UNIVERSITÀ DEGLI STUDI DI PADOVA

Sede Amministrativa: Università degli Studi di Padova
Dipartimento di Chimica

SCUOLA DI DOTTORATO IN SCIENZE MOLECOLARI
INDIRIZZO SCIENZE CHIMICHE
CICLO XXIII

SVILUPPO DI DERIVATI DI POLIFENOLI NATURALI DI INTERESSE FARMACOLOGICO

DEVELOPMENT OF DERIVATIVES OF NATURAL POLYPHENOLS FOR PHARMACOLOGICAL APPLICATIONS

Direttore della Scuola: Prof. Maurizio Casarin
Supervisore: Prof. Cristina Paradisi
Cosupervisore: Dott. Mario Zoratti

Dottorando: Andrea Mattarei

Contents

Riassunto dell'attività svolta

Il progetto di ricerca trattato in questa tesi di dottorato intende contribuire allo sfruttamento farmacologico dei polifenoli vegetali, una vasta famiglia di composti naturali presenti in molti cibi e bevande. Si tratta di un progetto marcatamente interdisciplinare, caratteristica che mi ha permesso di allargare il mio orizzonte culturale e allo stesso tempo di finalizzare il lavoro di sintesi a obiettivi ben definiti.

Gli effetti biomedici dei polifenoli vegetali sono oggetto di grande interesse e di molta ricerca, condotta in gran parte *in vitro*, usando sistemi modello come colture cellulari. Questi studi dimostrano che molti polifenoli possono stimolare o interferire con processi biochimici e che alcuni di essi potrebbero trovare utili applicazioni nella terapia e/o prevenzione di alcune patologie di grande interesse medico, ad esempio per prevenire l'insorgenza e inibire la crescita di molti tipi di cancro, per proteggere il sistema cardiovascolare o ancora per rallentare l'invecchiamento e il decorso di patologie neurodegenerative.

Queste potenzialità trovano però un grosso ostacolo nella loro esplicazione a causa della scarsa biodisponibilità di questi composti. Come risultato del loro scarso assorbimento e della cospicua metabolizzazione a livello intestinale ed epatico, infatti, solo piccole quantità di polifenoli entrano nel circolo sanguigno, e per lo più sotto forma di metaboliti.

Abbiamo individuato due possibili strategie per aumentare l'efficacia dei polifenoli. Una è di farli concentrare negli organi e/o nei comparti subcellulari in cui le loro proprietà possono avere il massimo impatto. Questo approccio, concretizzato nel targeting mitocondriale, ha portato alla realizzazione di sei lavori, ad oggi già pubblicati (Cap. 1-4), o inviati per la pubblicazione (Cap. 5-6), che costituiscono i primi sei capitoli della tesi.

Una seconda strategia per superare il problema della bassa biodisponibilità prevede la realizzazione di nuovi derivati che possano funzionare da veicoli di polifenoli (pro-drugs) resistenti alla metabolizzazione durante l'assorbimento e in grado di rigenerare il composto naturale una volta superata la barriera della metabolizzazione di primo passaggio. I risultati di questi studi sono descritti in due lavori a stampa che costituiscono i capitoli 7-8.

Infine, durante uno stage di sei mesi all'Università dell'Illinois, a Chicago, ho effettuato la sintesi di alcuni nuovi derivati della daidzeina, un importante isoflavone della soia, che incorporano la funzionalità per l'inibizione dell'istone deacetilasi, una classe di enzimi coinvolta nell'espressione genica (Capitolo 9). Questi nuovi composti sono tuttora in corso

di investigazione biologica al Burke/Cornell Medical Research Institute per verificare un possibile effetto nell'induzione dell'espressione di Arginasi 1.

Segue una breve descrizione dei più importanti risultati presentati nella tesi, mentre i principali nuovi composti sintetizzati sono presentati alla fine di questa sezione.

Derivati mitocondriotropici. I polifenoli sono molecole redox-attive e possono quindi intervenire nei processi radicalici che sono coinvolti in molte patologie. Il sito principale di produzione dei radicali sono i mitocondri, sede di eventi chiave nella morte cellulare sia per apoptosi che per necrosi, processi in cui hanno un ruolo determinante le specie reattive dell'ossigeno.

Importante per la genesi di questa ricerca è stata l'osservazione che la quercetina (3,3',4',5,7-pentaidrossiflavone) è in grado di inibire o indurre l'apertura del poro di transizione di permeabilità mitocondriale, a seconda che prevalga la sua attività anti- o pro-ossidante. Questo dipende da diversi fattori, tra cui l'azione di ioni metallici e di enzimi redox, il pH e la concentrazione del polifenolo stesso.

Ho sintetizzato alcuni nuovi derivati mitocondriotropici di quercetina e resveratrolo (3,4',5-triidrossi-*t*-stilbene), due polifenoli naturali molto diffusi e molto studiati in quanto dotati di interessanti proprietà. Questi composti sono resi mitocondriotropici grazie alla funzionalizzazione con un gruppo trifenilfosfonio (TPP^+), un catione in grado di diffondere attraverso le membrane biologiche e di accumularsi in regioni a potenziale negativo, quali la matrice mitocondriale. La quercetina possiede 5 ossidrili di cui nessuno è equivalente ad un altro. Per queste sintesi è stato quindi rilevante sviluppare approcci regioselettivi ma allo stesso tempo relativamente semplici e ad alta resa. La strategia generale per la sintesi dei derivati della quercetina ha pertanto richiesto passaggi di protezione/deprotezione selettiva delle funzionalità ossidriliche (Capitoli 1 e 3).

I composti sintetizzati si sono comportati come previsto in saggi *in vitro*, nei quali è stato possibile verificare un effettivo accumulo in organelli subcellulari a morfologia mitocondriale (Capitoli 1 e 2).

Le possibili applicazioni in campo biomedico dei derivati "mitocondriotropici" possono essere interessanti sia nel caso prevalga una loro azione anti-ossidante/citoprotettiva che pro-ossidante/citotossica.

Una prima indagine su quale sia l'effetto biologico di questi nuovi composti è stata condotta con mitocondri isolati, utilizzando due derivati della quercetina modificati in posizione 3, ovvero il 3-O-(4-trifenilfosfoniobutil) quercetina ioduro (3-QBTPI), e il suo analogo peracetilato (3-QTABTPI). In accordo con osservazioni fatte in precedenza con la

quercetina, questi composti si sono rivelati potenziali co-induttori della transizione di permeabilità mitocondriale e inibitori dell'ATP sintasi mitocondriale (Capitolo 4).

Per verificare la rilevanza della posizione occupata dal sostituente sullo scheletro della quercetina ho inoltre sintetizzato l'isomero mitocondriotropico di 3-QBTPI recante la funzionalizzazione con il fosfonio in posizione 7 (Capitolo 3).

E' stata quindi eseguita una caratterizzazione del comportamento redox dei due isomeri mitocondriotropici 3- e 7-(4-O-trifenilfosfoniobutil) quercetina ioduro. Sia nella determinazione del potenziale anodico di ossidazione che nel saggio di attività antiossidante utilizzando l'1,1-difenil-2-picrilidrazil (DPPH), l'isomero 7-sostituito si è comportato in maniera simile alla quercetina, mentre l'isomero 3-sostituito è risultato meno reattivo. Il derivato 7-sostituito ha inoltre manifestato una maggiore attività citotossica nei saggi di vitalità cellulare effettuati: è stato quindi selezionato come candidato ideale per ulteriori studi (Capitolo 5).

I derivati mitocondriotropici della quercetina inducono processi di morte cellulare non programmata (necrosi) e agiscono da proossidanti, generando anione superossido nei mitocondri. La morte cellulare è causata dalla generazione di superossido. L'induzione della necrosi è selettiva e colpisce cellule di tipo tumorale (C-26) e fibroblasti embrionali murini a crescita rapida (MEF) ma non fibroblasti embrionali murini a crescita lenta. Quantificazioni del contenuto mitocondriale e della produzione di superossido suggeriscono che la selettività dell'effetto citotossico potrebbe essere messa in relazione con la concentrazione di superossido mitocondriale (Capitolo 6).

Prodrugs di polifenoli. L'interesse per questi derivati nasce dall'idea di utilizzare reazioni comuni nella sintesi organica per sintetizzare derivati del resveratrolo, il polifenolo modello utilizzato per questo studio, recanti gruppi protettori sulle funzionalità ossidriliche. Lo scopo di questa protezione è di rallentare o eliminare i processi metabolici in fase di assorbimento, ottenendo quindi livelli sistemici del polifenolo più elevati in seguito alla rimozione dei gruppi protettori per idrolisi catalizzata da enzimi ubiquitari.

La strategia adottata inizialmente è basata sulla protezione degli ossidrili mediante legami di tipo carbossiestereo e ha prodotto diversi derivati del resveratrolo (Capitolo 7). Studi di stabilità in sangue, *in vivo* (farmacocinetiche nel ratto) ed *ex vivo* (camerette di Ussing) hanno però dimostrato che questo gruppo protettore è inadatto ai nostri scopi, in quanto troppo velocemente idrolizzato da attività esterasiche aspecifiche del sangue e della superficie intestinale.

Sono stati quindi selezionati altri tipi di legame da utilizzare per la protezione reversibile degli ossidrili e per realizzare derivati meno suscettibili all'idrolisi di quanto non siano i derivati carbossiesterei. Il primo tipo di legame saggiato è stato l'estere metansolfonico (mesilato) ($–O(SO_2)CH_3$) (Capitolo 7). Questo derivato si è dimostrato stabile in saggi *in vitro* a differenza dei derivati carbossiesterei che si idrolizzano lentamente in soluzioni a pH simili a quelli di stomaco e intestino e si convertono rapidamente a resveratrolo in sangue murino. In esperimenti di permeazione *ex vivo* utilizzando segmenti di intestino di ratto espiantati e montati in camerette di Ussing i derivati carbossiesterei si ritrovano nel comparto basolaterale essenzialmente come una miscela di metaboliti. Il precursore trimesilato si ritrova invece nel comparto basolaterale senza che sia possibile evidenziare prodotti di idrolisi o modificazioni metaboliche dovute al passaggio della parete intestinale. Esperimenti preliminari di farmacocinetica hanno suggerito che questo tipo di legame è troppo stabile e non suscettibile di idrolisi enzimatica anche *in vivo*, impedendo quindi la rigenerazione della forma attiva del polifenolo. Risultati analoghi sono stati ottenuti con il secondo tipo di derivati sintetizzato in cui gli ossidrili del resveratrolo sono stati protetti da funzionalità alchil eteree.

I polifenoli sono scarsamente solubili in acqua, e la solubilità è un fattore determinante per la biodisponibilità di un composto e per una comoda somministrazione.

Abbiamo quindi sintetizzato un primo derivato del resveratrolo (RGS) legando gli ossidrili del polifenolo al glucosio mediante un ponte succinico (Capitolo 8). Studi di farmacocinetica con questo composto dimostrano che l'assorbimento è ritardato rispetto al resveratrolo, un risultato potenzialmente utile. I livelli e la natura dei metaboliti in circolo sono però del tutto analoghi a quelli ottenuti somministrando resveratrolo; questo risultato suggerisce che il derivato subisca idrolisi a resveratrolo nel tratto intestinale, prima dell'assorbimento, compatibilmente con la nota instabilità del legame carbossiestereo *in vivo*.

Derivati della daidzeina. Durante un periodo di sei mesi (marzo/agosto 2010) presso il gruppo di ricerca del Prof. Alan Kozikowski alla UIC (University of Illinois at Chicago) ho effettuato la sintesi di alcuni nuovi derivati della daidzeina, un importante polifenolo naturale appartenente alla famiglia degli isoflavoni della soia. La daidzeina induce l'espressione dell'arginasi 1 (Arg 1), un enzima coinvolto nella biosintesi delle poliammine, che hanno un ruolo protettivo e favoriscono la rigenerazione di neuriti nel sistema nervoso centrale traumatizzato. Essa inoltre è un ben noto agonista del recettore estrogenico β e può agire anche da inibitore delle istone deacetilasi (HDACs), enzimi

coinvolti nella regolazione dell'espressione genica. Abbiamo quindi cercato di combinare in una sola molecola queste varie proprietà, producendo dei derivati che inducessero l'espressione di Arg1 rimanendo comunque capaci di interagire con il recettore degli estrogeni, e con una maggiore affinità per le HDACs. Per potenziare l'attività inibitoria nei confronti di questi ultimi enzimi ho unito la funzionalità dell'acido idrossammico allo scheletro molecolare della daidzeina, usando strumenti chimici come l'addizione di Michael sulla daidzeina protetta e la "click chemistry". La ritenzione della struttura dell'isoflavone e le funzionalità ossidriliche libere dovrebbero assicurare la ritenzione dell'attività estrogenica. In cinque passaggi sintetici sono giunto a quattro prodotti stereoisomerici, la cui farmacologia è ancora sotto studio.

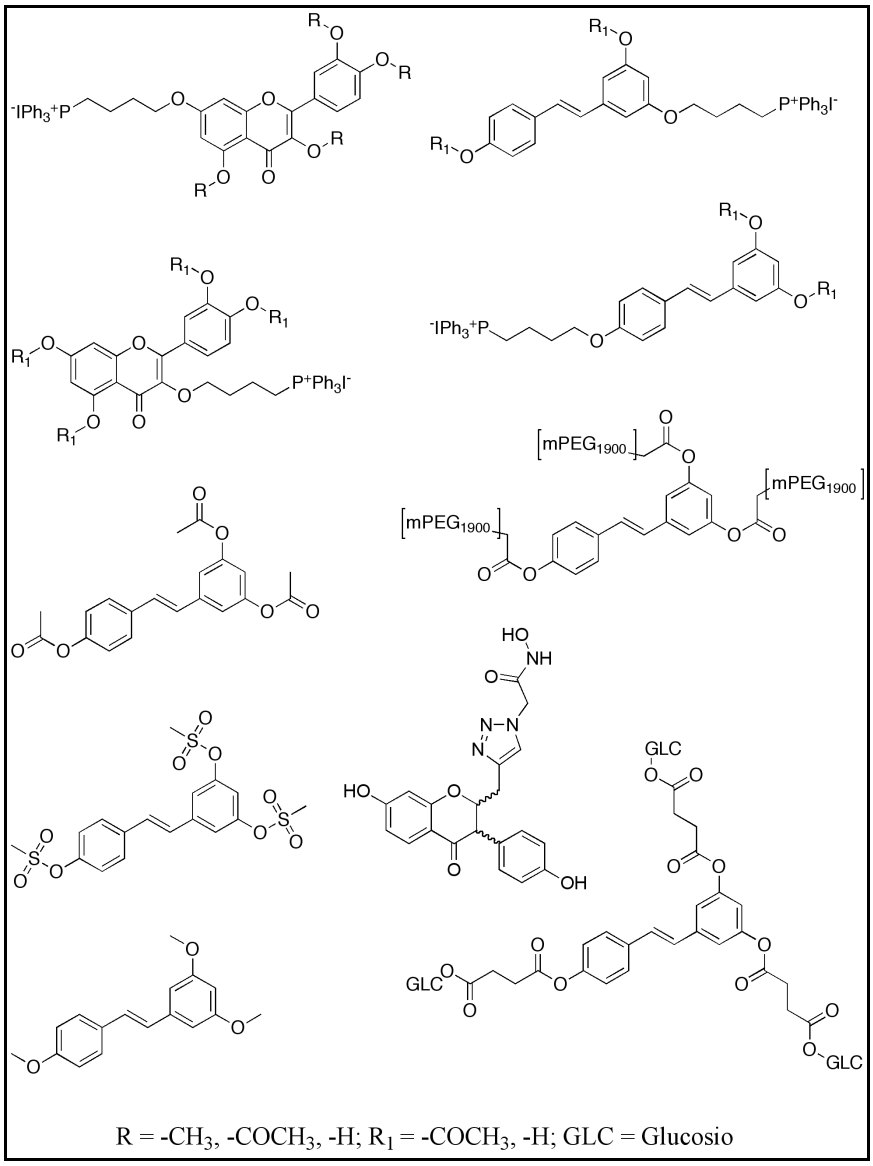

Principali nuovi composti sintetizzati

Summary

The research project I have been engaged in during my graduate studies is meant to open the way to the pharmacological exploitation of plant polyphenols, a vast family of natural compounds present in many foods and drinks. Its marked interdisciplinary characteristics have allowed me to expand my scientific interests while at the same time finalizing my synthesis work for well-defined goals.

The biomedical effects of plant polyphenols are of great interest and have been stimulating much research, conducted largely *in vitro*, using model systems such as cell cultures. These studies show that many polyphenols can stimulate or interfere with biochemical processes, and that several of them may find useful applications in the therapy and/or prevention of diseases and conditions of great medical interest. For example some polyphenols are reported to prevent the onset and to inhibit the growth of several types of cancer, to protect the cardiovascular system and to slow down senescence and the course of neurodegenerative diseases.

Applications such as these are however severely hindered by the low bioavailability of these compounds. As a result of a low level of absorption and of a rapid metabolism/degradation in the intestinal and hepatic compartments, only small amounts of polyphenols are found in the bloodstream, and then mostly as metabolites.

We have identified two possible strategies to increase the effectiveness of polyphenols. One is to concentrate them in the organs and/or subcellular compartments in which their properties can have a major impact. This approach, embodied in mitochondrial targeting, has led to six scientific papers, already published (Chapt.s 1-4) or submitted for publication (Chapt.s 5-6), which form the first part of the thesis.

A second strategy to reduce the obstacle of low bioavailability involves the production of new derivatives (prodrugs) that can act as vehicles of polyphenols, being more resistant to metabolism during the absorption and capable of regenerating the natural compound once the barrier of first-pass metabolism has been overcome. The results of these efforts are described in two papers and are reported in Chapters 7-8.

Finally, during a 6-months stage at the University of Illinois in Chicago I carried out the synthesis of new derivatives of daidzein, a major natural soy isoflavone, which incorporate a histone deacetylase (HDAC)-inhibitory functionality (Chapter 9). These new compounds are presently being tested at Burke/Cornell Medical Research Institute to assess possible effects on the expression of Arginase 1.

A brief description of the major results presented in the thesis follows, and the major new compounds produced are presented at the end of this section.

Mitochondriotropic derivatives. Polyphenols are redox-active molecules, and can thus intervene in oxidative processes involved in several pathologies. Mitochondria are the major source of reactive oxygen species (ROS) production and the site of key events for cell death in both the apoptotic and necrotic modes, processes in which ROS play a key role.

This part of the project originated from the observation that quercetin (3,3',4',5,7-pentahydroxyflavone) can either inhibit or induce the mitochondrial permeability transition, depending on whether its anti- or pro-oxidant activity prevails. This depends on a series of factors including the presence of metal ions with easily interconverting oxidation states, and/or enzymes with redox activity, the pH, and the concentration of the polyphenol itself.

I have synthesized some mitochondriotropic derivatives of model polyphenols quercetin and resveratrol (3,4',5-trihydroxy-trans-stilbene), both common and much studied natural compounds with interesting properties. The synthesized derivatives are mitochondriotropic thanks to functionalization with the triphenylphosphonium (TPP^+) group, a cation capable of diffusing through biological membranes and of concentrating in regions at negative electrical potential, such as the mitochondrial matrix. Quercetin has five non-equivalent hydroxyls. For these syntheses it has been therefore important to develop approches that would insure regioselectivity with relative simplicity and high yields. The general strategy for the synthesis of quercetin derivatives has thus involved the selective protection/deprotection of hydroxyls (Chapters 1 and 3).

These compounds exhibited the expected mitochondriotropic behaviour in *in vitro* assays involving isolated mitochondria and cultured cells (Chapters 1 and 2).

Since they are polyphenols, *a priori* these compounds may display an anti-oxidant/cytoprotective action or, on the contrary, a pro-oxidant/cytotoxic behaviour. Interesting possible biomedical applications can be envisioned in either case.

A first investigation on the biological effects of these new compounds has been carried out with isolated mitochondria, using two quercetin derivatives modified at position 3, namely 3-O-(triphenylphosphoniumbutyl) quercetin iodide (3-QBTPI), and its peracetylated analogue (3-QTABTPI). As expected on the basis of previous observations with quercetin, these compounds turned out to be potential co-inducers of the mitochondrial permeability transition, and inhibitors of the mitochondrial ATP synthase (Chapter 4).

To verify the relevance of the position occupied by the TPP-carrying substituent on the quercetin skeleton I also synthesized the mitochondriotropic analogues of 3-QBTPI and 3-QTABTPI with the phosphonium ion linked to position 7 (7-QBTI and 7-QTABTPI) (Chapter 3). We have then characterized the redox behaviour of the two mitochondriotropic isomers, 3- and 7-O-(4-triphenylphosphoniumbutyl) quercetin iodide. In both cyclic voltammetric determinations of the oxidation potential and in radical scavenging assays with 1,1-diphenyl-2-picrylhydrazyl (DPPH) the 7-substituted isomer behaved much like quercetin itself, while the 3-substituted isomer was more difficult to oxidize at the electrode and much less reactive towards DPPH. Moreover, the 7-substituted isomer proved to be more active (cytotoxic) in cell vitality assays, and thus emerges as the isomer of choice for further studies (Chapter 5).

The mitochondriotropic quercetin derivatives cause necrotic cell death and act as prooxidants, inducing generation of superoxide anion in the mitochondria. The generation of superoxide is what causes cell death. Necrosis induction is selective, hitting faster-growing C-26 tumoral cells and Mouse Embryonic Fibroblasts (MEFs) and sparing slower-growing MEFs. Measurements of mitochondrial content and superoxide production suggest that the selectivity of the cytotoxic effect might be related to the concentration of mitochondrial superoxide attained. (Chapter 6).

Prodrugs of polyphenols. Interest in these derivatives originated from the idea of using common reactions in organic synthesis to produce derivatives of resveratrol (used as a model polyphenol in this study) bearing protecting groups on the hydroxyls. The purpose of these protections is to slow down or eliminate metabolic processes during the absorption phase, thus resulting in higher systemic levels of polyphenol following the removal of protective groups by hydrolysis promoted by ubiquitous enzymes.

Our first choice was to protect the phenol hydroxyl moieties using the carboxyester bond and several derivatives of resveratrol were synthesized (Chapter 7). However, the results of stability studies in blood, of absorption experiments using *ex vivo* intestine segments mounted in Ussing chambers and of *in vivo* (rat) pharmacokinetic determinations have pointed out an excessive instability of the carboxyester linkage in these biological contexts. Its usefulness for *in vivo* applications turns out therefore to be limited.

Other types of protecting linkages were thus considered, which are expected to be less susceptible to hydrolysis than the carboxyesters. The first alternative protecting bond tested was the methanesulfonate ester ($–O(SO_2)CH_3$) (resveratrol trimesylate) (Chapter 7). This compound proved to be stable *in vitro*, while the carboxyester derivatives are slowly

hydrolysed in solutions at pH values mimicking the gastric or intestinal environment and are rapidly converted to resveratrol in blood. In *ex vivo* permeation experiments with explanted intestinal segments, resveratrol and carboxyester derivatives appeared in the basolateral compartment essentially as a mixture of Phase II metabolites. On the other hand, the trimesylate precursor was transported from the apical to the basolateral side without hydrolytic or metabolic modifications. Pharmacokinetic determinations also indicated that this type of bond is too stable and not susceptible to enzymatic hydrolysis thus preventing the regeneration of the active deprotected form of the polyphenol. An analogous conclusion was reached for ether derivatives.

Polyphenols generally have low solubilities in water, and solubility is a key factor contributing to the bioavailability of a compound and allowing convenient means of administration.

We therefore synthesized a first soluble resveratrol derivative (RGS) linking the hydroxyls to glucose moieties via a succinic acid group (Chapt. 8). Pharmacokinetic studies with this compound showed that absorption kinetics are delayed in comparison to resveratrol, a potentially useful outcome. The levels and the composition of the metabolite mix in the bloodstream are however analogous to those obtained using resveratrol itself. This suggests that the compound is hydrolysed to resveratrol in the gastro-intestinal tract, before absorption, due to the poor stability of the carboxyester linkage (Chapter 8).

Derivatives of daidzein. During the third year of my graduate studies I also carried out a project over six months (March-August 2010) spent in the group of Prof. Alan Kozikowski at the University of Illinois at Chicago (UIC). During this period I performed the synthesis of a few new derivatives of daidzein, a major polyphenol belonging to the family of soy isoflavones (Chapter 9).

Daidzein potentiates the expression of arginase 1 (Arg 1), a key enzyme in the biosynthesis of polyamines, which have a protective role in the central nervous system and favour neurite regeneration after a trauma. This isoflavone is furthermore a well-known agonist of the β estrogen receptor, and can also act as an inhibitor of histone deacetylases (HDACs), enzymes involved in the control of gene expression.

I have therefore worked to combine in a single molecule these various properties, producing derivatives capable of inducing Arg1 expression while maintaining the ability to interact with the estrogen receptor, and endowed with a higher affinity for HDACs. To achieve this enhancement of inhibitory effectiveness I attached the hydroxamic acid moiety to the daidzein skeleton, using chemical tools such as Michael addition on

protected daidzein and so-called “click chemistry”. The retention of the isoflavone structure and the free hydroxyls in our products should ensure the retention of the estrogenic activity. In five synthetic steps I have obtained four stereoisomeric products, whose pharmacology is still under investigation.

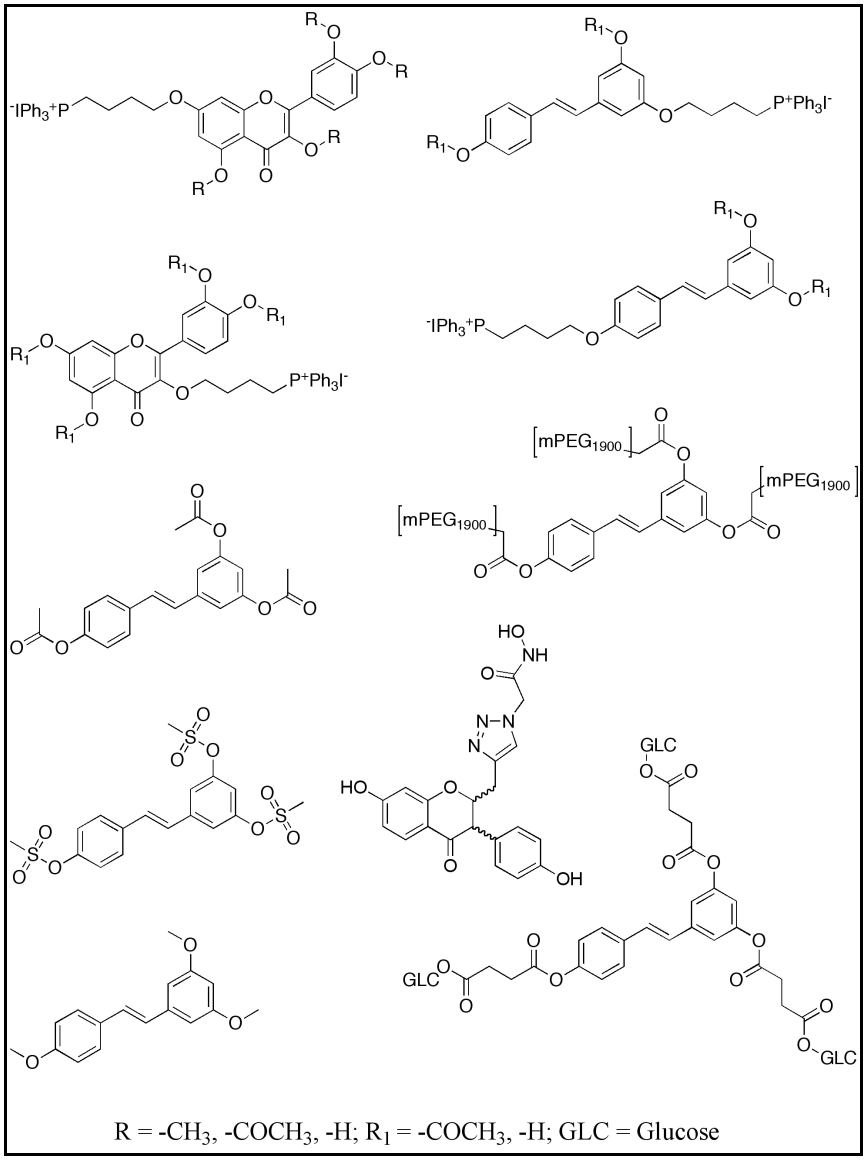

Major new compounds producted

Organization of the thesis

After a short general introduction, the bulk of this thesis is organized in nine chapters, corresponding each to a specific topic of research within the common subject of this thesis: development of new derivatives for the pharmacological exploitation of natural polyphenols. This organization has been favoured over a more traditional, monograph-style layout in part because my work actually developed as a series of closely related - but distinct - activities, and mainly with the intent of facilitating reading. Each chapter corresponds to a paper already published (Chapters 1-4, 7-8) or to a manuscript submitted for publication and presently under evaluation (Chapters 5-6) or, finally, to a manuscript in preparation (Chapter 9). Thus, the chapters are not homogenous in length and relevance. On the other hand each is self-standing and presents and discusses in detail a relatively complete piece of research work. My contribution to this interdisciplinary research was obviously limited to the chemical activities, which included the synthesis and characterization of all new derivatives and all studies of their stability, solubility and redox reactivity. The contribution of the other participants to this research is acknowledged by their names as coauthors in each individual chapter. I hope the benefits of such an organization outweigh its disadvantages.

Introduction

Polyphenols are a vast and diversified class of plant-made molecules characterized by the presence of a few phenolic hydroxyls. They are present in a great variety of foods of vegetable origin; Fig.1 shows the structures of some of the most important polyphenol subfamilies.

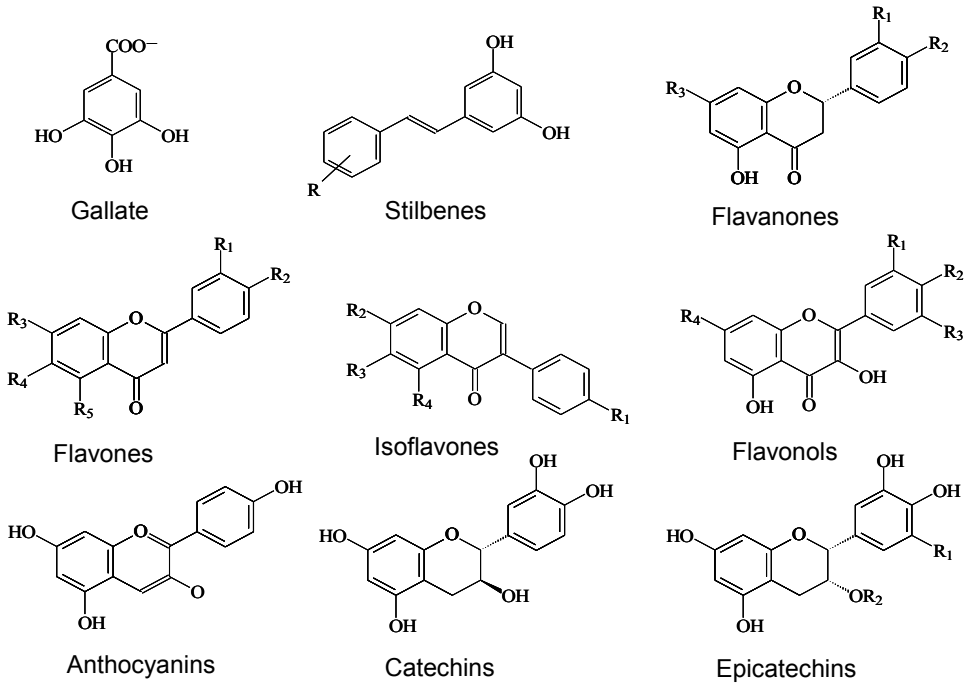

Figure 1. Some of the most important polyphenol subfamilies.

These compounds exhibit, at least *in vitro*, a variety of activities of potential relevance for many areas of health care, such as protection of the cardiovascular system, improving performance impaired by old age or neurodegeneration, contrasting inflammation and prevention and therapy of cancer.

The biological effects of polyphenols are ascribed both to their redox properties and to interaction with proteins.

Polyphenols are redox-active compounds. Their aromatic structure allows delocalization of charges or unpaired electrons, rendering them greatly more acidic than alcohols and good radical scavengers (and thus antioxidants). Radical scavenging may result from hydrogen donation or, more plausibly, electron transfer after deprotonation (Scheme 1).

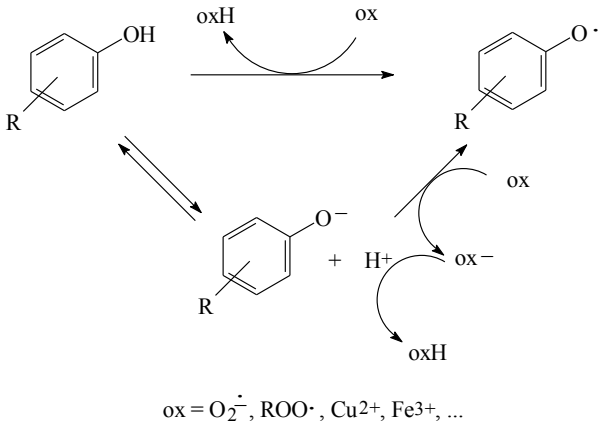

Scheme 1. Radical scavenging by a generic phenolic compound.

Anti-oxidant action has been given credit for the alleged antagonistic effects of polyphenols against processes involving radical-inflicted damage and/or radical-mediated signalling, such as aging and neurodegeneration. However, polyphenols can also act as pro-oxidants, depending on corollary factors such as their concentration, pH, and the presence of $Fe^{2+/3+}$ or $Cu^{+/2+}$ and/or oxidases such as the appropriately named "polyphenol oxidases". In the presence of iron or copper ions, they may act as catalysts of redox cycling leading to the oxidation of glutathione and other cellular components by atmospheric oxygen. They may thus become key participants in a "redox catastrophe" whereby an oxidative chain reaction may be amplified to the point of overwhelming the cellular redox defenses. In less extreme circumstances, the generation of H_2O_2 may have important consequences at the cellular level via redox-sensitive signalling proteins (e.g. phosphatases and kinases) and transcription factors (e.g. NFkB, AP-1). The cytotoxic pro-oxidant mode of action is as potentially useful as the anti-oxidant one, since it might be exploited to induce death of cancerous cells.

Various polyphenols are known to bind to and to modulate directly a number of key proteins, including metalloproteinases, membrane receptors, channels (e.g. CFTR), cyclooxygenases, transcription factors, deacetylases (sirtuins), cytoskeleton components (tubulin) and many kinases as well as proteins of the blood (albumin, haemoglobin) and some toxins (e.g. anthrax toxin, vacA). Effects on gene expression are very important, and in fact much of the antioxidant activity of polyphenols seems to be actually mediated by redox-sensitive transcription factors and enzymes. In many cases however potentially

useful interactions are relatively weak, and thus the question arises of whether the concentrations needed to exert a significant effect are reached in a physiological setting.

The notoriously low bioavailability of these compounds is a formidable obstacle for their pharmacological exploitation, and is believed to be a major reason why the epidemiological evidence for effects of polyphenol-rich diets is generally spotty and controversial. Since they are, by definition, ready-made Phase II metabolism substrates, they are rapidly sulfated, glucuronidated by enterocyte and liver transferases, and then rapidly eliminated. Only low (nM-μM) concentrations of any given polyphenol are found in plasma and lymph even after a polyphenol-rich meal, and mostly in the form of conjugates.

Low absorption and metabolism must be contrasted if the pharmacological potential of natural polyphenols is to be more fully exploited. Many drugs are afflicted by analogous bioavailability and metabolism problems, and one of the main strategies used to enhance effectiveness is based on protecting the reactive sites with removable groups, i.e. on the development of "prodrugs".

A more detailed overview of these various themes can be found in the introductory sections of the various chapters, where more specific information is presented to provide a context for each aspect of this work.

The project

My thesis developed as a proof-of-principle project intended to promote the exploitation of the biomedical potentialities of polyphenols *in vivo*, stimulating the development of a real pharmacology of these compounds.

For this work we adopted two widely used model polyphenols, quercetin and resveratrol, both credited with remarkably useful properties and widely used as representatives of the superfamily of compounds.

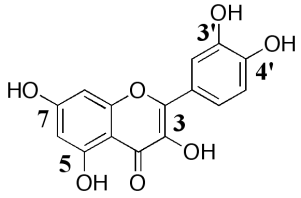

Quercetin

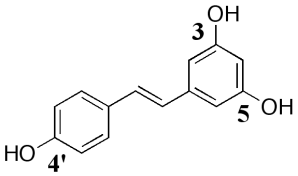

Resveratrol

As the project developed, two main themes came into focus: one was to target these compounds to a subcellular site where they might be expected to be most effective; the other was to increase the bioavailability and efficacy of polyphenols.

Since Reactive Oxygen Species (ROS) in cells are mostly produced by mitochondria, the development of polyphenol-based, redox-active derivatives targeted to these organelles allows one to place these compounds in the most appropriate subcellular location for exerting their anti-oxidant (protective) or pro-oxidant (cytotoxic) effects.

To increase bioavailability, we are developing derivatives protected at the sites of metabolic modification and with improved solubility characteristics, thus obtaining "pro-drugs" capable of crossing epithelia with higher absorption efficiency, and less prone to the action of detoxifying enzymes.

Furthermore in the last chapter of this thesis I describe a project performed in the United States under the supervision of the Prof. Alan P. Kozikowski at the College of Pharmacy, University of Illinois at Chicago. During this period I worked on the synthesis of some derivatives of daidzein (Fig. 2) an important natural polyphenol belong to the group of soy isoflavones.

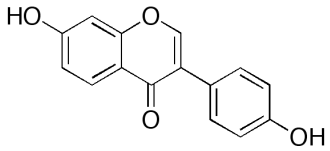

Daidzein

Figure 2. Chemical structure of daidzein

Recently it was discovered that daidzein induces arginase 1 (Arg 1) expression in a hippocampal cell line. Arg 1 has been shown to protect motor neurons from trophic factor deprivation and to allow sensory neurons to overcome neurite outgrowth inhibition by myelin proteins. Daidzein has both estrogenic and anti-estrogenic effects; estrogen receptor activation is required for daidzein to induce Arg 1 expression. Furthermore preliminary data suggested that it may also weakly inhibit histone deacetylases (HDAC). The HDAC inhibitor TSA has been shown to robustly induce arginase 1 expression whereas estrogen itself does not. Based on these results we undertook the synthesis of a novel series of compounds that link an HDAC-inhibitory functionality to the molecular frame of daidzein. These compounds will in turn allow us to assess whether the combination of estrogenic activity and enhanced HDAC inhibitory activity might lead to an enhancement of neuroprotective action.

Chapter 1

A mitochondriotropic derivative of quercetin: a strategy to increase the effectiveness of polyphenols[1]

Summary

Mitochondria-targeted compounds are needed to act on a variety of processes involving these subcellular organelles and having great pathophysiological relevance. In particular, redox-active molecules capable of homing in on mitochondria provide a tool to intervene on a major cellular source of reactive oxygen species and on the processes they induce, notably the mitochondrial permeability transition and cell death. We have linked the 3-OH of quercetin (3,3',4',5,7-pentahydroxy flavone), a model polyphenol, and the triphenylphosphonium moiety, a membrane-permeant cationic group, to produce proof-of-principle mitochondriotropic quercetin derivatives. The remaining hydroxyls were, or not, acetylated to hinder metabolism and improve solubility. The new compounds do accumulate in mitochondria in a transmembrane potential-driven process and are only slowly metabolized by cultured human colon cells. They inhibit mitochondrial ATPase activity much as quercetin does and are toxic for fast-growing cells.

Introduction

Polyphenols are a large family of natural compounds exhibiting, at least *in vitro*, a variety of biomedically important activities. A vast literature documents effects of potential relevance for such major health-care endeavours as protection of the cardiovascular[1] and nervous[2] systems, prevention and therapy of cancer,[1,3] contrasting aging,[2,4] reducing chronic inflammation[4,5] and lengthening the lifespan of model organisms.[6-8]

These effects are attributed in part to direct interactions of polyphenols with proteins, and in part to their redox properties as reducing agents and ROS (Reactive Oxygen Species) scavengers, i.e., antioxidants.[9,10] This antioxidant character has been proposed to underlie the alleged antagonistic effects of polyphenols vs. processes involving ROS-inflicted damage and/or radical-mediated signalling, such as aging and neurodegeneration.[11,12] The level of reactive polyphenol attainable at the site of action is of obvious importance: cells

[1] Published as: Mattarei, A.; Biasutto, L.; Marotta, E.; De Marchi, U.; Sassi, N.; Garbisa, S.; Zoratti, M.; Paradisi, C. *ChemBioChem*, **2008**, 16, 2633-2642.

normally maintain redox homeostasis thanks to a mM-range pool of molecules such as glutathione; to have a measurable effect as general reducing agents polyphenols ought therefore to reach concentrations of the same order of magnitude.

Mitochondria are the subcellular compartment in which most ROS are produced, and the site of key events in both apoptosis and necrosis. Oxidative processes are of major importance in both cases.[13-15] In apoptosis, for example, oxidation of cardiolipin is needed for the release of cytochrome c.[15] The ROS-induced Mitochondrial Permeability Transition (MPT)[16,17] is now believed to have a fundamental role in necrotic death, such as occurs, e.g., upon reoxygenation following ischemia.[18,19] Enhanced ROS production is the common theme of mitochondrial dysfunctions.[20,21]

A new sector of pharmacology targets mitochondria to prevent or to induce, as the case may be, cell death.[22-25] The control of mitochondrial redox processes is an attractive perspective in this context, and the development of drugs capable of accumulating specifically in mitochondria - "mitochondriotropic" compounds - is of obvious importance for such an effort. Important progress in this direction has been made exploiting the matrix-negative voltage difference of about 180 mV maintained by energized mitochondria across their inner membrane. Compounds formed by a redox-active part linked to a membrane-permeant permanent cation (most often triphenylphosphonium, TPP) accumulate in regions held at negative potential, i.e. the cytoplasm and the mitochondrial matrix.[25,26] Importantly, no significant toxic effects of these compounds have been observed *in vivo*.[25]

We reasoned that polyphenol-TPP conjugates may act as anti-oxidants *in vivo* and be useful in counteracting "basal" ROS production and long-term effects such as chronic inflammation and neurodegeneration. Furthermore, they may find application against acute pathologies, e.g. those caused by ischemia. Antioxidants (and MPT inhibitors) would be expected to counteract this process, and indeed this seems to be the case.[14,24,27] In a relevant piece of work the mitochondriotropic antioxidant decylquinone-TPP^+ ($MitoQ_{10}$) was administered to rats before explanting the hearts and subjecting them to ischemia/reperfusion (I/R).[28] Treatment resulted in a significant reduction of the necrotic area. A similar protective effect was afforded by high doses of intravenous resveratrol in models of cerebral[29] and cardiac[30] ischemia.

Polyphenols can also induce a potentiation, rather than a reduction, of oxidative and radical chain processes, i.e., they may act as "pro-oxidants".[31-33] Which behaviour predominates depends on the abundance of metal ions capable of maintaining a redox cycle and/or of

redox-active enzymes such as tyrosinases ("polyphenol oxidases") and peroxidases, on the ion-chelating properties of the polyphenols themselves, and on pH. Additional factors may be the concentration of the polyphenol[33] and even the subcellular compartment involved.[34] Depending on such factors, and on the particular polyphenol involved, polyphenol-TPP conjugates may therefore act as cytotoxic, apoptosis- or necrosis-inducing pro-oxidants.

The pro-oxidant mode of action is as potentially useful as the anti-oxidant one, since it may be exploited to induce death of unwanted, i.e. cancerous, cells. Cancer cells live under oxidative stress,[35] which in principle makes them more vulnerable to ROS-mediated damage. Cell death and/or MPT induction by "redox cycling" compounds such as menadione or adriamycin is well known, and anti-tumoral, mitochondrion-targeted, pro-oxidant-based chemotherapeutic approaches have been proposed.[36,37] *In vivo* it may be possible to focus the action on cancerous cells because in many tumour types mitochondria maintain a higher transmembrane potential than in normal tissue.[22,38,39] This approach has already been used in pioneering pharmacological work.[22,40,41] Mitochondriotropic polyphenols may provide significant oncological benefits also if they turn out to act as anti-oxidants. Recent studies have shown that mitochondrial ROS production is an important determinant of the metastatic potential of cancerous cells,[42] and that polyphenols are capable of reducing cell shedding from tumoural masses.[43]

The sheer number and variety of properties of natural polyphenols, their varied reactivity and the relevance of the pathophysiological processes for which they offer promise suggest that mitochondriotropic polyphenol derivatives may find clinically relevant applications. This is not necessarily limited to circumstances involving redox processes.

Here we report the proof-of-principle synthesis, characterization and initial biological assessment of triphenylphosphonium-comprising derivatives of quercetin, a widely used model polyphenol.

Results

Quercetin (1) and potentially useful target mitocondriotropic derivatives considered in this work are shown in Chart I.

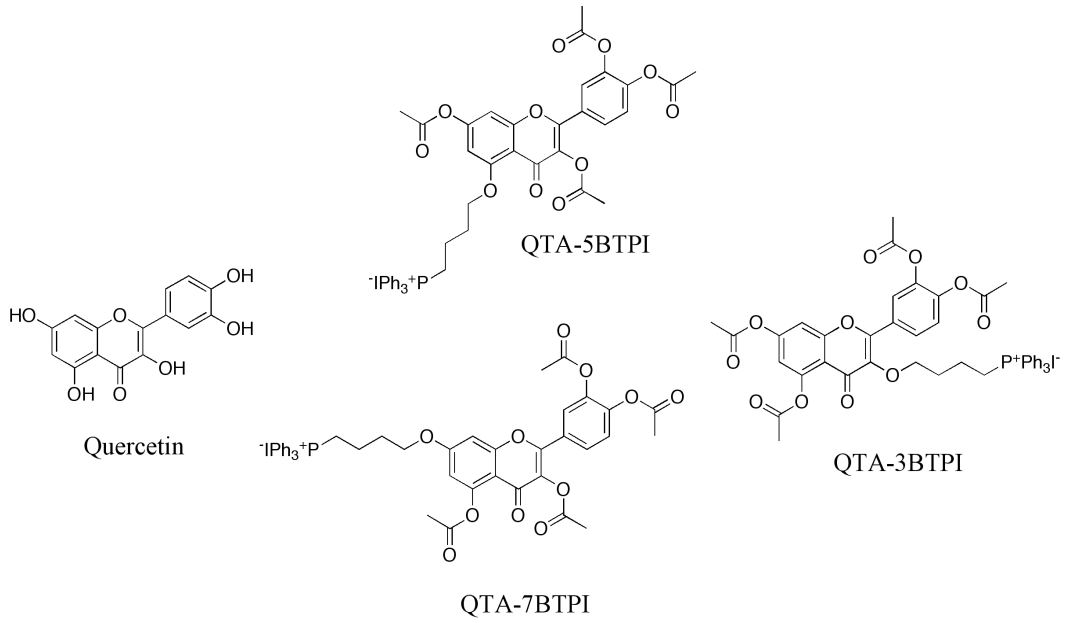

Chart 1. Quercetin (**1**) and potentially useful target mitocondriotropic derivatives

Such derivatives were identified on the basis of the following considerations: i) the hydroxyls of quercetin provide convenient sites to connect, through an ethereal bond, a linker bearing the TPP group; ii) since the catecholic hydroxyls determine to a large extent the redox properties of quercetin, they should be maintained as such in the target derivative. The connection to the TPP group ought therefore to involve one of the hydroxyls on the A or C rings; iii) to hinder metabolism and limit the formation of negative charges due to conjugation or ionization, it was desirable to protect the remaining hydroxyls with groups expected to be rapidly removed by cellular enzymes, such as acetyl moieties. Moreover, hydroxyl groups are also in part responsible for the well-known tendency of polyphenols to form colloidal particles and for aspecific interactions with proteins. The introduction of the TPP group and the protection of the hydroxyls were thus also expected to increase the low solubility of quercetin and possibly to counteract its notorious tendency to bind to proteins such as haemoglobin and albumin.[44,45]

Chemistry

Synthesis

Following the strategy outlined in Scheme 1 we succeeded in synthesizing the target derivative with the TPP-bearing linker on the C ring of quercetin, **7**. Briefly, the sequence involves protection of the cathecolic hydroxyls, selective O-alkylation to introduce a

chloroalkyl group, unblocking of the cathecolic hydroxyls, acetylation and introduction of the TPP^+ group via nucleophilic substitution on the chloroalkyl linker. By skipping the acetylation step, the non-acetylated derivative **9** was also prepared by the same route, so as to compare it with **7** and assess the effects of the free hydroxyl groups on the behaviour of these mitochondriotropic new compounds.

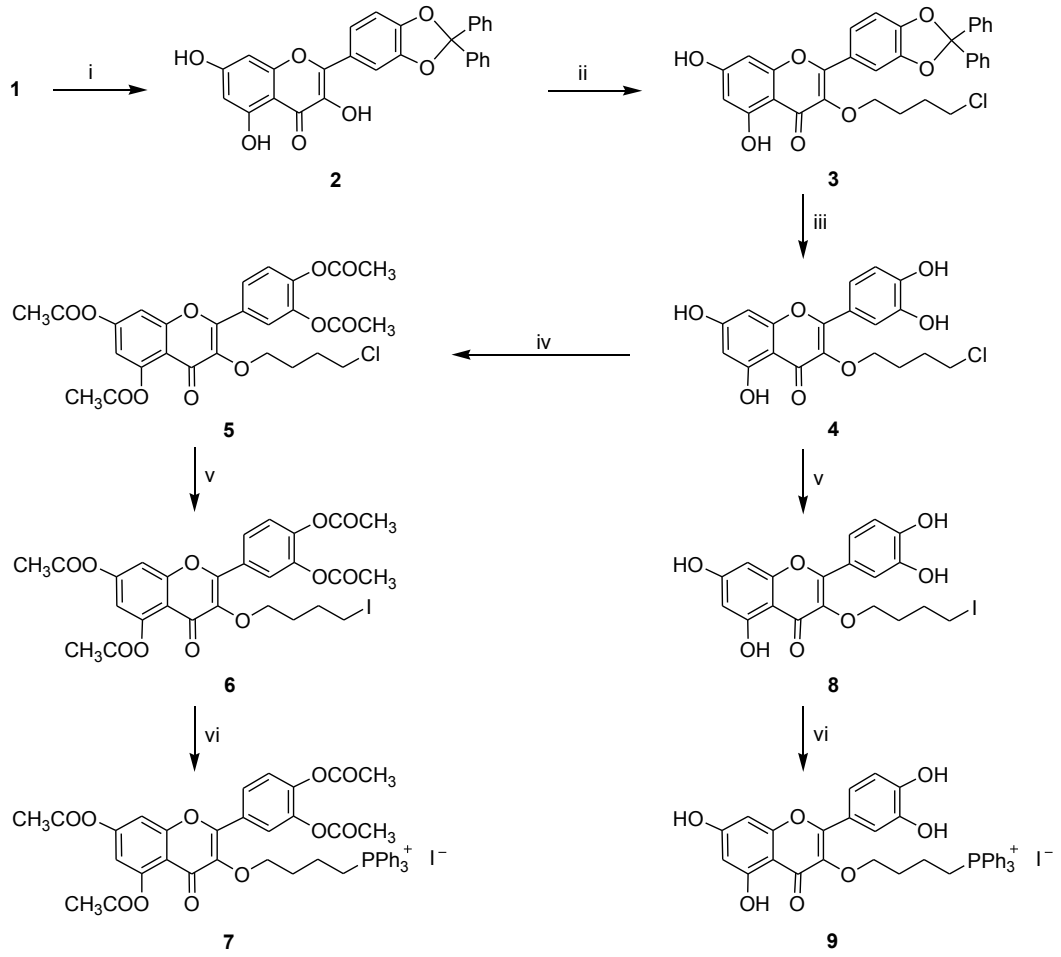

i: Ph_2CCl_2 (3 eq), 180°C, 10 min; ii 1-bromo-4-chlorobutane (1.2 eq), K_2CO_3 (1.3 eq), DMF, Ar, r.t., 20 h;
iii: $AcOH/H_2O$ 8:2, reflux, 2 h; iv: $CH_3C(=O)Cl$, pyr, r.t., 24 h; v: NaI, acetone, reflux, 20 h; vi: PPh_3, 95°C, 6h.

Scheme 1. Synthesis of mitochondriotropic derivatives **7** and **9**.

Ketal 2 was readily obtained following the procedure by Bouktaib et al.[46] with only small modifications. Reaction of **2** with 1.2 equivalents of 1-bromo-4-chlorobutane in the presence of K_2CO_3 yielded **3** in reasonably good yield (45% after purification). The assignment of the site of O-alkylation in **3** was based on NMR data. Specifically, the presence of a characteristically narrow NMR peak at ca. 12 ppm indicates the presence of the slowly exchanging proton of the hydroxyl at C-5.[47,48] To distinguish the two remaining possibilities, i.e. alkylation at C-3 or at C-7, either of which would have been a useful outcome in this study, we went on to unblock **3** and to compare the NMR chemical shifts of the ring protons of the resulting product, **4**, with those of **1**. We found (Table 1)

that the presence of a $–O(CH_2)_4Cl$ group in place of an –OH group does not affect the chemical shifts of H-6 and H-8, whereas a considerable difference is observed for H-2' and H-6', thus indicating that substitution is at C-3.

Table 1. Chemical shifts (δ) and, enclosed in parenthesis, chemical shift changes (Δδ) of the aromatic protons of quercetin (**1**) and 3-*O*-(4-chlorobutyl) quercetin (**4**) in DMSO-d_6 for the assignment of the O-alkylation site.

Compound	***Chemical shif s(δ) and chemical shifts changes (Δδ)***				
	δ(H-6)	***δ(H-8)***	***δ(H-5')***	***δ(H-6')***	***δ(H-2')***
Quercetin (1)	6.194	6.405	6.887	6.544	7.683
Compound 4	6.189 (-0.005)	6.397 (-0.008)	6.893 (+0.006)	7.436 (+0.892)	7.514 (-0.169)

Deprotection of the catecholic hydroxyls (step iii in Scheme 1) according to a literature procedure[46] gave the desired product 4 in 80% yield after purification. Careful control of the reaction progress was required to avoid, at prolonged treatment times, hydrolysis of the ether linkage. Acetylation of the free hydroxyls in **4** (step iv in Scheme 1), gave the Cl-derivative **5**. NMR analysis of this intermediate provided additional support for the attribution of the O-alkylation site to C-3: comparison of the NMR spectra of **5** and of pentaacetylquercetin showed significant differences in the chemical shifts of ring protons H-2' and H-6', thus confirming C-3 as the site of O-alkylation (Table 2). A similar analysis was not applicable to the final product **7** due to heavy spectral interferences by the TPP^+ group.

Compound **5** was converted to **7** via the iodo-derivative **6**. This indirect route avoided the high temperature necessary for direct reaction of triphenylphosphine with the primary chloro-derivative, which caused some decomposition. Compound **4** was converted to **9** in a similar manner.

Table 2. Chemical shifts (δ) and, enclosed in parenthesis, chemical shift changes (Δδ) in $CDCl_3$ of the aromatic protons of pentaacetylquercetin and of compound **5**, for the assignment of the O-alkylation site.

Compound	***Chemical shif s(δ) and chemical shifts changes (Δδ)***				
	δ(H-6)	***δ(H-8)***	***δ(H-5')***	***δ(H-6')***	***δ(H-2')***
Pentaacetylquercetin	6.876	7.333	7.351	7.717	7.690
Compound 5	6.822 (-0.054)	7.297 (-0.036)	7.346 (-0.005)	7.975 (+0.258)	7.919 (+0.229)

Solubility in water

The solubility of **7** in water was $(4.96 \pm 0.21)\cdot10^{-4}$ mol/L as determined by spectrophotometric measurements (see the Experimental section). This solubility is at least 200-fold higher than that of quercetin.[49] This derivative thus satisfies the requirement of increased solubility in aqueous media. The solubility of **9** turned out to be less than 2 μM, presumably because the free hydroxyls facilitate the formation of large aggregates. Since this concentration is too low for recording fluorescence spectra and performing metabolism studies, solutions for those experiments were prepared in HBSS (Hank's Balanced Saline Solution) containing 0.1% DMSO.

Stability in acqueous solution

Both **7** and **9** are stable for at least 24 hours in deionized water, as determined by spectrophotometric and HPLC analysis. **9** is also stable in 90% HBSS, 10% CH_3CN (added to insure solubility of the reaction products), while in this medium **7** undergoes very slow hydrolysis of the protective acetyl groups (Figure 1).

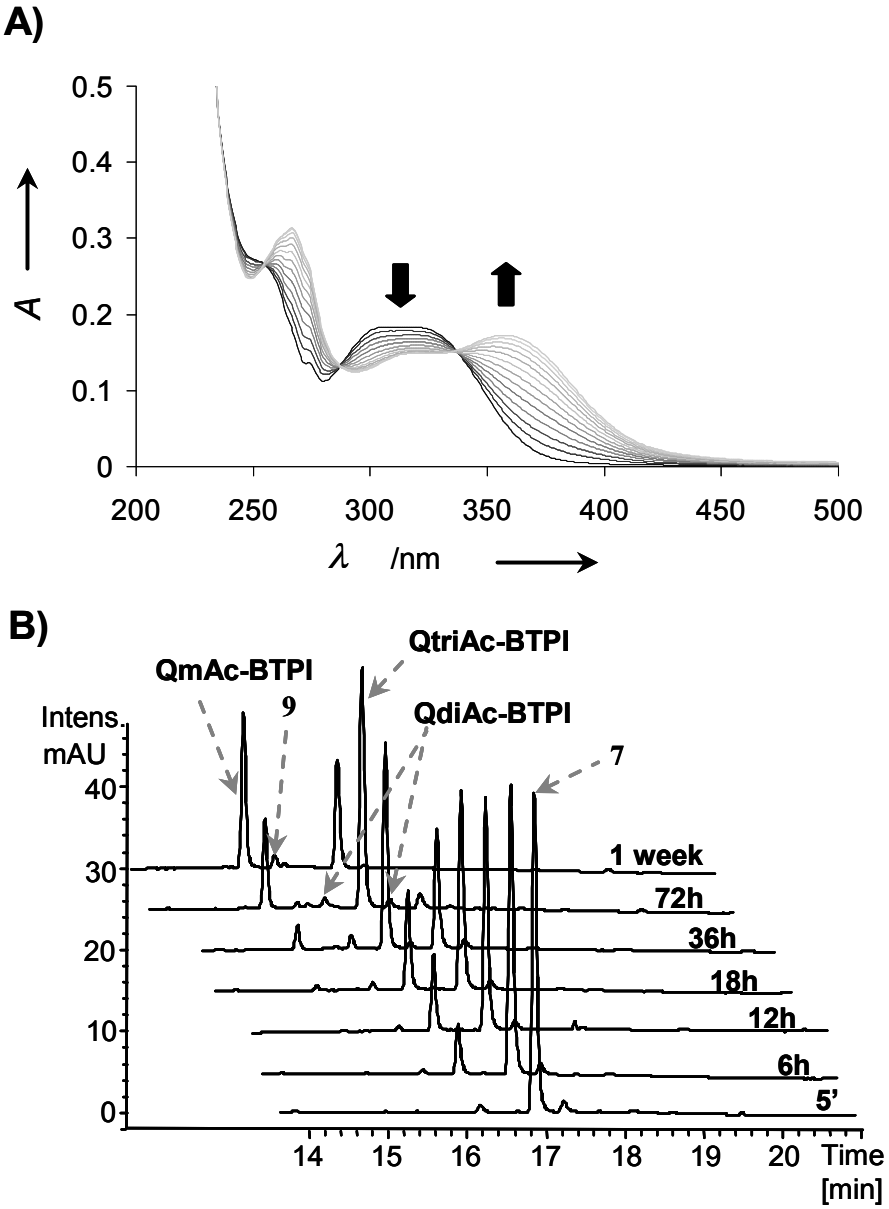

Figure 1. Hydrolysis of **7** in HBSS:CH_3CN 9:1. (A) UV-Vis spectra recorded every 6 hours for 72h. (B) HPLC traces recorded at 300 nm at different reaction times. Abbreviations: QmAc-BTPI: acetyl-3-*O*-(4-triphenylphosphoniumbutyl) quercetin iodide, QdiAc-BTPI: diacetyl-3-*O*-(4-triphenylphosphoniumbutyl) quercetin iodide, QtriAc-BTPI: triacetyl-3-*O*-(4-triphenylphosphoniumbutyl) quercetin iodide.

Metabolism

We assayed metabolism of **1**, **7** and **9** by HCT116 cells, i.e., the cells used in the experiments concerning mitochondriotropic behaviour (see below). HPLC and LC/MS analysis of the culture medium and cell extracts (see the Experimental section) showed that **1** and **9** were metabolized only to a very limited extent by these cells over an 8-hour period. Modification consisted in the introduction of a methyl group. In analogous experiments **7** was progressively deacylated with the eventual transformation of most of it

into the mono-acylated compound, but also underwent little conjugation. Figure 2 shows representative HPLC records.

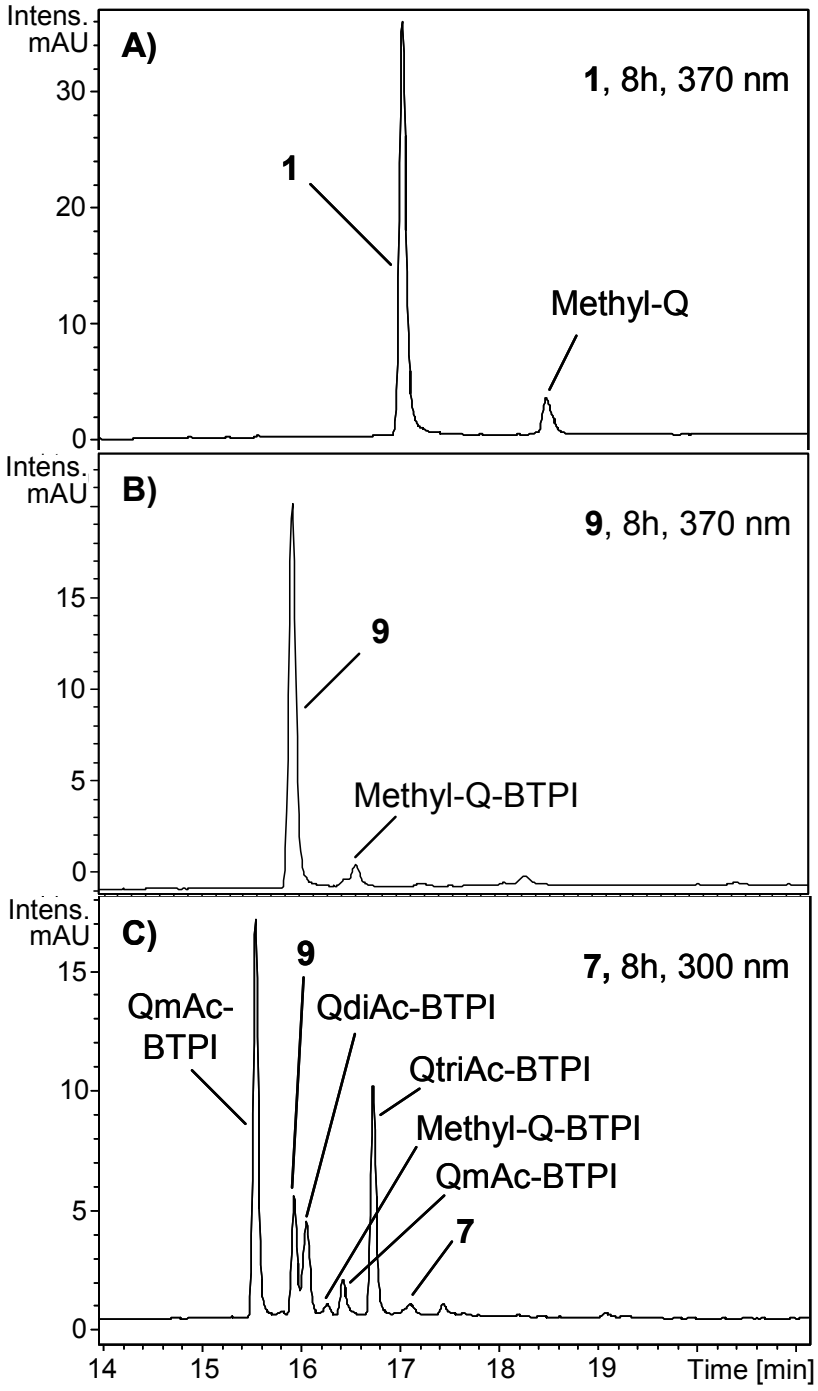

Figure 2. HPLC chromatograms, recorded at 300 or 370 nm, as indicated, of the extracts obtained after 8 hours of incubation of 1 (A), 9 (B) and 7 (C) with HCT116 cells. See the Experimental section for details. Abbreviations as in Figure 1 and: methyl-Q: methylquercetin, methyl-Q-BTPI: methyl-3-*O*-(4-triphenylphosphoniumbutyl) quercetin iodide.

Mitochondriotropic behaviour

We verified that compounds **7** and **9** indeed accumulate in mitochondria by two methods. In the first approach we monitored their uptake by isolated, respiring rat liver mitochondria using a TPP-sensitive electrode (see Experimental Section).[50] A representative experiment with **7** is shown in Figure 3.

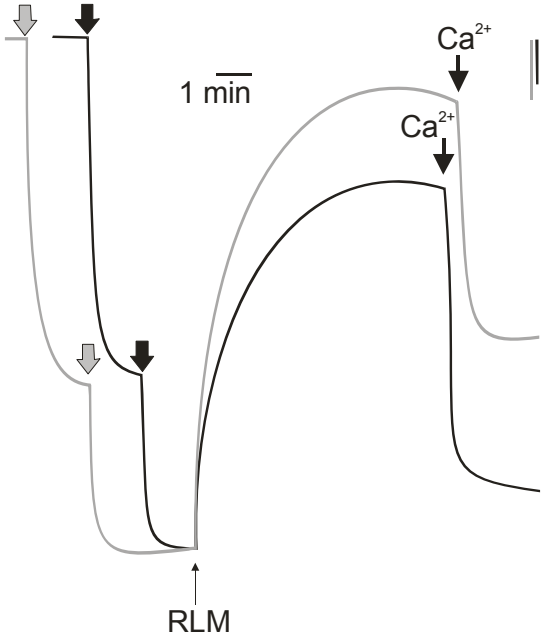

Figure 3. Accumulation of tetraphenylphosphonium (Ph_4P^+) (black trace) and **7** (gray trace) by Rat Liver Mitochondria (RLM). Thick arrows indicate the addition of 0.16 μM $Ph_4P^+I^-$ or **7** to the medium (in mM: sucrose 200, HEPES/K^+ 10, succinate/K^+ 5, NaH_2PO_4 1, rotenone $1.25x10^{-3}$; pH 7.4). Addition of RLM (1 mg prot.·mL^{-1}) and of $CaCl_2$ (40 μM) are also shown. The traces have been normalized to take into account the different response of the electrode in the two cases, which is quantified by the bars in the upper right corner.

The introduction of mitochondria causes a decrease (upward deflection of the trace) of the concentration of our compounds in the incubation medium, since they become partly sequestered in the mitochondrial matrix. The subsequent addition of excess Ca^{2+} induces the mitochondrial permeability transition, with loss of mitochondrial transmembrane potential ($\Delta\psi_m$) and release of the TPP derivatives. Release is also induced by addition of a $\Delta\psi_m$-dissipating protonophore (carbonyl cyanide p-trifluoromethoxyphenylhydrazone, FCCP). The accumulation ratio (i.e., the fraction of compound which is taken up by the organelles) differs somewhat from one compound to the other. This can be attributed to different extents of binding to mitochondrial constituents (lipids, proteins, nucleic acids), which is well known to cause apparent deviations from Nernst's law. This interpretation is

supported by the observation that the "excess" **7** taken up is retained also after depolarization. Analogous results were obtained with compound **9** (not shown).
In the second approach we exploited the fluorescence of **7** to follow its accumulation in the mitochondria of cultured cells (Figure 4).

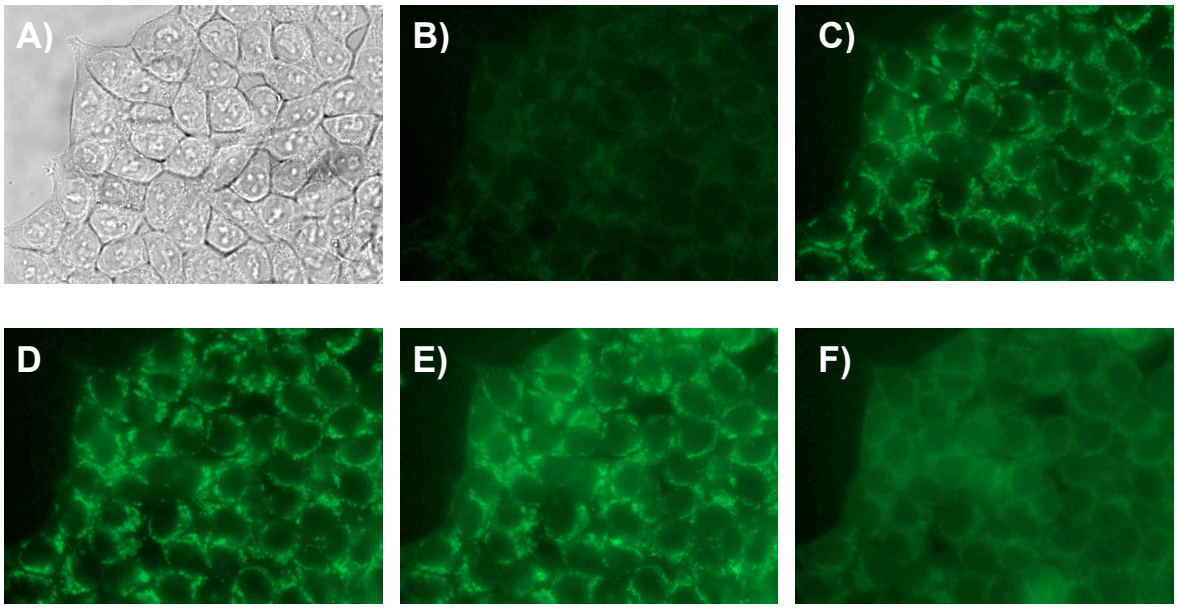

Figure 4. $\Delta\psi_m$-dependent accumulation of compound **7** in the mitochondria of cultured HCT116 cells. A) Phase contrast image, taken shortly before the start of the sequential automatic acquisition of 20 fluorescence images taken 1 min. apart. About 20 sec. after the first image was recorded, **7** was added to give a final concentration of 4 μM. B-D) Fluorescence images of the same field, taken approximately 0.7, 10 and 20 min., respectively, after the addition of **7**. The compound accumulates into perinuclear organelles having mitochondrial morphology. E-F) Images recorded approximately 1 and 10 min., respectively, after the subsequent addition of 2 μM FCCP, a classic $\Delta\psi_m$-dissipating protonophore (uncoupler). The fluorescence is released from the mitochondria and diffuses into the cytoplasm.

The spectral properties of the compound, similar to those of quercetin itself, allowed monitoring of its fluorescence upon excitation in the near-UV (380 nm) (see Experimental section). Mitochondria are easily recognizable by their characteristic granulated/filamentous morphology and perinuclear distribution. After the addition of **7** to the medium, their weak autofluorescence due to pyridine nucleotides is progressively overwhelmed by the much more intense signal due to accumulation of the quercetin derivative (Panels B-D). Addition of FCCP causes the rapid release of **7** (and partially deacylated derivatives) from the mitochondrial matrix (Panels E-F). Some of it remains in the cytoplasm of the cells due to the presence of a cytoplasm-negative voltage difference, maintained by K^+ diffusion, across the plasma membrane. Compound **9** is expected to

behave in the same manner, but its low fluorescence quantum yield hindered the observation of its accumulation in mitochondria *in situ*.

We compared the inhibition by quercetin, **7** and **9** of the activity of the mitochondrial ATPase. The results were in substantial agreement with previous reports of an inhibition by quercetin with an IC_{50} in the 50 μM range,[51] and showed that the introduction of the linker and TPP groups did not have a major effect on this action (Figure 5).

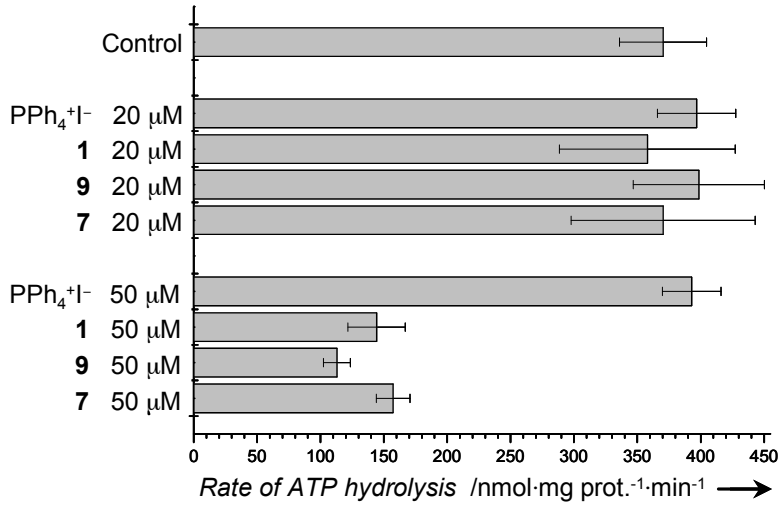

Figure 5. Effects of **7**, **9**, quercetin and tetraphenylphosphonium on the rate of ATP hydrolysis by permeabilised Rat Liver Mitochondria. See the experimental section for details. Determinations were carried out in triplicate and averages ± s.d. are reported.

As a preliminary test of possible anti-cancer activity, we also verified the effects of these compounds, and, as controls, of the parent polyphenol quercetin, of two phosphonium salts and of quercetin plus these latter compounds on cultured cells. We used the murine colon cancer cell line C-26 and, as controls, fast- and slow-growing non-tumoural mouse embryonic fibroblast (MEF) lines. Cell growth and viability was quantified using the tetrazolium salt reduction (MTT) assay (see Experimental section). As illustrated by Figure 6A, the various compounds had little effect on C-26 cell proliferation at the 1 μM level. At 5 μM, quercetin, with or without $Ph_4P^+I^-$ or TPMP (triphenylmethylphosphonium chloride), significantly hindered cell growth, while the phosphonium salts by themselves remained innocuous. The mitochondriotropic quercetin derivatives displayed marked cytotoxicity. A similar pattern was followed with a rapidly growing line of cells of non-tumoural origin, i.e. SV-40 immortalized Mouse Embryo Fibroblasts (MEF; Figure 6B), while none of the compounds tested had a significant effect, either at 1 or 5 μM, on a

distinct, slower-growing MEF line (Figure 6C and not shown). Alternative protocols, in which the various compounds were provided only once at the beginning of the three-day period, or were added every day (thus reaching formal final concentrations of 3 or 15 μM) gave results in line with those of the substitution protocol (not reported).

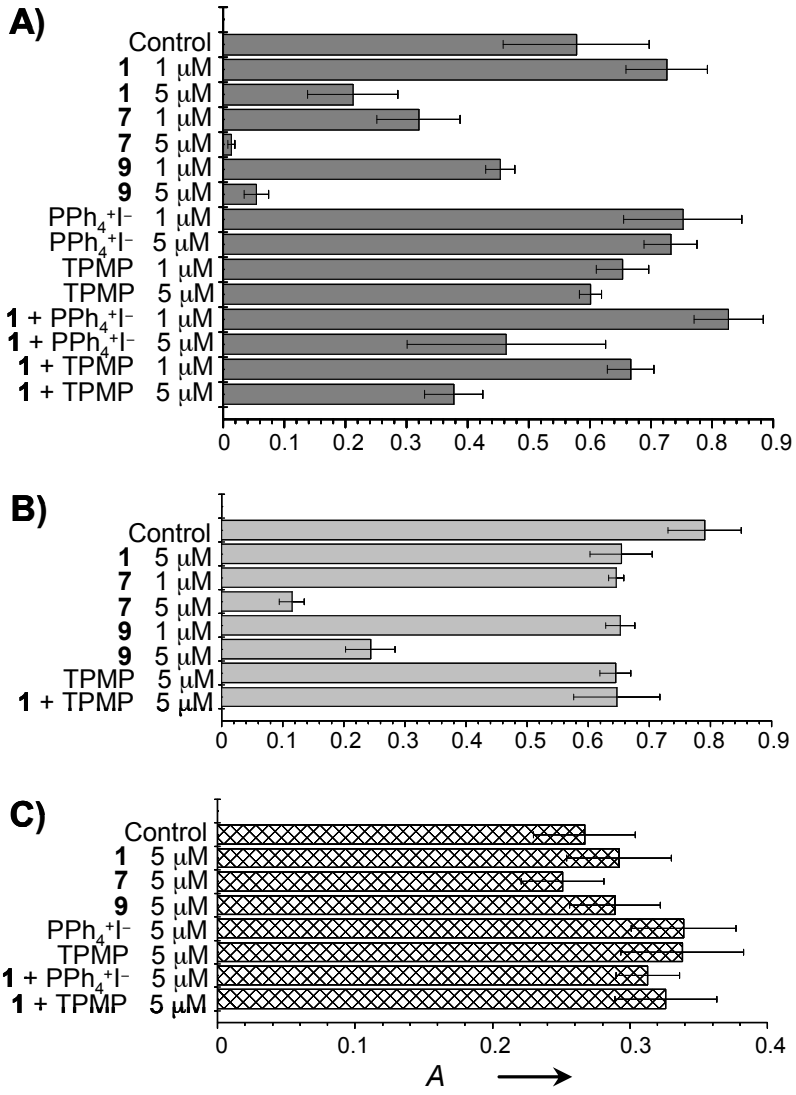

Figure 6. Effect of the mitochondriotropic quercetin derivatives and control compounds on the readout of tetrazolium reduction cell proliferation assays. Cells were allowed to grow for 3 days in the presence of the specified compounds (see the Experimental section for details). The panels show the results of individual experiments representative of four (A,C) or three (B) similar ones. All measurements were performed in quadruplicate. Averages ± s.d. are given. A) C-26 mouse colon tumour cells. B) Fast-growing Mouse Embryonic Fibroblasts (MEF). C) Slow-growing MEF (note different scale).

Discussion

We have synthesized the target compound 7 as well as its non-acylated analogue 9 from the natural polyphenol quercetin (1). Both carry a TPP group at the end of a 4-carbon saturated linker connected through an ethereal bond at C-3 of the quercetin skeleton. Both

7 and 9 exhibit the expected mitochondriotropic behaviour. Since a cytoplasm-negative voltage difference also exists across the plasma membrane, the charged compounds are also more concentrated in the cytoplasm than in the surrounding medium. This is best appreciated in fluorescence images taken after protonophore-induced release from the mitochondria, e.g. in Figure 4E-F.

As an initial verification of whether the modifications introduced have altered the pharmacological properties of the quercetin ring system, we have compared their activity as mitochondrial F_0F_1 ATPase inhibitors to that of quercetin. The latter is known to inhibit the enzyme,[51] presumably as a consequence of its binding to a site in the F_1 portion, which has been characterized by X-ray crystallography of the enzyme/polyphenol complex.[52] In our assays the mitochondrial membranes had been permeabilised with alamethicin (see Experimental section). Therefore no transmembrane electrical potential could be maintained, no accumulation of mitochondriotropic compounds could occur, and inhibition was expected to take place with similar dose-dependence unless the substituent(s) interfered. No major such interference was revealed (Figure 5). **7** and **9** behave similarly suggesting that interactions with the aromatic core of the molecule are most relevant for binding and inhibition. ATP synthase inhibition is thus expected to take place upon accumulation of mitochondriotropic polyphenols in mitochondria, and it might well contribute to their overall effects on cells and organisms.

7 and **9** behave as cytostatic/cytotoxic agents against fast- but not against slow-growing cells in culture (Figure 6). This mode of action is characteristic of many chemotherapeutic agents. Inhibition of ATP synthesis might obviously be a component of this cytotoxic action. Another tentative mechanism may envision a fraction of the positively charged derivatives associating with DNA due to charge interactions. Quercetin itself is known to form covalent bonds to DNA.[53,54] This might result in a cytotoxic or cytostatic effect which may be more relevant in the case of fast-dividing cells, such as cancerous ones. It should at any rate be emphasized that the parent compound, quercetin, and phosphonium cations (TPP and TPMP), alone or in combination, have much weaker toxic effects. Clearly the activity of quercetin-TPP conjugates in this case is not simply the sum of the activities of quercetin and TPP.

These and related new compounds will be available for specific tests of their properties *in vivo*. Their production opens interesting perspectives since, in principle, they may either quench or promote radical oxidative processes. Thus, a class of natural compounds with

useful properties can now be targeted to subcellular compartments where they ought to realize their biomedical potential in full.

Experimental section

Materials and instrumentation: Starting materials and reagents were purchased from Aldrich, Fluka, Merck-Novabiochem, Riedel de Haen, J.T. Baker, Cambridge Isotope Laboratories Inc., Acros Organics, Carlo Erba and Prolabo, and were used as received. ^{1}H and ^{13}C NMR spectra were recorded with a Bruker AC 250F spectrometer operating at 250 MHz for ^{1}H NMR and 62.9 MHz for ^{13}C NMR. Chemical shifts (δ) are given in ppm relative to the signal of the solvent. LC/MS analyses and mass spectra were performed with a 1100 Series Agilent Technologies system, equipped with binary pump (G1312A) and MSD SL Trap mass spectrometer (G2445D SL) with ion trap detector and ESI source. Accurate mass measurements were obtained using a Mariner ESI-TOF mass spectrometer (PerSeptive Biosystems). TLCs were run on silica gel supported on plastic (Macherey-Nagel Polygram®SIL G/UV_{254}, silica thickness 0.2 mm), or on silica gel supported on glass (Fluka) (silica thickness 0.25 mm, granulometry 60Å, medium porosity) and visualized by UV detection. Flash chromatography was performed on silica gel (Macherey-Nagel 60, 230-400 mesh granulometry (0.063-0.040 mm)) under air pressure. The solvents were analytical or synthetic grade and were used without further purification. HPLC-UV analyses for assessing the purity of the compounds synthesized were performed by a Thermo Separation Products Inc. system with a P2000 Spectra System pump and a UV6000LP diode array detector (190-500 nm). UV-Vis spectra were recorded at 25 °C with a Perkin-Elmer Lambda 5 spectrophotometer (PerkinElmer) equipped with water-thermostated cell holders. Fluorescence spectra were recorded at 25 °C with a Perkin–Elmer LS-55 spectrofluorimeter equipped with a Hamamatsu R928 photomultiplier and thermostated cell holder. Quartz cells with an optical pathlength of 1 cm were used for measurements of both absorption and fluorescence spectra.

Synthetic procedures.

Synthesis of 3',4'-*O*-diphenylmethane quercetin (2): The protection of quercetin catechol ring was carried out by a slight modification of the procedure by Bouktaib et al.[46] Briefly, compound **1** (3.0 g, 8.9 mmol, 1 eq.) and dichlorodiphenylmethane (5.1 mL, 27 mmol, 3 eq.) were mixed and heated at 180°C for 10 min. The residue was diluted in minimal CH_2Cl_2, sonicated and purified by flash chromatography using CH_2Cl_2:EtOAc 95:5 as eluent to afford **2** in 67% yield. ^{1}H-NMR (250 MHz, DMSO-d_6) d (ppm): 6.22 (d,

1H, J=2.0 Hz, aromatic-H), 6.49 (d, 1H, J=2.0 Hz, aromatic-H), 7.20 (d, 1H, H-5', J=8.0 Hz), 7.39-7.60 (m, 10H, aromatic-H), 7.78-7.86 (m, 2H, H-2', H-6'), 9.68 (s br, 1H, OH), 10.87 (s br, 1H, OH), 12.41 (s, 5-OH); ESI-MS (ion trap): m/z 466, $[M+H]^+$.

Synthesis of 3',4'-*O*-diphenylmethan-3-*O*-(4-chlorobutyl) quercetin (3): K_2CO_3 (0.75 g, 5.4 mmol, 1.3 eq.) and 1-bromo-4-chlorobutane (0.86 g, 5.0 mmol, 1.2 eq.) were added under argon to a solution of **2** (1.94 g, 4.16 mmol) in DMF (10 mL). After stirring overnight, the mixture was diluted in CH_2Cl_2 (30 mL) and washed with distilled water (3 × 50 mL). The organic layer was dried over $MgSO_4$ and filtered. The solvent was evaporated under reduced pressure and the residue was purified by flash chromatography using EtOAc:petroleum ether 3:7 as eluent to afford **3** in 45% yield. ^{1}H-NMR (250 MHz, $CDCl_3$) d (ppm): 1.84 (m, 4H, CH_2), 3.46 (t, 2H, CH_2), 3.94 (t, 2H, CH_2), 6.32 (d, 1H, J=2.0 Hz, aromatic-H), 6.42 (d, 1H, J=2.0 Hz, aromatic-H), 6.98 (d, 1H, H-5', J=8.25 Hz), 7.34-7.44 (m, 5H, aromatic-H), 7.55-7.69 (m, 7H, aromatic-H), 12.60 (s, 5-OH); ^{13}C-NMR (62.9 MHz, DMSO-d_6) d (ppm): 27.0 (CH_2), 28.9 (CH_2), 45.2 (CH_2Cl), 71.5 (OCH_2), 94.1, 98.9, 104.5, 108.8, 109.1, 117.5, 124.2, 124.3, 126.0, 128.8, 129.8, 137.4, 139.4, 146.8, 148.7, 155.4, 156.6, 161.4, 164.5, 178.2 (C-4); ESI-MS (ion trap): m/z 557, $[M+H]^+$; HRMS (ESI-TOF): m/z 557.1329; calcd for $C_{32}H_{25}O_7Cl{\cdot}H^+$ 557.1362.

Synthesis of 3-*O*-(4-chlorobutyl) quercetin (4): The cathecol ring protection was removed according to the procedure employed by Bouktaib et al. for analogous quercetin derivatives.[46] Briefly: compound **3** (1.0 g, 1.80 mmol) was dissolved into a mixture of acetic acid/water 8:2 (50 mL) and the solution was heated at reflux for 2 h. Then H_2O (100 mL) and of EtOAc (50 mL) were added and the organic layer collected, washed with 100 mL of a $NaHCO_3$-saturated aqueous solution and dried over $MgSO_4$. After filtration the solvent was evaporated under reduced pressure and the residue was purified by flash chromatography using $CHCl_3$:acetone 4:1 as solvent to afford **4** in 80% yield. ^{1}H-NMR (250 MHz, DMSO-d_6) d (ppm): 1.82 (m, 4H, CH_2), 3.66 (t, 2H, CH_2), 3.94 (t, 2H, CH_2), 6.19 (d, 1H, H-6, J=1.75 Hz), 6.40 (d, 1H, H-8, J=1.75 Hz), 6.89 (d, 1H, H-5', J=8.25 Hz), 7.44 (dd, 1H, H-6', J=8.25, 2.0 Hz), 7.51 (d, 1H, H-2', J=2.0 Hz), 12.72 (s, 5-OH); ^{13}C-NMR (62.9 MHz, DMSO-d_6) d (ppm): 27.0 (CH_2), 28.9 (CH_2), 45.3 (CH_2Cl), 71.3 (OCH_2), 93.8, 98.7, 104.4, 115.7, 115.8, 120.9, 121.1, 136.8, 145.4, 148.8, 156.2, 156.6, 161.5, 164.3, 178.2 (C-4); ESI-MS (ion trap): m/z 393, $[M+H]^+$; HRMS (ESI-TOF): m/z 393.0736; calcd for $C_{19}H_{17}O_7Cl{\cdot}H^+$ 393.0736.

Synthesis of 3',4',5,7-tetraacetyl-3-*O*-(4-chlorobutyl) quercetin (5): Acetyl chloride (1.1 mL, 15 mmol, 20 eq.) was added dropwise and under continuous stirring to a mixture of **4**

(300 mg, 0.76 mmol, 1 eq.) and anhydrous pyridine (0.85 mL, 7.6 mmol, 10 eq.) cooled in a bath of dry ice/acetone (-78°C). A white precipitate (pyridinium chloride) formed immediately. The reaction mixture was subsequently allowed to warm to room temperature and stirred overnight. Then CH_2Cl_2 (50 mL) was added and the organic layer was washed with HCl 0.5 N (3 × 50 mL) and water (2 × 30 mL). The organic solution was dried over $MgSO_4$ and filtered. The solvent was evaporated under reduced pressure and the residue was purified by flash chromatography using CH_2Cl_2:petroleum ether:EtOAc 6:3:1 as solvent to afford the acetylated product **5** in 78% yield. ^{1}H-NMR (250 MHz, $CDCl_3$) d (ppm): 1.85 (m, 4H, CH_2), 2.33 (m, 9H, OAc), 2.45 (s, 3H, OAc), 3.56 (t, 2H, CH_2), 3.99 (t, 2H, CH_2), 6.82 (d, 1H, aromatic-H, J=2.25 Hz), 7.30 (d, 1H, aromatic-H, J=2.25 Hz), 7.35 (d, 1H, H-5', J=8.5 Hz), 7.92 (d, 1H, H-2', J=2.0 Hz), 7.96 (dd, 1H, H-6', J=8.5, 2.0 Hz); ^{13}C-NMR (62.9 MHz, DMSO-d_6) d (ppm): 20.5 (CH_3), 20.6 (CH_3), 21.1 (CH_3), 26.9 (CH_2), 28.8 (CH_2), 45.3 (CH_2Cl), 71.5 (OCH_2), 110.0, 114.2, 114.9, 124.0, 124.3, 127.1, 128.6, 140.4, 142.2, 144.1, 149.6, 153.1, 154.1, 156.3, 168.3 (C=O), 168.4 (C=O), 168.6 (C=O), 169.1 (C=O), 172.5 (C-4); ESI-MS (ion trap): m/z 561, $[M+H]^+$; HRMS (ESI-TOF): m/z 561.1120; calcd for $C_{27}H_{25}O_{11}Cl{\cdot}H^+$ 561.1158.

Synthesis of 3',4',5,7-tetraacetyl-3-*O*-(4-iodobutyl) quercetin (6): compound **5** (100 mg, 0.18 mmol, 1 eq.) was added to a saturated solution of NaI in anhydrous acetone (10 mL) and heated at reflux for 20 h. After cooling, the resulting mixture was diluted in $CHCl_3$ (30 mL), filtered and washed with water (3 × 30 mL). The organic layer was dried over $MgSO_4$ and filtered. The solvent was evaporated under reduced pressure to afford **6** in 86% yield. ^{1}H-NMR (250 MHz, $CDCl_3$) d (ppm): 1.74-2.00 (m, 4H, CH_2), 2.35 (m, 9H, OAc), 2.47 (m, 3H, OAc), 3.22 (m, 2H, CH_2), 3.99 (m, 2H, CH_2), 6.83 (m, 1H, aromatic-H), 7.32 (m, 2H, aromatic-H), 7.95 (m, 2H, H-2', H-6'); ^{13}C-NMR (62.9 MHz, DMSO-d_6) d (ppm): 8.6 (CH_2I), 20.6 (CH_3), 21.1 (CH_3), 29.7 (CH_2), 30.4 (CH_2), 71.1 (OCH_2), 110.0, 114.2, 114.9, 124.0, 124.3, 127.1, 128.6, 140.4, 142.2, 144.1, 149.6, 153.1, 154.1, 156.3, 168.3 (C=O), 168.4 (C=O), 168.6 (C=O), 169.0 (C=O), 172.5 (C-4); ESI-MS (ion trap): m/z 653, $[M+H]^+$; HRMS (ESI-TOF): m/z 653.0521; calcd for $C_{27}H_{25}O_{11}I{\cdot}H^+$ 653.0514.

Synthesis of 3',4',5,7-tetraacetyl-3-*O*-(4-triphenylphosphoniumbutyl) quercetin iodide (7): A mixture of **6** (100 mg, 0.15 mmol) and triphenylphosphine (200 mg, 0.76 mmol, 5 eq.) in toluene (10 mL) was heated at 95°C under argon. After 6 h, the solvent was eliminated under reduced pressure and the resulting white solid was dissolved in the minimum volume of dichloromethane (1 mL) and precipitated with diethyl ether (50 mL). The solvent was decanted and the precipitation was repeated 5 times. Residual solvent was

then removed under reduced pressure to afford compound **7** in 72% yield and 96-98% purity. The small amount of impurities consisted of a triacetyl derivative and of an isomer of **7**. ^{1}H-NMR (250 MHz, DMSO-d_6) d (ppm): 1.62-1.96 (m, 4H, CH_2), 2.17 (s, 3H, OAc), 3.32 (m, 9H, OAc), 3.68 (t, 2H, CH_2), 4.00 (t, 2H, CH_2), 7.10 (d, 1H, aromatic-H, J=2.25 Hz), 7.34 (d, 1H, H-5', J=9.25 Hz), 7.62 (d, 1H, aromatic-H, J=2.25 Hz), 7.72-8.04 (m, 1 7H, aromatic-H); ^{13}C-NMR (62.9 MHz, DMSO-d_6) d (ppm): 18.3 (CH_2), 19.6 (CH_2), 20.5 (CH_3), 20.6 (CH_3), 20.9 (CH_3), 21.1 (CH_3), 29.5 (CH_2), 70.3 (OCH_2), 110.1, 114.3, 114.8, 118.6 (Ph, J(^{13}C/^{31}P)=85.9 Hz), 123.8, 124.1, 127.1, 128.5, 130.5 (Ph, J(^{13}C/^{31}P)=12.4 Hz), 133.7 (Ph, J(^{13}C/^{31}P)=10.1 Hz), 135.1 (Ph, J(^{13}C/^{31}P)=2.8 Hz), 140.2, 142.2, 144.1, 149.5, 153.1, 154.1, 156.2, 168.2 (C=O), 168.4 (C=O), 168.6 (C=O), 168.9 (C=O), 172.7 (C-4); ESI-MS (ion trap): m/z 787, M^+; HRMS (ESI-TOF): m/z 787.2346; calcd for $C_{45}H_{40}O_{11}P^+$ 787.2303.

Synthesis of 3-*O*-(4-iodobutyl) quercetin (8): Compound **4** (100 mg, 0.25 mmol, 1 eq.) was added to a saturated solution of NaI in dry acetone (10 mL) and heated at reflux for 20 h. After cooling, the resulting mixture was diluted in $CHCl_3$ (30 mL), filtered and washed with water (3 × 30 mL). The organic layer was dried over $MgSO_4$ and filtered. The solvent was evaporated under reduced pressure to afford the product in 87% yield. ^{1}H-NMR (250 MHz, DMSO-d_6) d (ppm): 1.72 (quintet, 2H, CH_2), 1.88 (quintet, 2H, CH_2), 3.29 (t, 2H, CH_2), 3.92 (t, 2H, CH_2), 6.18 (d, 1H, aromatic-H, J=1.95 Hz), 6.39 (d, 1H, aromatic-H, J=1.95 Hz), 6.88 (d, 1H, H-5', J=8.3 Hz), 7.43 (dd, 1H, H-6', J=8.3, 1.95 Hz), 7.51 (d, 1H, H-2', J=2.0 Hz); ^{13}C-NMR (62.9 MHz, DMSO-d_6) d (ppm): 8.7 (CH_2I), 29.8 (CH_2), 30.5 (CH_2), 70.9 (OCH_2), 93.8, 98.7, 104.4, 115.6, 115.8, 120.9, 121.0, 136.8, 145.4, 148.8, 156.2, 156.6, 161.5, 164.3, 178.2 (C-4); ESI-MS (ion trap): m/z 485, $[M+H]^+$; HRMS (ESI-TOF): m/z 485.0060; calcd for $C_{19}H_{17}O_7I{\cdot}H^+$ 485.0092.

Synthesis of 3-*O*-(4-triphenylphosphoniumbutyl) quercetin iodide (9): A mixture of **8** (100 mg, 0.21 mmol) and triphenylphosphine (275 mg, 1.05 mmol, 5 eq.) in toluene (15 mL) was heated at 95°C under argon. After 6 h, the solvent was eliminated at reduced pressure and the resulting yellow solid was dissolved in the minimum volume of dichloromethane (1 mL) and precipitated with diethyl ether (5 × 50 mL). The solvents were decanted after each precipitation. Residual solvent was then removed under reduced pressure to afford compound **9** in 73% yield. ^{1}H-NMR (250 MHz, DMSO-d_6) d (ppm): 1.65 (quintet, 2H, CH_2), 1.84 (quintet, 2H, CH_2), 3.63 (t, 2H, CH_2), 3.96 (t, 2H, CH_2), 6.18 (d, 1H, aromatic-H, J=2.0 Hz), 6.39 (d, 1H, aromatic-H, J=2.0 Hz), 6.74 (d, 1H, H-5', J=8.4 Hz), 7.33 (dd, 1H, H-6', J=8.4, 2.0 Hz), 7.44 (d, 1H, H-2', J=2.0 Hz), 7.50-7.93 (m,

15H, aromatic-H); ^{13}C-NMR (62.9 MHz, DMSO-d_6) d (ppm): 18.6 (CH_2), 19.6 (CH_2), 29.7 (CH_2), 70.4 (OCH_2), 93.8, 98.8, 104.3, 115.5, 115.7, 118.6 (Ph, J(^{13}C/^{31}P)=85.8 Hz), 120.9, 121.0, 130.4 (Ph, J(^{13}C/^{31}P)=12.4 Hz), 133.7 (Ph, J(^{13}C/^{31}P)=10.1 Hz), 135.1 (Ph, J(^{13}C/^{31}P)=2.8 Hz), 136.6, 145.4, 148.8, 156.1, 156.5, 161.4, 164.4, 178.1 (C-4); ESI-MS (ion trap): m/z 619, M^+; HRMS (ESI-TOF): m/z 619.1893; calcd for $C_{37}H_{32}O_7P^+$ 619.1882.

Solubility in water: Seven standard solutions of **7** of concentration within the range 2-6×10^{-5} M were prepared by diluting with water a 10^{-3} M mother solution in H_2O:CH_3CN 9:1. The absorbance of each solution was measured at 300 nm, which corresponds to a plateau region in the UV absorption spectrum of **7**, and plotted against concentration. Linear regression analysis of the data points yielded a slope of (1.244 ± 0.009)·10^4. This curve (Figure S6 of Supporting Information) was used to interpolate the concentration of an aqueous saturated solution of **7** prepared by vigorously stirring **7** (2 mg) in water (1 mL). After sedimentation, the clear supernatant (200 μL) was added to water (3 mL) and the absorbance of the resulting solution measured at 300 nm. Three repetitions of this experiment yielded an average value of A = 0.379 ± 0.011, from which a concentration of (3.23 ± 0.06)·10^{-5} M was interpolated using the calibration curve. Correcting for the dilution factor, a solubility of (4.96 ± 0.21)·10^{-4} mol/L is obtained.

Chemical stability studies: The chemical stability of compounds **7** and **9** in water and in HBSS buffer at 25°C was tested following changes in the UV-Vis spectra between 190 and 500 nm and by HPLC analysis of samples withdrawn at different reaction times. The reaction was initiated by adding a freshly prepared CH_3CN solution of the compound of interest (100 μL) to a HBSS:CH_3CN 9:1 mixture (3 mL) to give a final concentration in the μM range. The composition of HBSS was (in mM units): NaCl 136.9, KCl 5.36, $CaCl_2$ 1.26, $MgSO_4$ 0.81, KH_2PO_4 0.44, Na_2HPO_4 0.34, Glucose 5.55, pH 7.4 (with NaOH). Spectral changes were followed with a Perkin-Elmer Lambda 5 spectrophotometer (PerkinElmer) equipped with water-thermostated cell holders. Quartz cells with an optical path of 1 cm were used for all measurements. HPLC analyses were performed with the Thermo Separation Products Inc. system using a reversed phase column (Gemini C18, 3 μm, 150 x 4.6 mm i.d.; Phenomenex). Solvents A and B were H_2O containing 0.1% HCOOH and CH_3CN, respectively. The gradient for B was as follows: 10% for 5 min, then from 10% to 100% in 20 min; the flow rate was 0.7 mL/min. The eluate was preferentially monitored at 300 nm.

Mitochondria: Rat liver mitochondria were isolated by conventional differential centrifugation procedures[55] from fasted male albino Wistar rats weighing approximately 300 grams, raised in the local stabulary. The standard isolation medium was 250 mM sucrose, 5 mM HEPES (pH 7.4) and 1 mM EGTA; EGTA was omitted in the final resuspension step. Protein content was measured by the biuret method with bovine serum albumin as standard.[56]

TPP-selective electrode: The setup used to monitor the concentration of TPP-bearing compounds in solution was built in-house following published procedures.[57,58] A calomel electrode was used as reference and the potentiometric output was directed to a strip chart recorder. The experiments illustrated by Figure 3 and S1 were conducted in a water-jacketed cell at 20°C. The suspension medium contained 200 mM sucrose, 10 mM HEPES, 5 mM succinate, 1 mM phosphate, 1.25 mM rotenone, pH 7.4 (with KOH).

Cells: Human Colon Tumor (HCT116) cells,[59] kindly provided by B. Vogelstein, as well as fast- and slow-growing SV-40 immortalized Mouse Embryo Fibroblast (MEF) cells (kindly provided by L. Scorrano and W.J. Craigen, respectively) and murine colon cancer C-26 cells were grown in Dulbecco's Modified Eagle Medium (DMEM) plus 10 mM HEPES buffer, 10% (v/v) fetal calf serum (Invitrogen), 100 U/mL penicillin G (Sigma), 0.1 mg/mL streptomycin (Sigma), 2 mM glutamine (GIBCO) and 1% nonessential amino acids (100X solution; GIBCO), in a humidified atmosphere of 5% CO_2 at 37 °C.

Metabolism studies: HCT116 cells were seeded onto a 12-well plate, and allowed to grow to about 80% of confluence. They were then washed with warm HBSS, and incubated for the specified periods with 1 mL/well of 20 mM solutions of **7**, **9** or quercetin. The compounds were used as aliquots from 20 mM freshly made stock solutions in DMSO, which were diluted into HBSS just prior to adding the resulting solution to the washed cells. Medium and cells were collected together after 1, 3, 6 and 8 hours of incubation. Acetic acid (100 mL, 0.6 M) and fresh ascorbic acid (100 mL, 10 mM) solutions were added, and the samples were immediately stored at –20°C until treatment and analysis. Treatment consisted in addition of acetone (1 mL), followed by sonication (2 min), filtration through 0.45 mm PTFE syringe filters (Chemtek Analytica) and concentration under N_2. HPLC analyses were performed with the Agilent Technologies system using a diode array detector operating from 190 to 500 nm (G1315B) and the ion trap mass spectrometer with ESI source. Mass spectra were acquired in positive ion mode operating in full-scan from 100 to 1500 m/z. The HPLC protocol was the same as that employed for the chemical stabilities studies.

Fluorescence microscopy: HCT116 cells were sown onto 24 mm round coverslips and allowed to grow for 48 hours. The coverslips were then washed with HBSS, mounted into supports, covered with HBSS (1 mL) and placed onto the microscope stage. The imaging apparatus consisted of an Olympus IX71 microscope equipped with an MT20 light source and Cell$^{R©}$ software. Excitation wavelength was 380 nm and fluorescence was collected in the 500-550 nm range in the images shown in Figure 4. Sequential images were automatically recorded following a preordained protocol. The acquisition and display parameters of all fluorescence images shown were the same, i.e., fluorescence intensities can be compared.

ATP hydrolysis assays: The enzymatically coupled NADH oxidation assay was used.[60] Mitochondria (0.25 mg prot.·mL^{-1}) were incubated for about 1 min. in 250 mM sucrose, 10 mM TrisCl, 20 μM EGTA-Tris, 1 mM NaH_2PO_4, 6 mM $MgCl_2$, 2 μM rotenone, pH 7.6, plus 1 mM phosphoenolpyruvate (PEP), 0.1 mM NADH, 20 μM alamethicin, 20 units of pyruvate kinase (PK), 50 units of lactate dehydrogenase (LDH) (all from Sigma) and the desired compound in a thermostated (25°C), magnetically stirred cuvette in an Aminco DW-2000 UV-Vis spectrophotometer operating in the dual wavelength mode. Membrane-permeabilising alamethicin was used in order to measure ATPase activity without potential kinetic complications associated with transmembrane transport of the adenine nucleotides.[61] Differential absorbance at 340-372 nm was sampled every 0.6 sec. The reaction was started by the addition of 0.5 mM ATP. In this assay the ADP formed by ATP hydrolysis is re-phosphorylated by PK, generating pyruvate as the other product. Pyruvate is reduced to lactate by LDH, using NADH which is oxidised to NAD with a decrease in absorbance which is the parameter monitored. Rates of hydrolysis were determined as the best linear fit of the data.

Cell growth/viability (MTT) assays: C-26 or MEF cells were seeded in standard 96-well plates and allowed to grow in DMEM (200 μL) for 24 hours to insure attachment. In the experiments of Figure 6 initial densities were 1000 (C-26, fast MEF) or 2000 (slow MEF) cells/well. The growth medium was then replaced with medium containing the desired compound from a mother solution in DMSO. DMSO final concentration was 0.1% in all cases (including controls). Four wells were used for each of the compounds to be tested. The solution was substituted by a fresh aliquot twice, at 24-hour intervals. At the end of the third 24-hour period of incubation with the drugs the medium was removed and substituted, after a wash with PBS, with 100 μL of CellTiter 96® solution (Promega; for

details: www.promega.com/tbs). After a one-hour colour development period at 37°C absorbance at 490 nm was measured using a Packard Spectra Count 96-well plate reader.

Bibliography

[1] S. Shankar, G. Singh, R.K. Srivastava, Front. Biosci. **2007**, 12, 4839-4854.
[2] J.A. Joseph, B. Shukitt-Hale, F.C. Lau, Ann. N. Y. Acad. Sci. **2007**, 1100, 470-485.
[3] S. Shankar, S. Ganapathy, R.K. Srivastava, Front. Biosci. **2007**, 12, 4881-4899.
[4] N. Labinskyy, A. Csiszar, G. Veress, G. Stef, P. Pacher, G. Oroszi, J. Wu, Ungvari, Z. Curr. Med. Chem. **2006**, 13, 989-996.
[5] N.H. Nam, Mini Rev. Med. Chem. **2006**, 6, 945-951.
[6] J.A. Baur, D.A. Sinclair, Nat. Rev. Drug Discov. **2006**, 5, 493-506.
[7] D.R. Valenzano, E. Terzibasi, T. Genade, A. Cattaneo, L. Domenici, A. Cellerino, Curr. Biol. **2006**, 16, 296-300.
[8] S. Quideau, ChemBioChem. **2004**, 5, 427-430.
[9] W. Bors, C. Michel, Ann. N.Y. Acad. Sci. **2002**, 957, 57-69.
[10] H.E. Seifried, D.E. Anderson, E.I. Fisher, J.A. Milner, J. Nutr. Biochem. **2007**, 18, 567-579.
[11] O. Weinreb, S. Mandel, T. Amit, M.B. Youdim, J. Nutr. Biochem. **2004**, 15, 506-516.
[12] S. Mandel, T. Amit, L. Reznichenko, O. Weinreb, M.B. Youdim, Mol. Nutr. Food Res. **2006**, 50, 229-234.
[13] H.U. Simon, A. Haj-Yehia, F. Levi-Schaffer, Apoptosis **2000**, 5, 415-418.
[14] J. Neuzil, C. Widén, N. Gellert, E. Swettenham, R. Zobalova, L.F. Dong, X.F. Wang, C. Lidebjer, H. Dalen, J.P. Headrick, P.K. Witting, Redox Rep. **2007**, 12, 148-162.
[15] S. Orrenius, Drug Metab. Rev. **2007**, 39, 443-455.
[16] M. Zoratti, I. Szabò, Biochim. Biophys. Acta **1995**, 1241, 139-176.
[17] A. Rasola, P. Bernardi, Apoptosis **2007**, 12, 815-833.
[18] A.P. Halestrap, S.J. Clarke, S.A. Javadov, Cardiovasc. Res. **2004**, 61, 372-385.
[19] F. Di Lisa, P. Bernardi, Cardiovasc. Res. **2006**, 70, 191-199.
[20] K.C. Kregel, H.J. Zhang, Am. J. Physiol. Regul. Integr. Comp. Physiol. **2007**, 292, R18-R36.
[21] D.C. Wallace, Annu. Rev. Genet. **2005**, 39, 359-407.
[22] V.R. Fantin, P. Leder, Oncogene **2006**, 25, 4787-4797.
[23] L. Galluzzi, N. Larochette, N. Zamzami, G. Kroemer, Oncogene **2006**, 25, 4812-4830.
[24] S.S. Sheu, D. Nauduri, M.W. Anders, Biochim. Biophys. Acta **2006**, 1762, 256-265.
[25] M.P. Murphy, R.A.J. Smith, Annu. Rev. Pharmacol. Toxicol. **2007**, 47, 629-656.
[26] H.M. Cochemè, G.F. Kelso, A.M. James, M.F. Ross, J. Trnka, T. Mahendiran, J. Asin-Cayuela, F.H. Blaikie, A.-R.B. Manas, C.M. Porteous, V.J. Adlam, R.A.J. Smith, M.P. Murphy, Mitochondrion **2007**, 7, S94-S102.
[27] C.P. Baines, R.A. Kaiser, N.H. Purcell, N.S. Blair, H. Osinska, M.A. Hambleton, E.W. Brunskill, M.R. Sayen, R.A. Gottlieb, G.W. Dorn, J. Robbins, J.D. Molkentin, Nature **2005**, 434, 658-662.
[28] V.J. Adlam, J.C. Harrison, C.M. Porteous, A.M. James, R.A. Smith, M.P. Murphy, I.A. Sammut, FASEB J. **2005**, 19, 1088-1095.
[29] Q. Wang, J. Xu, G.E. Rottinghaus, A. Simonyi, D. Lubahn, G.Y. Sun, A.Y. Sun, Brain Res. **2002**, 958, 439-447.
[30] M. Shen, G.L. Jia, Y.M. Wang, H. Ma, Vascul. Pharmacol. **2006**, 45, 122-126.

[31] G. Galati, T. Chan, B. Wu, P.J. O'Brien, Chem. Res. Toxicol. **1999**, 12, 521-525.
[32] E.J. Choi, K.M. Chee, B.H. Lee, Eur. J. Pharmacol. **2003**, 482, 281-285.
[33] M. Kanadzu, Y. Lu, K. Morimoto, Cancer Lett. **2006**, 241, 250-255.
[34] H. Raza, A. John, Toxicol. Appl. Pharmacol. **2005**, 207, 212-220.
[35] H. Pelicano, D. Carney, P. Huang, Drug Resist. Update **2004**, 7, 97-110.
[36] J. Neuzil, X.-F. Wang, L.-F. Dong, P. Low, S.J. Ralph, FEBS Lett. **2006**, 580, 5125 –5129.
[37] J.S. Armstrong, Br. J. Pharmacol. **2006**, 147, 239-248.
[38] L.B. Chen, Annu. Rev. Cell Biol. **1988**, 4, 155-181.
[39] B. Kadenbach, Biochim. Biophys. Acta. **2003**,1604, 77-94.
[40] V.R. Fantin, P. Leder, Cancer Res. **2004**, 64, 329-336.
[41] V.R. Fantin, M.J. Berardi, L. Scorrano, S.J. Korsmeyer, P. Leder, Cancer Cell **2002**, 2, 29-42.
[42] K. Ishikawa, K. Takenaga, M. Akimoto, N. Koshikawa, A. Yamaguchi, H. Imanishi, K. Nakada, Y. Honma, J. Hayashi, Science **2008**, 320, 661-664.
[43] S. Günther, C. Ruhe, M.G. Derikito, G. Böse, H. Sauer, M. Wartenberg, Cancer Lett. **2007**, 250, 25-35.
[44] H.M. Rawel, K. Meidtner, J. Kroll, J Agric Food Chem. **2005**, 53, 4228-4235.
[45] M.I. Kaldas, U.K. Walle, H. van der Woude, J.M. McMillan, T. Walle, J. Agric. Food Chem. **2005**, 53, 4194-4197.
[46] M. Bouktaib, S. Lebrun, A. Atmani, C. Rolando, Tetrahedron **2002**, 58, 10001-10009.
[47] P.O. de Beck, M.G. Dijoux, G. Cartier, A.M. Mariotte, Phytochemistry **1998**, 47, 1171-1173.
[48] I.M. Rietjens, H.M. Awad, M.G. Boersma, M.L. van Iersel, J. Vervoort, P.J. Van Bladeren, Adv. Exp. Med. Biol. **2001**, 500, 11-21.
[49] L. Biasutto, E. Marotta, U. De Marchi, M. Zoratti, C. Paradisi, J. Med. Chem. **2007**, 50, 241-253.
[50] M.P. Murphy, K.S. Echtay, F.H. Blaikie, J. Asin-Cayuela, H.M. Cochemè, K. Green, J.A. Buckingham, E.R. Taylor, F. Hurrell, G. Hughes, S. Miwa, C.E. Cooper, D.A. Svistunenko, R.A. Smith, M.D. Brand, J. Biol. Chem. **2003**, 278, 48534-48545.
[51] J. Zheng, V.D. Ramirez, Brit. J. Pharmacol. **2000**, 130, 1115-1123.
[52] J.R. Gledhill, M.G. Montgomery, A.G. Leslie, J.E. Walker, Proc. Natl. Acad. Sci. U S A. **2007**, 104, 13632-13637.
[53] T. Walle, T.S. Vincent, U.K. Walle, Biochem. Pharmacol. **2003**, 65, 1603-1610.
[54] H. van der Woude, G.M. Alink, B.E. van Rossum, K.Walle, H. van Steeg, T. Walle, I.M. Rietjens, Chem. Res. Toxicol. **2005**, 18, 1907-1916.
[55] W.C. Schneider, H.G. Hogeboon, J. Biol. Chem. **1953**, 204**,** 233–238.
[56] A.G. Gornall, C.J. Bardawill, M.M. David, J. Biol. Chem. **1949**, 177**,** 751–766.
[57] N. Kamo, M. Muratsugu, R. Hongoh, Y. Kobatake, J. Membr. Biol. **1979**, 49, 105-121.
[58] M. Zoratti, M. Favaron, D. Pietrobon, V. Petronilli, Biochim. Biophys. Acta **1984**, 767, 231-239.
[59] L. Zhang, J. Yu, B.H. Park, K.W. Kinzler, B. Vogelstein, Science **2000**, 290, 989-992.
[60] S. Luvisetto, D. Pietrobon, G.F. Azione, Biochemistry. **1987**, 26, 7332-7338.
[61] See for example: I.S. Gostimskaya, V.G. Grivennikova, T.V. Zharova, L.E. Bakeeva, A.D.Vinogradov, Anal Biochem. **2003**, 313, 46-52.

Chapter 2

Development of mitochondria-targeted derivatives of resveratrol[2]

Summary

To target natural polyphenols to the subcellular site where their redox properties might be exploited at best, i.e., mitochondria, we have synthesized new proof-of-principle derivatives by linking resveratrol (3,4',5-trihydroxy-*trans*-stilbene) to the membrane-permeable lipophilic triphenylphosphonium cation. The new compounds, (4-triphenylphosphoniumbutyl)-4'-O-resveratrol iodide and its bis-acetylated derivative, the latter intended to provide transient protection against metabolic conjugation, accumulate into energized mitochondria as expected and are cytotoxic for fast-growing but not for slower-growing cells. They provide a powerful potential tool to intervene on mitochondrial and cellular redox processes of pathophysiological relevance.

Introduction

Plant polyphenols are the object of intense interest because they display, at least *in vitro*, properties and effects of relevance for physiopathological conditions ranging from aging to cancer. These effects are ascribed to their redox properties and to interactions with signalling proteins. Polyphenols can act either as anti- or pro-oxidants, i.e. inhibitors or enhancers of oxidative and radical chain processes [1]. Whether an anti- or a pro-oxidant effect predominates depends, besides the redox potential of the polyphenol, on the abundance of metal ions sustaining a redox cycle ($Fe^{2+/3+}$, $Cu^{+/2+}$) and/or of oxidizing enzymes, on the ion-chelating properties of the molecule, on pH, on the concentration of the polyphenol, and on the subcellular compartment. Either pro-oxidant or anti-oxidant activity may lead to useful oncological applications. Reactive Oxygen Species (ROS) are thought to be a major factor in cancerogenesis [2]. In particular, ROS production by mitochondria [3,4] is emerging as a key factor. The metastatic potential of cell lines has been convincingly related to this parameter [5]. Mitochondrial ROS are involved in the activation of Hypoxia Inducible Factor (HIF) [6,7], which influences angiogenesis and other aspects of

[2] Published as: Biasutto, L.; Mattarei, A.; Marotta, E.; Bradaschia, A.; Sassi, N.; Garbisa, S.; Zoratti, M.; Paradisi, C. *Bioorg. Med. Chem. Lett.* **2008**, 18, 5594-5597.

tumor development [7,8]. Thus, an anti-oxidant action may limit metastasis and tumor growth. Indeed resveratrol, the representative polyphenol selected for this work, inhibits cell shedding from primary tumors [9]. On the other hand, ROS play fundamental roles in apoptosis [10] and can induce the Mitochondrial Permeability Transition (MPT) [11], promoting in both cases cell death. Cancer cells are constitutively under oxidative stress [4] and an intensification of this stress may lead to their selective elimination. Resveratrol, in addition to other important activities [12], reportedly exerts anti-proliferative and pro-apoptotic effects on various tumor-derived cells [13,14] and antagonizes growth of xenografts and mutagen-induced cancers [15]. It has been recently shown that resveratrol-induced death of cultured colorectal carcinoma cells involves generation of superoxide anion, i.e., pro-oxidant action, at mitochondria [14]. The IC_{50} for death induction was found to be in the hundreds of μM range, a concentration which cannot be reached *in vivo* due to the poor bioavailability of polyphenols [16].

We are interested in exploiting the potential of polyphenols through chemical modifications designed to serve specific purposes. Thus, an increase in solubility was achieved via esterification with amino acids [17]. The present work aims at targeting polyphenols to the subcellular compartment where they are expected to best realize their anti-cancer potential (as well as other functions), i.e. mitochondria. We report here the synthesis and properties of new mitochondriotropic derivatives of resveratrol obtained by coupling it to the membrane-permeable lipophilic cation triphenylphosphonium (TPP^+) [18] which drives accumulation in compartments held at negative relative voltage, such as the mitochondrial matrix, according to Nernst's law. Since the mitochondria of cancer cells maintain a higher-then-normal transmembrane potential, [19] mitochondria-targeted drugs may be cancer-selective.

Results

The target derivative **4** was synthesised starting from resveratrol **(1)** in three steps as outlined in Scheme 1. Briefly, O-alkylation introduces a chlorobutyl group which is then converted to the desired TPP^+ derivative via two consecutive nucleophilic substitution steps: $-Cl \rightarrow -I \rightarrow - TPP^+I^-$. Direct substitution of chloride by triphenylphosphine was unsatisfactory because it required high temperatures, which led to some decomposition. The assignment of the site of O-alkylation in **2** is based on ^{1}H-NMR data: a unique signal is found for H-2 and H-6 indicating that these protons are equivalent. The acetylated derivative **6** was also prepared (Scheme 1), so as to compare it with **4** and assess the

importance of the free hydroxyl groups for the behaviour of these new mitochondriotropic molecules.

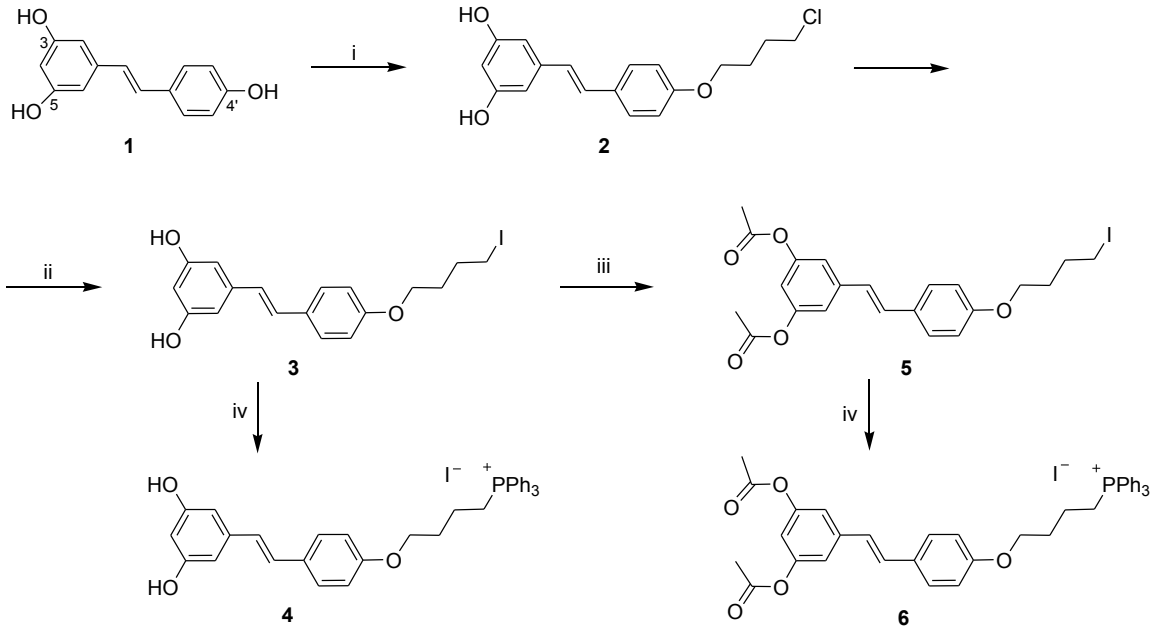

i: 1-bromo-4-chlorobutane (1.5 eq), K_2CO_3 (1.1 eq), DMF, Ar, r.t., 20 h, yield 33%; ii:NaI, acetone, reflux, 20 h, yield 89%; iii: $CH_3C(=O)Cl$ (20 eq), pyr, CH_2Cl_2, yield 73%; iv: PPh_3 (5 eq), toluene, 100°C, 6h, yield 78%.

Scheme 1. Synthesis of mitochondriotropic derivatives **4** and **6**.

The solubility in water of the resveratrol derivatives is $(3.12 \pm 0.20)\cdot10^{-5}$ mol·L^{-1} and $(9.7 \pm 0.6)\cdot10^{-5}$ mol·L^{-1} for **4** and **6** respectively. These solubilities are significantly higher (15 and 45-fold, respectively) than that of resveratrol. Both new compounds are essentially stable in aqueous media: **4** for at least one week both in deionised water and in Hank's Balanced Saline Solution (HBSS) with 10% CH_3CN (added to insure solubility of hypothetical reaction products); **6** for at least 24 h in deionised water, while in HBSS acetyl groups were slowly hydrolised (about 7% conversion to the monoacetylated derivative in 6 h). There were no detectable metabolic modifications of either **4** or **6** by cultured Human Colon Tumor (HCT) 116 cells[20] over 6 hours (Fig. 1) or whole freshly drawn rat blood over 75 min. (not shown), except for the hydrolysis of the acetyl ester groups of **6** in both cases.

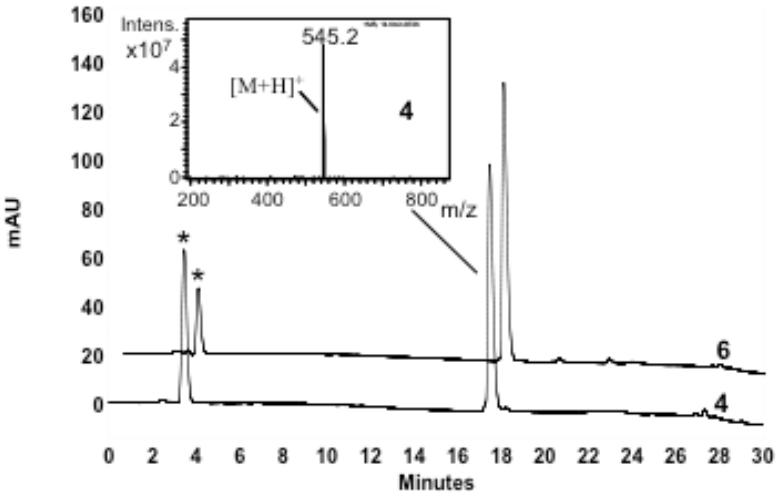

Figure 1. HPLC chromatograms recorded at 320 nm of the extracts obtained after incubation of **4** (lower trace) and **6** (upper trace) with HCT116 cells for 6 hours. Inset: positive ESI-MS spectrum of **4.** For clarity, the upper trace was shifted slightly to the right along the time axis: the retention time and the mass spectrum of the major peak in this chromatogram match perfectly those of **4**. Peaks marked with * are due to residual traces of acetone from the sample work-up.

Two methods were used to verify accumulation of the new compounds into mitochondria. First, their uptake by isolated, respiring rat liver mitochondria (RLM) was monitored using a TPP^+-sensitive electrode. A representative experiment with **6** is shown in Fig. 2. The introduction of mitochondria causes a decrease (upward deflection of the signal) of **6** in the medium, due to uptake into the mitochondrial matrix. After addition of excess Ca^{2+}, which induces the MPT, or of uncouplers (not shown), **6** is partially released. The release is incomplete presumably due to binding of the resveratrol derivative to mitochondrial constituents. Analogous results were obtained with **4** (not shown).

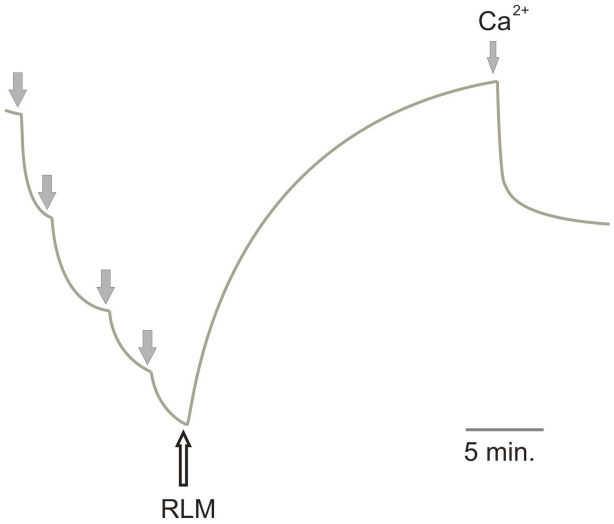

Figure 2. TPP^+-selective electrode response to additions of **6** (thick gray arrows; 0.5 µM each), Rat Liver Mitochondria (RLM) (1 mg prot.·mL^{-1}) and $CaCl_2$ (50 µM) at 20°C.

In the second approach we exploited the spectral properties of **6** and **4**, similar to those of resveratrol itself, to follow their accumulation in the mitochondria of cultured cells by monitoring of their fluorescence upon excitation at 340 nm. Images from one such experiment are shown in Fig. 3. After addition of **6** to the medium, intracellular structures become progressively fluorescent due to accumulation of the resveratrol derivative (panel B). Addition of a transmembrane potential ($\Delta\psi_m$)-dissipating protonophore (carbonyl cyanide p-trifluoromethoxyphenylhydrazone (FCCP)) causes a loss of fluorescence due to efflux of the polyphenol (panel C). Some **6** remains in the cytoplasm of the cells due to the plasma membrane potential maintained by K^+ diffusion. **4** behaved analogously (not shown).

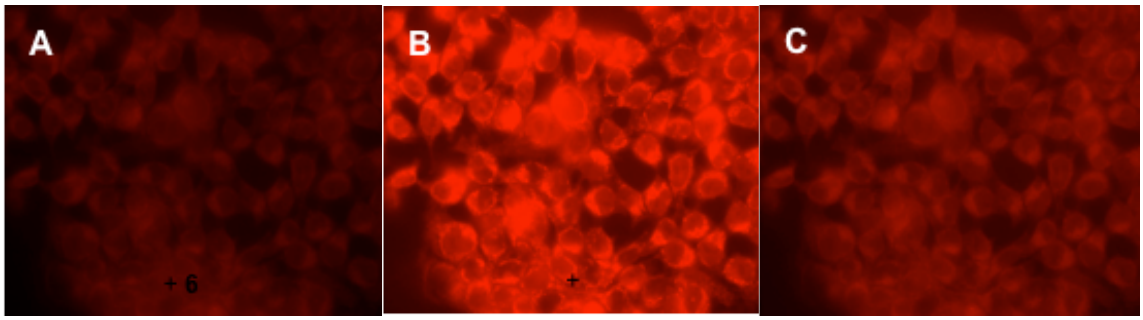

Figure 3. Fluorescence microscope images of cultured HCT116 cells: A) just before the addition of 10 μM **6**, B) 25 min after the addition of **6** and just before the addition of 2 μM FCCP and C) 10 min after the addition of FCCP.

As a first test of potential anti-cancer activity, we verified the effects of **4** and **6**, and of control compounds, on cultured cells (Fig. 4). Controls consisted of the parent polyphenol resveratrol, of the phosphonium salt Triphenylmethylphosphonium Iodide (TPMP) and of resveratrol plus this latter compound. We used the murine colon cancer cell line C-26 and, as controls, fast- and slow-growing non-tumoral mouse embryonic fibroblast (MEF) lines. Cell growth and viability was quantified using the tetrazolium salt reduction (MTT) assay. The various compounds had little effect on cell proliferation at the 1 μM level. At 5 μM, **4** and **6** displayed a marked cytotoxic effect on the two rapid-growth cell types, i.e. C-26 (Fig. 4A) and non-tumoral "fast" MEFs (Fig. 4B), but not on the slow-growth MEFs (Fig. 4C). Resveratrol, TPMP and their combination had little effect also at 5 μM and with all three cell types, showing that the activity of the resveratrol-TPP conjugates is not just the sum of the activity of the two components. Selective cytotoxicity for fast-growing cells is characteristic of many chemotherapeutic drugs.

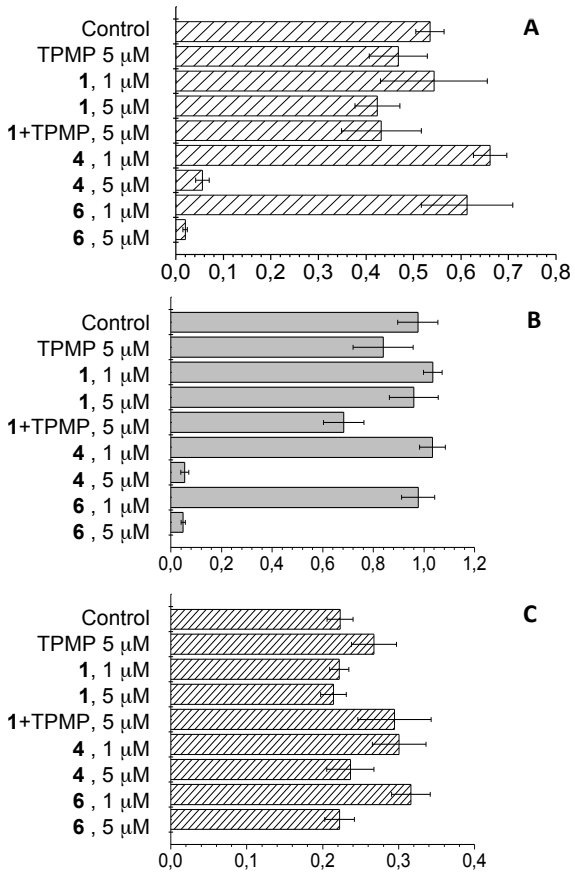

Figure 4. Effect of the mitochondriotropic resveratrol derivatives and control compounds on cell proliferation. Cells were allowed to grow for 3 days in the presence of the specified compounds and assayed using the tetrazolium salt reduction assay. All measurements were performed in quadruplicate. Averages ± s.d. are given. A) C-26 mouse colon tumor cells. B) Fast-growing Mouse Embryonic Fibroblasts (MEF). C) Slow-growing MEF (note different scale).

In conclusion we have produced mitochondriotropic resveratrol derivatives with good solubility and stability in aqueous media, which accumulate as expected in regions at negative potential. A class of natural compounds with useful properties can now be targeted to subcellular compartments where they ought to realize their biomedical potential in full. The results of initial cytotoxicity assessments encourage further experimentation *in vivo* to determine absorption, pharmacokinetics and possible anti-tumoral action.

Experimental section

Materials and instrumentation:

Chemicals were purchased from Aldrich, Fluka, Merck-Novabiochem, Riedel de Haen, J.T. Baker, Cambridge Isotope Laboratories Inc., Acros Organics, Carlo Erba and Prolabo, and were used as received. ^{1}H NMR spectra were recorded with a Bruker AC 250F spectrometer operating at 250 MHz. Chemical shifts (δ) are given in ppm relative to the

solvent signal (δ 2.49 ppm, DMSO-d_6). LC/MS analyses and mass spectra were performed with a 1100 Series Agilent Technologies system, equipped with MSD SL Trap mass spectrometer with ESI source. HPLC/UV analyses were performed with a Thermo Separation Products Inc. system with a P2000 Spectra System pump and a UV6000LP diode array detector (190-500 nm). Accurate mass measurements were obtained using a Mariner ESI-TOF mass spectrometer (PerSeptive Biosystems). UV-Vis spectra were recorded with a Perkin-Elmer Lambda 5 spectrophotometer. Fluorescence spectra were recorded with a Perkin–Elmer LS-55 spectrofluorimeter equipped with a Hamamatsu R928 photomultiplier. All absorption and fluorescence spectra were recorded at 25°C using thermostated quartz cells with an optical pathlength of 1 cm. Flash chromatographic separations were run on silica gel (Macherey-Nagel 60, 230-400 mesh) under air pressure. Elemental analyses were performed by the Microanalysis Laboratory of the Dept. of Chemical Sciences of the University of Padova.

Solubility of **4** *and* **6** *in water.* Calibration curves were built by plotting absorbance at 320 nm (a plateau in the UV absorption spectrum of both **4** or **6**) *vs* concentration for seven standard solutions in the 10^{-6} - 10^{-4} M range, prepared from a 10^{-3} M mother solution in CH_3CN by dilution with water:CH_3CN/9:1. The concentration of aqueous saturated solutions of **4** and **6** was determined by interpolation (5 repetitions each).

Stability **4** *and* **6** *in water and in HBSS buffer.* At time zero, a 60 μL volume of a freshly prepared 10^{-3} M CH_3CN solution of either **4** or **6** was added to 3 mL of the medium of interest, i.e. water or HBSS:CH_3CN 9:1, at 25°C. The composition of HBSS (Hank's Balanced Saline Solution) was (in mM units): NaCl 136.9, KCl 5.36, $CaCl_2$ 1.26, $MgSO_4$ 0.81, KH_2PO_4 0.44, Na_2HPO_4 0.34, Glucose 5.55, pH 7.4 (with NaOH). Aliquots were withdrawn at desired times and analyzed by HPLC/UV (at 320 nm) and LC/MS on a reversed phase column (Gemini C18, 3 μm, 150 x 4.6 mm i.d.; Phenomenex). Solvents A and B were H_2O containing 0.1% HCOOH and CH_3CN, respectively. The gradient for B was as follows: 30% for 5 min, up to 60% in 15 min, up to 100% in 5 min; the flow rate was 0.7 mL·min^{-1}. For HPLC/UV analyses the 190 - 500 nm range was considered; in the LC/MS analyses mass spectra were acquired in positive ion mode operating in full-scan from 100 to 1500 m/z.

Cells. Human Colon Tumor (HCT116) cells (kindly provided by B. Vogelstein) as well as fast- and slow-growing SV-40 immortalized Mouse Embryo Fibroblast (MEF) cells (kindly provided by L. Scorrano and W.J. Craigen, respectively) and murine colon carcinoma C-26 cells were grown in Dulbecco's Modified Eagle Medium (DMEM), plus

10 mM HEPES buffer, 10% (v/v) fetal calf serum (Invitrogen), 100 U/mL penicillin G (Sigma), 0.1 mg/mL streptomycin (Sigma), 2 mM glutamine (GIBCO) and 1% nonessential amino acids (100X solution; GIBCO), in a humidified atmosphere of 5% CO_2 at 37 °C.

Metabolism studies. HCT116 cells were grown to ~90% of confluence in a 6-well plate, washed with warm HBSS, and incubated with 1 ml/well of 20 μM solution of **4**, **6** or resveratrol. Medium and cells were collected together after 6 hours of incubation. 100 μL of 0.6 M acetic acid and of fresh 10 mM ascorbic acid were added and the samples stored at –20°C until treatment and HPLC and LC/MS analysis. Treatment consisted in addition of acetone (1 mL), followed by sonication, filtration through 0.45 μm Teflon® syringe filters (Chemtek Analytica) and concentration under N_2. The HPLC protocol was the same used for stability studies.

Mitochondria. Rat liver mitochondria were isolated by conventional differential centrifugation procedures from fasted male albino Wistar rats. The standard isolation medium was 250 mM sucrose, 5 mM HEPES (pH 7.4) and 1 mM EGTA. Protein content was measured by the biuret method with bovine serum albumin as standard.

TPP^+-selective electrode. The setup used to monitor the concentration of TPP^+-bearing compounds was built in-house following published procedures (Zoratti, M.; Favaron, M.; Pietrobon, D.; Petronilli, V. *Biochim. Biophys. Acta* **1984**, *767*, 231-239). A calomel electrode was used as reference. The suspension medium contained 200 mM sucrose, 10 mM Hepes, 5 mM succinate, 1 mM phosphate, 1.25 μM rotenone, pH 7.4 (with KOH).

Fluorescence microscopy. Cells were sown onto 24 mm round coverslips and allowed to grow for 48 hours. The coverslips were then washed with HBSS, mounted into supports, covered with 1 mL of HBSS and placed onto the microscope stage. The imaging apparatus consisted of an Olympus IX71 microscope equipped with an MT20 light source and Cell$^{R©}$ software. Excitation wavelength was 340 nm and fluorescence was collected in the 450-475 nm range. Sequential images were automatically recorded following a preordained protocol.

*Cell growth/viability (MTT) assays***.** C-26 or MEF cells were seeded in standard 96-well plates and allowed to grow in DMEM (200 μL) for 24 hours to insure attachment. In the experiments of Figure 3 initial densities were 1000 (C-26, fast MEF) or 2500 (slow MEF) cells/well. The growth medium was then replaced with medium containing the desired compound from a mother solution in DMSO. DMSO final concentration was 0.1% in all cases (including controls). Four wells were used for each of the compounds to be tested.

The solution was substituted by a fresh aliquot twice, at 24-hour intervals. At the end of the third 24-hour period of incubation with the drugs the medium was removed and substituted, after a wash with PBS, with 100 µL of CellTiter 96® solution (Promega; for details: www.promega.com/tbs). After a one-hour colour development period at 37°C absorbance at 490 nm was measured using a Packard Spectra Count 96-well plate reader.

Synthetic procedures:

4'-*O*-(4-chlorobutyl) resveratrol (2): K_2CO_3 (1.33 g, 9.64 mmol, 1.1 eq.) and 1-bromo-4-chlorobutane (2.25 g, 13.14 mmol, 1.5 eq.) were added under argon to a solution of resveratrol (1) (2.00 g, 8.76 mmol) in DMF (10 mL). After stirring overnight, the mixture was diluted in EtOAc (100 mL) and washed with 1 N HCl (3 × 50 mL). The organic layer was dried over $MgSO_4$ and filtered. The solvent was evaporated under reduced pressure and the residue was purified by flash chromatography using CH_2Cl_2:EtOAc 85:15 as eluent to afford 0.930 g of 2 (33%). ^{1}H-NMR (250 MHz, DMSO-d_6) δ (ppm): 1.76-1.98 (m, 4H, CH_2), 3.72 (t, 2H, CH_2), 4.02 (t, 2H, CH_2), 6.12 (t, 1H, H-4, J=2.0 Hz), 6.40 (d, 2H, J=2.0 Hz, H-2, H-6), 6.82-7.04 (m, 4H, =CH, H-2', H-6'), 7.50 (d, 2H, H-3', H-5', J=8.75 Hz), 9.21 (s, 2H, 3-OH, 5-OH); ^{13}C-NMR (62.9 MHz, DMSO-d_6) δ (ppm): 26.14 (CH_2), 28.90 (CH_2), 45.19 (CH_2Cl), 66.72 (OCH_2), 104.38, 114.62, 126.62, 127.45, 127.76, 129.62, 139.07, 158.16, 158.49; ESI-MS (ion trap): m/z 319, $[M+H]^+$; HRMS (ESI-TOF): m/z 319.1092; calcd for $C_{18}H_{19}ClO_3 \cdot H^+$ 319.1095. Anal.: calcd. for $C_{18}H_{19}ClO_3$ C 67.81, H 6.01; found: C 67.78, H 6.02.

4'-*O*-(4-iodobutyl) resveratrol (3): Compound 2 (500 mg, 1.57 mmol, 1 eq.) was added to a saturated solution of NaI in dry acetone (10 mL) and heated at reflux for 20 h. After cooling, the resulting mixture was diluted in EtOAc (100 mL), filtered and washed with water (3 × 30 mL). The organic layer was dried over $MgSO_4$ and filtered. The solvent was evaporated under reduced pressure and the residue was purified by flash chromatography using CH_2Cl_2:EtOAc 9:1 as eluent to afford 0.570 g of 3 (89%). ^{1}H-NMR (250 MHz, DMSO-d_6) δ (ppm): 1.71-2.00 (m, 4H, CH_2), 3.35 (t, 2H, CH_2), 4.01 (t, 2H, CH_2), 6.12 (t, 1H, H-4, J=2.0 Hz), 6.40 (d, 2H, H-2, H-6, J=2.0 Hz), 6.82-7.04 (m, 4H, =CH, H-2', H-6'), 7.50 (d, 2H, H-3', H-5', J=8.75 Hz), 9.21 (s, 2H, 3-OH, 5-OH); ^{13}C-NMR (62.9 MHz, DMSO-d_6) δ (ppm): 8.54 (CH_2I), 29.66 (CH_2), 29.76 (CH_2), 66.39 (OCH_2), 104.38, 114.62, 126.61, 127.45, 127.76, 129.62, 139.07, 158.16, 158.49; ESI-MS (ion trap): m/z 411, $[M+H]^+$. Anal.: calcd. for $C_{18}H_{19}IO_3$ C 52.70, H 4.66; found: C 52.75, H 4.66.

4'-*O*-(4-triphenylphosphoniumbutyl) resveratrol iodide (4): A mixture of 3 (500 mg, 1.22 mmol) and triphenylphosphine (1.60 g, 6.09 mmol, 5 eq.) in toluene (15 mL) was

heated at 100 °C under argon. After 6 h, the solvent was eliminated at reduced pressure and the resulting white solid was dissolved in the minimum volume of acetone (3 mL) and precipitated with diethyl ether (100 mL). The solvents were decanted and the procedure repeated 4 more times. The precipitate was then filtered to afford 600 mg of 7 (73%). ^{1}H-NMR (250 MHz, DMSO-d_6) δ (ppm): 1.73 (quintet, 2H, CH_2), 1.92 (quintet, 2H, CH_2), 3.67 (t, 2H, CH_2), 4.06 (t, 2H, CH_2), 6.13 (t, 1H, H-4, J=1.9 Hz), 6.40 (d, 2H, H-2, H-6, J=1.75 Hz), 6.83-7.04 (m, 4H, =CH, H-2', H-6'), 7.50 (d, 2H, H-3', H-5', J= 8.75 Hz), 7.71-7.95 (m, 15H, aromatic-H), 9.22 (s, 2H, 3-OH, 5-OH). ^{13}C-NMR (62.9 MHz, DMSO-d_6) δ (ppm): 18.48 (CH_2), 20.07 (CH_2), 29.15 (CH_2), 65.93 (OCH_2), 104.38, 114.66, 118.47 (Ph, J(^{13}C/^{31}P)=85.6 Hz), 126.67, 127.41, 127.73, 129.72, 130.25 (Ph, J(^{13}C/^{31}P)=12.4 Hz), 133.59 (Ph, J(^{13}C/^{31}P)=10.1 Hz), 134.93 (Ph, J(^{13}C/^{31}P)=2.9 Hz), 139.03, 158.00, 158.49; ESI-MS (ion trap): m/z 545, M^+; HRMS (ESI-TOF): m/z 545.2236; calcd for $C_{36}H_{34}O_3P^+$ 545.2240.

3,5-diacetyl-4'-*O*-(4-iodobutyl) resveratrol (5): A solution of acetyl chloride (1.1 mL, 15 mmol, 20 eq.) in CH_2Cl_2 (20 mL) was added dropwise and under continuous stirring to a mixture of 3 (300 mg, 0.73 mmol, 1 eq.) and anhydrous pyridine (0.85 mL, 10.5 mmol, 15 eq.) in CH_2Cl_2 (20 mL) cooled in dry ice/acetone. The reaction mixture was then allowed to slowly warm up to room temperature. CH_2Cl_2 (50 mL) was added and the organic layer was washed with 1 N HCl (3 × 50 mL), dried over $MgSO_4$ and filtered. The solvent was evaporated under reduced pressure and the residue was purified by flash chromatography using CH_2Cl_2:n-hexane 4:1 as eluent to afford 280 mg of 5 (78%). ^{1}H-NMR (250 MHz, DMSO-d_6) δ (ppm): 1.73-2.02 (m, 4H, CH_2), 2.29 (s, 6H, OAc), 3.38 (t, 2H, CH_2), 4.02 (t, 2H, CH_2), 6.86 (t, 1H, H-4, J=1.9 Hz), 6.96 (d, 2H, H-2', H-6', J=8.5 Hz), 7.08 (d, 1H, =CH, J=16.5 Hz), 7.21-7.33 (m, 3H, H-2, H-6, =CH), 7.53 (d, 2H, H-3', H-5', J= 8.75 Hz); ^{13}C-NMR (62.9 MHz, DMSO-d_6) δ (ppm): 8.49 (CH_2I), 20.83 (CH_3), 29.62 (CH_2), 29.75 (CH_2), 66.43 (OCH_2), 114.74, 116.79, 124.25, 128.08, 129.10, 130.09, 139.81, 151.15, 158.61, 168.99; ESI-MS (ion trap): m/z 495, $[M+H]^+$; HRMS (ESI-TOF): m/z 495.0664; calcd for $C_{22}H_{23}O_5I{\cdot}H^+$ 495.0663.

3,5-diacetyl-4'-*O*-(4-triphenylphosphoniumbutyl) resveratrol iodide (6): a mixture of 5 (200 mg, 0.40 mmol) and triphenylphosphine (525 mg, 2.00 mmol, 5 eq.) in toluene (10 mL) was heated at 100°C under argon. After 6 h, the solvent was eliminated under reduced pressure and the resulting white solid was dissolved in the minimum volume of acetone (3 mL) and precipitated with diethyl ether (100 mL) five times. The solvents were decanted after each precipitation. The precipitate was than filtered to afford 210 mg of 6 of 96-98%

purity (69% yield). ^{1}H-NMR (250 MHz, DMSO-d_6) δ (ppm): 1.73 (quintet, 2H, CH_2), 1.93 (quintet, 2H, CH_2), 2.29 (s, 6H, OAc), 3.67 (t, 2H, CH_2), 4.07 (t, 2H, CH_2), 6.86 (t, 1H, H-4, J=2.2 Hz), 6.91 (d, 2H, H-2', H-6', J= 8.75 Hz), 7.08 (d, 1H, =CH, J=16.25 Hz),7.21-7.33 (m, 3H, H-2, H-6, =CH), 7.53 (d, 2H, H-3', H-5', J= 8.5 Hz), 7.72-7.96 (m, 15H, aromatic-H). ^{13}C-NMR (62.9 MHz, DMSO-d_6) δ (ppm): 19.25 (CH_2), 20.84 (CH_2), 29.25 (CH_2), 65.98 (OCH_2), 114.79, 116.81, 118.46 (Ph, J(^{13}C/^{31}P)=85.9 Hz), 124.31, 128.06, 129.19, 130.05, 130.25 (Ph, J(^{13}C/^{31}P)=12.4 Hz), 133.59 (Ph, J(^{13}C/^{31}P)=10.1 Hz), 134.93 (Ph, J(^{13}C/^{31}P)=2.9 Hz), 139.76, 151.16, 158.46, 169.01; ESI-MS (ion trap): m/z 629, M^+; HRMS (ESI-TOF): m/z 629.2453; calcd for $C_{40}H_{38}O_5P^+$ 629.2451.

Bibliography

[1] (a) Cao, G.; Sofic, E.; Prior, R.L. Free Radic. Biol. Med. 1997, 22, 749-760. (b) Halliwell, B. Arch. Biochem. Biophys. 2008, 476, 107-112.
[2] Halliwell, B. Biochem J. 2007, 401, 1-11.
[3] Turrens, J.F. J. Physiol. 2003, 552, 335-344.
[4] Pelicano, H.; Carney, D.; Huang, P. Drug Resist. Update 2004, 7, 97-110.
[5] Ishikawa, K.; Takenaga, K.; Akimoto, M.; Koshikawa, N.; Yamaguchi, A.; Imanishi, H.; Nakada, K.; Honma, Y.; Hayashi, J. Science 2008, 320, 661-664.
[6] Qutub, A.A.; Popel, A.S. Mol. Cell. Biol. 2008, 28, 5106-5119.
[7] Patel, S.A.; Simon, M.C. Cell Death Differ. 2008, 15, 628-634.
[8] Rankin, E.B.; Giaccia, A.J. Cell Death Differ. 2008, 15, 678-685.
[9] Günther, S.; Ruhe, C.; Derikito, M.G.; Böse, G.; Sauer, H.; Wartenberg, M. Cancer Lett. 2007, 250, 25-35.
[10] Orrenius, S.; Gogvadze, V.; Zhivotovsky, B. Annu. Rev. Pharmacol. Toxicol. 2007, 47, 143-183.
[11] Rasola, A.; Bernardi, P. Apoptosis 2007, 12, 815-833.
[12] (a) Baur, J.A.; Sinclair, D.A. Nat. Rev. Drug Discov. 2006, 5, 493-506. (b) Pearson, K.J.; Baur, J.A.; Lewis, K.N.; Peshkin, L.; Price, N.L.; Labinskyy, N.; Swindell, W.R.; Kamara, D.; Minor, R.K.; Perez, E.; Jamieson, H.A.; Zhang, Y.; Dunn, S.R.; Sharma, K.; Pleshko, N.; Woollett, L.A.; Csiszar, A.; Ikeno, Y.; Le Couteur, D.; Elliott, P.J.; Becker, K.G.; Navas, P.; Ingram, D.K.; Wolf, N.S.; Ungvari, Z.; Sinclair, D.A.; de Cabo, R. Cell Metab. 2008, 8, 157-168.
[13] (a) Fulda, S.; Debatin, K.M. Cancer Detect. Prev. 2006, 30, 217-223. (b) Ma, X.; Tian, X.; Huang, X.; Yan, F.; Qiao, D. Mol. Cell. Biochem. 2007, 302, 99-109.
[14] Juan, M.E.; Wenzel, U.; Daniel, H.; Planas, J.M. J. Agric. Food Chem. 2008, 56, 4813-4818.
[15] (a) Kalra, N.; Roy, P.; Prasad, S.; Shukla, Y. Life Sci. 2008, 82, 348-358. (b) Pan, M.H.; Gao, J.H.; Lai, C.S.; Wang, Y.J.; Chen, W.M.; Lo, C.Y.; Wang, M.; Dushenkov, S.; Ho, C.T. Mol. Carcinog. 2008, 47, 184-196.
[16] Manach, C.; Williamson, G.; Morand, C.; Scalbert, A.; Rémésy, C. Am. J. Clin. Nutr. 2005, 81 (1 Suppl), 230S-242S.
[17] Biasutto, L.; Marotta, E.; De Marchi, U.; Zoratti, M.; Paradisi, C. J. Med. Chem. 2007, 50, 241-253.

[18] (a) Murphy, M.P.; Smith, R.A. Annu. Rev. Pharmacol. Toxicol. 2007, 47, 629-656. (b) Hoye, A.T.; Davoren, J.E.; Wipf, P.; Fink, M.P.; Kagan, V.E. Acc. Chem. Res. 2008, 41, 87-97.
[19] (a) Kadenbach, B. Biochim. Biophys. Acta 2003, 1604, 77-94. (b) Fantin, V.R.; Leder, P. Oncogene 2006, 25, 4787-4797.

Chapter 3

Regioselective *O*-derivatization of quercetin via ester intermediates. An improved synthesis of rhamnetin and development of a new mitochondriotropic derivative[3]

Summary

The regioselective synthesis of several quercetin (3,3',4',5,7-pentahydroxy flavone) tetraesters bearing the single free OH on 5-C was achieved in good yield using common esterification procedures by proper choice of reaction conditions. Tetracetylated quercetin with the free OH on 7-C was instead selectively obtained via imidazole-promoted deacylation of the corresponding pentaester. Unambiguous structural characterization of the two isomeric tetraacetyl quercetin derivatives was obtained by combined HSQC and HMBC 2D-NMR analysis. These molecules can be used as starting material for the regioselective synthesis of other derivatives. High yield syntheses of the natural polyphenol rhamnetin (7-*O*-methylquercetin) and of the new mitochondriotropic compound 7-(4-triphenylphosphoniumbutyl) quercetin iodide are reported as examples.

Introduction

Due to its large diffusion in many foodstuffs and to its complex and rich chemistry, quercetin (**1**), 2-(3,4-dihydroxyphenyl)-3,5,7-trihydroxy-4*H*-chromen-4-one, is an important and highly representative member of the vast family of natural polyphenols. Such compounds are drawing increasing interest by the scientific community in view of the potentially beneficial effects many of them exhibit *in vitro* (anti-inflammatory, anti-ageing, cardioprotective, anticancer) (for quercetin see, e.g., [1-4]). Despite the fact that several natural polyphenols are being exploited as additives in nutritional, cosmetic and over-the counter pharmacological formulations, their activity *in vivo* is difficult to demonstrate due to their low bioavailability [5-7]. This in turn is largely a consequence of their high susceptibility to metabolic modifications. Due to the presence of multiple -OH's, polyphenols are ready-made substrates for Phase II conjugative metabolism which rapidly converts them to sulfates, glucuronides and methyl ethers.

[3] Published as: Mattarei, A.; Biasutto, L.; Rastrelli, F.; Garbisa, S.; Marotta, E.; Zoratti, M.; Paradisi, C. *Molecules*, **2010**, 15, 4722-4736.

One interesting approach to overcome the low bioavailability of polyphenols, so as to test and hopefully exploit their activity *in vivo*, relies on chemical modification of the natural compound aimed at increasing solubility and at slowing down metabolism while maintaining the capability to regenerate the original molecule. Efforts are obviously concentrating on the protection of the polyphenol hydroxyls [8,9]. Another possibility is the modification of the parent molecule by the introduction of a stable substituent capable of conferring desirable properties. Recently, a charged, membrane-permeant triphenylphosphonium group has been linked to quercetin (at position 3) and resveratrol to produce derivatives targeted to mitochondria, where the polyphenol redox properties either as a pro- or anti-oxidant may be best exploited [10-12]. These products join the growing family of mitochondriotropic redox-active compounds [13], the best-known of which may be Mito-Q, a coenzyme Q derivative developed by the pioneering group of Murphy and Smith, currently undergoing clinical trials [14,15], and the plastoquinone-comprising "SkQs" of Skulachev and coworkers [16].

In such a context it is important to be able to modify selectively the various hydroxyls, which are far from equivalent from either the chemical or the biofunctional points of view. Thus, in the case of quercetin, the catechol moiety on the C ring (3'-OH, 4'-OH) is largely responsible for the redox properties of the molecule [17], the 3-OH is a key group for kinase inhibition [18], the 7-OH is chiefly responsible for the weak uncoupling activity [19], while the 5-OH is the least acidic and reactive one, due to intramolecular H-bonding to the carbonyl at 4-C. The literature reports the regioselective acylation of the 3-OH using enzymatic [20] or, after protection of the catecholic hydroxyls, chemical reactions [21].

We report here the synthesis and characterization of several ester derivatives of quercetin including pentaesters of a few carboxylic acids with different steric hindrance and selected regioisomers of tetraesters in which the free OH is either on 5-C or 7-C. The regioselective synthesis of tetraesters with a free 5-OH was achieved via esterification of quercetin under controlled conditions. Tetraesters with a free 7-OH can be obtained via selective hydrolysis of pentaester precursors, and we report here the tetraacetylated derivative. These molecules with a single free OH are meant to serve as entry points for the production of other compounds. To illustrate their usefulness we report the synthesis of rhamnetin (7-*O*-methylquercetin), a natural flavonoid and quercetin metabolite which possesses many of the activities of quercetin itself (e.g., it is an inhibitor of mitochondrial NADH oxidase [22]), and of 7-O-(4-triphenylphosphoniumbutyl)quercetin iodide. The latter is a novel mitochondria-targeted compound bearing a free OH at the important position 3.

Results

Acylation of all five hydroxyl groups of quercetin (**1**) with groups of different steric hindrance was carried out modifying published procedures [8,23] to obtain derivatives 2a–d in high yield (79-97%) (Scheme 1). By careful control of the reaction conditions, i.e. temperature (*T*), type and equivalents (n_{eq}) of acylating agent and reaction time (*t*), it is possible to stop the acylation at the 3,3',4',7-tetraester stage. Reaction yields did not systematically depend on the acyl group.

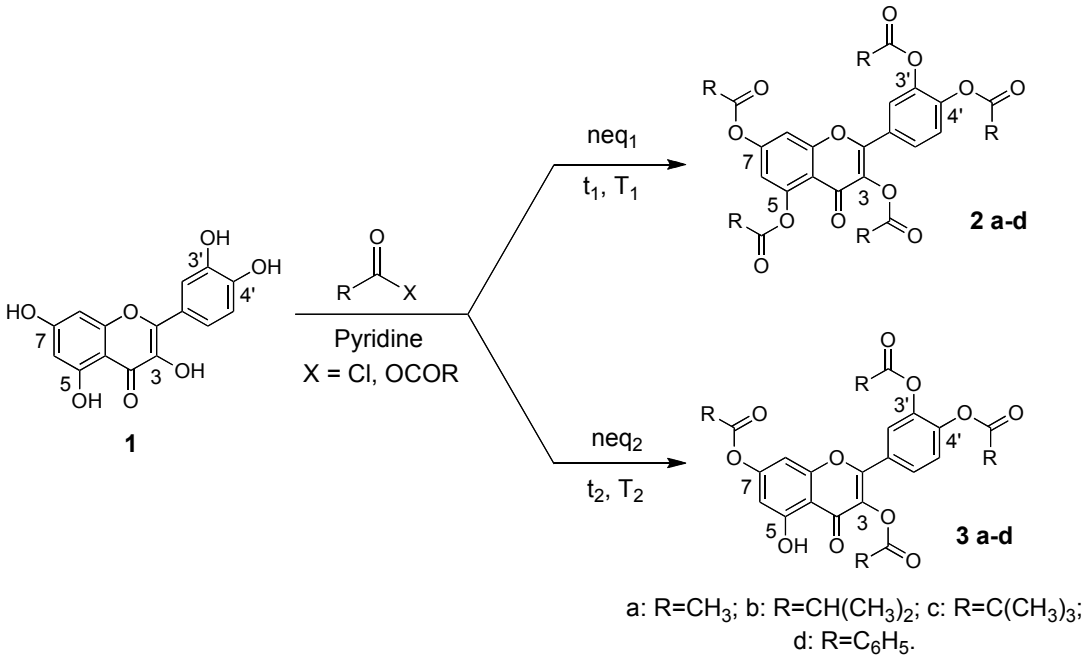

Scheme 1. Synthesis of pentaacyl and 3,3',4',7-tetraacyl derivatives of quercetin.

Thus, a single isomer of tetraacetyl quercetin was obtained in 75% isolated yield from the reaction with 5 equiv. of acetic anhydride at room temperature for 3 hours. The product is assigned the structure of 3,3',4',7-tetraacetyl quercetin (**3a**) based on ^{1}H-NMR analysis. Following literature protocols [24], the assignment of the single free hydroxyl group utilized the narrow peak shape and high chemical shift (12 ppm, 20 mM in $CDCl_3$) of the hydroxyl proton [25], and the difference in chemical shifts between the ring protons of the product and the corresponding ones of pentaacetylquercetin (**2a**) (Table 1). The chemical shifts of 2'-H, 5'-H and 6'-H are very similar in **2a** and in **3a**, while those of 6-H and 8-H differ significantly.

Table 1. Chemical shifts (δ) of the aromatic protons of pentaacetyl quercetin (**2a**), 3,3',4',7-tetraacetyl quercetin (**3a**) and 3,3',4',5-tetraacetyl quercetin (**4**) measured in $CDCl_3$. Chemical shift differences (Δδ) relative to **2a** are shown in parentheses.

Compound	δ(H-6)		δ(H-8)		δ(H-5')		δ(H-6')		δ(H-2')	
2a	6.88		7.33		7.35		7.72		7.69	
3a	6.60	(-0.28)	6.85	(-0.48)	7.36	(+0.01)	7.75	(+0.03)	7.72	(+0.03)
4	6.46	(-0.42)	6.71	(-0.62)	7.24	(-0.11)	7.64	(-0.08)	7.58	(-0.11)

HSQC (Heteronuclear Multiple-Quantum Correlation) and HMBC (Heteronuclear Multiple-Bond Correlation) 2D NMR analysis was then used to unambiguously establish the structure of **3a** (*Vide infra*). Compounds **3b-d** were synthesized in good yield (70-85%) and characterized by analogous procedures. Details about the specific reaction conditions used are given in the Experimental Section. The good regioselectivity of this reaction can be attributed to the low nucleophilic reactivity of the 5-OH.

The tetraacetyl isomer of quercetin with a free 7-OH (**4**) was instead prepared with high regioselectivity via imidazole-promoted hydrolysis of pentaester **2a** (equation 1). Selective deacylation to free the 7-OH group has been reported by Needs and Williamson [26] and Shin et al. [27] for daidzen and chrysin, respectively, which have only two hydroxyls. Recently Li et al. [28] performed the selective deacylation at 7-OH of pentahexanoyl quercetin using imidazole-catalyzed acyl transfer to an aromatic thiol under basic conditions. In our reaction, without thiols, using 0.2, 1 or 2 equivalents of imidazole produced compound 4 in 14, 44 and 87% isolated yield, respectively. Position 7 is preferentially involved presumably because the 7-OH is the most acidic hydroxyl of quercetin [29]. The assignment of the single free hydroxyl group in 4 is consistent with the observed differences in the chemical shifts of ring protons (Table 1) and was unambiguously established by combined HSQC and HMBC spectra (Figure 1 and 2).

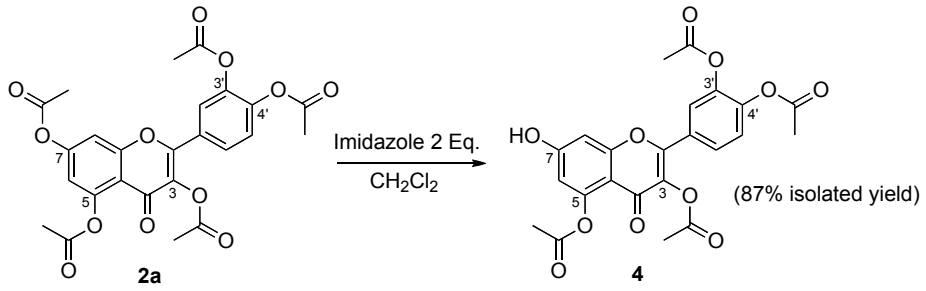

Compound 4 is a useful starting material. Two applications are described below dealing with a new synthesis of rhamnetin (7-*O*-methylquercetin) (**6**) and with the development of a new mitochondria-targeted derivative, 7-*O*-(4-triphenylphosphoniumbutyl) quercetin iodide (**9**).

HSQC and HMBC spectra were obtained in order to confirm the structures of **4** and **3a**. The 2D maps of the relevant spectral regions are shown in Fig.s 1 and 2 (the ^{13}C spectra displayed as a trace in the indirect dimension were obtained with the UDEFT pulse scheme) [30]. The singlet at 8 ppm in the spectrum of 4 clearly belongs to an exchangeable proton, since it has been found experimentally that trace amounts of water in the solvent mixture change both its lineshape and its position. From the HMBC spectrum (Figure 1, red) it is clear that this proton bears long-range correlations with both 6-C and 8-C (whatever their absolute assignment is) as demonstrated by the superimposed HSQC spectrum (black). This evidence is only compatible with structure **4**.

As a counterproof, in the HMBC spectrum of **3a** (Fig. 2), the OH proton appearing at 12.1 ppm bears a long-range correlation with 6-H, thus confirming the proposed structure. In this case the distinction between 6-H and 8-H is unambiguous, since the only proton-bearing carbon seen by the OH in the HMBC is 6-C, whose corresponding 6-H lies at 6.6 ppm as measured from the HSQC. Moreover, the cross peak between 5-C and the signal at 6.6 ppm of the ^{1}H spectrum indicates that this resonance indeed belongs to 6-H. Finally, a cross peak between 8-H and 9-C is observed at 156.2 ppm for **3a** and 158.2 ppm for **4**, which further helps to solve the ambiguity in the assignment of 8-H and 6-H.

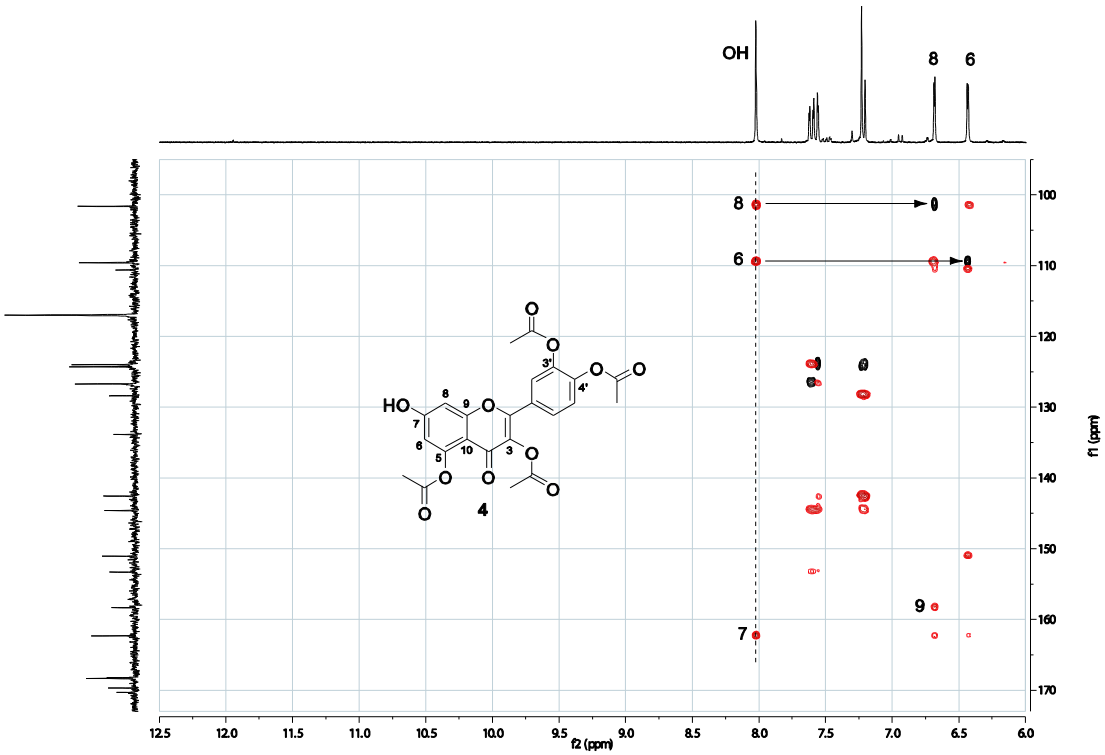

Figure 1. HSQC (black) and HMBC (red) spectra of **4**.

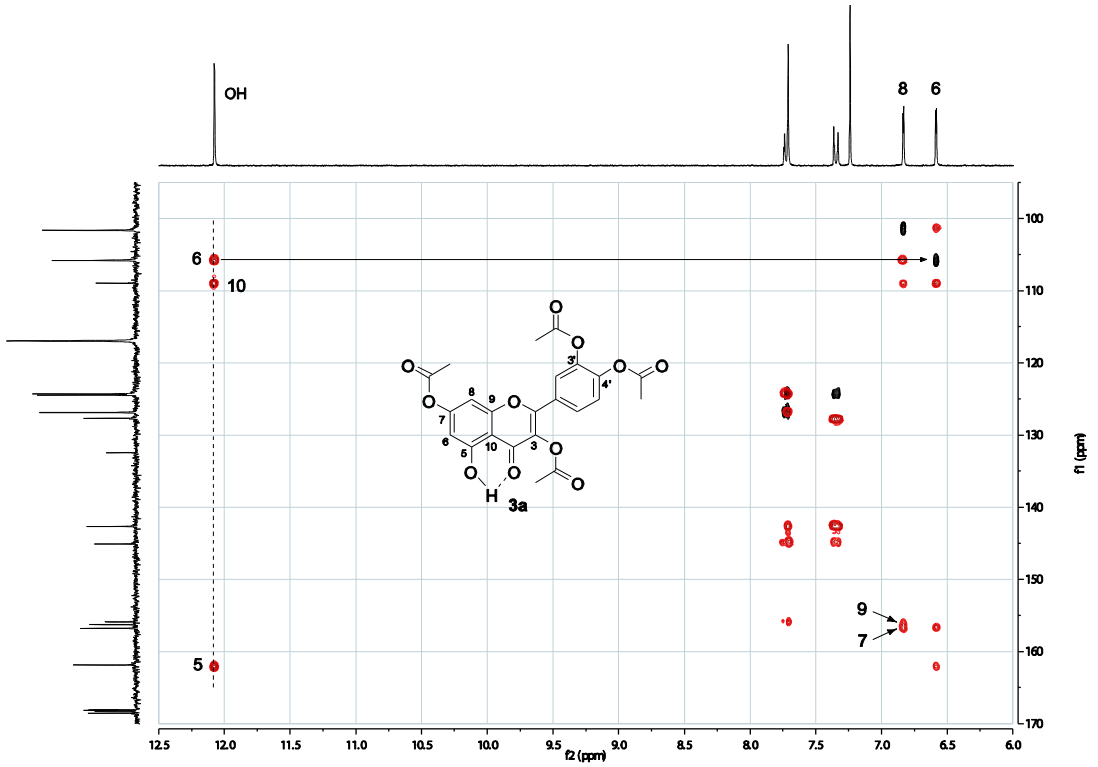

Figure 2. HSQC (black) and HMBC (red) spectra of **3a**.

Methylation of **4** followed by hydrolysis under acidic conditions afforded rhamnetin (**6**) in 67% overall yield (Scheme 2).

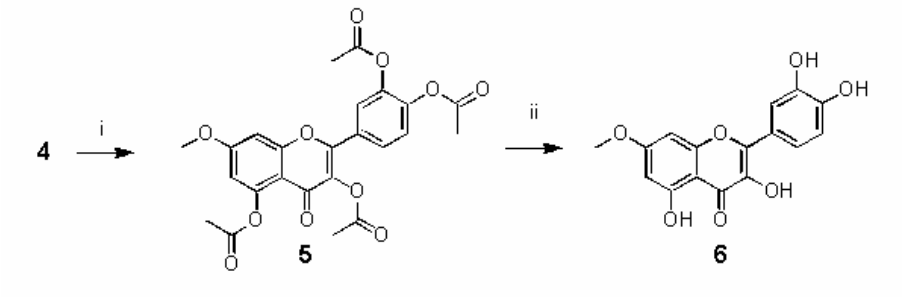

i) CH_3I (1.1 eq), K_2CO_3 (1 eq) in DMF; ii) conc. HCl/CH_3CN (1:2), reflux

Scheme 2. Synthesis of rhamnetin (**6**)

The intermediate product **5**, isolated by flash chromatography, contained some *O*-dimethyl derivative (about 20% by NMR analysis). It was used as such, without further purification, in the next step since we found that the final product **6** is easily separated by chromatography from any *O*-dimethylquercetins. In contrast, it is important to remove any unreacted **4** prior to the hydrolysis step to avoid the formation of quercetin which is almost impossible to separate from the major product **6** via silica gel flash chromatography. Our procedure, which converts quercetin to rhamnetin in four steps with an overall yield of 46%, is a considerable improvement over a previously reported synthesis also starting from quercetin [21]. The previous procedure requires two consecutive protection steps, the first for the *ortho*-dihydroxyl groups of the B ring, the second for the 3-OH, followed by methylation and two deprotection steps to yield the target compound in 11% overall yield.

The new mitochondriotropic derivative **9** was synthesized from **4** in three steps as outlined in Scheme 3.

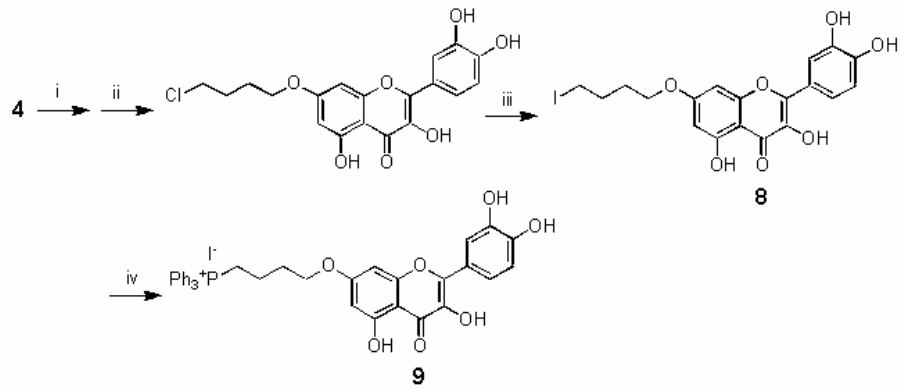

i) $Cl(CH_2)_4Br$ (1.2 eq), K_2CO_3 (1 eq), DMF, R.T.; ii) conc. HCl/CH_3CN (1:2), reflux; iii) saturated NaI in acetone, reflux; iv) PPh_3 (5 eq), toluene, 95 °C

Scheme 3. Synthesis of 7-O-(4-triphenylphosphoniumbutyl) quercetin iodide (**9**).

The synthesis involved one-pot O-alkylation of **4** to introduce the chlorobutyl group and complete deacetylation to yield 7-O-(4-butylchloro)-quercetin (**7**) in 61% yield. The triphenyl phosphonium (TPP^+) cation was then introduced via two consecutive nucleophilic substitution reactions first to replace chloride by iodide (giving **8** in 90% yield) and then to replace iodide by triphenylphosphine (giving **9** in 73% yield). This two-step procedure allowed us to avoid the high temperatures required by the direct –Cl → –$PPh_3^+I^-$ conversion, which were found to lead to some product decomposition.

Conclusions

Basic procedures and inexpensive and common reagents for esterification and ester hydrolysis were adapted to achieve the regioselective synthesis of quercetin tetraesters bearing the single free OH group either on 5-C or on 7-C. Selective hydrolysis of pentaacetyl quercetin to 3,3',4',5-tetraacetyl quercetin (**4**) formed the basis for a new, relatively easy synthesis of rhamnetin (**6**) and for the development of a new quercetin derivative of biomedical interest, the mitochondria-targeted 7-O-(4-triphenylphosphoniumbutyl) quercetin iodide (**9**). The cation of **9** is expected to accumulate into cells and mitochondria under the influence of the negative- inside transmembrane potential difference maintained across the cellular and inner mitochondrial membrane. Compound **9** is an isomer of already available 3-O-(4-triphenylphosphoniumbutyl) quercetin iodide [10], with which it may be compared in terms of redox reactivity and biological effects. The properties and effects of the two isomers differ significantly (Chapter 5 and 6), and the comparison will allow an informed choice of the most suitable compound to be tested in experimental models of pathophysiological relevance. The approaches used for the production of these quercetin derivatives may be easily extended to the regioselective modification of other flavonoids.

Experimental section

Materials and instrumentation:

Starting materials and reagents were purchased from Aldrich, Fluka, Merck-Novabiochem, Riedel de Haen, J.T. Baker, Cambridge Isotope Laboratories Inc., Acros Organics, Carlo Erba and Prolabo, and were used as received. ^1H and ^{13}C NMR spectra were recorded with a Bruker AC 250F spectrometer or a Bruker Avance DRX 300 spectrometer. Chemical shifts (δ) are given in ppm relative to the residual signal of the solvent (for ^1H: $CDCl_3$: δ =

7.26 ppm, DMSO-d_6: δ = 2.50 ppm, DMF-d_6: δ = 8.03 ppm, CD_3CN: δ = 1.94 ppm; for ^{13}C: $CDCl_3$: δ = 77.00 ppm, DMSO-d_6: δ = 39.52 ppm, DMF-d_6: δ = 29.76 ppm, CD_3CN: δ = 1.32 ppm). Mass spectra were performed with an Agilent Technologies MSD SL Trap mass spectrometer with ESI source coupled with a 1100 Series HPLC system. TLCs were run on silica gel supported on plastic (Macherey-Nagel Polygram®SIL G/UV_{254}, silica thickness 0.2 mm), or on silica gel supported on glass (Fluka) (silica thickness 0.25 mm, granulometry 60Å, medium porosity) and visualized by UV detection. Flash chromatography was performed on silica gel (Macherey-Nagel 60, 230-400 mesh granulometry (0.063-0.040 mm)) under air pressure. The solvents were analytical or synthetic grade and were used without further purification. Elemental analyses were performed by the Microanalysis Laboratory of the Dept. of Chemical Sciences of the University of Padova with a Fison EA1108 CHNS Analyzer.

HSQC and HMBC spectra. Spectra were obtained using a Bruker Avance DRX 300 spectrometer equipped with a 5-mm BBO *z*-gradient inverse probe. The experiments were conducted with 20 mM solutions in 1:5 CD_3CN:$CDCl_3$ (chosen to insure solubility during analysis). ^{13}C spectra were obtained with the UDEFT pulse scheme [30].

Synthetic procedures

Synthesis of 3,3',4',5,7-pentaacyl quercetins and 3,3',4',7-tetraacyl quercetins.

2-(3,4-diacetoxyphenyl)-4-oxo-4H-chromene-3,5,7-triyl triacetate (2a): Compound 2a was synthesized from 1, slightly modifying literature procedures [8,23]. Briefly, quercetin (1) (1.00 g, 3.0 mmol, 1 equiv.), acetic anhydride (6.13 g, 60.0 mmol, 20 equiv.) and pyridine (15 mL) were heated to reflux and stirred for 5 h. Ice-water (50 g) was added to the warm mixture. The resulting precipitate was filtered and washed with cold ethyl acetate to afford 2a as a white solid (1.22 g, 79% yield). ^1H NMR (250 MHz, DMSO-d_6, 25 °C): δ = 2.32 (s, 3H, CH_3), 2.34 (s, 12H, 4 × CH_3), 7.16 (d, $^4J_{H,H}$ = 2.2 Hz, 1 H, 6-H), 7.52 (d, $^3J_{H,H}$ = 8.6 Hz, 1 H, 5'-H), 7.64 (d, $^4J_{H,H}$ = 2.2 Hz, 1 H, 8-H), 7.35-7.65 (m, 2H, 2'-H, 6'-H) ppm. ^{13}C NMR (250 MHz, $CDCl_3$, 25 °C): δ = 170.0, 169.3, 167.9, 167.8, 167.8, 167.8, 156.8, 154.2, 153.7, 150.4, 144.4, 142.2, 134.0, 127.8, 126.4, 123.9, 123.8, 114.7, 113.9, 109.0, 21.2, 21.0, 20.7, 20.5 ppm. MS (ESI-MS): m/z 513, $[M+H]^+$. $C_{25}H_{20}O_{12}$: calcd. C 58.60, H 3.93; found C 58.62, H 3.97.

4-(3,7-diacetoxy-5-hydroxy-4-oxo-4H-chromen-2-yl)-1,2-phenylene diacetate (3a): 1 (1.00 g, 3.0 mmol, 1.0 equiv.) was dissolved in CH_2Cl_2 (20 mL) and pyridine (5 mL).

Acetic anhydride (1.53 g, 15.0 mmol, 5.0 equiv.) was then added dropwise and the mixture was stirred at room temperature for 3 hours. The obtained solution was diluted in CH_2Cl_2 (150 mL) and washed with 3 M aq. HCl (3 × 100 mL). The organic layer was then dried over $MgSO_4$, and filtered. The solvent was evaporated under reduced pressure and the residue was purified by silica gel flash chromatography (eluent CH_2Cl_2/hexane/ethyl acetate, 9:2:1) to afford 3a as a yellow solid (1.06 g, 75% yield). ^{1}H NMR (250 MHz, $CDCl_3$, 25 °C): δ = 2.34 (m, 9H, 3 × CH_3), 2.37 (s, 3H, CH_3), 6.60 (d, $^4J_{H,H}$ = 2.0 Hz, 1 H, 6-H), 6.85 (d, $^4J_{H,H}$ = 2.0 Hz, 1 H, 8-H), 7.36 (d, $^3J_{H,H}$ = 9.0 Hz, 1 H, 5'-H), 7.73-7.77 (m, 2H, 2'-H, 6'-H) ppm.^{13}C NMR (300 MHz, $CDCl_3$/CD_3CN (5:1), 25 °C): δ = 176.6, 168.5, 168.3, 168.1, 168.0, 161.8, 156.8, 156.3, 155.9, 145.1, 142.7, 132.5, 126.9, 124.5, 124.3, 117.0, 109.0, 105.8, 101.7, 21.3, 20.8, 20.6 ppm. MS (ESI-MS): m/z 471, $[M+H]^+$. $C_{23}H_{18}O_{11}$: calcd. C 58.73, H 3.86; found C 58.65, H 3.85.

2-(3,4-bis(isobutyryloxy)phenyl)-4-oxo-4H-chromene-3,5,7-triyl tris(2-methylpropanoate) (2b): isobutyric anhydride (4.75 g, 30.0 mmol, 10.0 equiv.) was added dropwise to a solution of 1 (1.00 g, 3.0 mmol, 1.0 equiv.) in pyridine (15 mL). The mixture was heated to reflux and stirred for 2 hours. The obtained solution was diluted in CH_2Cl_2 (150 mL) and washed with 3 M aq. HCl (6 × 100 mL). The organic layer was then dried over $MgSO_4$, and filtered. The solvent was evaporated under reduced pressure. The purification of the resulting residue by silica gel flash chromatography (eluent: CH_2Cl_2/hexane/ethyl acetate, 5:5:0.25) gave 2b as a pale yellow solid (1.90 g, 97% yield). ^{1}H NMR (250 MHz, CD_3CN, 25 °C): δ = 1.23-1.34 (m, 30H, 10 × CH_3), 2.79-2.94 (m, 5H, 5 × CH), 6.94 (d, $^4J_{H,H}$ = 2.2 Hz, 1 H, 6-H), 7.38-7.41 (m, 2 H, 8-H, 5'-H), 7.73 (d, $^4J_{H,H}$ = 2.0 Hz, 1 H, 2'-H), 7.81 (dd, $^3J_{H,H}$ = 8.8 Hz, $^4J_{H,H}$ = 2.2 Hz, 1 H, 6'-H) ppm. ^{13}C NMR (250 MHz, CD_3CN, 25 °C): δ = 175.9, 175.5, 175.3, 175.1, 174.8, 170.7, 157.9, 155.8, 154.5, 151.4, 145.9, 143.6, 134.8, 128.6, 127.6, 125.2, 124.7, 118.2, 115.5, 110.5, 34.9, 34.8, 34.7, 34.6, 34.5, 19.1, 19.0, 19.0, 18.9, 18.9 ppm. MS (ESI-MS): m/z 653, $[M+H]^+$. $C_{35}H_{40}O_{12}$: calcd. C 64.41, H 6.18; found C 64.45, H 6.22.

2-(3,4-bis(isobutyryloxy)phenyl)-5-hydroxy-4-oxo-4H-chromene-3,7-diyl bis(2-methylpropanoate) (3b): isobutyric anhydride (2.00 g, 12.6 mmol, 4.2 equiv.) was added dropwise to a solution of 1 (1.00 g, 3.0 mmol, 1.0 equiv.) in pyridine (15 mL). The mixture was stirred at 70°C for 1 hour. The obtained solution was diluted in CH_2Cl_2 (150 mL) and washed with 3 M aq. HCl (6 × 100 mL). The organic layer was then dried over $MgSO_4$, and filtered. The solvent was evaporated under reduced pressure and the resulting residue was purified by silica gel flash chromatography (eluent: CH_2Cl_2/hexane/ethyl acetate,

5:5:0.25) to afford 3b as a yellow solid (1.22 g, 70% yield). ^{1}H NMR (250 MHz, CD_3CN, 25 °C): δ = 1.24-1.30 (m, 24H, 8 × CH_3), 2.79-2.92 (m, 4H, 4 × CH), 6.61 (d, $^{4}J_{H,H}$ = 2.0 Hz, 1 H, 6-H), 6.92 (d, $^{4}J_{H,H}$ = 2.2 Hz, 1 H, 8-H), 7.41 (d, $^{3}J_{H,H}$ = 8.5 Hz, 1 H, 5'-H), 7.75 (d, $^{4}J_{H,H}$ = 2.2 Hz, 1 H, 2'-H), 7.82 (dd, $^{3}J_{H,H}$ = 8.8 Hz, $^{4}J_{H,H}$ = 2.2 Hz, 1 H, 6'-H) ppm. ^{13}C NMR (250 MHz, DMF-d_6, 25 °C): δ = 176.5, 174.7, 174.3, 174.1, 174.0, 161.4, 157.4, 156.4, 156.0, 145.7, 143.1, 132.3, 127.7, 127.3, 124.9, 108.6, 105.9, 102.3, 34.2, 34.0, 33.9, 18.7, 18.6, 18.5 ppm. MS (ESI-MS): m/z 583, $[M+H]^+$. $C_{31}H_{34}O_{11}$: calcd. C 63.91, H 5.88; found C 63.99, H 5.92.

2-(3,4-bis(pivaloyloxy)phenyl)-4-oxo-4H-chromene-3,5,7-triyl tris(2,2-dimethylpropanoate) (2c): 1 (1.00 g, 3.0 mmol, 1.0 equiv.) was dissolved in pyridine (15 mL). Pivaloyl chloride (3.62 g, 30.0 mmol, 10.0 equiv.) was then added dropwise and the mixture was heated to reflux and stirred for 2 hours. The obtained solution was diluted in CH_2Cl_2 (150 mL) and washed with 3 M aq. HCl (6 × 100 mL). The organic layer was then dried over $MgSO_4$, and filtered. The solvent was evaporated under reduced pressure. The purification of the resulting residue by silica gel flash chromatography (eluent: CH_2Cl_2/hexane/ethyl acetate, 9:1:0.5) gave 2c as a white solid (1.88 g, 87% yield). ^{1}H NMR (250 MHz, DMF-d_6, 25 °C): δ = 1.35-1.41 (m, 45H, 15 × CH_3), 7.27 (d, $^{4}J_{H,H}$ = 2.2 Hz, 1 H, 6-H), 7.64 (d, $^{3}J_{H,H}$ = 8.5 Hz, 1 H, 5'-H), 7.69 (d, $^{4}J_{H,H}$ = 2.2 Hz, 1 H, 8-H), 7.92 (d, $^{4}J_{H,H}$ = 2.0 Hz, 1 H, 2'-H), 8.01 (dd, $^{3}J_{H,H}$ = 8.8 Hz, $^{4}J_{H,H}$ = 2.2 Hz, 1 H, 6'-H) ppm. ^{13}C NMR (250 MHz, DMF-d_6, 25 °C): δ = 176.3, 176.1, 175.7, 175.6, 175.3, 169.8, 157.2, 155.6, 153.8, 151.1, 145.7, 143.2, 128.0, 127.1, 127.1, 124.9, 124.2, 115.0, 114.9, 110.2, 39.3, 39.3, 39.2, 39.1, 39.0, 27.0, 26.9, 26.9, 26.8, 26.7 ppm. MS (ESI-MS): m/z 723, $[M+H]^+$. $C_{40}H_{50}O_{12}$: calcd. C 66.47, H 6.97; found C 66.49, H 7.00.

2-(3,4-bis(pivaloyloxy)phenyl)-5-hydroxy-4-oxo-4H-chromene-3,7-diyl bis(2,2-dimethylpropanoate) (3c): pivalic anhydride (4.47 g, 24.0 mmol, 8.0 equiv.) was added dropwise to a solution of 1 (1.00 g, 3.0 mmol, 1.0 equiv.) in pyridine (15 mL). The mixture was heated to reflux and stirred for 45 minutes. The obtained solution was diluted in CH_2Cl_2 (150 mL) and washed with 3 M aq. HCl (6 × 100 mL). The organic layer was then dried over $MgSO_4$, and filtered. The solvent was evaporated under reduced pressure and the resulting residue was purified by silica gel flash chromatography (eluent: hexane/CH_2Cl_2/ethyl acetate, 9:1:0.5) to afford 3c as a pale green solid (1.62 g, 85% yield). ^{1}H NMR (250 MHz, DMF-d_6, 25 °C): δ = 1.36-1.38 (m, 36H, 12 × CH_3), 6.79 (d, $^{4}J_{H,H}$ = 2.0 Hz, 1 H, 6-H), 7.18 (d, $^{4}J_{H,H}$ = 2.2 Hz, 1 H, 8-H), 7.66 (d, $^{3}J_{H,H}$ = 8.5 Hz, 1 H, 5'-H), 7.94 (d, $^{4}J_{H,H}$ = 2.0 Hz, 1 H, 2'-H), 8.0 (dd, $^{3}J_{H,H}$ = 8.8 Hz, $^{4}J_{H,H}$ = 2.2 Hz, 1 H, 6'-H) ppm..

^{13}C NMR (250 MHz, DMF-d_6, 25 °C): δ = 176.6, 176.1, 175.7, 175.6, 175.4, 161.5, 157.7, 156.4, 156.0, 146.0, 143.2, 132.5, 127.7, 127.4, 125.0, 124.4, 108.6, 105.9, 102.3, 39.3, 39.3, 39.2, 39.1, 27.0, 26.9, 26.8, 26.7 ppm. MS (ESI-MS): m/z 639, $[M+H]^+$. $C_{35}H_{42}O_{11}$: calcd. C 65.82, H 6.63; found C 65.76, H 6.66.

2-(3,4-bis(benzoyloxy)phenyl)-4-oxo-4H-chromene-3,5,7-triyl tribenzoate (2d): 1 (1.00 g, 3.0 mmol, 1.0 equiv.) was dissolved in CH_2Cl_2 (20 mL) and pyridine (5 mL). Benzoyl chloride (4.22 g, 30.0 mmol, 10.0 equiv.) was then added dropwise and the mixture was stirred at room temperature for 3 hours. The obtained solution was diluted in CH_2Cl_2 (150 mL) and washed with 3 M aq. HCl (3 × 100 mL). The organic layer was then dried over $MgSO_4$, and filtered. The solvent was evaporated under reduced pressure and the resulting residue was purified by silica gel flash chromatography (eluent CH_2Cl_2/hexane/ethyl acetate, 5:5:0.5) to afford 2d as a white solid (2.4 g, 97% yield). ^{1}H NMR (250 MHz, DMF-d_6, 25 °C): δ = 7.49-7.83 (m, 15 H, Ar-H), 7.87 (d, $^3J_{H,H}$ = 8.5 Hz, 1 H, 5'-H), 8.01-8.08 (m, 5 H, Ar-H), 8.19-8.29 (m, 8 H, Ar-H), 8.43 (d, $^4J_{H,H}$ = 2.0 Hz, 1 H, 2'-H) ppm. ^{13}C NMR (250 MHz, DMF-d_6, 25 °C): δ = 168.8, 164.9, 164.4, 164.1, 163.9, 163.6, 157.4, 155.5, 154.5, 150.7, 145.6, 143.4, 134.8, 134.7, 134.6, 134.5, 134.2, 133.1, 130.6, 130.5, 130.4, 130.2, 130.2, 129.8, 129.7, 129.4, 129.4, 129.3, 129.1, 128.9, 128.9, 128.6, 128.5, 128.4, 128.4, 127.7, 125.1, 124.6, 115.8, 115.2, 111.0 ppm. MS (ESI-MS): m/z 823, $[M+H]^+$. $C_{50}H_{30}O_{12}$: calcd. C 72.99, H 3.67; found C 72.98, H 3.63.

4-(3,7-bis(benzoyloxy)-5-hydroxy-4-oxo-4H-chromen-2-yl)-1,2-phenylene dibenzoate (3d): 1 (1.00 g, 3.0 mmol, 1.0 equiv.) was dissolved in CH_2Cl_2 (20 mL) and pyridine (5 mL). Benzoyl chloride (1.77 g, 12.6 mmol, 4.2 equiv.) was then added dropwise and the mixture was stirred at room temperature for 2 hours. The obtained solution was diluted in CH_2Cl_2 (150 mL) and washed with 3 M aq. HCl (3 × 100 mL). The organic layer was then dried over $MgSO_4$, and filtered. The solvent was evaporated under reduced pressure. The purification of the resulting residue by silica gel flash chromatography (eluent: CH_2Cl_2/hexane/ethyl acetate (5:5:0.5)) gave 3d as a pale yellow solid (1.55 g, 72% yield). ^{1}H NMR (250 MHz, DMF-d_6, 25 °C): δ = 7.08 (d, $^4J_{H,H}$ = 2.0 Hz, 1 H, 6-H), 7.49-7.57 (m, 5 H, Ar-H), 7.65-7.75 (m, 6 H, Ar-H), 7.80-7.82 (m, 2 H, Ar-H), 7.88 (d, $^3J_{H,H}$ = 8.5 Hz, 1 H, 5'-H), 8.02-8.06 (m, 4 H, Ar-H), 8.22-8.33 (m, 5 H, Ar-H), 8.44 (d, $^4J_{H,H}$ = 2.0 Hz, 1 H, 2'-H) ppm. ^{13}C NMR (250 MHz, DMF-d_6, 25 °C): δ = 176.6, 164.4, 164.0, 163.9, 163.8, 161.6, 157.5, 156.6, 156.4, 151.1, 145.9, 143.4, 135.0, 134.7, 134.6, 132.7, 130.7, 130.4, 130.2, 130.2, 129.5, 129.4, 129.3, 129.1, 128.6, 128.5, 128.3, 128.2, 127.9, 125.2, 124.8,

108.9, 106.3, 102.8 ppm. MS (ESI-MS): m/z 719, $[M+H]^+$. $C_{43}H_{26}O_{11}$: calcd. C 71.86, H 3.65; found C 71.79, H 3.61.

Synthesis of 4-(3,5-diacetoxy-7-hydroxy-4-oxo-4H-chromen-2-yl)-1,2-phenylene diacetate (4): A solution of imidazole (0.05 g, 0.78 mmol, 2.00 equiv.) in CH_2Cl_2 (5 mL) was added dropwise to a solution of 2a (0.20 g, 0.39 mmol, 1.00 equiv.) in CH_2Cl_2 (10 mL) at –15 °C in an ice/acetone bath. The resulting solution was allowed to warm to room temperature and stirred for 2 hours. The reaction mixture was diluted in CH_2Cl_2 (50 mL) and washed with 3 M aq. HCl (3 × 50 mL). The organic layer was then dried over $MgSO_4$, and filtered. The solvent was evaporated under reduced pressure. The purification of the resulting residue by silica gel flash chromatography (eluent: $CHCl_3$/methanol, 97:3) gave 4 as a white solid (0.16 g, 87% yield). ^{1}H NMR (300 MHz, $CDCl_3/CD_3CN$ 5:1, 25 °C): δ = 2.23-2.30 (m, 9H, 3 × CH_3), 2.34 (s, 3H, CH_3), 6.48 (d, $^4J_{H,H}$ = 2.2 Hz, 1 H, 6-H), 6.74 (d, $^4J_{H,H}$ = 2.2 Hz, 1 H, 8-H), 7.26 (d, $^3J_{H,H}$ = 9.0 Hz, 1 H, 5'-H), 7.60-7.67 (m, 2H, 2'-H, 6'-H) ppm. ^{13}C NMR (300 MHz, $CDCl_3/CD_3CN$ (5:1), 25 °C): δ = 170.31, 169.67, 168.32, 168.2, 162.3, 158.3, 153.3, 151.1, 144.6, 142.6, 133.9, 128.4, 126.7, 124.3, 124.0, 117.0, 110.6, 109.6, 101.6, 21.3, 20.9, 20.7 ppm. MS (ESI-MS): m/z 471, $[M+H]^+$. $C_{23}H_{18}O_{11}$: calcd. C 58.73, H 3.86; found C 58.68, H 3.83.

Synthesis of 2-(3,4-dihydroxyphenyl)-3,5-dihydroxy-7-methoxy-4H-chromen-4-one (6): a solution of methyl iodide (0.13 g, 0.95 mmol, 1.1 equiv.) in DMF (10 mL) was added dropwise to a solution of 4 (0.4 g, 0.85 mmol, 1 equiv.) and potassium carbonate (0.12 g, 0.85 mmol, 1.0 equiv.) in DMF (20 mL). The mixture was stirred at –78 °C in a bath of dry ice/acetone for 10 minutes and then allowed to warm and stirred for 12 hours at room temperature. The reaction mixture was diluted in CH_2Cl_2 (100 mL) and washed with 3 M aq. HCl (6 × 100 mL). The organic layer was then dried over $MgSO_4$, and filtered. The solvent was evaporated under reduced pressure. The purification of the resulting residue by silica gel flash chromatography (eluent: $CHCl_3$/ethyl acetate, 7:3) gave a white solid (0.38 g) composed of 5 and of a dimethylated product in 8:2 ratio, as determined by NMR analysis. ^{1}H NMR (250 MHz, DMSO-d_6, 25 °C, signals of 5): δ = 2.27-2.34 (m, CH_3), 3.93 (s, OCH_3), 6.87 (d, $^4J_{H,H}$ = 2.2 Hz, 6-H), 6.30 (d, $^4J_{H,H}$ = 2.5 Hz, 8-H), 7.53 (d, $^3J_{H,H}$ = 9.2 Hz, 5'-H), 7.83-7.90 (m, 2'-H, 6'-H) ppm. MS (ESI-MS): m/z 485, $[M+H]^+$, m/z 457, $[M'+H]^+$. Without further purification, crude 5 (0.30 g) was added to a solution of acetonitrile (20 mL) and 6 M aq. HCl (10 mL). The resulting solution was stirred and refluxed for 1.5 hours. Then ethyl acetate (100 mL) and water (100 mL) were added. The organic layer was washed with 3 M aq. HCl (3 × 100 mL), dried over $MgSO_4$, and filtered.

The solvent was evaporated under reduced pressure and the purification of the resulting residue by silica gel flash chromatography (eluent: $CHCl_3$/methanol, 9:1) gave 6 as a bright yellow solid (0.14 g, 67% yield with respect to 4). ^{1}H NMR (250 MHz, DMSO-d_6, 25 °C): δ = 3.86 (s, 3H, OCH_3), 6.35 (d, $^4J_{H,H}$ = 2.0 Hz, 1 H, 6-H), 6.70 (d, $^4J_{H,H}$ = 2.0 Hz, 1 H, 8-H), 6.89 (d, $^3J_{H,H}$ = 8.5 Hz, 1 H, 5'-H), 7.58 (dd, $^3J_{H,H}$ = 8.5 Hz, $^4J_{H,H}$ = 2.0 Hz, 1 H, 6'-H), 7.73 (d, $^4J_{H,H}$ = 2.0 Hz, 1 H, 2'-H) ppm. ^{13}C NMR (250 MHz, DMSO-d_6, 25 °C): δ = 175.9, 164.8, 160.3, 156.0, 147.8, 147.2, 145.0, 136.0, 121.8, 119.9, 115.5, 115.1, 103.9, 97.4, 91.8, 55.9 ppm. MS (ESI-MS): m/z 317, $[M+H]^+$. $C_{16}H_{12}O_7$: calcd. C 60.76, H 3.82; found C 60.72, H 3.80.

Synthesis of 7-(4-chlorobutoxy)-2-(3,4-dihydroxyphenyl)-3,5-dihydroxy-4H-chromen-4-one (7). 1-Bromo-4-chlorobutane (0.62 g, 3.59 mmol, 1.20 equiv) and potassium carbonate (0.413 g, 2.97 mmol, 1.00 equiv.) were added to a solution of 4 (1.39 g, 2.97 mmol, 1.00 equiv.) in DMF (20 mL) under nitrogen and stirred overnight at R.T. The reaction mixture was diluted in CH_2Cl_2 (100 mL) and washed with 3 M aq. HCl (3 × 100 mL). The organic layer was then dried over $MgSO_4$ and filtered. The solvent was evaporated under reduced pressure. Without further purification, the crude product was added to a mixture of acetonitrile (60 mL) and 3 M aq. HCl (30 mL). The resulting solution was stirred and refluxed for 1 hour, and then ethyl acetate (100 mL) and water (100 mL) were added. The organic layer was washed with 3 M aq. HCl (3 × 100 mL), dried over $MgSO_4$, and filtered. The solvent was evaporated under reduced pressure and the purification of the resulting residue by silica gel flash chromatography (eluent: toluene/methanol, 8:2) gave 7 as a bright yellow solid (0.71 g, 61% yield). ^{1}H NMR (250 MHz, DMSO-d_6, 25 °C): δ = 1.80-2.01 (m, 4H, 2 × CH_2), 3.66-3.80 (m, 2H, CH_2), 4.00-4.22 (m, 2H, CH_2), 6.34 (d, $^4J_{H,H}$ = 2.2 Hz, 1 H, 6-H), 6.70 (d, $^4J_{H,H}$ = 2.0 Hz, 1 H, 8-H), 6.89 (d, $^3J_{H,H}$ = 8.5 Hz, 1 H, 5'-H), 7.57 (dd, $^3J_{H,H}$ = 8.5 Hz, $^4J_{H,H}$ = 2.0 Hz, 1 H, 6'-H), 7.73 (d, $^4J_{H,H}$ = 2.0 Hz, 1 H, 2'-H) ppm. ^{13}C NMR (250 MHz, DMSO-d_6, 25 °C): δ = 175.5, 163.7, 159.9, 155.6, 147.4, 146.8, 144.6, 135.6, 121.5, 119.6, 115.1, 114.8, 103.6, 97.4, 91.9, 67.3, 44.7, 28.3, 25.5 ppm. MS (ESI-MS): m/z 393, $[M+H]^+$. $C_{19}H_{17}ClO_7$: calcd. C 58.10, H 4.36; found C 58.18, H 4.41.

Synthesis of 7-(4-iodobutoxy)-2-(3,4-dihydroxyphenyl)-3,5-dihydroxy-4H-chromen-4-one (8): Compound 7 (0.50 g, 1.27 mmol, 1 equiv.) was added to a saturated solution of NaI in dry acetone (20 mL) and heated at reflux for 20 h. After cooling, the resulting mixture was diluted in EtOAc (100 mL), filtered and washed with water (3 × 30 mL). The organic layer was dried over $MgSO_4$ and filtered. The solvent was evaporated under

reduced pressure to afford the product in 90% yield after flash chromatography using $CHCl_3$:Acetone 7:3. ^1H NMR (250 MHz, DMSO-d_6, 25 °C): δ = 1.71-1.98 (m, 4H, 2 × CH_2), 3.24-3.43 (m, 2H, CH_2), 4.06-4.23 (m, 2H, CH_2), 6.32 (d, $^4J_{H,H}$ = 2.2 Hz, 1 H, 6-H), 6.70 (d, $^4J_{H,H}$ = 2.0 Hz, 1 H, 8-H), 6.89 (d, $^3J_{H,H}$ = 8.5 Hz, 1 H, 5'-H), 7.57 (dd, $^3J_{H,H}$ = 8.5 Hz, $^4J_{H,H}$ = 2.0 Hz, 1 H, 6'-H), 7.73 (d, $^4J_{H,H}$ = 2.0 Hz, 1 H, 2'-H) ppm. ^{13}C NMR (250 MHz, DMSO-d_6, 25 °C): δ = 175.8, 164.0, 160.3, 155.9, 147.7, 147.1, 145.0, 141.5, 135.9, 121.8, 119.9, 115.5, 115.2, 103.9, 92.3, 67.3, 29.5, 29.3, 8.3 ppm. MS (ESI-MS): m/z 485, $[M+H]^+$. $C_{19}H_{17}IO_7$: calcd. C 47.13, H 3.54; found C 47.16, H 3.59.

Synthesis of 7-(4-triphenylphosphoniumbutoxy)-2-(3,4-dihydroxyphenyl)-3,5-dihydroxy-4H-chromen-4-one iodide (9): A mixture of 8 (300 mg, 0.63 mmol, 1 equiv.) and triphenylphosphine (0.825 g, 3.15 mmol, 5 eq.) in toluene (15 mL) was heated at 95°C under argon. After 3 h, the solvent was eliminated at reduced pressure and the resulting yellow solid was dissolved in the minimum volume of dichloromethane (1 mL) and precipitated with diethyl ether (5 × 50 mL). The solvents were decanted after each precipitation. Residual solvent was then removed under reduced pressure to afford compound 6 in 73% yield. ^1H NMR (250 MHz, DMSO-d_6, 25 °C): δ = 1.64-1.80 (m, 2H, CH_2), 1.88-2.00 (m, 2H, CH_2), 3.60-3.73 (m, 2H, CH_2), 4.13-4.20 (m, 2H, CH_2), 6.28 (d, $^4J_{H,H}$ = 2.0 Hz, 1 H, 6-H), 6.66 (d, $^4J_{H,H}$ = 2.0 Hz, 1 H, 8-H), 6.89 (d, $^3J_{H,H}$ = 8.5 Hz, 1 H, 5'-H), 7.55 (dd, $^3J_{H,H}$ = 8.5 Hz, $^4J_{H,H}$ = 2.0 Hz, 1 H, 6'-H), 7.72-7.93 (m, 16 H: 15 H = PPh_3, 1 H = 2'-H) ppm. ^{13}C NMR (250 MHz, DMSO-d_6, 25 °C): δ = 175.7, 163.7, 160.1, 155.8, 147.6, 147.1, 144.8, 135.8, 134.9 (Ph, $^4J(^{13}C/^{31}P)$ = 2.8 Hz), 133.4 (Ph, $^3J(^{13}C/^{31}P)$ = 10.1 Hz), 130.0 (Ph, $^2J(^{13}C/^{31}P)$ = 12.3 Hz), 121.6, 119.7, 118.1 (Ph, $^1J(^{13}C/^{31}P)$ = 86.1 Hz), 115.3, 115.1, 103.8, 97.5, 92.2, 74.1, 28.5, 19.1, 18.2 ppm. MS (ESI-MS): m/z 619, $[M]^+$. $C_{37}H_{32}IO_7P$: calcd. C 59.53, H 4.32; found C 59.60, H 4.30.

Bibliography

[1] Bischoff, S.C. Quercetin: potentials in the prevention and therapy of disease. Curr. Opin. Clin. Nutr. Metab. Care **2008,** 11, 733-740.

[2] Murakami, A.; Ashida, H.; Terao, J. Multitargeted cancer prevention by quercetin. Cancer Lett. **2008**, 269, 315-325.

[3] Boots, A.W.; Haenen, G.R.; Bast, A. Health effects of quercetin: from antioxidant to nutraceutical. Eur. J. Pharmacol. **2008**, 585, 325-337.

[4] Hirpara, K.V.; Aggarwal, P.; Mukherjee, J.; Joshi, N.; Burman, A.C. Quercetin and its derivatives: synthesis, pharmacological uses with special emphasis on anti-tumor properties and prodrug with enhanced bio-availability. Anticancer Agents Med. Chem. **2009**, 9, 138-161.

[5] Manach, C.; Williamson, G.; Morand, C.; Scalbert, A.; Rémésy, C. Bioavailability and bioefficacy of polyphenols in humans. I. Review of 97 bioavailability studies. Am. J. Clin. Nutr. **2005**, 81 (Suppl. 1), 230S-242S.
[6] Williamson, G.; Manach, C. Bioavailability and bioefficacy of polyphenols in humans. II. Review of 93 intervention studies. Am. J. Clin. Nutr. **2005**, 81 (Suppl. 1), 243S-255S.
[7] Silberberg, M.; Morand, C.; Mathevon, T.; Besson, C.; Manach, C.; Scalbert, A., Rémésy, C. The bioavailability of polyphenols is highly governed by the capacity of the intestine and of the liver to secrete conjugated metabolites. Eur. J. Nutr. **2006**, 45, 88-96.
[8] Biasutto, L.; Marotta, E.; De Marchi, U.; Zoratti, M.; Paradisi, C. Ester-based precursors to increase the bioavailability of quercetin. J. Med. Chem. **2007**, 50, 241-253.
[9] Biasutto, L.; Marotta, E.; Mattarei, A.; Beltramello, S.; Caliceti, P.; Salmaso, S.; Bernkop-Schnürch, A.; Garbisa, S.; Zoratti, M.; Paradisi, C. Absorption and metabolism of resveratrol carboxyesters and methanesulfonate by explanted rat intestinal segments. Cell. Physiol. Biochem. **2009**, 24, 557-566.
[10] Mattarei, A.; Biasutto, L.; Marotta, E.; De Marchi, U.; Sassi, N.; Garbisa, S.; Zoratti, M.; Paradisi, C. A mitochondriotropic derivative of quercetin: a strategy to increase the effectiveness of polyphenols. ChemBioChem **2008**, 16, 2633-2642.
[11] Biasutto, L.; Mattarei, A.; Marotta, E.; Bradaschia, A.; Sassi, N.; Garbisa, S.; Zoratti, M.; Paradisi, C. Development of mitochondria-targeted derivatives of resveratrol. Bioorg. Med. Chem. Lett. **2008**, 18, 5594-5597.
[12] Biasutto, L.; Sassi, N.; Mattarei, A.; Marotta, E.; Cattelan, P.; Toninello, A.; Garbisa, S.; Zoratti, M.; Paradisi, C. Impact of mitochondriotropic quercetin derivatives on mitochondria. Biochim. Biophys. Acta **2010**, 1797, 189-196.
[13] Hoye, A.T.; Davoren, J.E.; Wipf, P.; Fink, M.P.; Kagan, V.E. Targeting mitochondria. Acc. Chem. Res. **2008**, 41, 87-97.
[14] Murphy, M.P.; Smith, R.A. Targeting antioxidants to mitochondria by conjugation to lipophilic cations. Annu. Rev. Pharmacol. Toxicol. **2007**, 47, 629-656.
[15] Murphy, M.P. Targeting lipophilic cations to mitochondria. Biochim. Biophys. Acta **2008**, 1777, 1028-1031.
[16] Skulachev, V.P.; Anisimov, V.N.; Antonenko, Y.N.; Bakeeva, L.E.; Chernyak, B.V.; Erichev, V.P.; Filenko, O.F.; Kalinina, N.I.; Kapelko, V.I.; Kolosova, N.G.; Kopnin, B.P.; Korshunova, G.A.; Lichinitser, M.R.; Obukhova, L.A.; Pasyukova, E.G.; Pisarenko, O.I.; Roginsky, V.A.; Ruuge, E.K.; Senin, I.I.; Severina, I.I.; Skulachev, M.V.; Spivak, I.M.; Tashlitsky, V.N.; Tkachuk, V.A.; Vyssokikh, M.Y.; Yaguzhinsky, L.S.; Zorov, D.B. An attempt to prevent senescence: a mitochondrial approach. Biochim. Biophys. Acta **2009**, 1787, 437-461.
[17] Metodiewa, D.; Jaiswal, A.K.; Cenas, N.; Dickancaité, E. Quercetin may act as a cytotoxic prooxidant afyer its metabolic activation to semiquinone and quinoidal product. Free Radic. Biol. Med. **1999**, 26, 107-116.
[18] Sarno, S.; Moro, S.; Meggio, F.; Zagotto, G.; Dal Ben, D.; Ghibellini, P.; Battistutta, R.; Zanotti, G.; Pinna, L.A. Toward the rational design of protein kinase casein kinase-2 inhibitors. Pharmacol. Ther. **2002**, 93, 159-168.
[19] van Dijk, C.; Driessen, A.; Recourt, K. The uncoupling efficiency and affinity of flavonoids for vesicles. Biochem. Pharmacol. **2000**, 60, 1593–1600.
[20] Montenegro, L.; Carbone, C.; Maniscalco, C.; Lambusta, D.; Nicolosi, G.; Ventura, C.A.; Puglisi, G. In vitro evaluation of quercetin-3-O-acyl esters as topical drugs. Int. J. Pharm. **2007**, 336, 257-262.
[21] Bouktaib, M.; Lebrun, S.; Atmani, A.; Rolando, C. Hemisynthesis of all the O-monomethylated analogues of quercetin including the major metabolites, through selective protection of phenolic functions. Tetrahedron **2002**, 58, 10001-10009.

[22] Hodnick, W.F.; Duval, D.L.; Pardini, R.S. Inhibition of mitochondrial respiration and cyanide-stimulated generation of reactive oxygen species by selected flavonoids. Biochem. Pharmacol. **1994**, 47, 573-80.
[23] Picq, M.; Prigent, A.F.; Némoz, G.; André, A.C.; Pacheco, H. Pentasubstituted quercetin analogues as selective inhibitors of particulate 3':5'-cyclic-AMP phosphodiesterase from rat brain. J. Med. Chem. **1982**, 25, 1192-1198.
[24] Op de Beck, P.; Dijoux, M.G.; Cartier, G.; Mariotte, A.-M. Quercitrin-3'-sulphate from leaves of Leea guinensis. Phytochemistry **1998**, 47, 1171-1173.
[25] Rietjens, I.M.; Awad, H.M.; Boersma, M.G.; van Iersel, M.L.; Vervoort, J.; Van Bladeren, P.J. Structure activity relationship for the chemical behaviour and toxicity of electrophilic quinones/quinone methides. Adv. Exp. Med. Biol. **2001**, 500, 11-21.
[26] Needs, P.W.; Williamson, G. Syntheses of daidzein-7-yl beta-D-glucopyranosiduronic acid and daidzein-4',7-yl di-beta-D-glucopyranosiduronic acid. Carbohydr. Res. **2001**, 330, 511-515.
[27] Shin, J.S.; Kim, K.S.; Kim, M.B.; Jeong, J.H.; Kim, B.K. Synthesis and hypoglycemic effect of chrysin derivatives. Bioorg. Med. Chem. Lett. **1999**, 9, 869-874.
[28] Li, M.; Han, X.; Yu, B. Facile synthesis of flavonoid 7-O-glycosides. J. Org. Chem. **2003**, 17, 6842-6845.
[29] Musialik, M.; Kuzmicz, R.; Pawlowski, T.S.; Litwinienko, G. Acidity of hydroxyl groups: an overlooked influence on antiradical properties of flavonoids. J. Org. Chem. **2009**, 74, 2699-2709.
[30] Piotto, M.; Bourdonneau, M.; Elbayed, K.; Wieruzeski, J.M.; Lippens, G. New DEFT sequences for the acquisition of one-dimensional carbon NMR spectra of small unlabelled molecules. Magn. Reson. Chem. **2006**, 44, 943-947.

Chapter 4

Impact of mitochondriotropic quercetin derivatives on mitochondria[4]

Summary

Mitochondria-targeted polyphenols are being developed with the intent to intervene on the levels of reactive oxygen species (ROS) in mitochondria. Polyphenols being more than just anti-oxidants, the interaction of these derivatives with the organelles needs to be characterised. We have studied the effects of two quercetin derivatives, 3-*O*-(4-triphenylphosphoniumbutyl)quercetin iodide (Q3BTPI) and its tetracetylated analogue (QTA3BTPI), on the inner membrane aspecific permeability, transmembrane voltage difference and respiration of isolated rat liver mitochondria. While the effects of low concentrations were too small to be reliably defined, when used in the 5-20 μM range these compounds acted as inducers of the mitochondrial permeability transition (MPT), an effect due to pro-oxidant activity. Furthermore, Q3BTPI behaved as an uncoupler of isolated mitochondria, causing depolarisation and stimulating oxygen consumption. When applied to tetramethylrhodamine methyl ester (TMRM)-loaded HepG2 or Jurkat cells uptake of the compounds was predictably associated with a loss of TMRM fluorescence, but there was no indication of MPT induction. A production of superoxide could be detected in some cells upon prolonged incubation of MitoSOX®-loaded cells with QTA3BTPI. The overall effects of these model mitochondriotropic polyphenols may thus differ considerably depending on whether their hydroxyls are protected or not and on the experimental system. In vivo assays will be needed for a definitive assessment of their bioactivities.

Introduction

The production of Reactive Oxygen Species (ROS) in cells, and in particular by mitochondria, is considered to be a major factor in aging and degenerative processes (e.g.: [1-5]) with the implication that undesirable organism deterioration may be slowed down by anti-oxidants. Anti-oxidants, including polyphenols, are thus included in some cosmetics

[4] Published as: Biasutto, L.; Sassi, N.; Mattarei, A.; Marotta, E.; Cattelan, P.; Toninello, A.; Garbisa, S.; Zoratti, M.; Paradisi, C. *Biochim. Biophys. Acta*, **2010**, 1797**,** 189-196.

and nutritional supplements. In ischemia/reperfusion (I/R) injury, much of the damage is sustained when circulation is reinstated. A major role in cell death under these circumstances is played by the Mitochondrial Permeability Transition (MPT), a process induced by matrix Ca^{2+} overload and oxidative conditions [6-8]. The involvement of ROS in MPT induction is clearly recognised (e.g.: [2,9,10], and antioxidants may be expected to exert a protective effect. This has led to an on-going effort to develop "mitochondriotropic" antioxidants [11-18], including polyphenols [19,20], mainly with the goal of counteracting these undesirable redox-mediated effects. However, μM concentrations of mitochondria-targeted quercetin and resveratrol derivatives proved to be cytotoxic for rapidly dividing cultured cells [19,20], suggesting a potential as chemotherapeutic agents. Understanding the reasons for this cytotoxicity ought to help the design of other mitochondria-targeted antioxidants and the utilisation of already available ones.

It is therefore important to characterise the effects of these mitochondria-targeted compounds on isolated mitochondria and on the organelles in cells to gain a sense of what may happen *in vivo*. Here we report our observations with isolated rat liver mitochondria (RLM), cultured HepG2 and Jurkat cells, and two mitochondria-targeted quercetin derivatives, 3-*O*-(4-triphenylphosphoniumbutyl)quercetin iodide (Q3BTPI) and 3',4',5,7-tetra-O-acetyl-3-*O*-(4-triphenylphosphoniumbutyl)quercetin iodide (QTA3BTPI).

Results

To assess the effects of Q3BTPI and QTA3BTPI on isolated rat liver mitochondria we monitored three classical readouts of bioenergetics experiments: mitochondrial volume (as reflected by light scattering), transmembrane potential and oxygen consumption. These parameters, and their variation in response to pharmacological agents, vary to some extent from one preparation to the other. The direct comparisons presented in this paper are based on data obtained with the same preparation.

As an initial step we simply mixed the compounds with RLM suspended in an isotonic sucrose-based medium. Both QTA3BTPI [19] and Q3BTPI (Fig. 1) can be observed to accumulate into isolated mitochondria by monitoring their concentration with a TPP-responsive electrode.

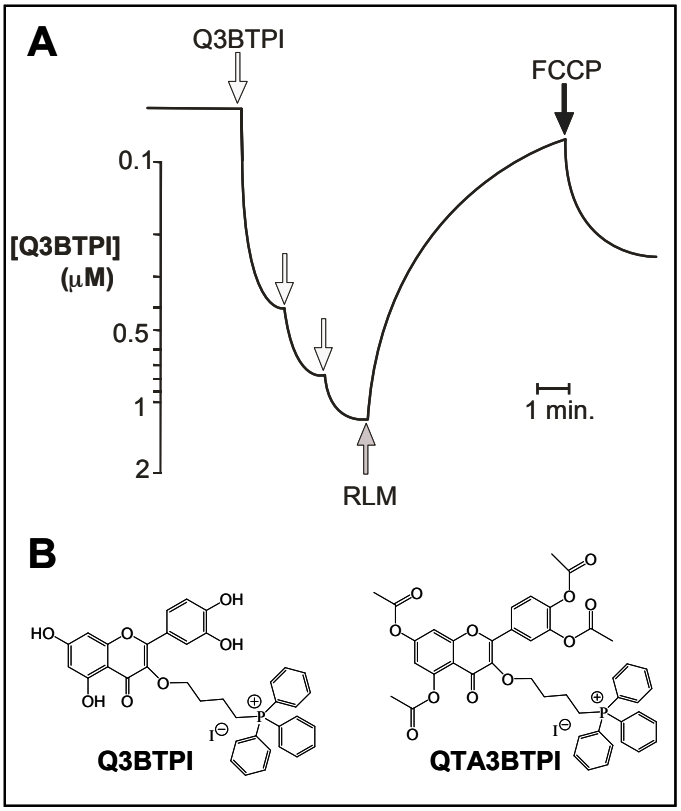

Figure 1. A) Accumulation of Q3BTPI by RLM. The response of a TPP-sensitive electrode is shown. Arrows indicate the addition of 0.4 μM Q3BTPI to standard medium. Addition of RLM (1 mg prot.·mL^{-1}) causes an upward deflection of the trace since respiring mitochondria take up the positively charged compound, which also bind in part to mitochondrial components. Addition of FCCP causes release. **B)** Chemical structures of Q3BTPI and QTA3BTPI.

Note that Q3BTPI is only partially released upon uncoupling of the organelles indicating that much of the compound is actually bound. Polyphenols are well known to bind avidly to proteins, and the TPP moiety is also understood to participate in interactions with membranes and with macromolecules bearing negative charges (DNA). The group of Smith and Murphy has recently produced a quantitative study of the partition of mitoQ in cells: most of the compound was found to bind to cellular components [24]. Acetylation of the OH groups allows faster redistribution and less extensive binding of QTA3BTPI [19].

Fig. 2A illustrates the results of light-scattering experiments with Q3BTPI under these conditions (N = 3). In this as well as in the other figures representative experiments are shown, utilising concentrations of the compounds producing a marked change of the readout parameter.

Lower concentrations always had similar, but less evident, effects or produced variations too small for a reliable assessment. In the presence of 20 μM Q3BTPI (trace 1) swelling ensued which was not observed when no addition was made (trace 7, with oxygenation) or in the presence of 20 μM tetraphenylphosphonium chloride (trace 6). The latter induced

only a much slower and lower-amplitude swelling, presumably due to the energy-driven uptake of the osmotically active solute since it was abolished by FCCP (not shown). The pseudo-absorbance decrease induced by Q3BTPI was in turn more modest than that associated with full-blown Ca^{2+}-induced permeability transition (trace 8), it was partly sensitive to Cyclosporin A (trace 2) and EGTA (trace 9), abolished by FCCP (trace 3) and it was interrupted by a sudden inversion (traces 1,2). The latter was associated with the near-exhaustion of the oxygen supply in the spectrophotometer cuvette, since saturating the suspension medium with oxygen beforehand delayed the phenomenon (traces 4,5). This behaviour indicates that oxygen consumption was strongly enhanced by Q3BTPI. This could not be confirmed directly by measurements with a Clark electrode, because Q3BTPI reacted at the electrode surface producing a tarry substance which rapidly rendered the electrode useless. Oxygenation on the other hand increased the CsA-sensitive portion of the pseudo-absorbance decrease (compare traces 1,2 vs. 4,5), i.e., the rate of propagation of the permeability transition in the suspension, confirming that this phenomenon is mediated by oxidative events [23].

The acetylated derivative - QTA3BTPI - and quercetin affected swelling differently, as illustrated in fig. 2B. In the absence of added Ca^{2+} quercetin in the 10-50 μM range had little effect (cf. trace 4 in Fig. 2B). QTA3BTPI on the other hand induced large amplitude swelling (trace 1) which was essentially abolished by both cyclosporin A and EGTA (traces 2 and 3), and can thus be attributed to the permeability transition taking place in the presence of "contaminating" Ca^{2+}.

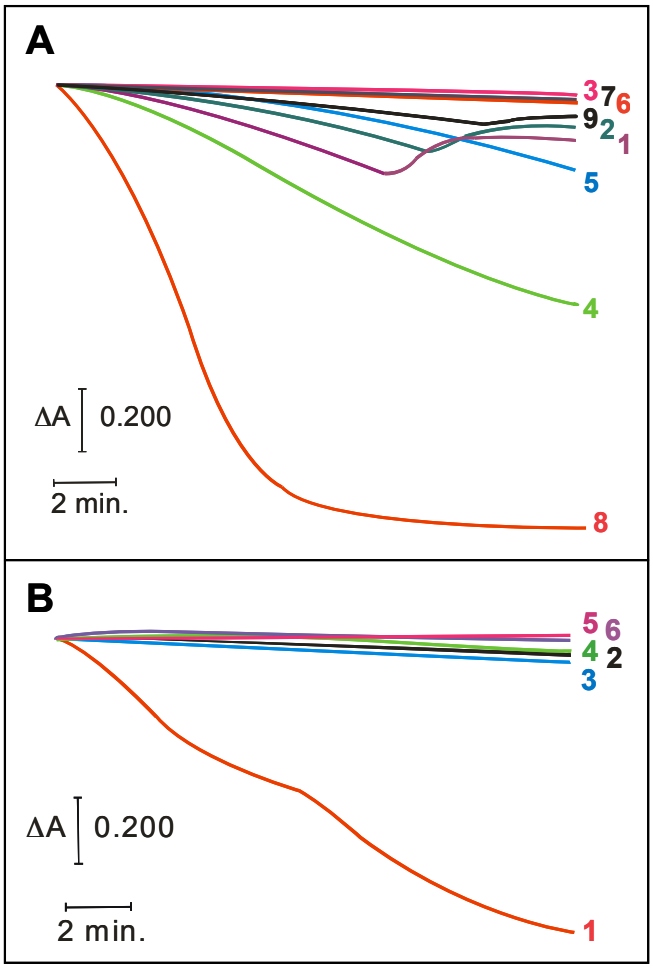

Figure 2. Effects of Q3BTPI and QTA3BTPI on isolated rat liver mitochondria in the absence of added Ca^{2+}. Parallel light scattering experiments initiated by the addition of 1 mg.prot.ml^{-1} RLM to the cuvettes. Pseudo-absorbance was monitored at 540 nm. The medium contained: **A)** traces 1-5 and trace 9: Q3BTPI 20 µM; traces 2,5: CsA 1 µM; trace 3: FCCP 1 µM; trace 6: $Ph_4P^+Cl^-$ 20 µM; trace 8: $CaCl_2$ 80 µM; trace 9: EGTA 100 µM; traces 4,5,7,8: the incubation medium saturated with oxygen; **B)** traces 1-3: QTA3BTPI 20 µM; trace 2: CsA 1 µM; trace 3: EGTA 100 µM; traces 4-6: Q 20 µM; trace 5: CsA 1 µM; trace 6: EGTA 100 µM.

These results suggested that both Q3BTPI and QTA3BTPI acted as inducers of the MPT in synergy with any Ca^{2+} present. In this capacity QTA3BTPI seemed to be more efficient than Q3BTPI (in Fig. 2 compare trace 1 minus trace 2 in panel B for QTA3BTPI vs. trace 1 minus trace 2 in panel A for Q3BTPI), which in turn was more efficient than quercetin itself (trace 4 minus trace 5 in panel B). These indications were confirmed by experiments performed in the presence of near-threshold [Ca^{2+}], i.e. of a concentration of Ca^{2+} sufficient for only a slowly-developing MPT-associated swelling in the absence of another inducing agent (Fig. 3) (N = 31). QTA3BTPI-induced swelling was always profoundly inhibited by CsA, at variance from that caused by Q3BTPI, which was only partially

sensitive (in Fig. 3 compare trace 2 for QTA3BTPI + CsA with trace 4 for Q3BTPI + CsA).

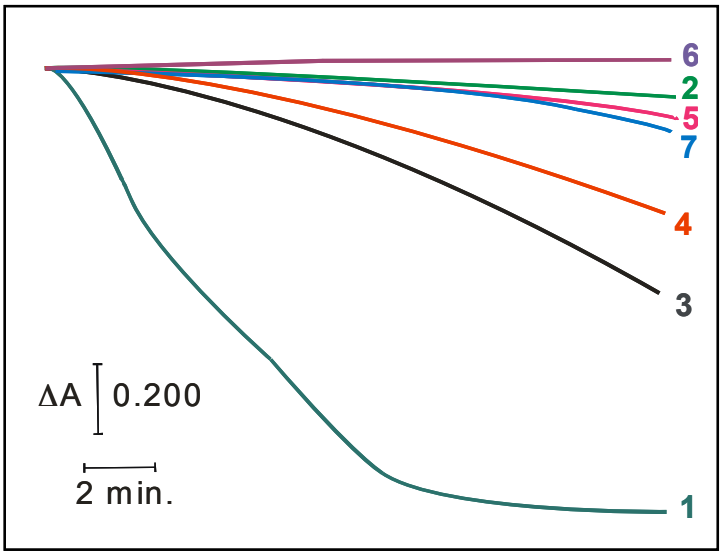

Figure 3. Effects of Q, Q3BTPI and QTA3BTPI on isolated rat liver mitochondria in the presence of exogenous Ca^{2+}. Light scattering experiments analogous to those of Fig. 2. In all cases the medium was saturated with oxygen and contained $CaCl_2$ 50 µM plus: traces 1,2: QTA3BTPI 10 µM; trace 2: CsA 1 µM; traces 3,4: Q3BTPI 20 µM; trace 4: CsA 1 µM; traces 5,6: Q 40 µM; trace 6: CsA 1 µM.

Thus, while QTA3BTPI is more efficient at inducing the MPT, Q3BTPI is more efficient at inducing CsA-insensitive swelling. These properties clearly must be related to the presence of free OH groups in Q3BTPI. Quercetin has been shown to induce the MPT via a metal ion-catalyzed oxidative process [23] and the same mechanism may be envisioned for the present compounds. In the presence of metal ions with multiple possible oxidation states (mainly $Fe^{2+/3+}$ and $Cu^{+/2+}$) polyphenols, especially if comprising a catechol moiety, may oxidize in chain reactions producing superoxide and hence H_2O_2. The latter can then undergo Fenton-type reactions producing more aggressive hydroxy and peroxy radicals [25,26]. Oxygen radicals, or, in general, oxidising conditions, are well known to favour the onset of the MPT by acting on key thiol residues [27-29].

MPT induction by QTA3BTPI was somewhat unexpected because the hydroxyls, the sites of oxidation in quercetin, are protected by acetylation. LC/MS analysis revealed that QTA3BTPI undergoes partial deacetylation, producing oxidisable species still capable of electrophoretic accumulation into energised mitochondria (Fig. 4). However over the time course of a swelling experiment essentially no Q3BTPI is produced: the main species found at 15 min. still retain two or three of the original four acetyl groups.

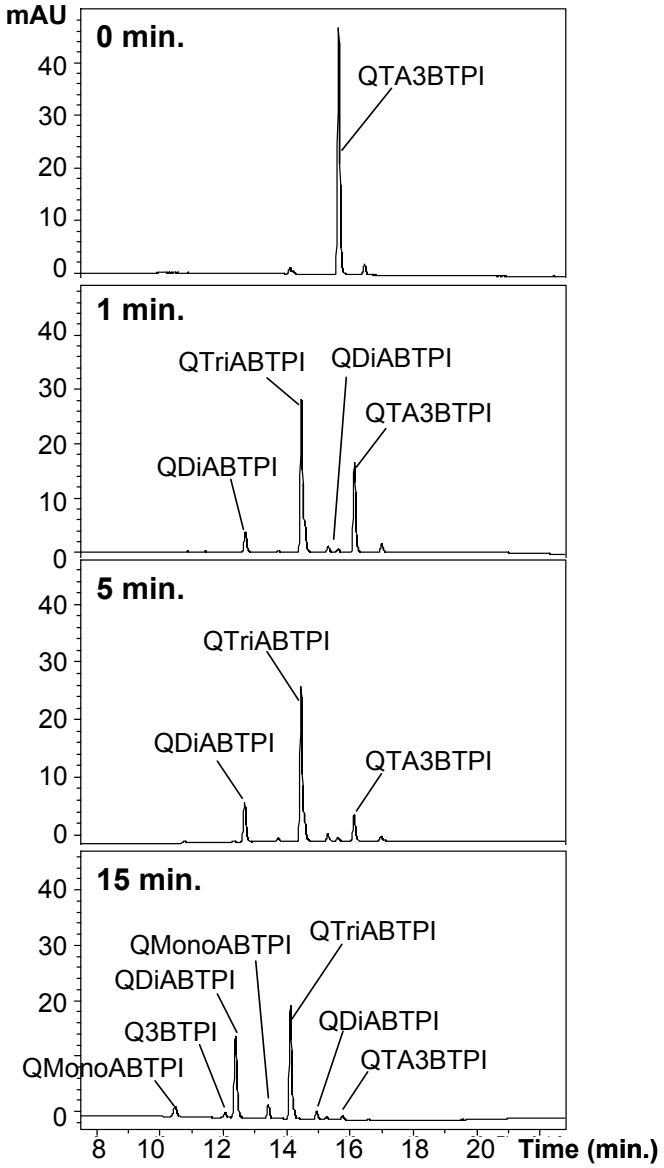

Figure 4. Deacetylation of QTA3BTPI in the presence of RLM. HPLC chromatograms (300 nm) recorded after different incubation periods of QTA3BTPI with a RLM suspension (1 mg.prot.ml^{-1}). Peak identity was determined by ESI/MS analysis.

The intervention of radicalic/oxidative processes in the onset of QTA3BTPI-induced MPT and, in part, of Q3BTPI-induced swelling was confirmed by the inhibition afforded by BHT + DTT (Fig. 5A) (N = 3). In the case of quercetin, MPT induction was antagonised by Fe and Cu chelating agents [23], indicating the involvement of Fenton reactions catalysed by metallic species released by or associated with the mitochondria themselves.

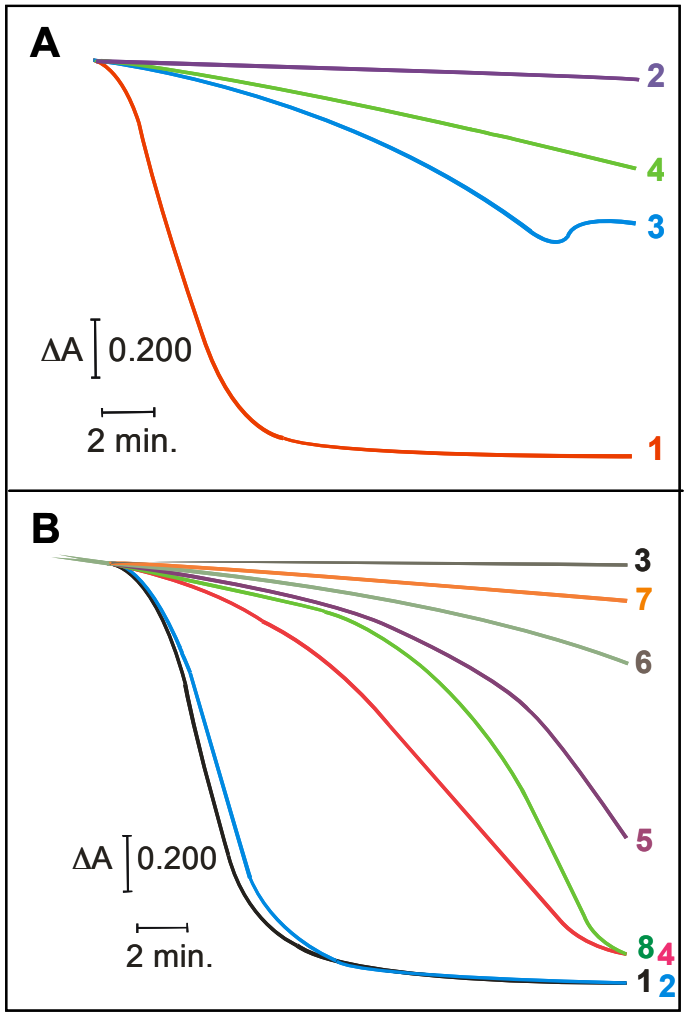

Figure 5. Contribution of Fe and Cu ions and radical species to the induction of the mitochondrial permeability transition by Q3BTPI and QTA3BTPI. Light scattering experiments analogous to those in Figs 2 and 3. In all cases the medium was saturated with oxygen. **A)** All traces: $CaCl_2$ 50 µM. Traces 1,2: QTA3BTPI 10 µM; trace 2: BHT and DTT, 1 mM each; traces 3,4: Q3BTPI 20 µM; trace 4: BHT and DTT, 1 mM each. **B)** The medium contained $CaCl_2$ 40 µM plus: traces 1-3: QTA3BTPI 10 µM; trace 2: BF and BC, 10 µM each; trace 3: CsA 1 µM; traces 4-7: Q3BTPI 20 µM; trace 5: BF and BC, 10 µM each; trace 6: CsA 1 µM; trace 7: BF and BC, 10 µM each, and CsA 1 µM.

Selective chelators also affected Q3BTPI and Ca^{2+}-associated swelling (Fig. 5B) (N = 3), reducing not only the CsA-sensitive component of the swelling curve, but also the CsA-insensitive one (compare traces 6 and 7 in Fig. 5B). This suggests that CsA-insensitive swelling is also largely mediated by ROS produced by metal-catalysed processes, presumably via aspecific membrane permeabilisation by lipoxidation.

On the other hand in the case of QTA3BTPI this protective effect was practically absent (compare traces 1 and 2). This would be expected if in this case the relevant redox events took place mostly in the mitochondrial matrix, where QTA3BTPI accumulates. The matrix is inaccessible to BC and BF which are sulfonated (i.e., negatively charged) molecules.

QTA3BTPI is much less reactive than Q3BTPI at the Clark electrode surface, and its effects on respiration can therefore be assessed by polarography. As expected, in the presence of Ca^{2+} its addition caused an acceleration of the rate of oxygen consumption which was blocked by CsA (not shown). An increase in respiratory rate normally implies "uncoupling" of the mitochondrial energy conversion process, which in turn, according to the chemiosmotic model, implies a decrease of the transmembrane electrochemical proton gradient ($\Delta\tilde{\mu}_H$). To verify whether such a decrease was taking place we used the fluorescent transmembrane potential ($\Delta\Psi$) indicator dye Rhodamine 123 (Rh123). In these experiments Rh123 was added to the suspension and equilibrated, so that some was always present outside mitochondria. The high (0.5 mg.prot./mL) density of the latter then insured that any dye released upon depolarisation could be rapidly taken up again upon repolarisation. Q3BTPI indeed induced a sustained recovery of Rh123 fluorescence, corresponding to a decrease of $\Delta\Psi$, when added to a suspension of RLM, also if no Ca^{2+} was added and CsA was present to block the MPT (Fig. 6A) (N = 3). QTA3BTPI had an analogous depolarising effect (Fig. 6B).

In the presence of CsA, however, the increase of Rh123 fluorescence was transient, suggesting a rapid depolarisation due to influx of the permeant cation followed by a slower repolarisation taking place on the time scale of a few minutes (Fig. 6C; N = 4), as the compound was taken up and an equilibrium distribution was approached. Quercetin itself had little effect under the same conditions (not shown).

We then checked whether our compounds affected mitochondria inside cultured cells (Fig. 7). We followed the mitochondrial potential via TMRM fluorescence. In the experiments of Fig. 7A, representative of 37 separate ones under various conditions, HepG2 cells were loaded with TMRM in the presence of CsH (to inhibit MDR pumps; CsH, contrary to CsA, does not prevent the MPT) and then incubated in HBSS without any pharmacological agent. Under these conditions there was a background loss of TMRM fluorescence (plot "a"), which was hardly affected by the addition of 5 μM Q3BTPI (plot "b"), while 20 μM resulted in a modest acceleration (plot "c"). This sluggishness may be explainable in terms of the sequestration of a fraction of this compound by cellular structures.

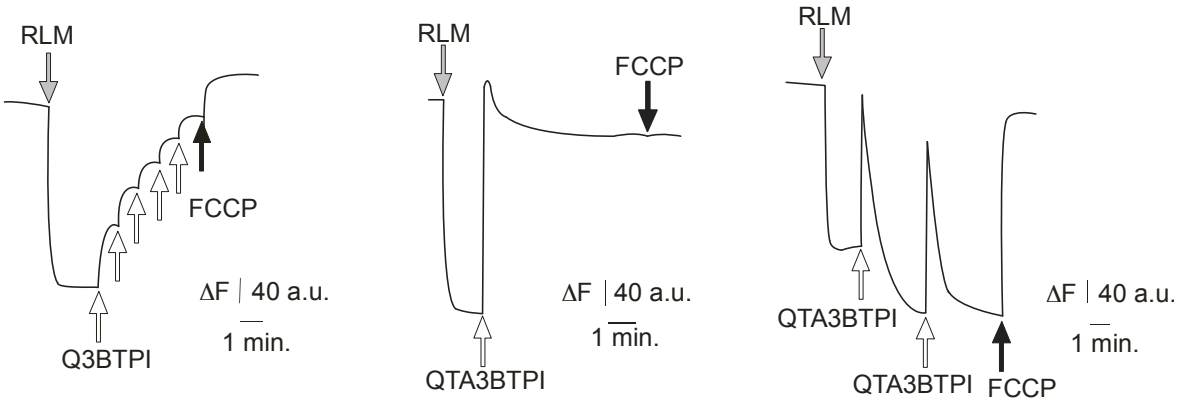

Figure 6. Effects of Q3BTPI and QTA3BTPI on mitochondrial membrane potential. Variations of Rhodamine 123 fluorescence upon additions of: **A**) Q3BTPI (each arrow represents a 10 μM addition); **B,C**) QTA3BTPI (each arrow represents a 20 μM addition). In A) and C), CsA 1 μM was present during the experiment.

QTA3BTPI is expected to bind less avidly, since its hydroxyls are capped, and it has been directly observed to accumulate into *in situ* mitochondria [19]. Accordingly, its addition induced a more pronounced but transient acceleration of the fluorescence decrease (plot "d"), which was not affected by either CsA or BHT+DTT (1 mM each) (not shown), ruling out the MPT as its origin. Fluorescence loss proceeded with kinetics comparable to those of QTA3BTPI uptake [19], suggesting that the two phenomena are correlated, i.e., the process may be ascribable to the depolarisation associated with uptake of a permeant cation. A protonophoric cycle by (partially) deacylated species may also intervene. The same type of behaviour by QTA3BTPI was observed when Jurkat cells were analysed by cytofluorimetry (Fig. 7B,C). In the case of Q3BTPI reliable data could not be obtained (see Materials and Methods). In experiments with cells loss of TMRM fluorescence does not necessarily indicate an irreversible, permanent depolarisation of the mitochondria. Cells are pre-loaded with TMRM and then washed, so that no dye is present outside cells, a non-equilibrium situation. Indeed, TMRM slowly leaks out of cells under our control conditions. The cells face an extremely larger volume of incubation medium. Under these conditions, any TMRM lost because of a transient depolarisation would not be expected to be regained upon a subsequent recovery of the mitochondrial potential. Thus, fluorescence loss indicates depolarisation, but does not necessarily indicate by itself a *permanent* depolarisation or damage.

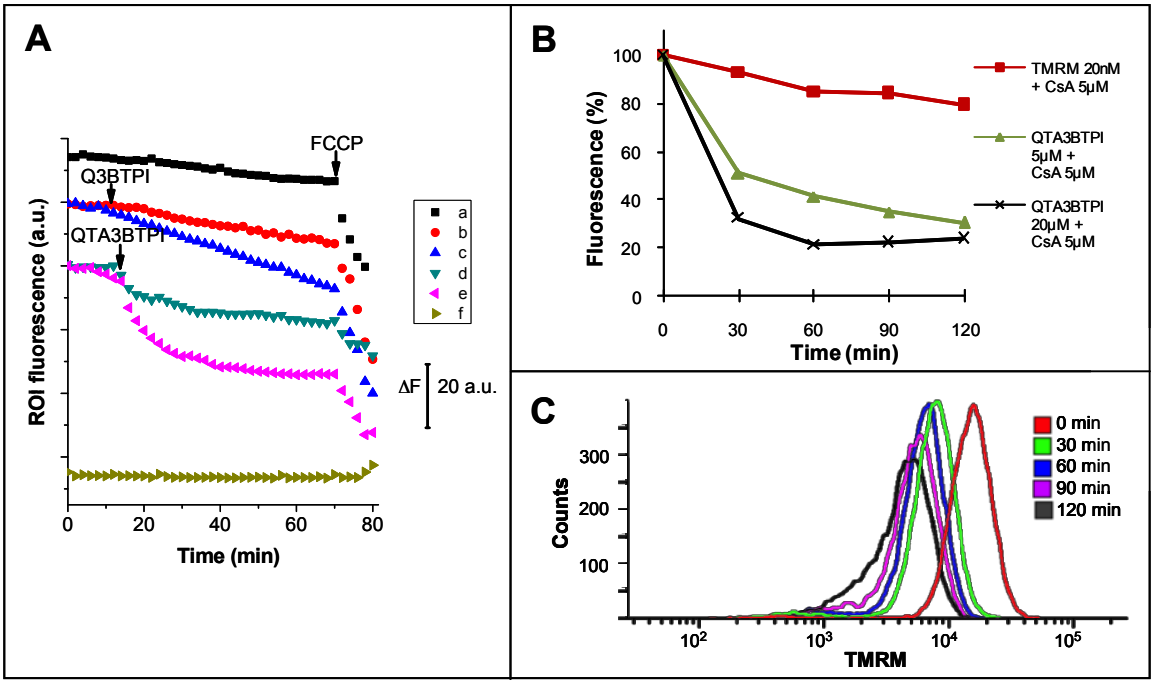

Figure 7. Mitochondrial membrane potential in cells exposed to Q3BTPI and QTA3BTPI, monitored using TMRM. **A**) Representative fluorescence microscopy experiments with TMRM-loaded HepG2 cells. Computer-generated plots of the fluorescence emitted by the field areas (Regions Of Interest, ROI) coinciding with one cell or a portion of background (f). Images were acquired every 60 seconds. Plot "a" represents a control experiment without addition. Plot "b": Q3BTPI 5 μM; plot "c": Q3BTPI 20 μM; plot "d": QTA3BTPI 5 μM; plot "e": QTA3BTPI 20 μM. Compound additions are indicated by arrows. Plots have been shifted along the ordinate axis for clarity. See Materials and Methods for details. **B**) Representative FACS experiments with 0 (red; control), 5 (green) or 20 μM (black) QTA3BTPI additions. The experiment was conducted in the presence of 5 μM CsA. Plotted are the normalised median values of histograms such as those shown in panel C). The median of the histogram recorded immediately after the addition of QTA3BTPI was set as 100%. **C**) The set of histograms obtained in the experiment with 5 μM QTA3BTPI shown in panel B) is shown as an example.

Quercetin induces the production of superoxide anion by isolated mitochondria as well as by cultured cells [23]. We could not obtain clear evidence of an analogous effect by Q3BTPI or QTA3BTPI on isolated mitochondria using HE or mitoSOX®. A reliable assessment of the effect of Q3BTPI on the response of MitoSOX® in HepG2 or Jurkat cells was made difficult by technical problems at 20 μM (see Materials and Methods) and was not robust enough to reach definite conclusions at the 5 μM level. Addition of QTA3BTPI resulted instead in a fluorescence increase, which took place also in the presence of CsA (Fig. 8). In microscopy experiments an heterogeneity of cell behaviour was evident, as illustrated by the different increases of the fluorescence associated with two cells in the same field shown in Fig. 8A (plots "b" and "c").

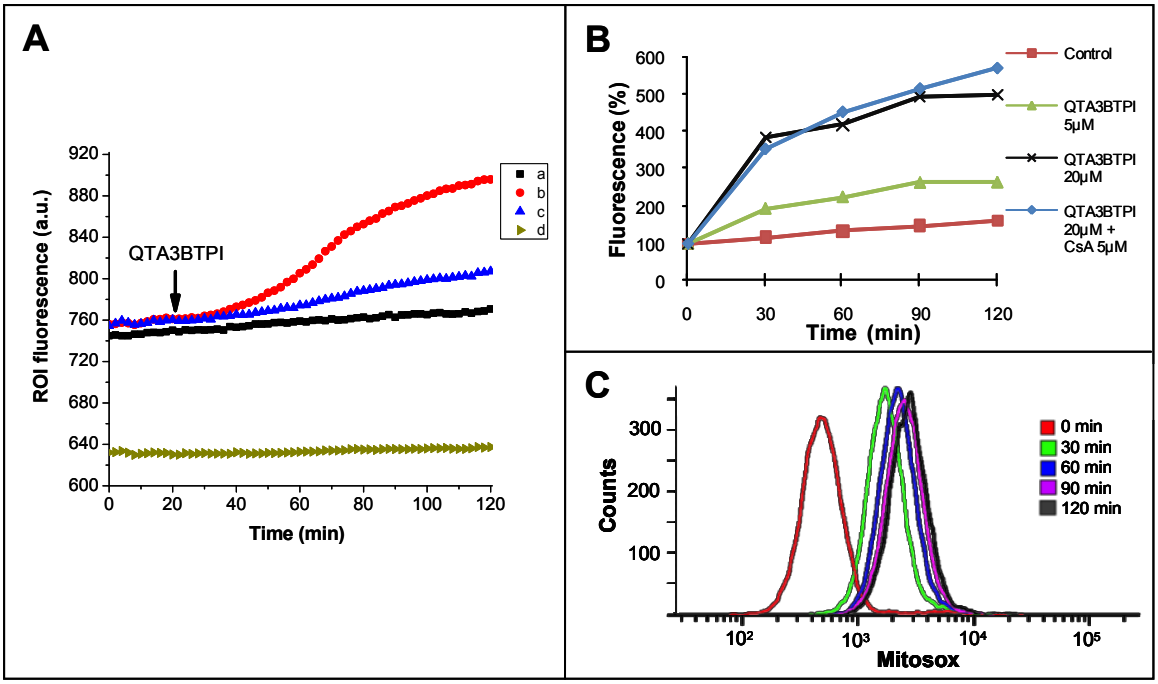

Figure 8. Superoxide production in cells exposed to QTA3BTPI, monitored using MitoSOX Red®. **A**) Representative fluorescence microscopy experiments with MitoSOX Red®-loaded HepG2 cells. A computer-generated plot of the fluorescence emitted by field areas (Regions Of Interest, ROI) coinciding with a cell (a-c) or a portion of background (d). Images were acquired every 2 min. Plot "a" presents the fluorescence associated with a cell in a separate control experiment without additions. 20 µM QTA3BTPI was added, when indicated, in plots "b" and "c", which report the fluorescence associated with two cells in the same field (plot "d" also comes from the same experiment). See Materials and Methods for details. **B**) Representative FACS experiments with 0 (red; control), 5 (green) or 20 µM (black) QTA3BTPI additions. The graph plotted in blue refer to a parallel experiment with 20 µM QTA3BTPI in the presence of 5 µM CsA. Plotted are the normalised median values of histograms such as those shown in panel C). The median of the histogram recorded immediately after the addition of QTA3BTPI was set as 100%. **C**) The set of histograms obtained in the experiment with 20 µM QTA3BTPI in the presence of CsA shown in panel B) (blue plot) is shown as an example.

Discussion

The results presented above plausibly identify the mechanisms responsible for the cytotoxicity of Q3BTPI and QTA3BTPI. They have been obtained *in vitro*, with relatively high concentrations, but we believe they are relevant also for an eventual *in vivo* utilisation of the compounds, since much the same mechanisms and requirements would be expected to apply. Polyphenols *per se* have rather poor bioavailability, and when administered in foods or beverages they are unlikely to reach µM-range concentrations in blood and organs (except as phase II conjugates). Here we are however considering not the natural compounds, but their derivatives, which may be considered as drugs, and administered in

various ways. Pharmacological delivery methods can be expected to result in much higher levels, at least locally.

We rationalise the behaviour of Q3BTPI vs. isolated mitochondria in terms of three major concomitant processes: uncoupling of the mitochondria by Q3BTPI acting as a protonophore (Fig. 9), MPT induction - involving Ca^{2+} and ROS in analogy to the process induced by quercetin itself under similar conditions [23] - and CsA-insensitive permeabilisation of the IMM, with consequent swelling, due to the action of ROS on membrane lipids.

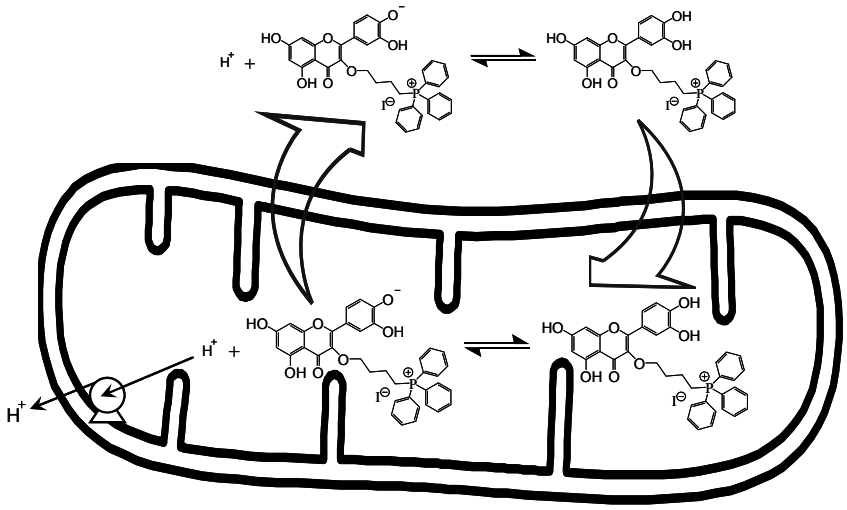

Figure 9 An illustration of how Q3BTPI may act as a protonophore and uncoupler. See text for details.

The uncoupling effect of Q3BTPI can be explained as follows: Q3BTPI exists in solution as a mixture of instantaneously fully protonated (i.e., positively charged due to the TPP group) and deprotonated species (the first pKa of quercetin is close to 7 [30-32]). The mitochondrial $\Delta\Psi$ will drive the uptake of fully protonated molecules, the chemical gradient between the matrix and the suspension medium will drive the efflux of the unprotonated, zwitterionic specie. A $\Delta\Psi$-decreasing, respiration-stimulating protonophoric futile cycle will thus be generated. Flavonoids have already been identified as potential uncouplers [33], but the presence of the membrane-permeating positive charge enhances this characteristic: quercetin itself is not active as an uncoupler at concentrations below 1 mM [33], while Q3BTPI uncouples in the μM range. Active uptake of Q3BTPI by energised mitochondria is therefore self-limiting.

Direct comparison shows that both QTA3BTPI and Q3BTPI are more efficient MPT co-inducers than quercetin (Fig. 3) in RLM. Since these compounds are accumulated inside suspended mitochondria, this indicates that induction can be mediated by phenomena taking place in the matrix. The higher efficiency is then presumably accounted for by the

higher concentration of inducer on the matrix side of the inner mitochondrial membrane (IMM) (in comparison with an analogous experiment with quercetin). While the two mitochondriotropic compounds are better inducers than quercetin, the difference is less marked than might have been expected. In the case of Q3BTPI this may be explained by uncoupling, which limits matrix accumulation of both Ca^{2+} and inducer. QTA3BTPI is expected to be less effective than quercetin or Q3BTPI, at parity of concentration, because its hydroxyls are at least initially blocked (see Fig. 4).

The observations on cultured cells differ in some respects from those with isolated mitochondria, indicating that the MPT is much less readily induced in *in situ* mitochondria. This is coherent with the low concentration of Ca^{2+} and of transition metals – the two factors involved in MPT induction with isolated RLM - in the cytoplasm. At least in the case of QTA3BTPI, MPT-independent (because CsA-insensitive) production of superoxide and some loss of $\Delta\Psi$ takes place. Other mitochondriotropic polyphenols may well behave differently, depending on their physico-chemical properties, but compounds of this class are in any case to be studied with care: it is not clear that *in vivo* they would behave only as beneficial antioxidants and ROS quenchers. The results of this investigation may be taken into consideration for the design of other mitochondriotropic compounds: features conferring protonophoric/uncoupling properties will best be avoided if the intention is to produce a cell-saving anti-oxidant molecule, and may conversely be desirable if a candidate for chemotherapeutic applications is desired. Usefulness in oncology may also be maximised by taking into account the findings that cancer cells have elevated levels of copper ions [34] and of oxidative stress [35]. On the other hand mild uncoupling of mitochondria is proposed to have potentially beneficial effects, such as mimicking life-extending caloric restriction (e.g.: [36,37]) and protecting neurons against excitotoxicity (e.g.: [38]). Thus, a less readily oxidisable polyphenol derivative with mild uncoupling activity may also find applications.

Literature reports suggest that concentration, or dosage, may well an important parameter determining the overall effect a (mitochondriotropic) polyphenol. For example, EpiGalloCatechinGallate (EGCG) may have anti-oxidant and "cell-protective" effects at low dosages (< 1μM), and pro-oxidant, cytotoxic effects at higher levels [39]. MitoQ, the best studied mitochondriotropic antioxidant, changes from an anti-oxidant to a pro-oxidant behaviour over a relatively small concentration range ([5] and references therein). Low doses of mitochondria-targeted plastoquinone derivatives reportedly exert very beneficial effects in vivo [5]. It remains to be seen whether the present compounds may display

divergent effects at very low concentration, and whether there may be relatively sharp thresholds for these hypothetical different activities. It also remains to be seen what concentrations may be attained in the organs of laboratory animals, and by what means. Furthermore, as mentioned, the bioactivity of polyphenols is not limited to redox effects. The investigation of the activity of mitochondriotropic polyphenols *in vivo* will need therefore to consider several "readout" parameters, the most important obviously being the impact on physiological or pathological conditions of interest.

Experimental section

Materials and methods:

Cells and mitochondria.

HepG2 cells were grown in Dulbecco's Modified Eagle Medium (DMEM) (GIBCO) plus 10 mM HEPES buffer, 10% (v/v) fetal calf serum (Invitrogen), 100 U/mL penicillin G (Sigma), 0.1 mg/mL streptomycin (Sigma), 2 mM glutamine (GIBCO) and 1% nonessential amino acids (100X solution; GIBCO), in a humidified atmosphere of 5% CO_2 at 37 °C. Jurkat cells were grown in RPMI-1640 medium supplemented as above plus 50 μM β-mercaptoethanol. Rat liver mitochondria (RLM) were prepared by standard differential centrifugation procedures and obtained as a suspension in 0.25 M sucrose, 5 mM Hepes/K^+, pH 7.4.

TPP-sensitive electrode.

The setup used to monitor the concentration of triphenylphosphonium-bearing compounds in solution was built in-house following published procedures [21,22]. In these electrodes the diffusion of the charged, permeant compound across a permeable polyvinylchloride (PVC) film gives rise to a half-cell potential logarithmically related to the concentration of the compound according to Nernst's law. The film is permeable because doped with tetraphenylborate anion, which acts as a carrier. Such an electrode will respond to all cations capable of diffusing into the PVC film as an ionic couple with tetraphenylborate, i.e., in practice, to triphenylphosphonium-comprising organic molecules. A calomel electrode was used as reference and the potentiometric output was directed to a strip chart recorder. The experiment illustrated in Figure 1 was conducted at 20°C.

Swelling and respiration assays.

Preparation of RLM and swelling and respiration assays were carried out as described in [23]. The standard medium contained 250 mM sucrose, 10 mM Hepes/K^+, 5 mM succinate/K^+, 1.25 μM rotenone, 1 mM P_i/K^+, pH 7.4, supplemented with the desired

concentration of $CaCl_2$. RLM were used at a concentration of 1 or 0.5 mg.prot.mL^{-1}. Direct determinations of the effects of Q3BTPI on respiration using a Clark electrode could not be carried out because Q3BTPI diffused through the semi-permeable Teflon membrane covering the working surface of the electrode (a cathode at which approximately -0.7 V are applied), and reacted there forming black polymeric products which rapidly gummed up the surface making the electrode unserviceable.

Fluorimetric assays of mitochondrial potential.

Rhodamine 123 (75 nM) fluorescence was used to monitor the transmembrane potential of isolated RLM suspended (0.5 mg.prot.mL^{-1}) in standard medium in a stirred quartz cuvette placed in a Shimadzu RL-5000 spectrofluorimeter at R.T. Excitation was at 503 nm (3 nm slit), and fluorescence was collected at 523 nm (5 nm slit).

Tetramethylrhodamine methyl ester (TMRM; Invitrogen/Molecular Probes) staining of cells was used to monitor mitochondrial transmembrane potential in cultured cells. HepG2 cells were seeded onto 24-mm coverslips in 6-well plates and grown for about two days, avoiding confluence. Coverslips were mounted onto holders, exposed to 20 nM TMRM in DMEM or HBSS (in mM units: NaCl 136.9, KCl 5.36, $CaCl_2$ 1.26, $MgSO_4$ 0.81, KH_2PO_4 0.44, Na_2HPO_4 0.34, glucose 5.55, pH 7.4 with NaOH) for about 20 min, generally in the presence of 4 μM Cyclosporin H or 2 μM Cyclosporin A depending on the details of the experimental protocol, and washed twice. Cells were then covered with 1 mL of the desired medium and observed at room temperature. Images were acquired automatically at 1- or 2-min intervals, using an Olympus Biosystems apparatus comprising an Olympus IX71 microscope and MT20 light source, and processed with Cell$^{R©}$ software. Excitation was at 568 ± 25 nm and fluorescence was collected using a 585 nm longpass filter. Additions were performed by withdrawing 0.5 mL of incubation medium, adding the desired solute to this aliquot, mixing, and adding back the solution into the chamber at a peripheral point.

A Beckton Dickinson Canto II flow cytometer was used to monitor TMRM fluorescence of Jurkat cells. The cells were washed in HBSS, suspended in FACS buffer (135 mM NaCl, 10 mM Hepes, 5 mM $CaCl_2$, pH 7.4) at a density of $1.5x10^6$/mL and loaded with 20 nM TMRM (37° C, 20 min). Cells were then diluted 1:5 in FACS buffer and divided into the desired number of identical aliquots. At time zero the desired compound was added, and data collected after the desired incubation times, exciting at 545 nm and measuring fluorescence at 585 nm. Data were analysed using the BD VISTA software. Experiments

could be performed only with QTA3BTPI because Q3BTPI significantly altered the scatter parameters of a large fraction of the cells.

Superoxide production assays.

Dihydroethidine (Invitrogen/Molecular Probes) assays were used as described in [23] to detect the production of $O_2^{\cdot-}$ in RLM suspensions. Superoxide generation in cells was followed using the mitochondriotropic probe MitoSOX Red® (Invitrogen/Molecular Probes) used as specified by the producer. Cells were incubated for 15 min with 1 or 2 μM MitoSOX Red® in HBSS, washed twice, covered with 1 mL HBSS, and placed on the microscope stage. Excitation was at 500-520 nm, and fluorescence was collected at $\lambda >$ 570 nm. Images were automatically acquired at 1 or 2 min intervals as above. These experiments could be conducted only with QTA3BTPI and 5 μM Q3BTPI, because 20 μM Q3BTPI apparently interacted with mitoSOX to produce strongly fluorescent microaggregates giving rise to a "snowstorm" effect which masked any fluorescence increase.

FACS experiments with Jurkat cells were conducted as described for TMRM fluorescence determinations, loading with 1 μM MitoSOX Red®. Also in this case analyses could be performed only with QTA3BTPI.

QTA3BTPI stability in mitochondrial suspensions.

QTA3BTPI was added to a 1 mg.prot.ml^{-1} suspension of RLM in standard medium to give a 20 μM solution. 100 μL samples were withdrawn, stabilised with 1 mM ascorbate and 0.06 M acetic acid, and mixed with an equal volume of acetone. After sonication the solids were separated by centrifugation. The supernatant was concentrated under N_2 and analysed. LC-ESI/MS analyses and mass spectra were performed with a 1100 Series Agilent Technologies system, equipped with binary pump (G1312A) and MSD SL Trap mass spectrometer (G2445D SL) with ESI source. Samples (20 μL) were injected onto a reversed phase column (Gemini C18, 3 μm, 150 x 4.6 mm i.d.; Phenomenex). Solvents A and B were H_2O containing 0.1% formic acid and CH_3CN, respectively. The gradient for B was as follows: 30% for 5 min, from 30% to 60% in 15 min, from 60% to 100% in 3 min; the flow rate was 0.7 mL/min. The eluate was monitored at 300 nm.

Bibliography

[1] K.C. Kregel, H.J. Zhang, An integrated view of oxidative stress in aging: basic mechanisms, functional effects, and pathological considerations, Am. J. Physiol. Integr. Comp. Physiol. 292 (2007) R18-R36.
[2] M. Valko, D. Leibfritz, J. Moncol, M.T. Cronin, M. Mazur, J. Telser, Free radicals and antioxidants in normal physiological functions and human disease, Int. J. Biochem. Cell Biol. 39 (2007) 44-84.
[3] A. Carpi, R. Menabò, N. Kaludercic, P. Pelicci, F. Di Lisa, M. Giorgio, The cardioprotective effects elicited by p66(Shc) ablation demonstrate the crucial role of mitochondrial ROS formation in ischemia/reperfusion injury, Biochim. Biophys. Acta 1787 (2009) 774-780.
[4] H. Du, S.S. Yan, Mitochondrial permeability transition pore in Alzheimer's disease: Cyclophilin D and amyloid beta, Biochim. Biophys. Acta, in press (2009) (doi:10.1016/j.bbadis.2009.07.005)
[5] V.P. Skulachev, V.N. Anisimov, Y.N. Antonenko, L.E. Bakeeva, B.V. Chernyak, V.P. Erichev, O.F. Filenko, N.I. Kalinina, V.I. Kapelko, N.G. Kolosova, B.P. Kopnin, G.A. Korshunova, M.R. Lichinitser, L.A. Obukhova, E.G. Pasyukova, O.I. Pisarenko, V.A. Roginsky, E.K. Ruuge, I.I. Senin, I.I. Severina, M.V. Skulachev, I.M. Spivak, V.N. Tashlitsky, V.A. Tkachuk, M.Y. Vyssokikh, L.S. Yaguzhinsky, D.B. Zorov, An attempt to prevent senescence: a mitochondrial approach, Biochim. Biophys. Acta 1787 (2009) 437-461.
[6] P. Bernardi, A. Krauskopf, E. Basso, V. Petronilli, E. Blachly-Dyson, F. Di Lisa, M.A. Forte, The mitochondrial permeability transition from in vitro artifact to disease target, FEBS J. 273 (2006) 2077-2099.
[7] A. Rasola, P. Bernardi, The mitochondrial permeability transition pore and its involvement in cell death and in disease pathogenesis, Apoptosis 12 (2007) 815-833.
[8] A.P. Halestrap, What is the mitochondrial permeability transition pore? J. Mol. Cell. Cardiol. 46 (2009) 821-831.
[9] J.L. Zweier, M.A. Talukder, The role of oxidants and free radicals in reperfusion injury, Cardiovasc. Res. 70 (2006) 181-190.
[10] V. Petronilli, J. Sileikyte, A. Zulian, F. Dabbeni-Sala, G. Jori, S. Gobbo, G. Tognon, P. Nikolov, P. Bernardi, F. Ricchelli, Switch from inhibition to activation of the mitochondrial permeability transition during hematoporphyrin-mediated photooxidative stress. Unmasking pore-regulating external thiols, Biochim. Biophys. Acta 1787 (2009) 897-904.
[11] V. Weissig, Targeted drug delivery to mammalian mitochondria in living cells. Expert Opin. Drug Deliv. 2 (2005) 89-102.
[12] M.P. Murphy, R.A. Smith, Targeting antioxidants to mitochondria by conjugation to lipophilic cations, Annu. Rev. Pharmacol. Toxicol. 47 (2007) 629-656.
[13] A.T. Hoye, J.E. Davoren, P. Wipf, M.P. Fink, V.E. Kagan, Targeting mitochondria, Acc. Chem. Res. 41 (2008) 87-97.
[14] M.P. Murphy, Targeting lipophilic cations to mitochondria, Biochim. Biophys. Acta 1777 (2008) 1028-1031.
[15] H.H. Szeto, Development of mitochondria-targeted aromatic-cationic peptides for neurodegenerative diseases, Ann. N.Y. Acad. Sci. 1147 (2008) 112-121.
[16] H.H. Szeto, Mitochondria-targeted cytoprotective peptides for ischemia-reperfusion injury, Antiox. Redox Signal. 10 (2008) 601-619.
[17] T.A. Prime, F.H. Blaikie, C. Evans, S.M. Nadtochiy, A.M. James, C.C. Dahm, D.A. Vitturi, R.P. Patel, C.R. Hiley, I. Abakumova, R. Requejo, E.T. Chouchani, T.R. Hurd, J.F. Garvey, C.T. Taylor, P.S. Brookes, R.A. Smith, M.P. Murphy, A mitochondria-targeted S-

nitrosothiol modulates respiration, nitrosates thiols, and protects against ischemia-reperfusion injury, Proc. Natl. Acad. Sci. USA 106 (2009) 10764-10769.
[18] J. Ripcke, K. Zarse, M. Ristow, M. Birringer, Small-molecule targeting of the mitochondrial compartment with an endogenously cleaved reversible tag, Chembiochem 10 (2009) 1689-1696.
[19] A. Mattarei, L. Biasutto, E. Marotta, U. De Marchi, N. Sassi, S. Garbisa, M. Zoratti, C. Paradisi, A mitochondriotropic derivative of quercetin: a strategy to increase the effectiveness of polyphenols, Chembiochem 9 (2008) 2633-2642.
[20] L. Biasutto, A. Mattarei, E. Marotta, A. Bradaschia, N. Sassi, S. Garbisa, M. Zoratti, C. Paradisi, Development of mitochondria-targeted derivatives of resveratrol, Bioorg. Med. Chem. Lett. 18 (2008) 5594-5597.
[21] N. Kamo, M. Muratsugu, R. Hongoh, Y. Kobatake, Membrane potential of mitochondria measured with an electrode sensitive to tetraphenyl phosphonium and relationship between proton electrochemical potential and phosphorylation potential in steady state. J. Membr. Biol. 49 (1979) 105-121.
[22] M. Zoratti, M. Favaron, D. Pietrobon, V. Petronilli, Nigericin-induced transient changes in rat-liver mitochondria. Biochim. Biophys. Acta 767 (1984) 231-239.
[23] U. De Marchi, L. Biasutto, S. Garbisa, A. Toninello, M. Zoratti, Quercetin can act either as an inhibitor or an inducer of the mitochondrial permeability transition pore: A demonstration of the ambivalent redox character of polyphenols, Biochim. Biophys. Acta 1787 (2009) 1425-1432.
[24] M.F. Ross, T.A. Prime, I. Abakumova, A.M. James, C.M. Porteous, R.A. Smith, M.P. Murphy, Rapid and extensive uptake and activation of hydrophobic triphenylphosphonium cations within cells, Biochem. J. 411 (2008) 633-645.
[25] Y. Sakihama, M.F. Cohen, S.C. Grace, H. Yamasaki, Plant phenolic antioxidant and prooxidant activities: phenolics-induced oxidative damage mediated by metals in plants, Toxicology 177 (2002) 67-80.
[26] U. Shamim, S. Hanif, M.F. Ullah, A.S. Azmi, S.H. Bhat, S.M. Hadi, Plant polyphenols mobilize nuclear copper in human peripheral lymphocytes leading to oxidatively generated DNA breakage: implications for an anticancer mechanism, Free Radic. Res. 42 (2008) 764-72.
[27] V. Petronilli, P. Costantini, L. Scorrano, R. Colonna, S. Passamonti, P. Bernardi, The voltage sensor of the mitochondrial permeability transition pore is tuned by the oxidation-reduction state of vicinal thiols. Increase of the gating potential by oxidants and its reversal by reducing agents, J. Biol. Chem. 269 (1994) 16638-16642.
[28] P. Costantini, B.V. Chernyak, V. Petronilli, P. Bernardi, Modulation of the mitochondrial permeability transition pore by pyridine nucleotides and dithiol oxidation at two separate sites, J. Biol. Chem. 271 (1996) 6746-67451.
[29] P. Costantini, R. Colonna, P. Bernardi, Induction of the mitochondrial permeability transition by N-ethylmaleimide depends on secondary oxidation of critical thiol groups. Potentiation by copper-ortho-phenanthroline without dimerization of the adenine nucleotide translocase, Biochim. Biophys. Acta 1365 (1998) 385-392.
[30] S.V. Jovanovic, S. Steenken, M. Tosic, B. Marjanovic, M.G. Simic, Flavonoids as antioxidants, J. Am. Chem. Soc. 116 (1994) 4846-4851.
[31] N. Sauerwald, M. Schwenk, J. Polster, E. Bengsch, Spectrophotometric pK Determination of Daphnetin, Chlorogenic Acid and Quercetin, Z. Naturforsch. 53b (1998) 315-321.
[32] K. Lemanska, H. Szymusiak, B. Tyrakowska, R. Zielinski, A.E.M.F. Soffers, I.M.C.M. Rietjens, The influence of pH on antioxidant properties and the mechanism of antioxidant action of hydroxyflavones, Free Rad. Biol. Med. 31 (2001) 869-881.

[33] C. van Dijk, A.J. Driessen, K. Recourt, The uncoupling efficiency and affinity of flavonoids for vesicles, Biochem. Pharmacol. 60 (2000) 1593-1600.
[34] A. Gupte, R.J. Mumper, Elevated copper and oxidative stress in cancer cells as a target for cancer treatment, Cancer Treat. Rev. 35 (2009) 32-46.
[35] H. Pelicano, D. Carney, P. Huang, ROS stress in cancer cells and therapeutic implications, Drug Resist. Updat. 7 (2004) 97-110.
[36] C.E. Amara, E.G. Shankland, S.A. Jubrias, D.J. Marcinek, M.J. Kushmerick, K.E. Conley, Mild mitochondrial uncoupling impacts cellular aging in human muscles in vivo, Proc. Natl. Acad. Sci. USA 104 (2007) 1057-1062.
[37] C.C. Caldeira da Silva, F.M. Cerqueira, L.F. Barbosa, M.H. Medeiros, A.J. Kowaltowski, Mild mitochondrial uncoupling in mice affects energy metabolism, redox balance and longevity, Aging Cell. 7 (2008) 552-560.
[38] D. Liu, M. Pitta, M.P. Mattson, Preventing NAD(+) depletion protects neurons against excitotoxicity: bioenergetic effects of mild mitochondrial uncoupling and caloric restriction, Ann. N.Y. Acad. Sci. 1147 (2008) 275-282.
[39] S. Mandel, O. Weinreb, T. Amit, M.B. Youdim, Cell signaling pathways in the neuroprotective actions of the green tea polyphenol (-)-epigallocatechin-3-gallate: implications for neurodegenerative diseases, J. Neurochem. 88 (2004) 1555-1569.

Chapter 5

Isomeric mitochondriotropic quercetin derivatives have different redox properties and cytotoxicity[5]

Summary

Mitochondria-targeted redox-active polyphenol derivatives are being developed to intervene on radical processes in the organelles and as a tool either to protect cells from oxidative insults or to precipitate their death. Since the properties of the compounds may be modified by the substituents introduced to determine mitochondrial delivery, we have characterized the redox behaviour of two isomeric mitochondriotropic quercetin-based compounds, 3- and 7-*O*-(4-triphenylphosphoniumbutyl)quercetin iodide. In both cyclic voltammetric determinations of the oxidation potential and in 1,1-diphenyl-2-picrylhydrazyl (DPPH) radical scavenging assays the 7-substituted isomer behaved much like quercetin itself, while the 3-substituted isomer was less reactive. In the low-μM range both compounds proved to be cytotoxic for cancerous and, to a lesser extent, non-cancerous fast-growing cultured cells, while sparing slow-growing cells. The 7-substituted isomer proved more active, and thus emerges as the isomer of choice for further studies. Cells died by necrosis, as shown by the lack of effect of the deletion of pro-apoptotic Bax and Bak and of the presence of the pan-caspase inhibitor z-VAD-fmk.

Introduction

In most cells, mitochondria are the main site of Reactive Oxygen Species (ROS) production. Radicals are produced via one-electron transfer to oxygen from sites of the respiratory chain [1,2], and, under appropriate circumstances, by diversion from cytochrome c to oxygen with the intermediacy of p66Shc [3,4] or as a product of MonoAmino Oxidase activity [5]. These ROS carry a considerable part of the blame for aging (e.g. [6]; but see [7]), neurodegenerative disorders [8,9], and ischemia/reperfusion damage [4,5]. ROS are also an important factor in apoptosis (e.g. [10-12]). Their regulated production is believed to constitute an important signalling pathway (e.g. [13, 14]). ROS are oncogenic, and their increased production is important for the maintenance of the cancerous phenotype (e.g.

[5] Submitted to *Free Radic. Biol. Med*. by: Mattarei, A.; Sassi, N.; Biasutto, L.; Durante, C.; Sandonà, G.; Marotta, E.; Garbisa, S.; Gennaro, A.; Zoratti, M.; Paradisi, C.

[15-19]). Mitochondrial ROS production increases the metastatic potential of cells [20-22] and anti-oxidant polyphenols decrease cell shedding from cancer spheroids in culture (a model of the metastatic process) [23]. On the other hand ROS can induce cell death and thus act as anti-cancer agents. Since cancerous cells in many cases have a higher-than-normal basal rate of ROS production, despite their enhanced redox defences an additional oxidative stress may push them over the brink of death more easily than normal cells (e.g. [24, 25]). Thus both anti-oxidant and pro-oxidant anti-cancer approaches have been proposed (e.g. [16, 18, 19, 24, 26-29]). These considerations explain the booming interest in the development of pharmacological tools allowing the modulation of the mitochondrial redox state, which in most studies take the form of mitochondria-targeted redox-active compounds [30-35].

Polyphenols, a vast family of natural compounds, can function as anti-oxidant or pro-oxidant agents depending on such factors as pH and the concentration of iron or copper ions (e.g.: [36-38]). Accordingly, we have recently shown that *in vitro* they can modulate the mitochondrial permeability transition, i.e. the Ca^{2+} and oxidative stress-induced loss of permeability of the inner mitochondrial membrane, in opposite ways depending on the experimental setup used [39]. Furthermore, they can exert effects of great potential biomedical relevance via interactions with enzymes and channels (for recent reviews on the activities of quercetin, the flavonoid used for this study, see, e.g. [40-43]). A major issue concerning their efficient use *in vivo* is their low bioavailability [44-46]. Only low (nM-μM) concentrations of polyphenols are found in plasma and lymph even after a polyphenol-rich meal, and mostly in the form of conjugates. Even a modest increase may however have remarkable effects through hormesis, the induction of a defensive anti-oxidant apparatus in response to a transient pro-oxidant stress (e.g. [47-49]), or via a catalytic effect precipitating the extensive oxidation of the cellular pools of antioxidants (glutathione, NADH and thioredoxin) with the concomitant reduction of oxygen and formation of H_2O_2 (e.g. [50, 51]).

With the long-term goal of increasing the concentration of redox-active polyphenols in the cytosol and in the subcellular compartment where they might be most useful, the mitochondria, we are developing "mitochondriotropic" derivatives obtained by linking a membrane-permeable, positively charged triphenylphosphonium (TPP) moiety to the polyphenol kernel ([52, 53]; for a discussion of the method see, e.g.: [32, 33]). The rationale of such an approach calls for the delivery and accumulation into mitochondria of compounds with physico-chemical properties and bioactivities similar to those of the

parent compound (quercetin in our case). On the other hand, any modification of the chemical structure will imply a modification of the properties; thus, quercetin conjugates produced in metabolism are much less oxidation-prone than quercetin itself [54, 55]. This consideration may apply also to isomers. In the case in hand, oxidation of flavonoids with a catechol group on the B ring is generally considered to involve the cathecol group [56-59] (for a discussion of why this is so, see, e.g., [60]), but the rate of the electrochemical process [61, 62] and the identity of the products eventually formed [63] depend on the presence of a free OH at position 3, which plays a key role for oxidative degradation of the flavonoid ring system (Fig. 1).

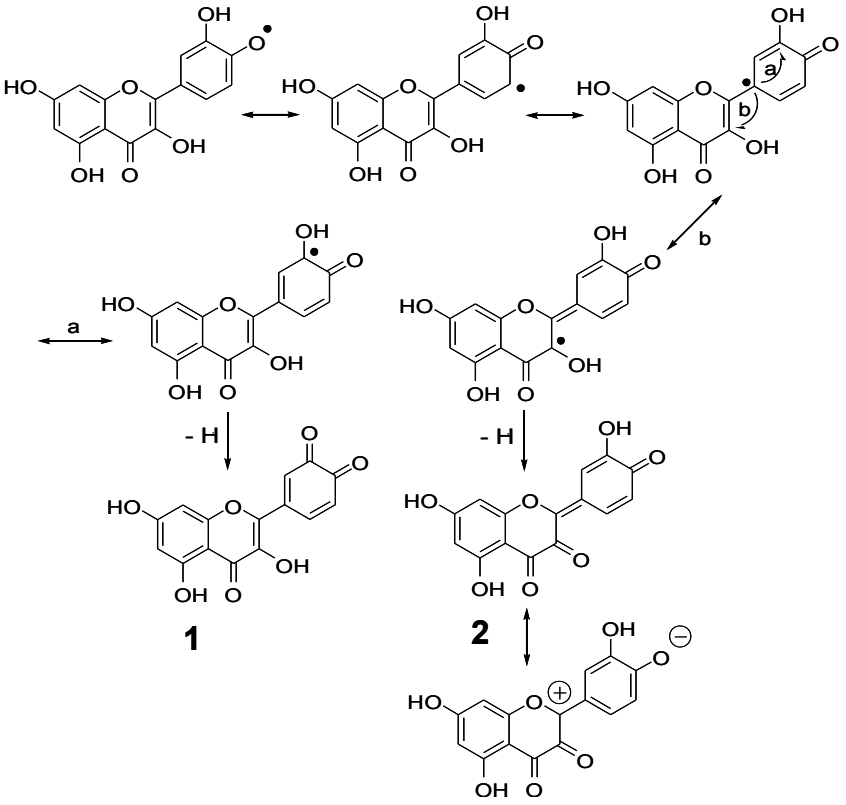

Figure 1. Quercetin oxidation.

For oxidation product **2** (but not for **1**) a resonance structure can be written showing a positive charge on C-2. This site can therefore be attacked by nucleophiles (water) with consequent opening of the C ring and formation of a set of products, which are not accessible if the 3-OH is blocked (e.g. [64, 65]). Reactivity depends, besides structure, also on the solvent and its characteristics, and the outcome of comparisons may depend on the type of assay used. A discussion of these topics can be found in recent publications [58, 60, 66, 67]. In assays based on the reaction with stable radicals, in solvents supporting ionisation, the acidity of the available free OH groups has an important role in determining the reducing power of the compound [60].

A mitochondria-targeting group can in principle be attached at any one of 10 positions in quercetin. In view of planned future elaborations allowing reversibility, i.e. the regeneration of the parent compound once inside mitochondria (e.g. [68]), and to avoid destruction via C ring opening, we initially chose to link the TPP group via an ether bond and a 4-methylene connection to the 3-OH [52, 53]. As mentioned, modifications of this group can however be predicted to affect oxidation potential, reactivity and possibly biological activity as well, making it interesting to assess the extent of the variation with respect to quercetin and to another regioisomer, carrying the substituent at position 7, which was recently synthesized in our laboratory [69]. We therefore decided to characterize the redox properties of the two isomeric derivatives Q-3BTPI and Q-7BTPI, and to compare them with those of quercetin (Q) (Fig. 2).

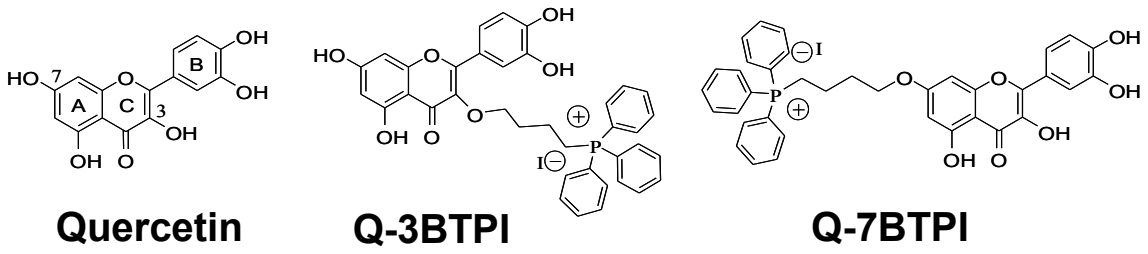

Figure 2. Structures of quercetin and of its mitochondriotropic derivatives used in this study.

The oxidation of phenols can proceed via different mechanisms, depending on experimental conditions such as solvent and pH (e.g. [67], refs therein) and lead to complex sets of products (at least 20 have been identified for quercetin [58]). Processes *in vivo* are likely to involve multiple pathways and are difficult to reproduce *in vitro*. To compare the redox behaviour of our compounds we used cyclic voltammetry (CV) and the DPPH reactivity assay, one of the most widely used methods to rank molecules on the basis of their ROS scavenging power. These two quite different experimental approaches may be taken to represent two extremes of the spectrum of possible oxidative reaction conditions. While they cannot be considered to fully reflect the complete range of reactions our compounds may undergo in a biological setting, coherent results may be taken to provide a reliable indication of relative redox reactivity in settings of physiological relevance.

To identify a biological comparative readout we built on our recent findings that Q-3BTPI and its peracetylated derivative are cytotoxic [52], and proceeded to compare Q-3BTPI and Q-7BTPI from this point of view. Q-7BTPI outperformed Q-3BTPI as a cytotoxic agent

also, inducing necrosis. In Chapter 6 we describe the characterization of the death induction process.

Results and Discussion

TPP-quercetin conjugates accumulate in the mitochondria of cultured cells

While our compounds can be predicted, on the basis of their structure and of their behaviour with suspensions of isolated mitochondria, to concentrate in mitochondria due to the transmembrane potential, with cells this has actually been shown only for the acetylated derivatives [52, 82]. Unprotected quercetin derivatives may be expected to bind avidly to cellular components because of the simultaneous presence of H-bonding hydroxyls, the planar flavonoid structure which can engage in hydrophobic stacking, and the charged and lipophilic triphenylphosphonium group. We therefore assessed their mitochondriotropic behaviour by fluorescence microscopy. The assays were complicated by the low intrinsic fluorescence of these compounds (especially of Q-3BTPI, which in practice cannot be monitored with this approach). Furthermore, the expected binding is indeed observed: the accumulation process is relatively slow, and the "background" due to the molecules bound to non-mitochondrial cellular structures reduces contrast and resolution. Accumulation into mitochondria is not, therefore, as marked and evident as with the acetylated derivatives. Nonetheless, as illustrated in Fig. 3, the compounds do concentrate in discrete subcellular structures which are shown to be mitochondria by their morphology and by the releasing effect of uncoupler.

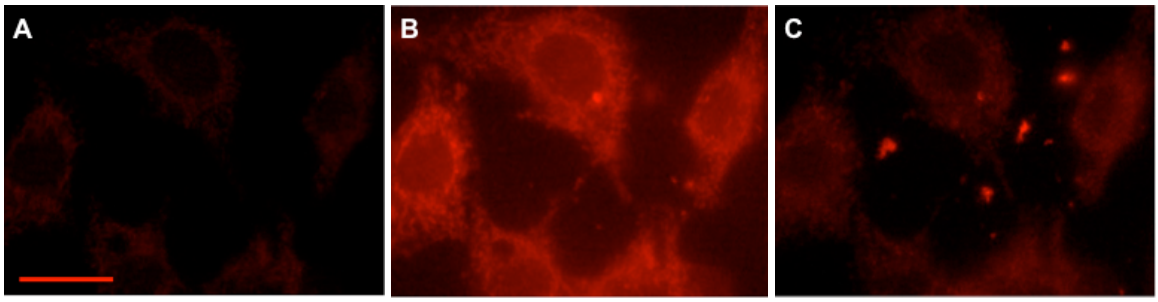

Figure 3. Cellular localization. Fluorescence microscopy images of HepG2 cells. For details see Materials and Methods. A) No addition. B) A few minutes after the addition of 20 μM Q-7BTPI. C) After the subsequent addition of 2 μM FCCP. The strongly fluorescent objects are granules of precipitated Q-7BTPI. Bar: 25 μm. Images were acquired using the same settings and displayed with the same parameters, allowing comparison.

Cyclic voltammetry of quercetin and its mitochondriotropic derivatives.

A major purpose of these determinations has been the comparison of the electrochemical behaviour of the mitochondriotropic derivatives Q-3BTPI and Q-7BTPI with that of the parent compound, quercetin, to assess the effect of the chemical modifications introduced.

To our knowledge, this is the first such study involving mitochondriotropic redox-active compounds.

The voltammetric behaviour of quercetin at the glassy carbon electrode is shown in Fig. 4a. The voltammogram presents three oxidation peaks indicated in the graph as A_1, A_2 and A_3 at 0.114, 0.485 and 0.86 V vs. SCE, respectively (Table 1). The first voltammetric wave A_1 corresponds to the cathodic counter part C_1, which becomes clearer if the potential scan is inverted before the second oxidation event A_2 takes place (solid line). The first redox event is indicative of an almost reversible electrochemical process since the ΔE_p, expressed as the difference between the anodic $E_{p,a}$ and cathodic $E_{p,c}$ peak potentials, is 80 mV. The ΔE_p values increase as the scan rate is increased, indicating that the electrochemical process is dependent both on diffusion and on the rate of electron transfer, which, in this case, is relatively slow.

Peak A_2 is irreversible for all the scan rates ranging from 0.01 to 20 V/s, and so is peak A_3, which appears as a shoulder of the solvent discharge. On the cathodic scan (not shown) an almost reversible reduction process takes place at a cathodic potential peak of −1.685 V vs. SCE. Although the electrochemical oxidation process of quercetin has been investigated using various solvents and supporting electrolytes [58, 59, 61, 63], the oxidation mechanism has not yet been completely understood. However, it is commonly accepted that the first oxidation process A_1 is the reversible bielectronic oxidation of the cathecolic moiety of quercetin to yield the corresponding quinonic derivative. The subsequent peak A_2 has been assigned to the oxidation of OH group in position 3 of the C ring, while peak A_3 is probably due to the oxidation of a OH group on the A ring. On the cathodic scan, peak at −1.685 V vs. SCE may be ascribed to the reduction of the carbonyl on the C ring.

When the electrochemical process is reversible or quasi-reversible, cyclic voltammetry allows the estimation of the standard potential as $E° = (E_{p,a} + E_{p,c})/2$. The standard potential value for the first oxidation of quercetin in these experimental conditions is $E° = 0.074$ V vs. SCE, in line with the values reported in the literature [83]. The standard potential of quercetin and other flavonoid molecules is often correlated to their antioxidant activity. Since the latter is of interest here, we focused on the first oxidation process.

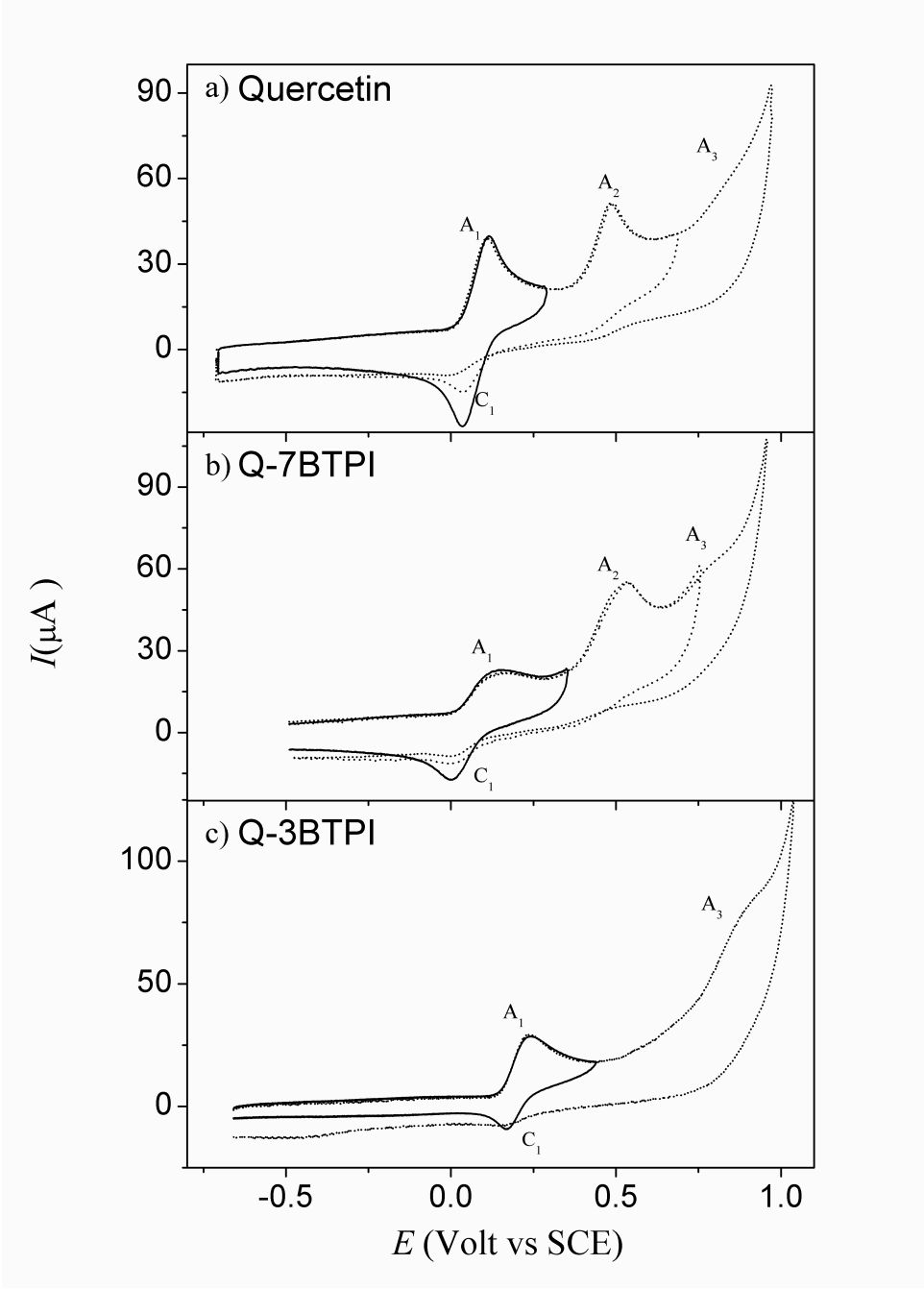

Figure 4. Cyclic voltammetry of the compounds of interest. Voltammograms were recorded with 1 mM: a) Quercetin, b) Q-7BTPI, c) Q-3BTPI, in 9/1 DMF/TrisHCl buffer solution, 0.1 M Bu_4NBF_4 as supporting electrolyte, and with a Glassy Carbon working electrode at $v = 0.2$ Vs^{-1}.

The redox behaviour of Q-7BTPI (Fig. 4b) also shows three oxidation steps, the first of which (A_1) is quasi-reversible, as shown by the ΔE_p value considerably greater than the 60 mV expected for a fully reversible electron transfer (Table 1). Although the anodic peak potential $E_{p,a1}$ is more positive than the corresponding peak potential of quercetin by 0.029 V, the standard potential $E°$ (0.072 V vs. SCE) is quite close in value to that of quercetin (Table 1). It is worth noting that peak A_1 is more "stretched" and of lower intensity in the case of Q-7BPTI with respect to quercetin as reflected by the values of J_p, ΔE_{p1} and $\Delta E_{p/2}$

reported in Table 1. This may be ascribed to the contribution of two different effects: (i) a lower diffusion coefficient due to a different solvation sphere induced by the BTPI group, (ii) a slower electron transfer rate with respect to quercetin. A confirmation of this assumption is provided by the observation that ΔE_{p1} values increase with the scan rate much more markedly than in the case of quercetin suggesting that a slower electron transfer takes place in Q-7BTPI with respect to quercetin.

In the case of Q-3BTPI the alkylation of the OH group causes a positive shift of the first oxidation peak and the loss of the second peak in the voltammetric pattern. This is in agreement with the notion that the 3-OH is profoundly involved in the first electron transfer process due to its implication in resonance structures which stabilize the intermediates of the electrochemical process. Furthermore, the first peak A_1 is characterized by a lower chemical reversibility even when the scan rate is reversed just after the A_1 peak potential (Fig. 4c solid line). Chemical reversibility is completely lost at a scan rate of 0.01 V s^{-1} (Fig. 5).

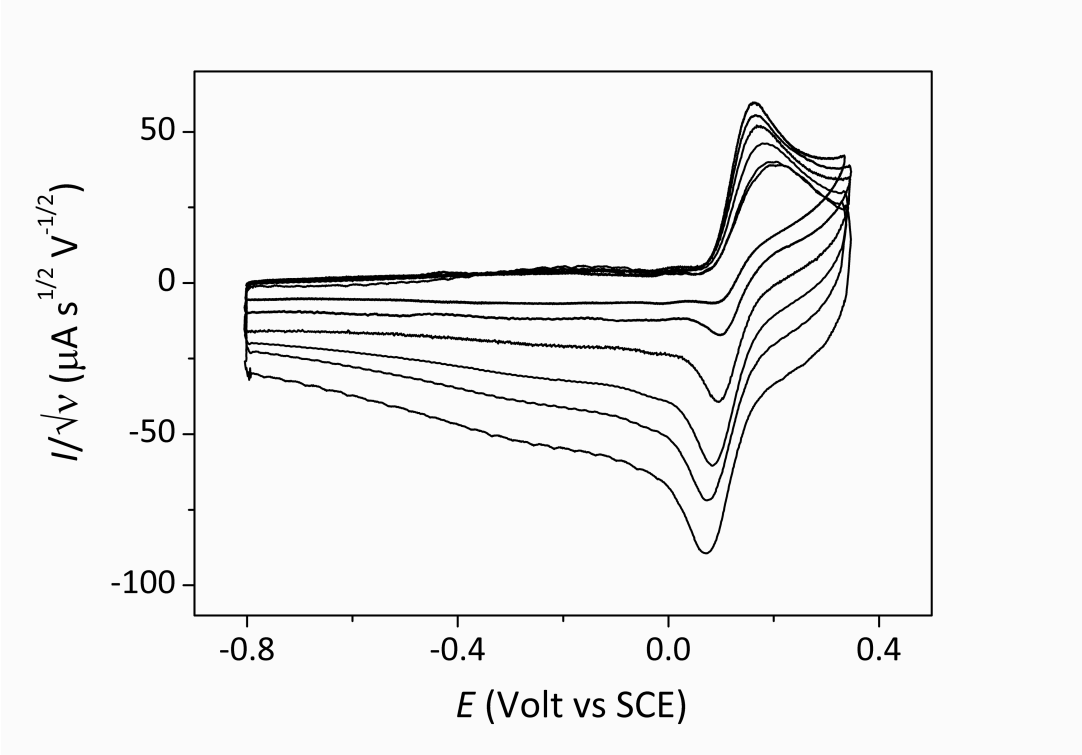

Figure 5. Cyclic voltammetry of Q-3BTPI as a function of scan rate. Voltammograms were recorded with 1 mM Q-3BTPI in 9/1 DMF/TrisHCl buffer solution, 0.1 M Bu_4NBF_4 as supporting electrolyte, using a Glassy Carbon working electrode at scan rates ranging from 0.01 to 2 V s^{-1}.

However, increasing the scan rate the anodic current peak decreases and on the contrary the cathodic counterpart increases (Fig. 5). This behaviour, associated with the increase of the $\Delta E_{p/2}$ with the scan rate, may be ascribed to an ECE mechanism, which involves a first

electron transfer that induces a chemical reaction to generate a new species that may be further oxidized. However at high scan rates the chemical step may be prevented, so that the species that is produced upon oxidation may be reduced at the electrode before it has a chance to undergo any chemical reaction.

In this case, the evaluation of the standard potential as the average of oxidation and reduction peak potentials of A_1 is not straightforward, because at low scan rates the peak potentials are influenced by the chemical reaction of the ECE mechanism, while at high scan rates they are influenced by a slow electron transfer kinetic that causes the "stretching" of the peaks. However, the standard potentials can be roughly estimated at scan rates higher than 1 V s^{-1} while the peak is still fully chemically reversible (0.166 V vs SCE). This value is more positive by about 90 mV with respect to both quercetin and Q-7BTPI, reflecting a lower oxidability of Q-3BTPI.

Assessment of the radical scavenging properties of quercetin and derivatives by the DPPH method.

DPPH is a stable free radical with an absorbance maximum at 520 nm (purple). Its conversion to DPPHH (yellow) is used as a readout of radical scavenging by an added antioxidant such as quercetin [71, 84, 85] (Fig. 6).

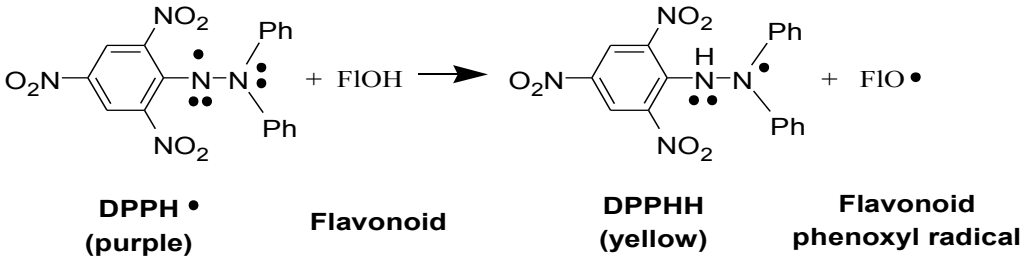

Figure 6. The reaction between DPPH and a generic flavonoid.

Fig. 7 presents the results of typical spectrophotometric experiments in which DPPH was titrated with quercetin, Q-7BTPI or Q-3BTPI. The results are displayed as plots of $[(A_{contr} - A_{sam})/(A_{contr} - A_{blank})] \times 100$, a quantity which is taken to represent the percent fraction of DPPH quenched, as a function of the polyphenol concentration (see Materials and Methods for details). The steeper the quenching curve the stronger the oxidizing power of the polyphenol.

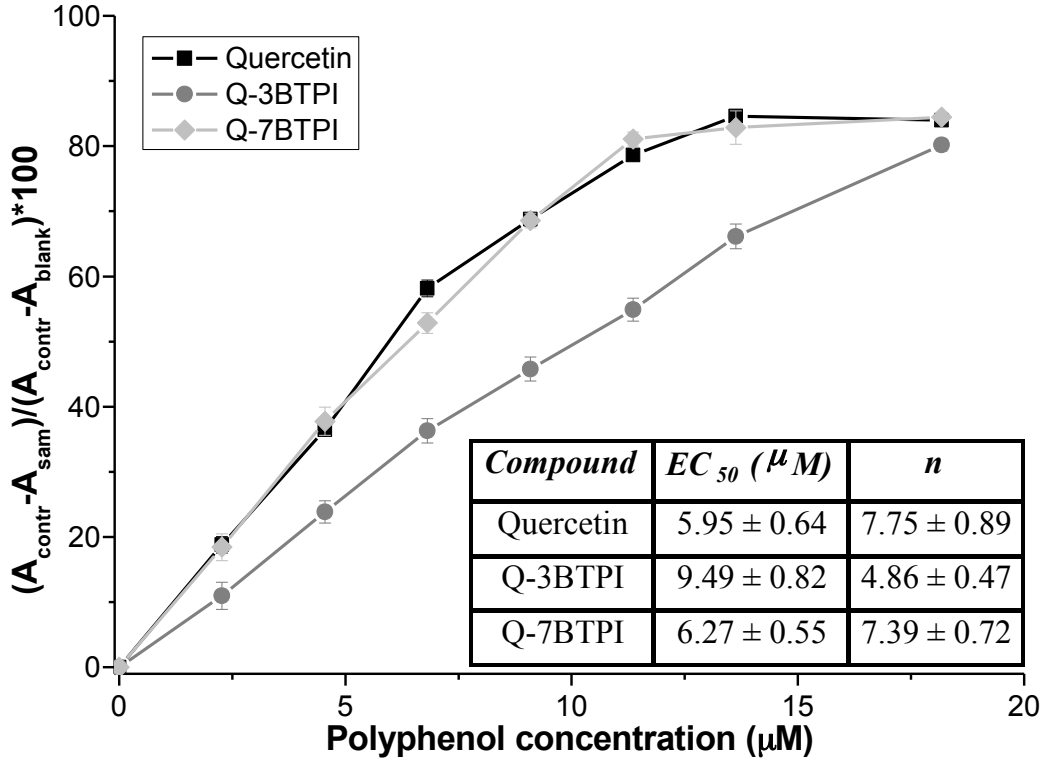

Compound	*EC 50 (μM)*	*n*
Quercetin	5.95 ± 0.64	7.75 ± 0.89
Q-3BTPI	9.49 ± 0.82	4.86 ± 0.47
Q-7BTPI	6.27 ± 0.55	7.39 ± 0.72

Figure 7. Reaction of DPPH with quercetin, Q-3BTPI and Q-7BTPI monitored spectrophotometrically at 520 nm. For each compound an exemplary experiment is shown. Data points are the average of triplicate measurements ± s.d. See Materials and Methods for details. Inset: EC_{50} and reaction coefficient values (averages ± s.d.; N = 3 for each compound).

From the titration curves values of EC_{50} and *n* are derived, which represent, respectively, the concentration of polyphenol necessary to quench the DPPH absorbance by 50% and the reaction coefficient. EC_{50} and *n* values derived from our experiments with quercetin, Q-3BTPI and Q-7BTPI are reported in the inset of Fig. 7.

Fig. 7 shows that, while quercetin and Q-7BTPI produce very similar titration curves and reaction coefficients, Q-3BPTI is less efficient at quenching DPPH. The presence of a free hydroxyl at position 3 is thus important for this reaction as well as for the electrochemical oxidation, whereas the OH at position 7 seems to be rather ininfluent. This behaviour, which is consistent with observations made by other groups [86-90] can be rationalised considering that the Sequential Proton Loss Electron Transfer (SPLET) reaction probably taking place at the catechol moiety [60] forms a delocalized radical which, in case there is a free OH in 3, can lead to the formation of a o-quinone group in the C ring upon further oxidation (Fig. 1). C-ring-opening products may then give further reactions with DPPH, thus presumably accounting for the different stoichiometries observed with quercetin and

Q-7BTPI on one hand and Q-3BTPI on the other. Further reaction of an initially formed product to give a higher overall stoichiometry has been reported, e.g., for the reaction of chrysin with the ABTS (2,2'-azinobis-(3-ethylbenzothiazoline-6-sulfonic acid)) radical in the TEAC assay [91].

In conclusion, both in direct electrochemical oxidation experiments and in radical quenching assays the performance of Q-7BTPI is very similar to that of quercetin. Its regioisomer Q-3BTPI is characterized by a higher electrochemical oxidation potential and a lower reactivity with DPPH. Based on these grounds, therefore, Q-7BTPI is *a priori* to be preferred to its isomer Q-3BTPI for the development of mitochondriotropic anti- or pro-oxidant prodrugs. However, Q-7BTPI may be expected to be more prone to oxidative degradation than Q-3BTPI also *in vivo*, for the reasons already mentioned.

Cytotoxicity of mitochondriotropic quercetin derivatives.

To verify whether a correlation exists between the observed oxidative behaviour and cytotoxicity for cultured cells we compared Q-3BTPI and Q-7BTPI in cytotoxicity assays. As controls, we checked also the action of quercetin, a simple phosphonium salt (triphenylphosphonium chloride; TPMP) and quercetin plus TPMP. Three cell lines were used for these studies: a murine colon cancer line (C-26), and fast- and slow-growing embryonic murine fibroblasts (MEF), non-tumoral cell lines. To evaluate the cytotoxic/cytostatic action of our compounds, we used the tetrazolium salt reduction (MTT) assay to quantify cell growth and viability. The results shown (Fig. 8) are representative of 5-7 repeated experiments. The effects were always reproduced, but with some quantitative variability especially in the case of Q-3BTPI. All compounds tested had little or no effect at 1 μM (not shown). At higher concentrations Q-7BTPI turned out to be more effective than Q-3BTPI, a result which is best appreciated at the 3 μM level. As already observed with Q-3BTPI, the cytotoxic/cytostatic effect of the mitochondriotropic quercetins is evident in the case of C-26 cells (Fig. 8a) and, more moderately, on fast-growing MEF cells (Fig. 8b), while it was insignificant on slow-growing MEF cells (Fig. 8c). This behaviour is typical of many chemotherapeutic drugs. The relative effectiveness of the two isomers also appears to depend, to an extent, on the cell type. The ratio of the MTT assay absorbance values (Q-3BTPI-treated cells) / (Q-7BTPI-treated cells) in each experiment (i.e., the relative number of viable cells) was always higher in the case of fast-growing MEF cells than for C-26 cells (averages: 3.62 ± 0.44 and 2.18 ± 0.66, respectively; N=4 for both).

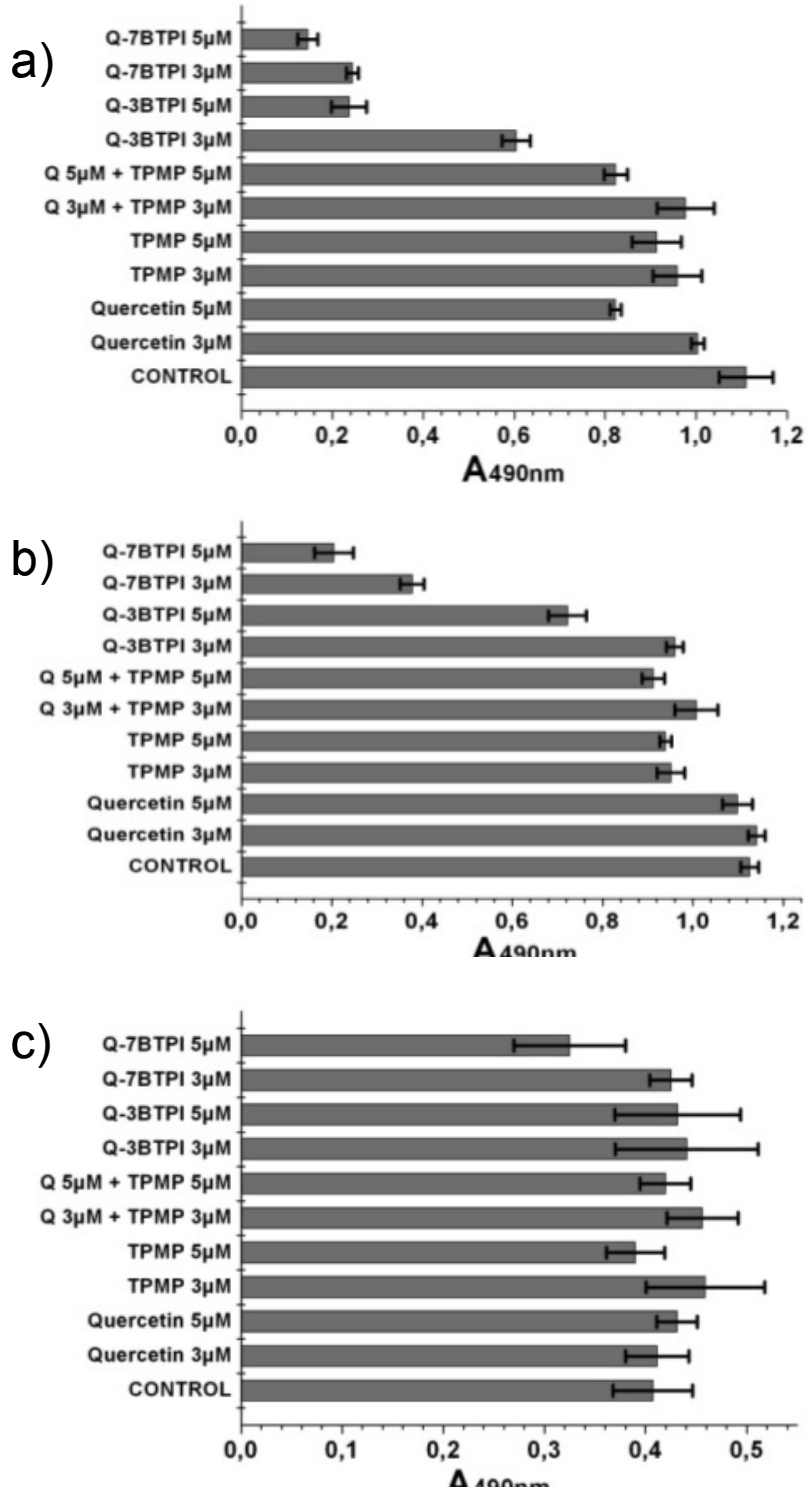

Figure 8. Effect of quercetin derivatives and control compounds on the readout of tetrazolium reduction assays. Cells were allowed to grow for 3 days in the presence of the specified compounds (see Materials and Methods for details). An individual representative experiment run in parallel with the three cell lines is shown. All measurements were performed in quadruplicate. Averages ± s.d. are given. a) C-26 mouse colon tumor cells. b) Fast-growing Mouse Embryonic Fibroblasts (MEF). c) Slow-growing MEF. Abbreviations: TPMP: methyltriphenylphosphonium; BTPI: n-(4-triphenylphosphonium)butyl iodide; Q: quercetin. In this experiment the number of cells seeded in each well was as follows: a): 3000; b): 1000; c): 2500.

The parent polyphenol and TPMP, alone or in combination, did not have a significant effect on cell vitality. The combination of the polyphenol kernel and the mitochondriotropic phosphonium moiety within the same molecule is thus necessary to observe cytotoxicity. The results of the MTT assay were confirmed by direct observation of the cell cultures at the microscope (not shown).

One possible factor contributing to the differential cytotoxicity may be a difference in the mitochondrial endowment of the different cell lines. Assuming transmembrane potentials to be the same, a larger average cell size, and/or a higher mitochondrial/cellular volume ratio would be expected to result in more mitochondriotropic compound being taken up per cell, and this may result in higher cytotoxicity if the latter is an extensive property of the compound. On the other hand, since a) if more compound is taken up by cells its equilibrium external concentration is bound to be lower, b) distribution tends to obey Nernst's law, and c) a larger cellular and/or mitochondrial mass implies more binding, the concentration of compound in the cytosol and/or mitochondria is expected to be lower in cells that are larger and/or have a larger mitochondrial compartment. This might actually result in a lower cytotoxicity if the latter is an intensive (i.e., linked to concentration) property of the compound.

To gain some information on this aspect we first measured for each of the three cell lines the average protein content per cell (see Materials and Methods). The values turned out to be similar (Fig. 9A). Mitochondrial content was compared instead by measuring by FACS the relative median fluorescence of cells loaded with NAO (10-N-nonyl Acridine Orange), a compound which binds tightly to IMM-specific cardiolipin and thus reports on the amount of this mitochondrial phospholipid and indirectly on the surface of the IMM [81] (Fig. 9B). C-26 cells, i.e., glycolysing tumor cells, and fast-growing MEFs turned out to have similar contents of cardiolipin, lower than that of slow-growing MEFs. Thus, the least affected cells are the ones with the most mitochondria. The point is elaborated further in the next chapter.

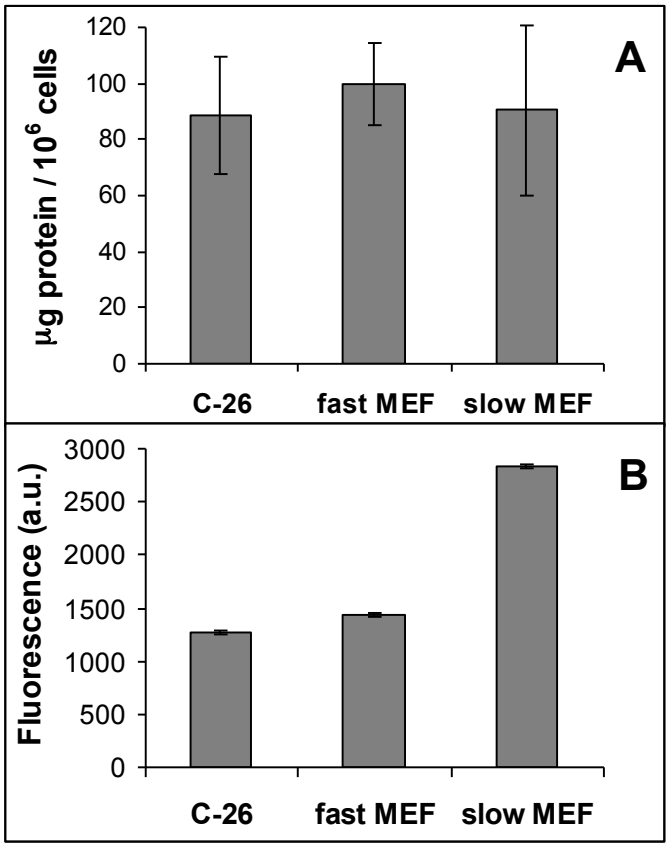

Figure 9. Relative mitochondrial content of the adherent cells used. A) The protein content per cell is similar in the three cases. The amount (µg) of total protein per million cells, based on the BCA protein assay. B) Slow-growing MEF cells have a higher amount of cardiolipin per cell than the other two lines. NAO fluorescence; medians of cell fluorescence distribution histograms. N = 3 in all cases. See Materials and Methods for details.

Cell death induced by Q-3BTPI and Q-7BTPI is necrotic

The results presented so far suggest that these compounds, in particular Q-7BTPI, may act as pro-oxidants, and that radical generation may underlie cell death. A vast consensus exists that reactive oxygen species can induce apoptosis (revs: [11, 92]). In this process, activation of kinase-based pro-apoptotic signaling can be of major importance [93], along with other process such as the oxidative dimerization and activation of Bax [94] and peroxidation of mitochondrial cardiolipin, important for the release of cytochrome c [10, 95]. ROS, especially at high levels, may also lead to necrosis (e.g. [96]). Necrosis, long considered as an uncontrolled, haphazard form of cell death, is now understood to comprise a set of interacting signalling cascades and biochemical phenomena forming a continuum with other forms of cell death (apoptosis, autophagy, parthanatos, pyroptosis etc.; see [97]) (e.g.: [98-100]). ROS may for example cooperate with Ca^{2+}-activated calpains to destabilize lysosomal membranes. Released cathepsins then determine generalized failure of cell bioenergetics and death (e.g. [101]). Membrane disruption may

have to do with the generation of very reactive oxygen species in Fenton reactions catalysed by the iron-rich, H_2O_2-permeable lysosomes [102]. In fact, permeable iron chelator desferrioxamine prevents lysosomal membrane permabilization and cell death [103].

Apoptosis may be characterized as involving the pro-apoptotic Bcl2-family proteins Bax and/or Bak, and the caspase family of proteases. We have therefore verified whether the toxic effects of the compounds would be reduced a) for $Bax^{-/-}/Bak^{-/-}$ MEFs in comparison with the corresponding parental strain (Fig. 10A) and b) in the presence of the pan-caspase inhibitor z-VAD-fmk (Fig. 10B).

For the former experiment we compared the results of MTT reduction assays. z-VAD-fmk has been reported to be toxic itself if applied at high concentration for prolonged periods, such as the three days of our standard cell viability determination protocol [104]. Therefore for the latter experiment we used FACS and Jurkat cells (a tumoral lymphocyte line of cells growing in suspension) to quantify cell labelling by annexin and propidium iodide (PI) after a much shorter (3 hrs) exposure to our compounds or to a recognized apoptosis inducer, staurosporine (e.g. [105]), with or without z-VAD-fmk. With both approaches, the results with the mitochondriotropic quercetin derivatives differed considerably from those with staurosporine. The readout of the MTT assay was markedly altered by the absence of Bax and Bak when staurosporine was used (note however that $Bax^{-/-}/Bak^{-/-}$ DKO cells also suffer in the presence of this aspecific kinase inhibitor), but not with Q-7BTPI or the less powerful Q-3BTPI. In the annexin/PI labelling experiments, control incubation in DMEM without serum for 3 hours resulted in a significant fraction (20% in the example shown) of the cells being labelled by PI, annexin or both, a fraction that was slightly reduced in the presence of z-VAD-fmk 100 μM.

With apoptosis-inducing staurosporine the fractions of cells labelled by PI or by both PI and annexin were similar to control, while, as expected, the percentage of cells labelled by annexin only was much higher (63% vs. 7.2% in the control), and was reduced to 9.3% in the presence of z-VAD-fmk.

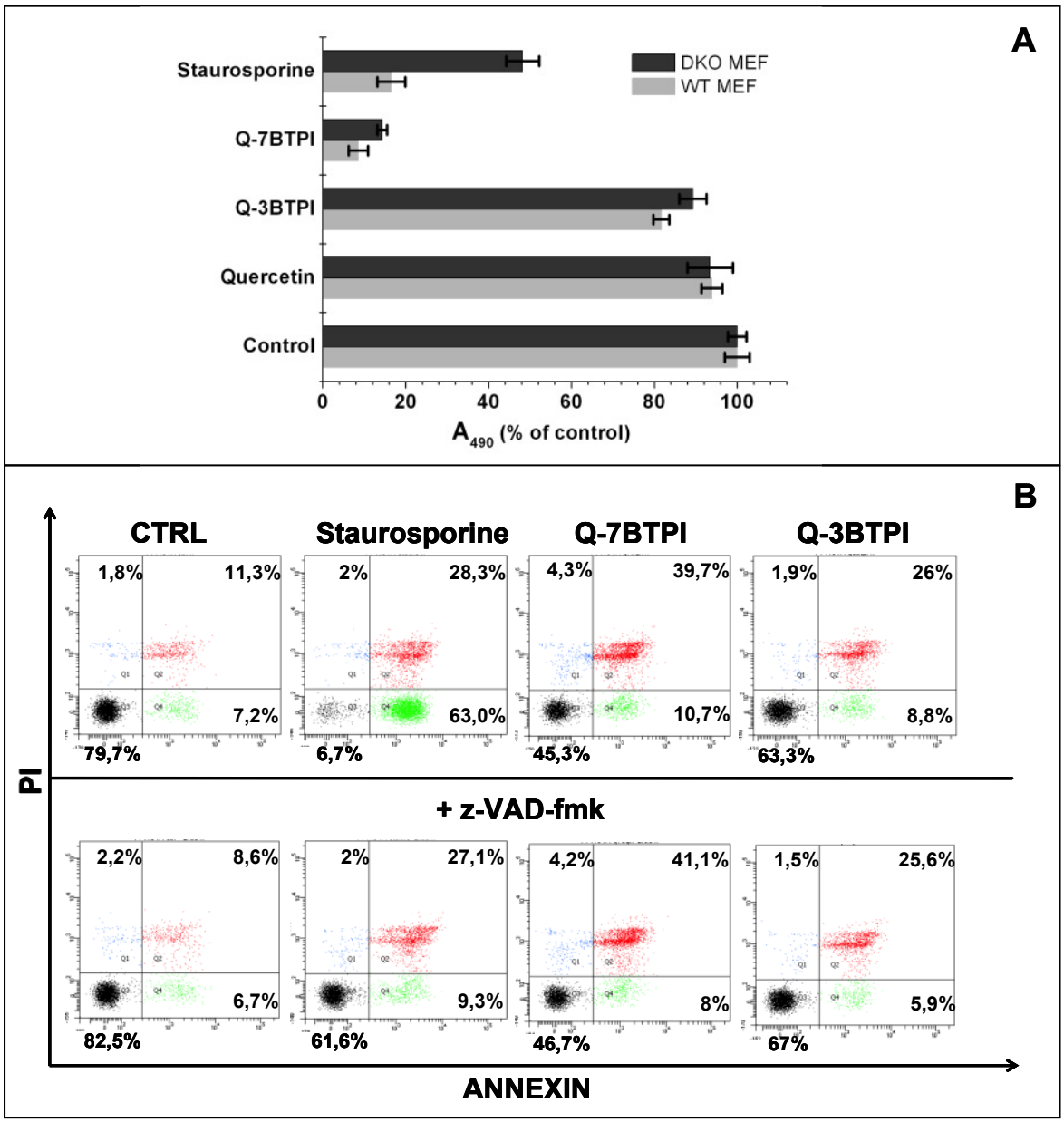

Figure 10. Cells death is necrotic. A) The cytotoxic/cytostatic effect of mitochondriotropic quercetin derivatives is only slightly affected by the presence or absence of the pro-apoptotic proteins Bax and Bak. MTT assay readout. One representative experiment out of three performed is shown. 1000 WT or $Bax^{-/-}/Bak^{-/-}$ (DKO) MEF cells were seeded in each well. Concentration of quercetin and derivatives was 5 µM, Stauroporine 100 nM. B) The pan-caspase inhibitor z-VAD-fmk has little effect on annexin/PI labelling of Jurkat cells exposed to Q-7BTPI or Q-3BTPI. FACS analysis of cells labelled after exposure to 5 µM of the indicated agents (2 µM for Staurosporine) for three hours. Cells were pre-incubated 30 minutes with or without z-VAD-fmk; experiments were conducted in DMEM without serum. One representative experiment out of five performed is shown. See Materials and Methods for details. 5.000 cells were counted for each condition.

With the mitochondriotropic quercetin derivatives, conversely, annexin-only labelling was similar to or below control levels, while a large portion of the cells displayed labelling by PI only - the characteristic mark of necrosis - or by both reagents (necrotic cells also

become annexin-positive when this reagent enters the cytoplasm and can react with PS in the inner leaflet of the PM). These phenomena were only slightly antagonized by z-VAD-fmk. Thus, the mechanisms involved in cell death in our experiments appear to have more a necrotic than an apoptotic character. This obviously does not exclude that under other circumstances apoptosis may intervene instead.

The mitochondrial permeability transition (revs: [106-110]) is believed to play a key role in many types of cell death, especially when Ca^{2+} levels and ROS production are disregulated. ROS can be produced by cells as a consequence of MPT induction. To avoid this possible complication and to minimize the possible re-exportation of our compounds by MDR pumps most experiments were conducted in the presence of cyclosporin A, the most reliable inhibitor of the MPT, which also blocks Pgp/MDR1 pumps [111, 112]. To verify whether, in its absence, the MPT may contribute to cell death we performed annexin/PI labelling experiments comparing the readouts without or in the presence of CSA or of CSH, a cyclosporin variant which inhibits MDR1, but not the permeability transition pore [113]. Unexpectedly, no significant difference was observed, suggesting that the MPT is not involved in the process (Fig. 11).

Q-3BTPI and Q-7BTPI show the same relationship whatever aspect is examined: the former is less easily oxidized, has a lower stoichiometry of reaction with DPPH and is less cytotoxic. Q-7BTPI thus appears to be the regioisomer of choice for further work aiming to understand the factors underlying cytotoxicity and to eventually exploit these compounds pharmacologically. Our investigation of the mechanism of cytotoxicity is described in the next chapter.

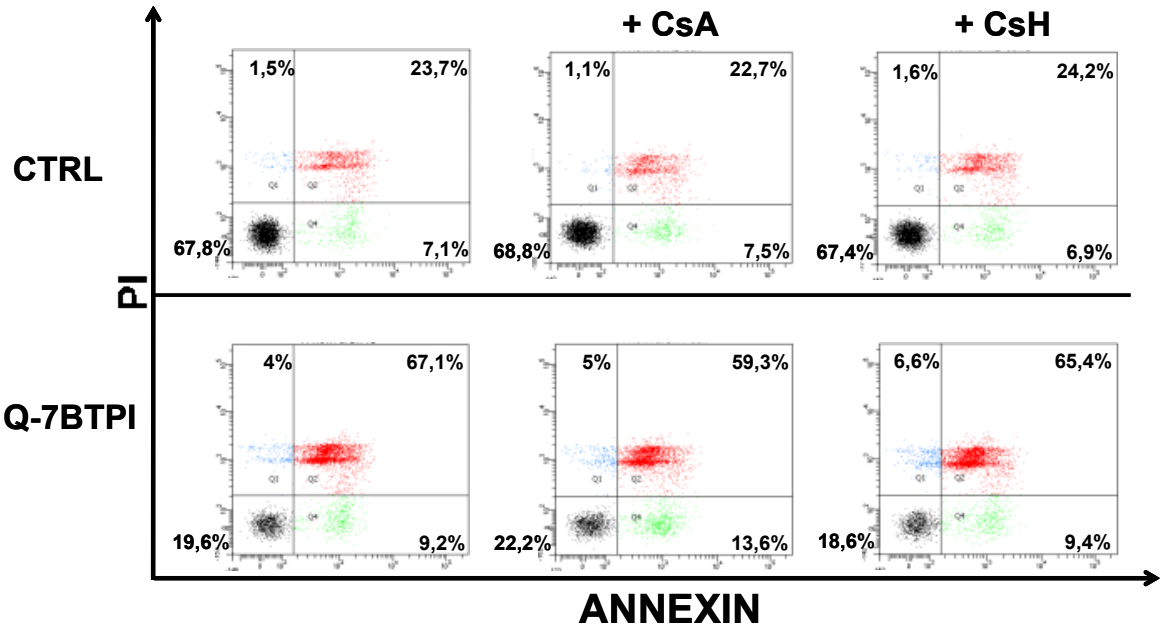

Figure 11. The lack or presence of CsA or CsH has little effect on annexin/PI labelling of Jurkat cells exposed to 5 μM Q-7BTPI. FACS analysis of cells labelled after exposure to the indicated agents for three hours in DMEM without serum. A representative experiment is shown. See Materials and Methods for details. 5.000 cells were counted for each condition.

Experimental section

Materials and methods:

Quercetin and other commercial chemicals were purchased from Sigma-Aldrich (Milan) unless otherwise specified. Chemicals for buffer preparations were of laboratory grade, obtained from J. T. Baker, Merck, or Sigma. Q-3BTPI [52] and Q-7BTPI [69] were synthesized as previously reported.

Electrochemistry.

Electrochemical experiment were performed in a 9/1 DMF/TrisHCl (pH 7.5) buffer solution and tetrabuthylammonium tetrafluoroborate as supporting electrolyte. This buffer was chosen to insure solubility of all compounds to be analysed. Dimethylformamide (DMF, Acros Organics, 99%) was treated with anhydrous Na_2CO_3 and doubly distilled at reduced pressure under a N_2 atmosphere. Tetrabuthylammonium tetrafluoroborate (Bu_4NBF_4 Fluka, > 98%) was recrystallized from ethanol/water (2/1) and dried at 70 °C under vacuum.

Electrochemical measurements were performed by an EG&G Princeton Applied Research Model 173A potentiostat connected to a computer by a DAQ National Instruments USB-9215A card for data monitoring and acquisition. Cyclic voltammetry experiments were

carried out in a three-electrode cell system with a glassy carbon disc as working electrode. The counter electrode and the reference electrode were a Pt wire and Ag|AgI|0.1M *n*-Bu_4NI in DMF, respectively. The latter was calibrated after each experiment against the ferricenium/ferrocene couple, which in DMF/TrisHCl has an $E°$ value of 0.432 V versus SCE. The potentials measured against the $Ag|AgI|I^-$ reference electrode were converted to the SCE scale, to which all potentials in the chapter are referred. The working electrodes were built from a 3 mm diameter Glassy Carbon (GC) rod (Tokai GC-20) and were cleaned with diamond paste (0.25 μm) and sonicated in ethanol for 5 min prior to each experiment; furthermore the GC electrode was electrochemically activated performing 20 cycles (from -0.6 to 1.8 V vs SCE at 0.1 $V\,s^{-1}$) in a Na_2SO_4 0.2 M solution. All experiments were carried out at 25 °C, under Argon, and with a 1 mM solution of the compound of interest.

1,1-diphenyl-2-picrylhydrazyl (DPPH) radical scavenging assays.

The assays were conducted using 96-well plates (Greiner Bio-One) following Fukumoto and Mazza (2000) [71]. Measurements were performed in triplicate (three wells per concentration). Each well contained 200 μL of 150 μM DPPH (i.e. 30 nmoles) in 5/1 methanol/Tris-HCl (pH 7.4). 20 μL Aliquots of appropriate solutions of the polyphenol in DMSO were added at time zero and mixed to produce the desired concentrations (at least seven per determination, within the range 0-200 μM). After 40 minutes at room temperature in the dark, absorbance was measured using a Tecan Infinite 200 plate reader (λ = 520 nm, 10 nm slit). Following literature precedents (e.g. [72-74]), the percent fraction of DPPH quenched during the 40-min incubation is approximated by the following quantity:

$[(A_{contr} - A_{sam})/(A_{contr} - A_{blank})] \times 100$

where A_{contr}, A_{sam} and A_{blank} are the absorbances of the control solution (only DPPH), of the polyphenol plus DPPH solution and of the blank solution (solvent system), respectively.

According to a common practice [75-79], the results of these assays are presented in terms of the parameters EC_{50} and n. EC_{50} is defined as the polyphenol concentration at which the quantity $[(A_{contr} - A_{sam})/(A_{contr} - A_{blank})] \times 100$ reaches a value of 50. This point was determined using the linear best fit of the initial, linear part of the plot $[(A_{contr} - A_{sam})/(A_{contr} - A_{blank})] \times 100$ vs. [polyphenol]. The ratio (moles of DPPH reacted)/(moles of polyphenol added) at EC_{50} constitutes the coefficient n.

Cells.

Fast- (doubling time 16 hours) and slow- (doubling time 3 days) growing SV-40 immortalized Mouse Embryo Fibroblast (MEF) cells and mouse colon cancer C-26 cells (doubling time 24 hours) were grown in Dulbecco's Modified Eagle Medium (DMEM) plus 10 mM HEPES buffer (pH 7.4), 10% (v/v) fetal calf serum (Invitrogen), 100 U/mL penicillin G, 0.1 mg/mL streptomycin, 2 mM glutamine (GIBCO) and 1% nonessential amino acids (100X solution; GIBCO), in a humidified atmosphere of 5% CO_2 at 37°C. Jurkat T lymphocytes (doubling time 24 hours) were grown in RPMI-1640 supplemented as above.

Fluorescence microscopy.

For the experiments on the mitochondrial accumulation of Q-7BTPI (Fig. 3) HepG2 cells were seeded onto 24-mm coverslips in 6-well plates and grown for about two days in DMEM. Coverslips were mounted onto holders, washed, covered with 1 mL of HBSS (in mM units: NaCl 136.9, KCl 5.36, $CaCl_2$ 1.26, $MgSO_4$ 0.81, KH_2PO_4 0.44, Na_2HPO_4 0.34, glucose 5.55, pH 7.4 with NaOH) and placed on the microscope stage. Fluorescence images were acquired automatically at 1- or 2-min intervals, using an Olympus Biosystems apparatus comprising an Olympus IX71 microscope and MT20 light source, and processed with CellR© software. Excitation was at 340 ± 15 nm and fluorescence was collected at $\lambda >$ 400 nm. Additions were performed by withdrawing 0.5 mL of incubation medium, adding the desired solute to this aliquot, mixing, and adding back the solution into the chamber at a peripheral point. Images are presented using the same display parameters; fluorescence intensities can thus be compared.

Cell growth/viability MTT assays.

These experiments were intended to compare the effects of the compounds on cells with different origin and proliferation rates. These effects are expected to depend not on the absolute concentration of compound in the growth medium, but rather on the amount accumulated by the cells, which is inversely related to the number of cells in the assay. The latter in turn changes with a different time course due to the different doubling times of the cultures. Furthermore, in assays with slow-growing cells it was necessary to begin the culture with a more numerous population in order to obtain significant readout values. Results must therefore be considered as of only semi-quantitative significance.

C-26 or MEF cells were seeded in standard 96-well plates and allowed to grow in DMEM + 10% FCS (200 μL) for 16-18 hours to ensure attachment. Initial densities were 1000 or 3000 (for C-26 and fast-growing MEF) or 2500/3000 (slow-growing MEF) cells/well. After the initial attachment period the growth medium was replaced with medium

containing the desired compound at 1, 3 or 5 μM from stock solutions in DMSO. DMSO final concentration was 0.1% in all cases (including controls). Experiments were performed in quadruplicate, i.e., four wells were used for each of the compounds to be tested. Cells were incubated with the compounds for 72 hours; the solution was substituted by a fresh aliquot twice, at 24-hour intervals. At the end of the incubation period, the medium was removed and substituted with 90 μl of PBS plus 10 μL of CellTiter 96® solution (Promega; for details: www.promega.com/tbs). After a one-hour color development period at 37 °C absorbance at 490 nm was measured using a Packard Spectra Count 96-well plate reader.

Annexin/PI labelling assays.

Cell death or committment to it was determined by staining cells with Annexin V-FLUOS (Roche) and Propidium Iodide (PI) (Sigma) and fluorescence analysis by flow cytometry. Jurkat lymphocytes were used to avoid cell aggregations and possible damage due to trypsinization and other procedures associated with the detachment of adherent cells. A Beckton Dickinson Canto II flow cytometer was used. Cells were washed in HBSS and resuspended at 3×10^5 cells/mL in DMEM without serum or in some experiments in HBSS. Aliquots were incubated for three hours with the desired compounds at 37°C, 5% CO_2. DMSO concentration was 0.2% in all cases. A 200 μL portion of each incubation was then placed in test tube and Propidium Iodide (final concentration 1 μg/mL) and annexin-V-FLUOS (Roche; cat. N. 11 828 681 001) (1 μL/sample) were added. FACS analysis was carried out after a further 20-min. labelling period at 37 °C in the dark. Data were processed by quadrant statistics using the BD VISTA software.

Estimating cell mass

Cells (C-26, fast MEFs and slow MEFs) were detached with trypsin/EDTA, washed with PBS and counted. They were then resuspended in PBS containing a protease inhibitors cocktail (Roche) (final concentration 2.5×10^6 cells/ml), and lysed by sonication.

Total protein amount per cell was estimated using bicinchoninic acid (BCA Protein Assay Reagent, Thermo Scientific) according to [80]. Briefly, samples were diluted 1:1 with 2% SDS; 10 μl of sample (about 12500 cells) were placed in duplicate on a 96-well plate; 200 μl of the BCA mixture (solutions A and B, 49:1; see manufacturer's instructions for details) were finally added, followed by 30 min incubation at 37°C. Protein amount was determined interpolating absorbance readouts at 540 nm with a calibration curve obtained by plotting absorbance of albumin reference solutions against concentration (0-500 μg/ml).

Mitochondrial content assays

This assay is based on the fact that Cardiolipin (CL) is found almost exclusively in the inner membranes of mitochondria. The dye 10-N-nonyl acridine orange (NAO), has been used as a specific fluorescence probe for Cardiolipin detection. The incorporation of NAO in inner mitochondrial membranes has been detected as the red fluorescence emitted by formation of NAO dimers [81]. The adherent cells (C-26 and MEFs) were washed in PBS, harvested by trypsinization, washed in HBSS and resuspended at a finally density of 1.5×10^6 cells/mL in HBSS with 0.2 μM NAO. After 10 min of incubation at 37°C in the dark, the cells were washed to remove excess NAO, resuspended in HBSS and analyzed directly by flow cytometry (excitation at 488 nm, fluorescence collected at 530 nm).

Bibliography

[1] Starkov, A. A. The role of mitochondria in reactive oxygen species metabolism and signaling. Ann. N. Y. Acad. Sci. **1147:** 37-52; 2008.
[2] Murphy, M. P. How mitochondria produce reactive oxygen species. Biochem. J. **417:** 1-13; 2009.
[3] Pinton, P.; Rizzuto, R. p66Shc, oxidative stress and aging: importing a lifespan determinant into mitochondria. Cell Cycle **7:** 304-308; 2008.
[4] Carpi, A.; Menabò, R.; Kaludercic, N.; Pelicci, P.; Di Lisa, F.; Giorgio, M. The cardioprotective effects elicited by p66(Shc) ablation demonstrate the crucial role of mitochondrial ROS formation in ischemia/reperfusion injury. Biochim. Biophys. Acta **1787:** 774-780; 2009.
[5] Di Lisa, F.; Kaludercic, N.; Carpi, A.; Menabò, R.; Giorgio, M. Mitochondrial pathways for ROS formation and myocardial injury: the relevance of p66(Shc) and monoamine oxidase. Basic Res. Cardiol. **104:** 131-139; 2009.
[6] Rajawat, Y. S.; Hilioti, Z.; Bossis, I. Aging: central role for autophagy and lysosomal degradative system. Ageing Res. Rev. **8:** 199-213; 2009.
[7] Pérez, V.I.; Bokov, A.; Van Remmen, H.; Mele, J.; Ran, Q.; Ikeno, Y.; Richardson, A. Is the oxidative stress theory of aging dead? Biochim. Biophys. Acta **1790**: 1005-1014; 2009.
[8] Lee, J.; Boo, J. H.; Ryu, H. The failure of mitochondria leads to neurodegeneration: Do mitochondria need a jump start? Adv. Drug Deliv. Rev. **30:** 1316-1323; 2009.
[9] Sayre, L. M.; Perry, G.; Smith, M. A. Oxidative stress and neurotoxicity. Chem. Res. Toxicol. **21:** 172-188; 2008.
[10] Ott, M.; Gogvadze, V.; Orrenius, S.; Zhivotovsky, B. Mitochondria, oxidative stress and cell death. Apoptosis **12:** 913-922; 2007.
[11] Circu, M.L.; Aw, T.Y. Reactive oxygen species, cellular redox systems, and apoptosis. Free Radic. Biol. Med. **48**: 749-762; 2010.
[12] Szabò, I.; Bock, J.; Grassmé, H.; Soddemann, M.; Wilker, B.; Lang, F.; Zoratti, M.; Gulbins, E. Mitochondrial potassium channel Kv1.3 mediates Bax-induced apoptosis in lymphocytes. Proc. Natl. Acad. Sci. U.S.A. **105:** 14861-14866; 2008.
[13] Feissner, R. F.; Skalska, J.; Gaum, W. E.; Sheu, S. S. Crosstalk signaling between mitochondrial Ca^{2+} and ROS. Front. Biosci. **14:** 1197-1218; 2009.
[14] Aon, M. A.; Cortassa, S.; O'Rourke, B. Mitochondrial oscillations in physiology and pathophysiology. Adv. Exp. Med. Biol. **641:** 98-117; 2008.

[15] Klaunig, J. E.; Kamendulis, L. M. The role of oxidative stress in carcinogenesis. Annu. Rev. Pharmacol. Toxicol. **44:** 239-267; 2004.
[16] Storz, P. Reactive oxygen species in tumor progression. Front. Biosci. **10:** 1881-1896; 2005.
[17] Valko, M.; Rhodes, C. J.; Moncol, J.; Izakovic, M.; Mazur, M. Free radicals, metals and antioxidants in oxidative stress-induced cancer. Chem. Biol. Interact. **160:** 1-40; 2006.
[18] Trachootham, D.; Alexandre, J.; Huang, P. Targeting cancer cells by ROS-mediated mechanisms: a radical therapeutic approach? Nat. Rev. Drug Discov. **8:** 579-591; 2009.
[19] Ralph, S. J.; Rodríguez-Enríquez, S.; Neuzil, J.; Saavedra, E.; Moreno-Sánchez, R. The causes of cancer revisited: "mitochondrial malignancy" and ROS-induced oncogenic transformation - why mitochondria are targets for cancer therapy. Mol. Aspects Med. **31:** 145-170; 2010.
[20] Ishikawa, K.; Takenaga, K.; Akimoto, M.; Koshikawa, N.; Yamaguchi, A.; Imanishi, H.; Nakada, K.; Honma, Y.; Hayashi, J. ROS-generating mitochondrial DNA mutations can regulate tumor cell metastasis. Science **320:** 661-664; 2008.
[21] Pani, G.; Giannoni, E.; Galeotti, T.; Chiarugi, P. Redox-based escape mechanism from death: the cancer lesson. Antioxid. Redox Signal **11:** 2791-2806; 2009.
[22] Pani, G.; Galeotti, T.; Chiarugi, P. Metastasis: cancer cell's escape from oxidative stress. Cancer Metastasis Rev. **29:** 351-378; 2010.
[23] Günther, S.; Ruhe, C.; Derikito, M. G.; Böse, G.; Sauer, H.; Wartenberg, M. Polyphenols prevent cell shedding from mouse mammary cancer spheroids and inhibit cancer cell invasion in confrontation cultures derived from embryonic stem cells. Cancer Lett. **250:** 25-35; 2007.
[24] Ralph, S. J.; Rodriguez-Enriquez, S.; Neuzil, J.; Moreno-Sánchez, R. Bioenergetic pathways in tumor mitochondria as targets for cancer therapy and the importance of the ROS-induced apoptotic trigger. Mol. Aspects Med. **31:** 29-59; 2010.
[25] Chen, G.; Wang, F.; Trachootham, D.; Huang, P. Preferential killing of cancer cells with mitochondria dysfunction by natural compounds. Mitochondrion **10**: 614-625; 2010.
[26] Cabello, C. M.; Bair, W. B.; Wondrak, G. T. Experimental therapeutics: targeting the redox Achilles' heel of cancer. Curr. Opin. Investig. Drugs **8:** 1022-1037; 2007.
[27] Wang, J.; Yi, J. Cancer cell killing via ROS: to increase or decrease, that is the question. Cancer Biol. Ther. **7:** 1875-1884; 2008.
[28] Hail, N.; Lotan, R. Cancer chemoprevention and mitochondria: Targeting apoptosis in transformed cells via the disruption of mitochondrial bioenergetics/redox state. Mol. Nutr. Food Res. **53:** 49-67; 2009.
[29] Ralph, S. J.; Neuzil, J. Mitochondria as targets for cancer therapy. Mol. Nutr. Food Res. **53:** 9-28; 2009.
[30] Sheu, S. S.; Nauduri, D.; Anders, M. W. Targeting antioxidants to mitochondria: a new therapeutic direction. Biochim. Biophys. Acta **1762:** 256-265; 2006.
[31] Victor, V. M.; Rocha, M. Targeting antioxidants to mitochondria: a potential new therapeutic strategy for cardiovascular diseases. Curr. Pharm. Design **13:** 845-863; 2007.
[32] Murphy, M. P.; Smith, R. A. Targeting antioxidants to mitochondria by conjugation to lipophilic cations. Annu. Rev. Pharmacol. Toxicol. **47:** 629-656; 2007.
[33] Hoye, A. T.; Davoren, J. E.; Wipf, P.; Fink, M. P.; Kagan, V. E. Targeting mitochondria. Acc. Chem. Res. **41:** 87-97; 2008.
[34] Murphy, M. P. Targeting lipophilic cations to mitochondria. Biochim. Biophys. Acta **1777:** 1028-1031; 2008.
[35] Skulachev, V. P.; Anisimov, V. N.; Antonenko, Y. N.; Bakeeva, L. E.; Chernyak, B. V.; Erichev, V. P.; Filenko, O. F.; Kalinina, N. I.; Kapelko, V. I.; Kolosova, N. G.; Kopnin, B. P.; Korshunova, G. A.; Lichinitser, M. R.; Obukhova, L. A.; Pasyukova, E. G.; Pisarenko, O. I.; Roginsky, V. A.; Ruuge, E. K.; Senin, I. I.; Severina, I. I.; Skulachev, M.

V.; Spivak, I. M.; Tashlitsky, V. N.; Tkachuk, V. A.; Vyssokikh, M. Y.; Yaguzhinsky, L. S.; Zorov, D. B. An attempt to prevent senescence: a mitochondrial approach. Biochim. Biophys. Acta **1787:** 437-461; 2009.
[36] Galati, G.; Sabzevari, O.; Wilson, J. X.; O'Brien, P. J. Prooxidant activity and cellular effects of the phenoxyl radicals of dietary flavonoids and othe rpolyphenolics. Toxicology **177:** 91-104; 2002.
[37] Choi, E. J.; Chee, K. M.; Lee, B. H. Anti- and prooxidant effects of chronic quercetin administration in rats. Eur. J. Pharmacol. **482:** 281-285; 2003.
[38] Halliwell, B. Are polyphenols antioxidants or pro-oxidants? What do we learn from cell culture and in vivo studies? Arch. Biochem. Biophys. **476:** 107-112; 2008.
[39] De Marchi, U.; Biasutto, L.; Garbisa, S.; Toninello, A.; Zoratti, M. Quercetin can act either as an inhibitor or an inducer of the mitochondrial permeability transition pore: A demonstration of the ambivalent redox character of polyphenols. Biochim. Biophys. Acta **1787:** 1425-1432; 2009.
[40] Bischoff, S. C. Quercetin: potentials in the prevention and therapy of disease. Curr. Opin. Clin. Nutr. Metab. Care **11:** 733-740; 2008.
[41] Murakami, A.; Ashida, H.; Terao, J. Multitargeted cancer prevention by quercetin. Cancer Lett. **269:** 315-325; 2008.
[42] Boots, A. W.; Haenen, G. R.; Bast, A. Health effects of quercetin: from antioxidant to nutraceutical. Eur. J. Pharmacol. **585:** 325-337; 2008.
[43] Hirpara, K. V.; Aggarwal, P.; Mukherjee, A. J.; Joshi, N.; Burman, A. C. Quercetin and its derivatives: synthesis, pharmacological uses with special emphasis on anti-tumor properties and prodrug with enhanced bio-availability. Anticancer Agents Med. Chem. **9:** 138-161; 2009.
[44] Manach, C.; Williamson, G.; Morand, C.; Scalbert, A.; Rémésy, C. Bioavailability and bioefficacy of polyphenols in humans. I. Review of 97 bioavailability studies. Am. J. Clin. Nutr. **81:** 230S-242S; 2005.
[45] Liu, Z.; Hu, M. Natural polyphenol disposition via coupled metabolic pathways. Expert Opin. Drug Metab. Toxicol. **3:** 389-406; 2007.
[46] Yang, C. S.; Sang, S.; Lambert, J. D.; Lee, M. J. Bioavailability issues in studying the health effects of plant polyphenolic compounds. Mol. Nutr. Food Res. **52 (Suppl. 1):** S139-S151; 2008.
[47] Lee-Hilz, Y. Y.; Boerboom, A. M.; Westphal, A. H.; Berkel, W. J.; Aarts, J. M.; Rietjens, I. M. Pro-oxidant activity of flavonoids induces EpRE-mediated gene expression. Chem. Res. Toxicol. **19:** 1499-1505; 2006.
[48] Hayes, J. D.; McMahon, M.; Chowdhry, S.; Dinkova-Kostova, A. T. Cancer chemoprevention mechanisms mediated through the Keap1-Nrf2 pathway. Antiox. Redox Signal. **13**: 1713-1748; 2010.
[49] Calabrese, V.; Cornelius, C.; Dinkova-Kostova, A. T.; Calabrese, E. J.; Mattson, M. Cellular stress responses, the hormesis paradigm and vitagens: novel targets for therapeutic intervention in neurodegenerative disorders. Antiox. Redox Signal. **13**: 1763-1811; 2010.
[50] Galati, G.; Chan, T.; Wu, B.; O'Brien, P. Glutathione-dependent generation of reactive oxygen species by the peroxidase-catalyzed redox cycling of flavonoids. Chem Res Toxicol. **12:** 521-525; 1999.
[51] Chan, T.; Galati, G.; O'Brien, P. Oxygen activation during peroxidase catalysed metabolism of flavones or flavanones. Chem Biol Interact. **122:** 15-25; 1999.
[52] Mattarei, A.; Biasutto, L.; Marotta, E.; De Marchi, U.; Sassi, N.; Garbisa, S.; Zoratti, M.; Paradisi, C. A mitochondriotropic derivative of quercetin: a strategy to increase the effectiveness of polyphenols. ChemBioChem **9:** 2633-2642; 2008.

[53] Biasutto, L.; Sassi, N.; Mattarei, A.; Marotta, E.; Cattelan, P.; Toninello, A.; Garbisa, S.; Zoratti, M.; Paradisi, C. Impact of mitochondriotropic quercetin derivatives on mitochondria. Biochim. Biophys. Acta **1797:** 189-196; 2010.
[54] Lodi, F.; Jiménez, R.; Menendez, C.; Needs, P. W.; Duarte, J.; Perez-Vizcaino, F. Glucuronidated metabolites of the flavonoid quercetin do not auto-oxidise, do not generate free radicals and do not decrease nitric oxide bioavailability. Planta Med. **74:** 741-746; 2008.
[55] Terao, J. Dietary flavonoids as antioxidants. Forum Nutr. **61:** 87-94; 2009.
[56] Krishnamachari, V.; Levine, L. H.; Paré, P. W. Flavonoid oxidation by the radical generator AIBN: a unified mechanism for quercetin radical scavenging. J. Agric. Food Chem. **50:** 4357-4363; 2002.
[57] Firuzi, O.; Lacanna, A.; Petrucci, R.; Marrosu, G.; Saso, L. Evaluation of the antioxidant activity of flavonoids by "ferric reducing antioxidant power" assay and cyclic voltammetry. Bichim. Biophys. Acta **1721:** 174-184; 2005.
[58] Zhou, A.; Sadik, O. A. Comparative analysis of quercetin oxidation by electrochemical, enzymatic, autoxidation, and free radical generation techniques: a mechanistic study. J. Agric. Food Chem. **56:** 12081-12091; 2008.
[59] He, J. B.; Yu, C. L.; Duan, T. L.; Deng, N. In situ spectroelectrochemical analysis of quercetin in acidic medium. Anal. Sci. **25:** 373-377; 2009.
[60] Musialik, M.; Kuzmicz, R.; Pawlowski, T. S.; Litwinienko, G. Acidity of hydroxyl groups: an overlooked influence on antiradical properties of flavonoids. J. Org. Chem. **74:** 2699-2709; 2009.
[61] Hendrickson, H. P.; Kaufman, A. D.; Lunte, C. E. Electrochemistry of catechol-containing flavonoids. J. Pharm. Biomed. Anal. **12:** 325-334; 1994.
[62] Montaña, M. P.; Pappano, N.; Giordano, S. O.; Molina, P.; Debattista, N. B.; García, N. A. On the antioxidant properties of three synthetic flavonols. Pharmazie **62:** 72-76; 2007.
[63] Jørgensen, L. V.; Cornett, C.; Justesen, U.; Skibsted, L. H.; Dragsted, L. O. Two-electron electrochemical oxidation of quercetin and kaempferol changes only the flavonoid C-ring. Free Radic. Res. **29:** 339-350; 1998.
[64] Jungbluth, G.; Rühling, I.; Ternes, W. Oxidation of flavonols with Cu(II), Fe(II) and Fe(III) in aqueous media. J. Chem. Soc., Perkin Trans. **2:** 1946 - 1952; 2000.
[65] Zhou, A.; Kikandi, S.; Sadik, O. A. Electrochemical degradation of quercetin: Isolation and structural elucidation of the degradation products. Electrochemistry Communications **9:** 2246-2255; 2007.
[66] Foti, M. C. Antioxidant properties of phenols. J. Pharm. Pharmacol. **59:** 1673-1685; 2007.
[67] Foti, M. C.; Daquino, C.; Mackie, I. D.; Dilabio, G. A.; Ingold, K. U. Reaction of phenols with the 2,2-diphenyl-1-picrylhydrazyl radical. Kinetics and DFT calculations applied to determine ArO-H bond dissociation enthalpies and reaction mechanism. J. Org. Chem. **73:** 9270-9282; 2008.
[68] Ripcke, J.; Zarse, K.; Ristow, M.; Birringer, M. Small-molecule targeting of the mitochondrial compartment with an endogenously cleaved reversible tag. ChemBioChem **10:** 1689-1696; 2009.
[69] Mattarei, A.; Biasutto, L.; Rastrelli, F.; Garbisa, S.; Marotta, E.; Zoratti, M.; Paradisi, C. Regioselective O-Derivatization of Quercetin via Ester Intermediates. An Improved Synthesis of Rhamnetin and Development of a New Mitochondriotropic Derivative. Molecules **15:** 4722-4736; 2010.
[70] Sassi, N.; Biasutto, L.; Mattarei, A.; Giorgio, V.; Carraro, M.; Citta, A.; Garbisa, S.; Szabò, I.; Paradisi, C.; Zoratti, M. Cytotoxicity of mitochondriotropic quercetin derivatives: mechanisms. Free Radic. Biol. Med., submitted.

[71] Fukumoto, L. R.; Mazza, G. Assessing antioxidant and prooxidant activities of phenolic compounds. J. Agric. Food Chem. **48:** 3597-3604; 2000.
[72] Choi, J. S.; Jung, M. J.; Park, H. J.; Chung, H. Y.; Kang, S. S. Further isolation of peroxynitrite and 1,1-diphenyl-2-picrylhydrazyl radical scavenging isorhamnetin 7-O-glucoside from the leaves of Brassica juncea L. Arch. Pharm. Res. **25:** 625-627; 2002.
[73] Kanatt, S. R.; Chander, R.; Radhakrishna, P.; Sharma, A. Potato peel extract - a natural antioxidant for retarding lipid peroxidation in radiation processed lamb meat. J. Agric. Food Chem. **53:** 1499-1504; 2005.
[74] Cheng, Z.; Moore, J.; Yu, L. High-throughput relative DPPH scavenging capacity assay. J. Agric. Food Chem. **54:** 7429-7436; 2006.
[75] Cai, Y.; Sun, M.; Corke, H. Antioxidant activity of betalains from plants of the amaranthaceae. J. Agric. Food Chem. **51:** 2288-2294; 2003.
[76] Huang, D.; Ou, B.; Prior, R. L. The chemistry behind antioxidant capacity assays. J. Agric. Food Chem. **53:** 1841-1856; 2005.
[77] Matkowski, A.; Piotrowska, M. Antioxidant and free radical scavenging activities of some medicinal plant from the Lamiaceae. Fitoterapia **77:** 346-353; 2006.
[78] Villaño, D.; Fernández-Pachón, M. S.; Moyá, M. L.; Troncoso, A. M.; García-Parrilla, M. C. Radical scavenging ability of polyphenolic compounds towards DPPH free radical. Talanta **71:** 230-235; 2007.
[79] Saito, S. T.; Gosmann, G.; Saffi, J.; Presser, M.; Richter, M. F.; Bergold, A. M. Characterization of the constituents and antioxidant activity of Brazilian green tea (Camellia sinensis var. assamica IAC-259 cultivar) extracts. J. Agric. Food Chem. **55:** 9409-9414; 2007.
[80] Smith, P. K.; Krohn, R. I.; Hermanson, G. T.; Mallia, A. K.; Gartner, F. H.; Provenzano, M. D.; Fujimoto, E. K.; Goeke, N. M.; Olson, B. J.; Klenk, D. C. Measurement of protein using bicinchoninic acid. Anal. Biochem. **150**: 76-85; 1985.

[81] Petit, J. M.; Huet, O.; Gallet, P. F.; Maftah, A.; Ratinaud, M. H.; Julien, R. Direct analysis and significance of cardiolipin transverse distribution in mitochondrial inner membranes. Eur. J. Biochem. **220**: 871-879; 1994.
[82] Biasutto, L.; Dong, L.F.; Zoratti, M.; Neuzil, J. Mitochondrially targeted anti-cancer agents. Mitochondrion **10**: 670-681; 2010.
[83] Sergediene, E.; Jönsson, K.; Szymusiak, H.; Tyrakowska, B.; Rietjens, I. M.; Cenas, N. Prooxidant toxicity of polyphenolic antioxidants to HL-60 cells: description of quantitaive structure-activity relationships. FEBS Lett. **462:** 392-396; 1999.
[84] Blois, M. S. Antioxidant determinations by the use of a stable free radical. Nature **181:** 1199-1200; 1958.
[85] Brand-Williams, W.; Cuvelier, M. E.; Berset, C. Use of a free radical method to evaluate antioxidant activity. Lebensm. Wiss. Technol. **28:** 25-30; 1995.
[86] Sichel, G.; Corsaro, C.; Scalia, M.; Di Bilio, A. J.; Bonomo, R. P. In vitro scavenger activity of some flavonoids and melanins against O2-. Free Radic. Biol. Med. **11:** 1-8; 1991.
[87] Ioku, K.; Tsushida, T.; Takei, Y.; Nakatani, N.; Terao, J. Antioxidative activity of quercetin and quercetin monoglucosides in solution and phospholipid bilayers. Biochim. Biophys. Acta **1234:** 99-104; 1995.
[88] Haenen, G. R.; Paquay, J. B.; Korthouwer, R. E.; Bast, A. Peroxynitrite scavenging by flavonoids. Biochem. Biophys. Res. Comm. **236:** 591-593; 1997.
[89] Firuzi, O.; Mladenka, P.; Petrucci, R.; Marrosu, G.; Saso, L. Hypochlorite scavenging activity of flavonoids. J. Pharm. Pharmacol. **56:** 801-807; 2004.

[90] Firuzi, O.; Lacanna, A.; Petrucci, R.; Marrosu, G.; Saso, L. Evaluation of the antioxidant activity of flavonoids by "ferric reducing antioxidant power" assay and cyclic voltammetry. Biochim. Biophys. Acta **1721:** 174-184; 2005.
[91] Arts, M. J.; Haenen, G. R.; Voss, H. P.; Bast, A. Antioxidant capacity of reaction products limits the applicability of the Trolox Equivalent Antioxidant Capacity (TEAC) assay. Food Chem. Toxicol. **42:** 45-49; 2004.
[92] Ueda , S.; Masutani, H.; Nakamura, H.; Tanaka, T.; Ueno, M.; Yodoi J. Redox control of cell death. Antiox. Redox Signal. **4**: 405-414; 2002.
[93] Takeda, K.; Naguro, I.; Nishitoh, H.; Matsuzawa, A.; Ichijo, H. Apoptosis signaling kinases: from stress response to health outcome. Antiox. Redox Signal. 2010, in press. (doi: 10.1089/ars.2010.3392).
[94] Ghibelli, L.; Diederich, M. Multistep and multitask Bax activation. Mitochondrion **10**: 604-613; 2010.
[95] Kagan, V. E.; Bayir, H. A.; Belikova, N. A.; Kapralov, O.; Tyurina, Y. Y.; Tyurin, V. A.; Jiang, J.; Stoyanovsky, D. A.; Wipf, P.; Kochanek, P. M.; Greenberger, J. S.; Pitt, B.; Shvedova, A. A.; Borisenko, G. Cytochrome c/cardiolipin relations in mitochondria: a kiss of death. Free Radic. Biol. Med. **46**: 1439-1453; 2009.
[96] Vanlangenakker, N.; Vanden Berghe, T.; Krysko, D. V.; Festjens, N.; Vandenabeele, P. Molecular mechanisms and pathophysiology of necrotic cell death. Curr. Mol. Med. **8**: 207-220; 2008.
[97] Kroemer, G.; Galluzzi, L.; Vandenabeele, P.; Abrams, J.; Alnemri, E. S.; Baehrecke, E. H.; Blagosklonny, M. V.; El-Deiry, W. S.; Golstein, P.; Green, D. R.; Hengartner, M.; Knight, R. A.; Kumar, S.; Lipton, S. A.; Malorni, W.; Nunez, G.; Peter, M. E.; Tschopp, J.; Yuan, J.; Piacentini, M.; Zhivotovsky, B.; Melino, G. Classification of cell death: recommendations of the Nomenclature Committee on Cell Death 2009. Cell Death Differ. **16**: 3–11; 2009.
[98] Nagley, P.; Higgins, G. C.; Atkin, J. D.; Beart, P. M. Multifaceted deaths orchestrated by mitochondria in neurones. Biochim. Biophys. Acta **1802:** 167-185; 2010.
[99] Proskuryakov, S. Y.; Gabai, V. L. Mechanisms of tumor cell necrosis. Curr. Pharm. Des. **16**: 56-68; 2010.
[100] Zhivotovsky, B.; Orrenius, S. Cell death mechanisms: cross-talk and role in disease. Exp. Cell Res. **316:** 1374-1383; 2010.
[101] Yamashima, T.; Oikawa, S. The role of lysosomal rupture in neuronal death. Prog. Neurobiol. **89**: 343-358; 2009.
[102] Kurz, T.; Eaton, J. W.; Brunk, U. T. Redox activity within the lysosomal compartment: implications for aging and apoptosis. Antiox. Redox Signal. **13**: 511-523; 2010.
[103] Berndt, C.; Kurz, T.; Selenius, M.; Fernandes, A. P.; Edgren, M. R.; Brunk, U. T. Chelation of lysosomal iron protects against ionizing irradiation. Biochem. J. **432**: 295-301; 2010.
[104] Wu, Y. T.; Tan, H. L.; Huang, Q.; Sun, X. J.; Shen, H. M. zVAD-induced necrosis in L929 cells depends on autocrine production of TNFalpha mediated by the PKC-MAPK-AP-1 pathway. Cell Death Differ. 2010, in press (doi: 10.1038/cdd.2010.72).
[105] Bertrand, R.; Solary, E.; O'Connor, P.; Kohn, K. W.; Pommier, Y. Induction of a common pathway of apoptosis by staurosporine. Exp. Cell Res. **211**: 314-321; 1994.
[106] Zoratti, M.; Szabò, I. The mitochondrial permeability transition. Biochim. Biophys. Acta **1241**: 139-176; 1995.
[107] Rasola, A.; Bernardi, P. The mitochondrial permeability transition pore and its involvement in cell death and in disease pathogenesis. Apoptosis **12**: 815-833; 2007.

[108] Azzolin, L.; von Stockum, S.; Basso, E.; Petronilli, V.; Forte, M. A.; Bernardi, P. The mitochondrial permeability transition from yeast to mammals. FEBS Lett. **584**: 2504-2509; 2010.
[109] Rasola, A.; Sciacovelli, M.; Pantic, B.; Bernardi, P. Signal transduction to the permeability transition pore. FEBS Lett. **584**: 1989-1996; 2010.
[110] Zoratti, M.; De Marchi, U.; Biasutto, L.; Szabò, I. Electrophysiology clarifies the megariddles of the mitochondrial permeability transition pore. FEBS Lett. **584**: 1997-2004; 2010.
[111] Loor, F.; Tiberghien, F.; Wenandy, T.; Didier, A.; Traber, R. Cyclosporins: structure-activity relationships for the inhibition of the human MDR1 P-glycoprotein ABC transporter. J. Med. Chem. **45**: 4598-4612; 2002.
[112] Morjani, H.; Madoulet, C. Immunosuppressors as multidrug resistance reversal agents. Methods Mol. Biol. **596**: 433-446; 2010.
[113] Bernardi, P.; Scorrano, L.; Colonna, R.; Petronilli, V.; Di Lisa, F. Mitochondria and cell death. Mechanistic aspects and methodological issues. Eur. J. Biochem. **264**: 687-701; 1999.

Chapter 6

Cytotoxicity of mitochondriotropic quercetin derivatives: mechanisms[6]

Summary

The mitochondriotropic compounds 3- and 7-*O*-(4-triphenylphosphoniumbutyl)quercetin iodide cause necrotic cell death and act as prooxidants, inducing generation of superoxide anion in the mitochondria. Mitochondrial depolarization, also induced by these compounds, may contribute to superoxide production, but a process involving the flavonol hydroxyls appears to be a major source, because 3,3',4',5-tetra-O-methyl-7-*O*-(4-triphenylphosphoniumbutyl)quercetin, the analogous compound without free hydroxyls, induces a similar depolarization but not superoxide production. Superoxide is the direct cause of cell death, since death is abated when superoxide is rapidly eliminated by externally added membrane-permeating superoxide dismutase. Permeant catalase has little effect. ROS formation can also be countered by drastically increasing cellular reduced glutathione levels with a permeant precursor of the tripeptide. Necrosis induction is selective, hitting faster-growing C-26 tumoral cells and Mouse Embryonic Fibroblasts (MEFs) and sparing slower-growing MEFs. Measurements of mitochondrial content and superoxide production suggest that the selectivity of the cytotoxic effect might be related to the concentration of mitochondrial superoxide attained.

Introduction

Mitochondria-targeted redox-active compounds have been generally considered to be protective anti-oxidants and have been shown to act as such in several experimental systems (revs.: [1-8]). Reports of cytotoxic and pro-oxidant effects are few. The Vitamin E redox-inactive analogue α-tocopheryl succinate (α-TOS) interacts with mitochondrial Succinate Dehydrogenase at a Coenzyme Q_{10} binding site, interfering with the normal flow of electrons along the respiratory chain and diverting a portion of them to the production of superoxide [9].

[6] Submitted to *Free Radic. Biol. Med.* by: Sassi, N.; Biasutto, L.; Mattarei, A.; Giorgio, V.; Carraro, M.; Citta, A.; Garbisa, S.; Szabò, I.; Paradisi, C.; Zoratti, M.

This results in cytotoxicity which has been found to offer promise against cancer in *in vivo* studies [10]. Introduction of a triphenylphosphonium group in the structure to promote mitochondrial delivery increases the efficacy of the compound without altering its mechanism of action [11]. MitoQ, an ubiquinol-TPP construct which is possibly the best-known mitochondriotropic redox-active compound, has been shown to act as an anti-oxidant in a number of studies [2, 8, 12]. It can nonetheless act as a pro-oxidant *in vitro*, causing an important production of ROS by cultured cells [13]. Such "duplicity" is not surprising, since polyphenols can act as either anti-oxidants or pro-oxidants. Both behaviours descend from the same physico-chemical property, namely a relatively low oxidation potential. Whether one or the other mode of action prevails depends on circumstances such as the presence of catalysts (often metal ions) that can induce redox cycling, and the concentration of the redox-active specie itself [14-20]. Whether quercetin, in particular, acts as an anti- or a pro-oxidant has been found to correlate also with the status of the cellular glutathione pool: low levels of reduced glutathione (GSH) are associated with pro-oxidant activity and cytotoxicity [21, 22].

Chapter 5 have shown that the mitochondriotropic quercetin derivatives induce necrotic cell death. The results of that study suggest that these compounds, in particular Q-7BTPI, may act as pro-oxidants, and that radical generation may underlie cell death. We report here our investigation of these matters.

Results and Discussion

ROS production.

We have monitored superoxide production in cells exposed to the mitochondriotropic quercetin derivatives, as fluorescence changes of the indicator MitoSOX® in FACS experiments with Jurkat lymphocytes, chosen as cell model because they grow in suspension, and thus need not undergo the traumatic detachment procedure before FACS analysis. The compounds were supplied at the highest concentration used in cytotoxicity experiments [23], 5 μM. CsA, the paradigmatic Mitochondrial Permeability Transition (MPT) inhibitor, was included to exclude possible effects due to onset of the MPT. We also verified that the absence of Cyclosporin, or substituting CsH for CsA in the assay cocktail did not have a detectable effect on the MitoSOX® response to mitochondriotropic quercetin derivatives, thus making it unlikely that the MPT is upstream of ROS production (Fig. 1).

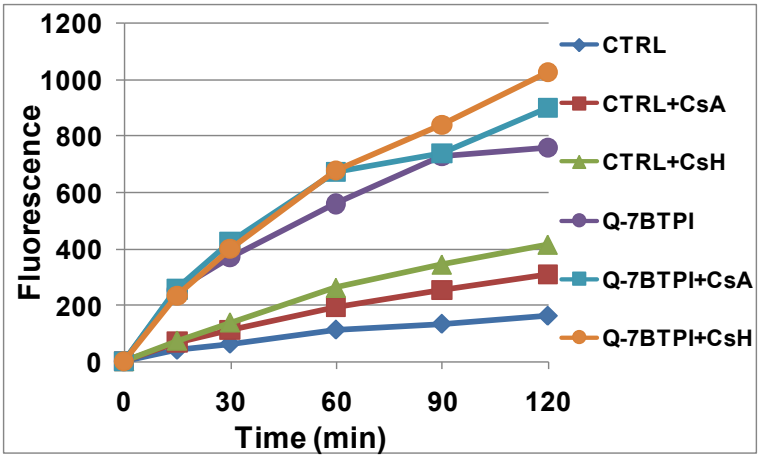

Figure 1. MitoSOX® fluorescence response elicited by quercetin derivatives in Jurkat cells in the absence or in the presence of 5µM CsA or CsH. Plots of the medians of cell fluorescence distribution histograms. For clarity, the value at time 0 was subtracted from each set of data.

The results are illustrated by the typical experiment presented in Fig. 2. Populations of cells were analyzed that displayed forward- and side-scatter parameters characteristic of healthy cells (Fig. 2A), i.e. cells not exhibiting morphological changes associated with advanced necrosis or apoptosis. Thus the effects observed are not consequences of the death process, but rather preceed or accompany it, and can be attributed to a direct effect of the compounds. MitoSOX® fluorescence increased significantly with both Q-3BTPI and Q-7BTPI, and more markedly with the latter. Fig. 2B shows the fluorescence distribution histograms obtained with 5 µM Q-7BTPI. Panel 1C plots the median values of histograms of this type for the various compounds and controls. The results appear to reflect the redox properties of the compounds: Q-3BTPI and Q-7BTPI both elicited a strong response, with Q-7BTPI easily surpassing Q-3BPTI.

Superoxide production seems to be specifically associated with mitochondriotropic compounds, since quercetin or the combination of quercetin and a phosphonium salt do not produce a similar effect. The redox properties and reactivity of Q-7BTPI however are very close to those of quercetin (and Q-3BTPI is more resistant to oxidation). An explanation for this behaviour must therefore consider the environmental conditions in which oxidation takes place. In other words, the abundant production of radicals must have to do with the concentration of Q-7BTPI or Q-3BTPI in mitochondria. Which specific factors are involved remains to be determined. The concentration of oxidizable species can itself be a factor in determining pro-oxidant behaviour [27].

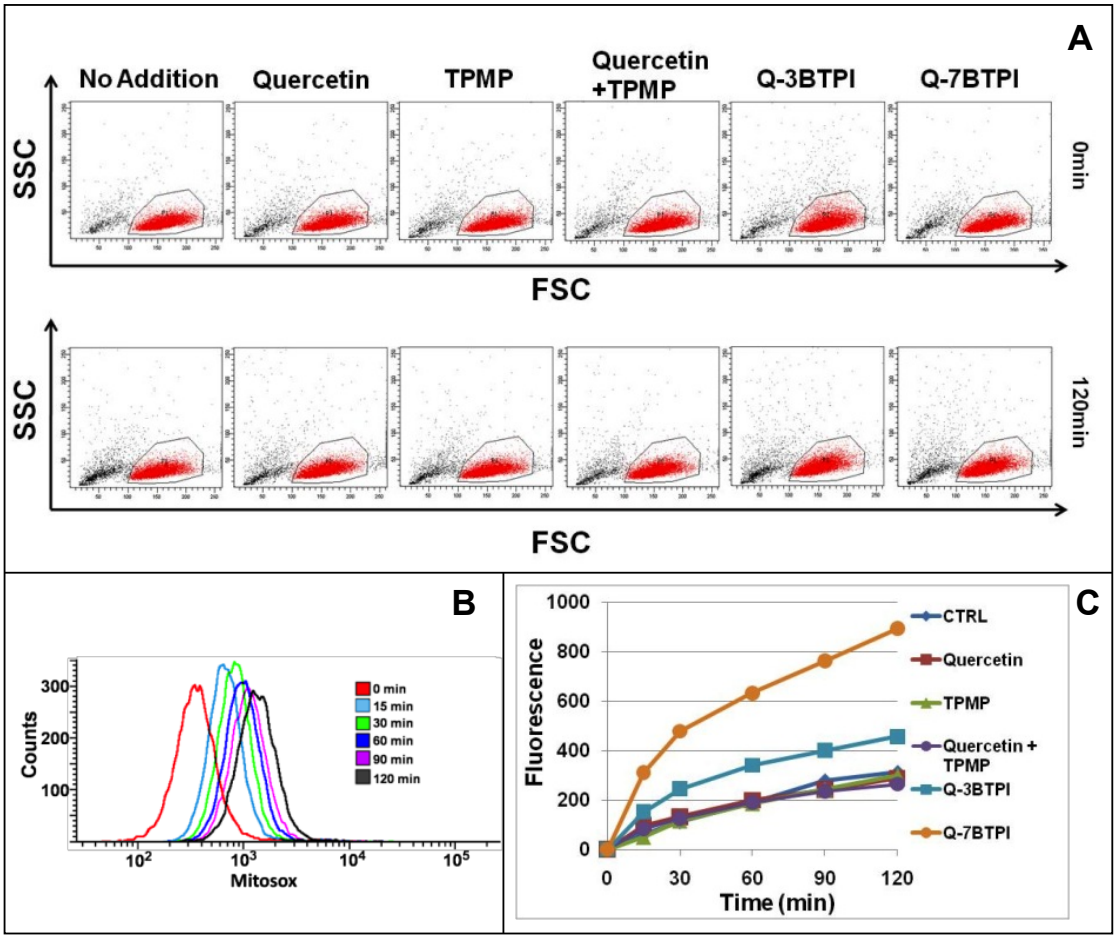

Figure 2. Mitochondriotropic quercetin derivatives elicit production of superoxide anion in Jurkat cells. A) The scatter parameters of Jurkat cells are not significantly altered by 5 µM Q-3BTPI or Q-7BTPI over a two-hour period. Side- vs. forward-scatter plots obtained by FACS from suspensions of cells treated with the indicated compounds for 0 or 120 minutes, as indicated. B) Fluorescence distribution histograms from the same experiment as in panel A. The cells were exposed to 5 µM Q-7BTPI in HBSS for the indicated times. 10.000 cells were counted in each case, and the fluorescence emitted by the selected population (circled and in red in panel A) was plotted. C) The MitoSOX® fluorescence response (same experiment). Plots of the medians of cell fluorescence distribution histograms analogous to those shown in panel B, for 5 µM of the indicated compounds. The median values plotted for Q-7BTPI are those of the histograms shown in panel B. For clarity, the value at time 0 was subtracted from each set of data.

Mitochondria maintain a slightly more alkaline pH, which is expected to favor oxidation, and are rich in copper and iron, which *a priori* can serve as mediators in electron transfer from the polyphenolic species to oxygen. Generically speaking, they are the seat of intense enzymatic redox activity which may entrain polyphenols.

ROS are responsible for cell death

While the literature contains abundant evidence that ROS can cause cell death, in principle the cytotoxicity of our compounds might have other causes. For example, flavonoids are known to be kinase inhibitors (e.g. [28]). To verify this point we checked whether

eliminating ROS would influence cell death. We tested a few permeant radical scavengers (Trolox, TEMPOL, NAC, PEG-SOD) by comparing the MitoSOX® response to our compounds in their presence. The best performance was provided by Pegylated SuperOxide Dismutase (PEG-SOD) (Sigma). Incubation of Jurkat cells with 40 units/mL of the reagent resulted in the reduction of the MitoSOX® response to Q3- and Q-7BTPI treatment nearly to control levels (Fig. 3A). This result confirms that the ROS being detected in these experiments is superoxide (since it is eliminated by superoxide dismutase), something that was not to be taken for granted [29, 30]. Indeed, the inclusion, in addition to PEG-SOD, of pegylated catalase (PEG-CAT) in the loading cocktail before the addition of mitochondriotropic quercetins and during the incubation did not induce a significant variation of the response (not shown).

Incubation with PEG-SOD also resulted in abolition of the Q-3/7BTPI-induced labelling by PI (and secondarily annexin) in FACS analyses (Fig. 3B). In the samples treated with Q-3BTPI or Q-7BTPI, PEG-SOD completely cancelled the effect of these compounds, so that the percentage of double-negative cells was very close to – or even higher than - that recorded for the PEG-SOD-treated, otherwise untreated control sample. Inclusion of PEG-CAT in the incubation did not bring further improvement (not shown).

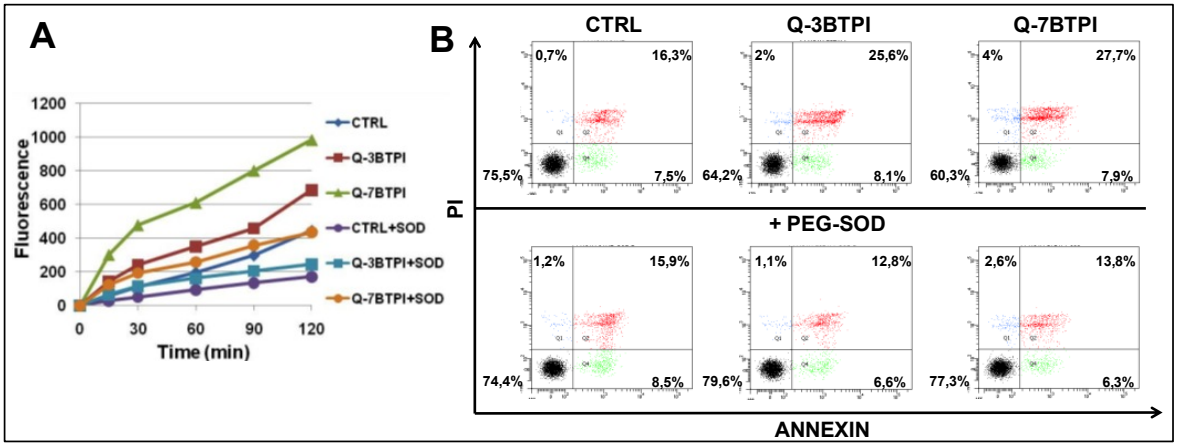

Figure 3: Permeant SOD reduces superoxide production and cell death. A) MitoSOX® fluorescence response elicited by quercetin derivatives (5 µM) in Jurkat cells. A representative FACS experiment out of three is shown. Plots of the medians of cell fluorescence distribution histograms. Preincubations (30 min) and treatments were performed in the presence or absence of PEG-SOD (40 units/mL) as indicated. The value at time 0 was subtracted from each set of data. B) Incubation with PEG-SOD affects annexin/PI labelling of Jurkat cells exposed to 5 µM Q-3/7BTPI. FACS analysis of cells labelled after exposure to the indicated agents for three hours in HBSS. A representative experiment out of five is shown. See Materials and Methods for details. 5.000 cells were counted for each condition.

Treating the cells only with 40 units/mL of permeable PEG-CAT led to different results. In annexin/PI labelling experiments catalase increased the percentage of doubly-negative (i.e.,

healthy) cells in the control sample as well as in the samples treated with Q-7BTPI. In this latter case however an approximately constant difference remained between the percentages of viable cells recorded for the control and the Q-7BTPI-treated cells (Suppl. Fig. 4). At variance from what observed in the experiments with PEG-SOD, a higher percentage of the cells treated with PEG-CAT and Q-7BTPI was positive for PI or both annexin and PI than in the case of the cells treated only with the permeant enzyme. Thus PEG-CAT behaved as if eliminating an underlying noxious process which contributed approximately to the same extent to the annexin/PI positivity in both untreated and treated samples, while having little impact on Q-3/7BTPI-induced markers of toxicity. This suggests that the toxic specie responsible for the effect of Q-3/7BTPI is not mainly H_2O_2 derived from superoxide.

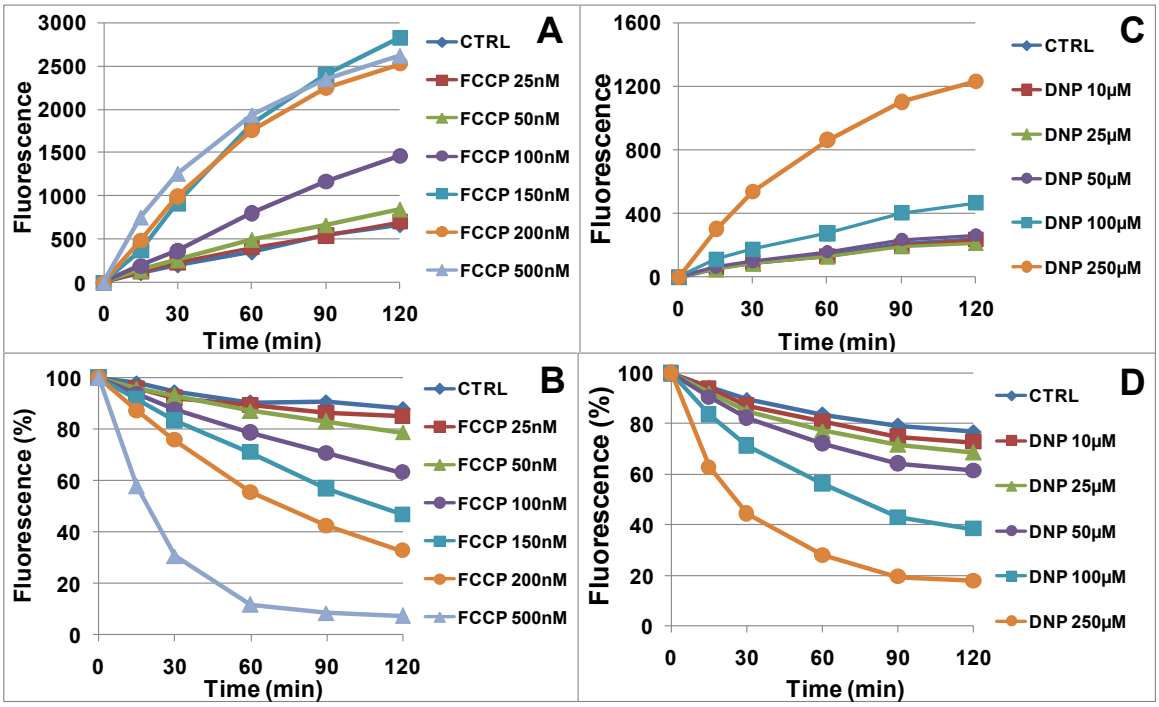

Figure 4. Effects of increasing uncoupler concentrations on superoxide generation and mitochondrial depolarization. A, C) MitoSOX® fluorescence response in Jurkat cells. Plots of the medians of cell fluorescence distribution histograms for increasing FCCP (A) or DNP (C) concentrations. For clarity, the value at time 0 (approx. 300 fluorescence units) was subtracted from each set of data. B, D) TMRM fluorescence loss at increasing FCCP (B) or DNP (D) concentrations. Same experiments as in the other panels. Data are expressed as percentage of the initial TMRM fluorescence value.

Thus, ROS may be considered to be responsible for cell death, in agreement with the hypothesis presented in [23], which was based on the correlation between the relative oxidizability, ROS-inducing power and cytotoxicity of Q-3BTPI and Q-7BTPI. It remains to be clarified whether toxicity is to be attributed to superoxide itself, to still-to-be-identified downstream reactive species (also other than hydrogen peroxide), or to

derivatives of quercetin (e.g. [31-36]) produced with the intermediacy of, or together with, superoxide.

Depolarization and relationship between depolarization and ROS.

Mitochondria are characterized by a transmembrane electrical potential gradient, maintained by the activity of the respiratory chain. The latter also results in the production of ROS, and the literature contains reports of increased ROS production following both inhibition of the electron flow due to a $\Delta\tilde{\mu}_H$ increase or its stimulation following a $\Delta\tilde{\mu}_H$ decrease by uncoupling (rev.: [37]). In fact, in FACS experiments assessing MitoSOX® fluorescence to monitor superoxide production and TMRM fluorescence as a reporter of transmembrane potential we have observed an increase of the former accompanying a decrease of the latter when using the classical protonophoric uncouplers FCCP or DNP (Fig. 4). Note however that at low concentrations of uncouplers, producing a moderate loss of TMRM fluorescence (up to about 40% after 2 hrs in the case of DNP), the corresponding MitoSOX® fluorescence increase was undetectable or weak. Both Q-3BTPI and Q-7BTPI induced a slowly-developing loss of TMRM fluorescence, which was more pronounced in the case of Q-7BTPI (Fig. 5A). This is in agreement with previous observations [24]. 5 μM Quercetin also induced a fluorescence decrease, which was not potentiated by the simultaneous presence of 5 μM TPMP, in the order of 20-40% after two hours (median values of the fluorescence distribution histograms; N = 6).

This depolarization was accompanied by little (5 experiments out of 7; not shown) or no (2 expts. out of 7; Fig. 2) superoxide production and cell death, in substantial agreement with the behaviour of FCCP and DNP. Quercetin has been observed to induce mitochondrial depolarization in other studies [38], although the reasons for this phenomenon to our knowledge have not been elucidated. According to the chemiosmotic model, unless the respiratory chain is inhibited a depolarization ought to be accompanied by stimulation of respiration. We were in fact able to detect a modest such increase in experiments with a Clark electrode and Jurkat cells exposed to Q-7BTPI (Fig. 5B).

In experiments with isolated mitochondria we had come to the conclusion that mitochondriotropic quercetins can act as protonophoric uncoupling agents [24]. To verify whether loss of mitochondrial potential in cells might be attributed to an analogous behaviour we compared the effect of Q-7BTPI with that of its per-*O*-methylated derivative (3,3',4',5-tetra-O-methyl,7-O-(4-triphenylphosphoniumbutyl)quercetin).

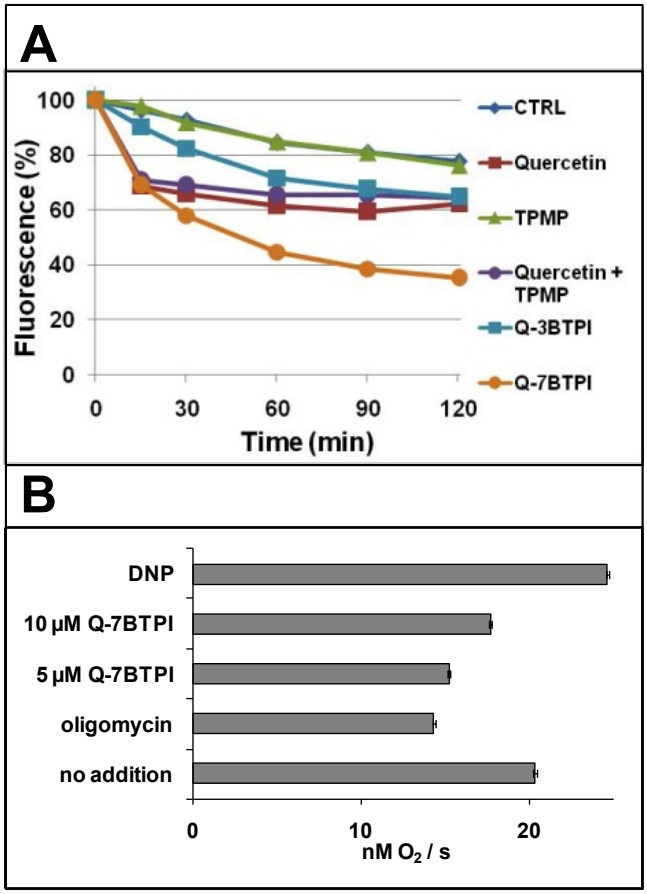

Figure 5: Mitochondriotropic quercetin derivatives induce depolarization. A) Decrease of TMRM fluorescence induced by Q-3BTPI and Q-7BTPI (5 µM) in Jurkat cells (a representative FACS experiment). Plots of the medians of cell fluorescence distribution histograms. Data are expressed as % of the initial TMRM fluorescence value. B) Effects of additions of Q-7BTPI and DNP (20 µM) on the respiration of Jurkat cells (3×10^6 cells/mL) in HBSS. Higher concentration of Q-7BTPI resulted in cell aggregation. Oligomycin (1 µg/mL) was also present together with Q-7BTPI and DNP. O_2 consumption was monitored as a decrease in the readout of a Clark electrode. Ten-minute segments of data sampled at 1 Hz were fitted with a linear fit, and the slopes are plotted.

This latter compound has no free hydroxyl group, and therefore it cannot behave as a weak acid and as the mediator of a futile protonophoric cycle. It nonetheless induced a TMRM fluorescence loss analogous to that produced by Q-7BTPI, but no superoxide production and no significant indication of cell death induction in annexin/PI labelling experiments (Fig. 6).

This result suggests that protonophoric cycling contributes only in a minor way to mitochondrial depolarization induced by mitochondriotropic quercetins in cells, perhaps because a large fraction of the compounds binds to cellular structures. The lack of generation of ROS by the tetramethylated derivative also strongly suggests, although it does not formally prove, that superoxide production is in considerable part dependent on

the presence of oxidizable groups on the quercetin derivative. The polyphenol moiety may well become oxidized in the mitochondrial environment, perhaps in a reversible manner acting as a redox cycler, and possibly via interaction with respiratory chain components (see below). Since no superoxide was detected in experiments with the tetramethylated derivative, the converse hypothesis that IMM depolarization may be downstream of superoxide generation appears unlikely.

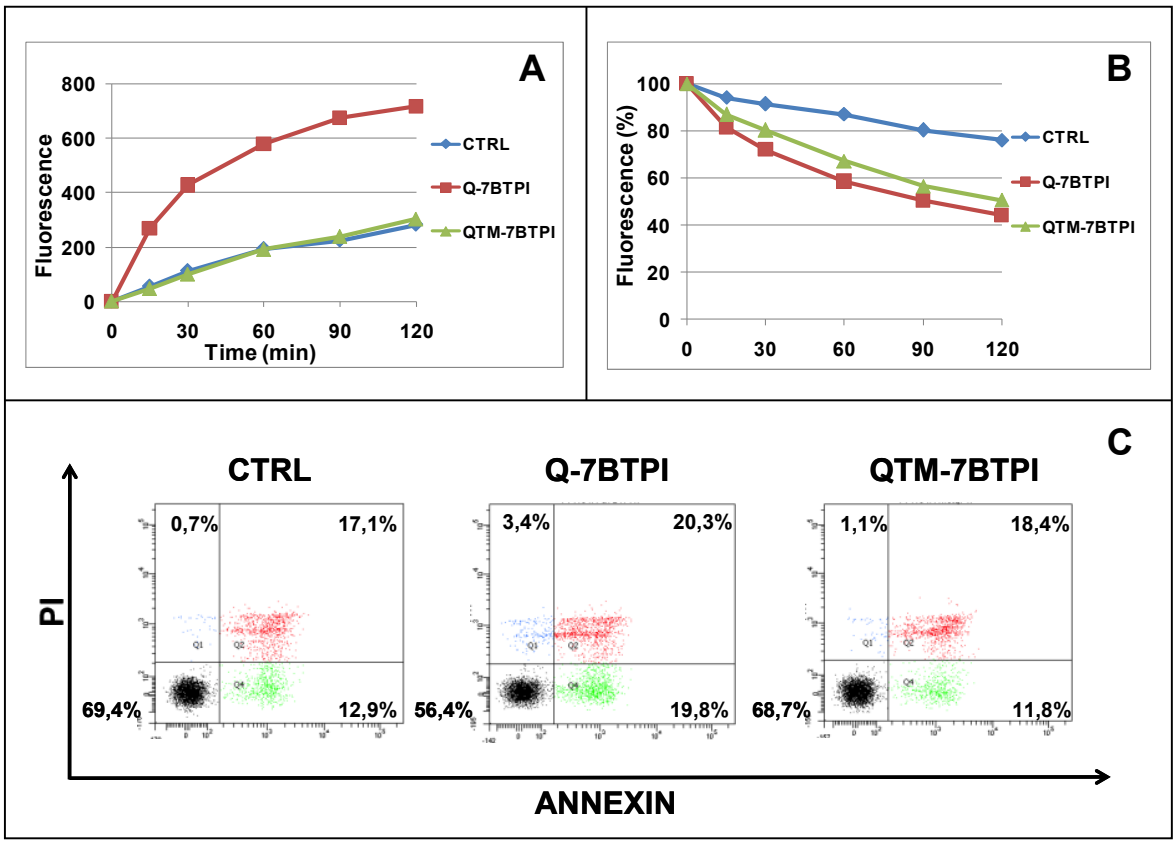

Figure 6. Tetramethylated Q-7BTPI has little effect on MitoSOX® fluorescence, although it induces a decrease of TMRM fluorescence, and is not cytotoxic. A) MitoSOX® response to 5 µM QTM-7BTPI or Q-7BTPI in Jurkat cells. B) TMRM fluorescence loss. Same experiment as in A. C) Effect on annexin/PI labelling of Jurkat cells. FACS analysis of cells labeled after exposure to the indicated agents for three hours. 5.000 cells were counted for each condition.

Indeed, treatment with PEG-SOD does not have a significant impact on Q-7BTPI-induced loss of TMRM fluorescence (Fig. 7), indicating that depolarization itself is not the cause of cell death (since PEG-SOD does strongly reduce death).

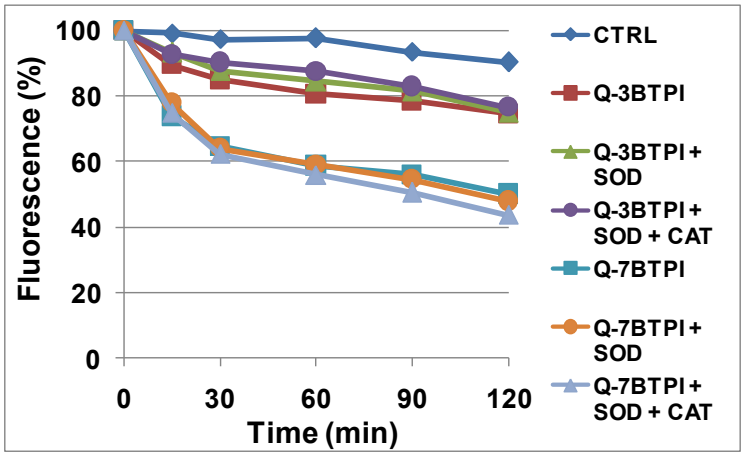

Figure 7. Lack of effect of pre-treatment (30 min., HBSS) and co-incubation with 40 U/mL PEG-SOD and PEG-CAT (as indicated) on TMRM fluorescence loss induced by quercetin derivatives (5 μM) in Jurkat cells.

Is resistance to death associated with a lower production of ROS?

Since now ROS generation has been identified as the crucial factor for death induction, one can return to the question of what the reason may be for the different sensitivity of the cell lines we tested (C-26, fast- and slow-growing MEFs) [23]. Is it a difference in the rate at which they produce ROS, a difference in the concentration of mitochondriotropic compounds in the organelles, or does it depend on their intrinsic vulnerability, associated with a different rate of proliferation?

To try to elucidate this point we monitored ROS production by detached C-26 and MEF cells treated with Q-3/Q-7BTPI (Fig. 8). Since the cells differ in their content of mitochondria [23], they take up different amounts of MitoSOX® per cell, so that the baseline (control) median cell fluorescence is different (highest for "slow" MEFs, as expected from the results of [23]). To compare the increase in MitoSOX® fluorescence during parallel incubations (control and plus the mitochondriotropic isomeric quercetin derivatives) we have therefore scaled the values obtained at each time point to that measured at time zero. The normalized MitoSOX® fluorescence increase is more pronounced for C-26 and fast MEFs, correlating with the stronger cytotoxicity of mitochondriotropic quercetins vs. these cell types. Along with the idea that the differential sensitivity may be ascribed to a different vulnerability of the cells, linked to their rate of growth, the hypothesis can therefore be considered that cytotoxicity may be related to the concentration profile of mitochondrial superoxide.

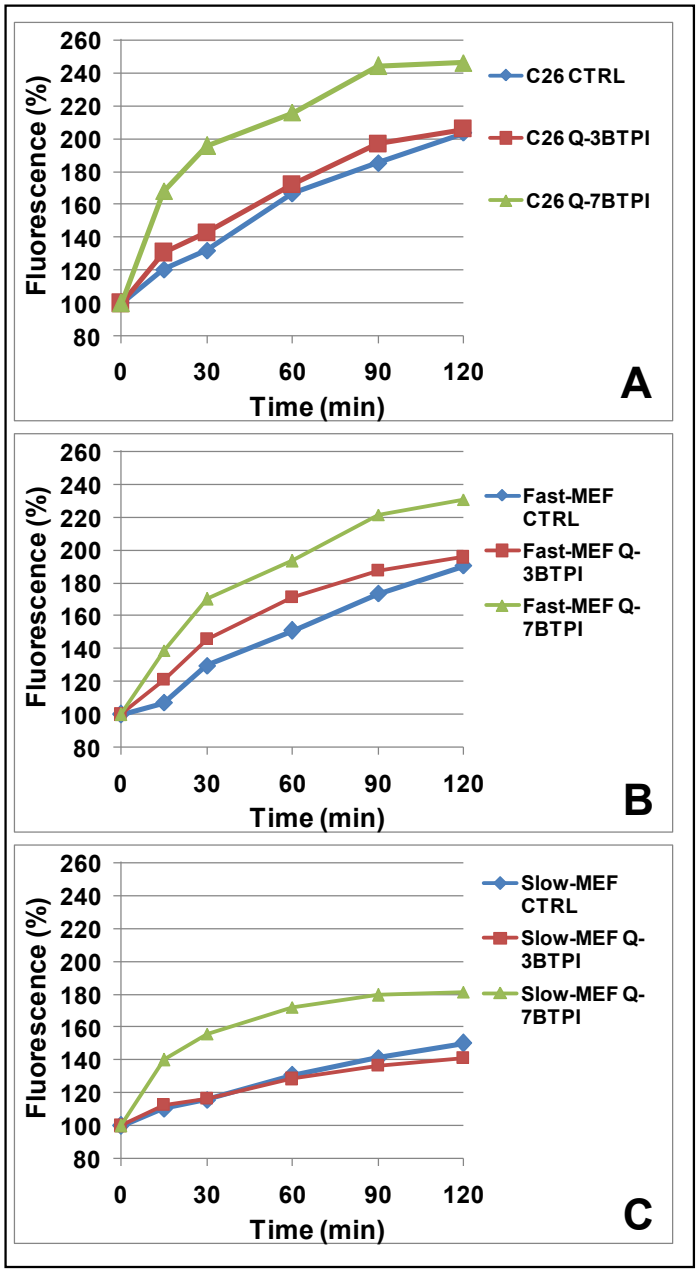

Figure 8. Superoxide generation by different cell lines. MitoSOX® fluorescence response elicited by quercetin derivatives. A) C-26; B) fast-growing MEFs; C) slow-growing MEF cells. Plots of the medians of cell fluorescence distribution histograms for 5 μM of the indicated compounds. Data are expressed as percentage of the initial MitoSOX® fluorescence value.

The origin of ROS

The question arises of how ROS are generated. The correlation with depolarization and with the behaviour of FCCP and DNP is indicative, but that depolarization can fully account for the intense production of superoxide is unlikely. ROS production can also be elicited by inhibition of respiration, as shown for example by experiments with Antimycin A (not shown). We observed stimulation of respiration by oligomycin-treated cells, but cells not exposed to this blocker of the F_0F_1 ATPase respire at a higher rate, and

mitochondriotropic compounds might inhibit, rather than stimulate, respiration if the cells have no "reserve capacity" [39, 40], i.e., no or little possibility to increase the rate of electron transfer to oxygen. In other words, our compounds may uncouple the mitochondria, and also act as mild inhibitors of respiration. However, our efforts to detect inhibition of maximally stimulated oxygen consumption by treatment with Q3- or Q-7BTPI using the oxygen indicator ("SeaHorse") technique failed.

Since mitoVESS interacts with Succinate Dehydrogenase to produce ROS [11], we also checked whether Q-7BTPI would inhibit succinate-driven respiration. The SeaHorse approach could not be used in this case because a) the permeating succinate precursor methylsuccinate proved unable to sustain respiration in our system and b) cells permeabilized to allow entry of succinate tended to become detached thus invalidating measurements. We therefore measured succinate-supported respiration by rotenone-treated rat liver mitochondria (RLM) using a Clark electrode. The effects on coupled respiration could not be assessed because of the uncoupling effect of the mitochondriotropic compound itself on isolated RLM [24]. Mitochondriotropic compounds cannot accumulate into uncoupled mitochondria because of the lack of a transmembrane potential. Thus, we measured their effect on uncoupled respiration at high concentrations, to mimick the mitochondrial concentrations in treated cells. As shown in suppl. Fig. 7B, Q-7BTPI inhibited respiration by about 12% at 50 μM and by about 37% at 100 μM. This suggests that a significant interaction with Complex II may take place in coupled *in situ* mitochondria. A full elucidation of this point is beyond the scope of this paper, and will be the object of further studies.

Metal ions may catalyze oxidative reactions leading to the consumption of polyphenol with the generation of superoxide [41-43], and we have observed that iron and copper chelators reduce the permeability transition in isolated mitochondria treated with Q-3BTPI [24]. We therefore also verified whether incubation of the cells with membrane-permeant copper and iron chelators (penicillamine, deferoxamine, o-phenanthroline) would significantly affect the MitoSOX® response. This was not the case. These chelators had a negative impact on the cells, acting as relatively weak death inducers when added by themselves (not shown). The Q-7BTPI-induced increase in the percentage of cells showing positivity for annexin/PI fluorescence in FACS experiments was also increased by their presence. These observations also suggests that H_2O_2-splitting Fenton reactions are not a major factor for the cytotoxicity of the mitochondriotropic quercetin derivatives.

In conclusion, radicals may be produced by different processes, including the oxidation of the quercetin derivatives, presumably promoted by as yet unspecified mitochondrial enzymes. Fig. 9 illustrates the reactions expected to take place in such an environment.

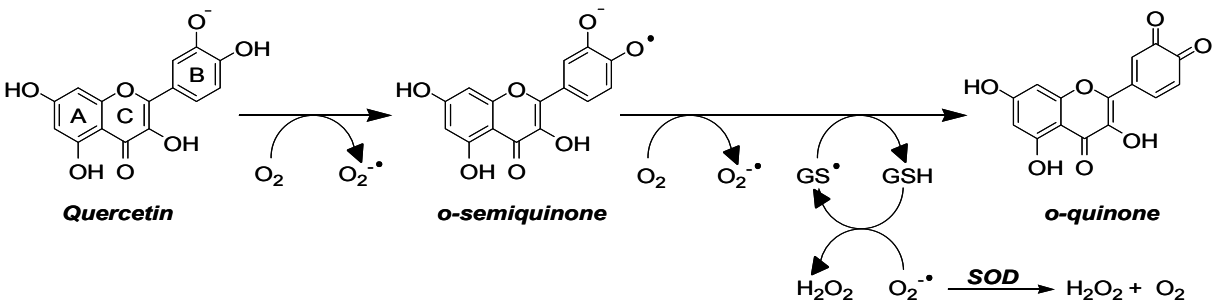

Figure 9. Redox chemistry of quercetin in cells.

The role of glutathione

Reduced glutathione, the major cellular antioxidant molecule, has been reported to have a direct role in regulating ROS production by mitochondria (rev.: [44]), and imbalances in the levels of glutathione have been linked to oxidative stress-induced death induction (e.g. [45-47]). GSH can directly reduce $O_2^{\cdot -}$ [48-50] and it reacts to reduce hydrogen peroxide to water with catalysis by GPx. Due to slow kinetics and efficient competition by SOD, direct reduction is expected to become important only at high concentrations of $O_2^{\cdot -}$ and/or GSH [50]. The product, GSSG, can in turn be re-reduced to GSH by Glutathione Reductase, which uses reducing equivalents provided by NADPH.

The literature reports that high (100 µM range) concentrations of quercetin inhibit GR from various sources [51-53], even upon *in vivo* long-term administration [54]. Inhibition by quercetin is reported to be irreversible [53] and to possibly be due to the formation of oxidized (quinonic) quercetin derivatives [52]. Our mitochondriotropic compounds accumulate not only in mitochondria, but also in the cytoplasm, which is also at a negative potential with respect to the extracellular space, and may reach concentrations sufficient for an inhibitory effect. Quercetin also inhibits at least Glutathione-S-Transferase [51, 55, 56], and, at sub-µM levels, Thioredoxin Reductase [57]. The effects of flavonoids on GSH levels in cultured cells seem to depend on cell type and on the experimental procedures. For example, quercetin (5-25 µM) has been reported to reduce the GSH content in three human leukemia cell lines, but not in a fourth [22], to either have no effect [58] or produce an increase [59] in cultured neurons, and to increase GSH in cultured astrocytes [58].

In our hands, treatment of Jurkat cells with 5 µM Q-7BTPI for 1 hour decreased GSH from 13.9 ± 2.3 to 10.4 ± 0.4 nmoles/mg.prot (N = 3). The same compound inhibited GR

activity in Jurkat cell lysate by 50% at 50 µM. GPx activity was inhibited by about 80% after 1-hr incubation of the cells with 5 µM Q-7BTPI, in agreement with the known sensitivity of this selenoenzyme to $O_2^{\cdot -}$ [60]. A marked decrease of the MitoSOX® response elicited by Q-7BTPI could be obtained by pre- and co-incubation with 10 mM GSHEE, a permeable precursor of glutathione, from which GSH can be regenerated by cellular esterases (Fig. 10).

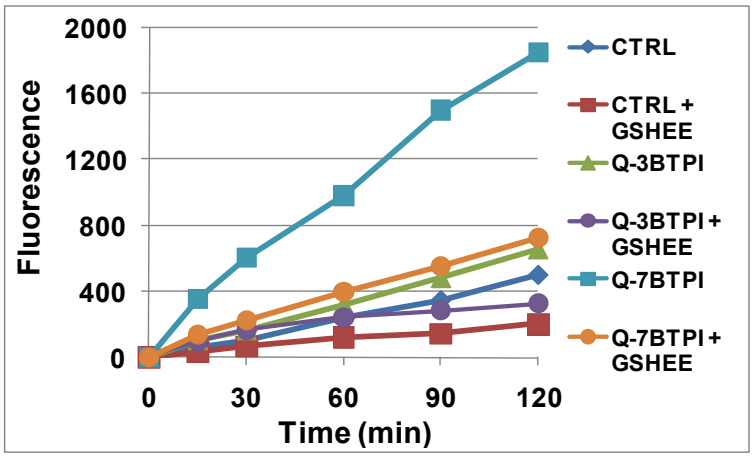

Figure 10. MitoSOX® fluorescence increase in Jurkat cells treated with the indicated compounds. Where indicated, cells were also pre-incubated with 10 mM GSHEE for 4 hours in DMEM plus FCS. The FACS experiment was carried out in HBSS. Q-3BTPI and Q-7BTPI were 5 µM.

Under these conditions cellular GSH increased to 250 ± 14 and 271 ± 25 nmoles/mg.prot. for otherwise untreated and Q-7BTPI treated cells, respectively.

Cytotoxicity by the mitochondriotropic quercetin derivatives can thus be concluded to due to the generation of oxidative stress. Pro-oxidant effects of this type, resulting in either apoptosis or necrosis, have been reported for various redox active compounds (e.g. [61-63]). In studies on cultured cells, quercetin has been recognized to act as an antioxidant at relatively low (roughly < 50 µM) concentrations, and as a prooxidant at higher levels (e.g. [64-66]). Its effects on cell growth and viability also depend on concentration and to some extent on cell line [67]. Several studies have found it to act as a pro-apoptotic agent for cultured cancer cells when applied in the tens-of-µM range (e.g.: [68-71]). It can exhibit pro-apoptotic cancer-selective action also in *in vivo* models [72]. At the concentrations used in our study, quercetin has little or no effect on proliferation or death of the cells we used. The mitochondriotropic derivatives however concentrate, as expected, inside cells and mitochondria, and they apparently locally achieve concentrations exceeding the threshold for pro-oxidant behaviour. Pro-oxidant activity is more marked in the case of Q-7BTPI, in agreement with its physico-chemical properties [23], and is the reason for cell death.

Necrosis-like death induction by prooxidants has been classified by some authors as a separate mode, autoschizis [73]. The molecular mechanisms of autoschizis have not been characterized in detail, but they are considered to involve widespread damage to cellular components by the oxidant species generated. In the case of quercetin, the formation of toxic adducts by the oxidation products is also a possibility (e.g. [31-36]). The onset of necrosis rather than of apoptosis may also reflect an impairment of ATP supply [74] due to inhibition of mitochondrial ATP synthase by these compounds [75].

It should be pointed out that the experiments reported here were performed *in vitro*, and that cytotoxic effects were observed only at what may be considered high concentrations (3 μM or higher) and, more relevantly, at high compound/cell ratios. What the effects of these compounds may turn out to be *in vivo* remains an open question, and much may depend on the attainable levels. Considerably lower dosages may have little effect or an hormetic action (rev.s on hormesis: [76-78]), inducing cytoprotective anti-oxidant responses through such signaling pathways as the Nrf2/ARE axis. In fact quercetin and its glycosylated derivatives have been associated with Nrf2 activation in some reports [79-83]. An hormetic action may account for the interesting anti-oxidant effects of the *in vivo* administration of another class of mitochondria-targeted polyphenolic compounds, the plastoquinones developed by Skulachev's group [6]. If high concentrations can be achieved, at least locally, they are likely to have a cytotoxic effect which may be put to use to fight established cancer. Selectivity vs. cancer cells may be expected to be achievable by topologically restricted delivery as well as because of the higher mitochondrial potential maintained by most cancer cells (e.g.: [84 and refs. therein, 85, 86]), of the already stressed redox situation of cancer cells, and of their higher rate of proliferation. In turn achievable levels *in vivo* are expected to depend on the mode of administration, efficiency of adsorption, metabolism, binding, rate of transport and excretion. All these aspects as well as toxicology need to be explored before the usefulness of compounds of this type can be assessed.

Experimental section

Materials and methods:

For materials, cells, and labelling by annexin and PI please see the chapter 5. All experiments were performed at least twice.

ROS production assays.

Superoxide generation in cells was assessed in Fluorescence-Activated Cell Scanner (FACS) experiments using a Beckton Dickinson Canto II flow cytometer and the mitochondriotropic superoxide anion-specific probe MitoSOX Red® (Invitrogen/Molecular Probes). Jurkat cells were washed and resuspended in HBSS at a density of 1.5×10^6 cells/mL and loaded with 1 μM MitoSOX Red® (37 °C, 20min). Cyclosporin A (CsA) (5 μM) was generally included as an inhibitor of MDR pumps, to obtain a higher accumulation ratio for the dye and to limit the rate of efflux during the experiment. After loading, cells were diluted 1:5 in HBSS (plus CsA) and divided into identical aliquots. At time zero the compound was added, and data collected after the desired incubation times, exciting at 488 nm and collecting fluorescence in the 542-585 nm interval. Data were analysed using the BD VISTA software. It should be mentioned that MitoSOX® is a mitochondriotropic compound, comprising a triphenylphosphonium group, which will therefore be released from the mitochondria if they undergo depolarisation. It can therefore only provide semi-quantitative information when depolarization is taking place.

Mitochondrial potential assays

Tetramethylrhodamine methyl ester (TMRM; Invitrogen/Molecular Probes) staining was used to monitor mitochondrial transmembrane potential of Jurkat lymphocytes by FACS. Procedures were essentially as described above for superoxide production assays, loading the cells with 20 nM TMRM in the presence of 5 μM CsA for approximately 20 min at 37°C. Excitation was at 488 nm and fluorescence was collected in the 542-585 nm interval.

Oxygen consumption assays.

Oxygen consumption by adherent cells was measured using an XF24 Extracellular Flux Analyzer (Seahorse, Bioscience) which measures in real time the oxygen consumption rate (OCR) in the medium immediately surrounding adherent cells cultured in an XF24-well microplate. Adherent C-26 cells were seeded at 5×10^4 cells/well in 200 μL of supplemented culture medium (DMEM; Sigma Aldrich) and incubated in a humidified atmosphere with 5% CO_2 at 37°C. After an overnight incubation, the medium was replaced with 670 μL of pre-warmed (37°C) DMEM supplemented with 4.5 g/L glucose, 0.58 g/L L-Glutamine, 0.11 g/L sodium pyruvate and 0.015 g/L phenol red. Microplates were incubated at 37°C for 30 min to allow media, temperature and pH to reach equilibrium before the measurements. OCR was measured at preset time intervals while the instrument automatically carried out the pre-programmed additions of the various compounds (including oligomycin 1 μg/mL final concentration, carbonyl cyanide 4-

(trifluoromethoxy)phenylhydrazone (FCCP) 0.1 µM, Antimycin A 1 µM), added as a solution in 70 µL of DMEM. All measurements were carried out in quadruplicate (4 wells per condition). For presentation purposes (suppl. Fig. 6A), the data were normalized to the initial OCR baseline measurement for each set of wells and are presented as % changes with respect to that level.

The rate of respiration by suspended Jurkat cells or Rat Liver Mitochondria (RLM) (purified as described in [24]) was measured in polarographic assays using a Clark electrode inserted in a thermostatted (25 °C) and stirred enclosed chamber with an illumination device and an airtight injection port. The electrode was controlled by an HansaTech CB1D control box and interfaced with a personal computer by a Microlink 751 digitizer. Jurkat cells were used as a suspension in HBSS, at the density of 3×10^6 cells/mL, RLM at 0.5 mg.prot.mL^{-1} in sucrose-based isoosmolar medium (250 mM sucrose, 10 mM Hepes/K^+, pH 7.4) supplemented with 1.25 µM Rotenone to block respiration at Site I of the respiratory chain. With RLM, respiration was started by the addition of 5 mM succinate.

Glutathione assays

Jurkat cells were counted, washed with warm PBS, and then incubated for 1 h in HBSS with or without 5 µM Q-7BTPI. In another experimental setting, cells were pre-treated for 3 hours with GSHEE (Reduced Glutathione Ethyl Ester, Sigma), and then treated for 1 h in HBSS with or without 5 µM Q-7BTPI in the presence of GSHEE. Cells were finally pelleted, and extracted with RIPA buffer (300 µL every 10 million cells; composition: NaCl 150 mM, Tris/HCl 50 mM, Triton X-100 1%, SDS 0.1%, sodium deoxycholate 0.5%, NaF 1mM, EDTA 1mM, PMSF 0.1 mM, protease inhibitors cocktail (Roche), pH 7.4) for 40 minutes at 4°C. Samples were then centrifuged 5 min at 10,000 *g*; and total protein in the supernatants was estimated using the Folin method [25].

Quantification of the cellular GSH pool. 750,000 Jurkat cells were used for each experimental condition. Cell extracts (180 µL) were deproteinized adding 100 µL of 6% metaphosphoric acid; after 3-5 min in ice, samples were centrifuged 5 min at 10,000 *g*. Supernatants were collected, their volumes measured, and pH neutralized with Na_3PO_4 15%. Phosphate buffer (0.2 M, pH 7.4, EDTA 5mM) was added to each sample (to 1 mL final volume); absorbance at 412 nm was measured before and after addition of 30 µL DTNB (5-5'-dithiobis[2-nitrobenzoic acid]) 0.1M [26]. Sample deproteinization assured selective detection of soluble free thiols, which can be attributed mainly to GSH. The amount of GSH was calculated from the absorbance change using Lambert-Beer's law

with 13.6 $M^{-1}\cdot cm^{-1}$ as the molar extinction coefficient of DTNB, and normalized to the protein content of each sample.

Glutathione Reductase activity. 10 million Jurkat cells were used for each experimental condition. In a cuvette, cell lysate (120 μg protein) and NADPH (250 μM final concentration) were added to 0.5 mL of TrisHCl buffer (0.2 M, pH 8.1, 5 mM EDTA). Glutathione Reductase (GR) activity was started adding 1 mM GSSG, and monitored at 25°C as a decrease in NADPH absorbance at 340 nm. The effect of Q-7BTPI on Glutathione Reductase activity was assessed by adding 50 μM Q-7BTPI to an untreated Jurkat cells lysate.

Glutathione Peroxidase Activity. 40 million Jurkat cells were used for each experimental condition. In a cuvette, cell lysate (800 μg protein), NADPH (250 μM final concentration), 25 nM Yeast Glutathione Reductase and 1 mM GSH (both from Sigma) were added to 0.5 mL of Hepes buffer (50 mM, pH 7.0, 3 mM EDTA). A Glutathione Peroxidase-catalyzed reaction was started by adding 50 μM tert-butyl-hydroperoxide, and monitored at 25°C as a decrease in NADPH absorbance at 340 nm. The effect of Q-7BTPI on Glutathione Peroxidase (GPx) activity was assessed both adding 50 μM Q-7BTPI to an untreated Jurkat cells lysate (with no effect, not shown), and by monitoring the activity of a lysate of Jurkat cells cultured for 1 h in the presence of 5 μM Q-7BTPI.

Synthesis of 3,3',4',5-tetra-O-methyl,7-O-(4-triphenylphosphoniumbutyl) quercetin iodide (QTM-7BTPI).

Methyl Iodide (1.0 mL, 16 mmol, 230 eq.) was added dropwise and under continuous stirring to a mixture of 7-O-(4-triphenylphosphoniumbutyl) quercetin iodide (Q-7BTPI) (50 mg, 0.07 mmol, 1 eq.) and K_2CO_3 (100 mg, 0.7 mmol, 10 eq.) in CH_3CN (5 mL) and heated at 45°C overnight. The solvent was than eliminated under reduced pressure. The resulting yellow solid was dissolved in the minimum amount of dichloromethane (1 mL) and precipitated with diethyl ether (20 mL). The mixture was centrifugated and the precipitation was repeated for 5 times. Residual solvent was then removed under reduced pressure to afford the title compound (45 mg, 0.06 mmol) in 84% yield.

^{1}H-NMR (250 MHz, $CDCl_3$) δ (ppm): 1.91-2.01 (m, 2H, CH_2), 2.27-2.35 (m, 2H, CH_2), 3.73-3.81 (m, 2H, CH_2), 3.86 (s, 3H, CH_3), 3.94-3.99 (m, 9H, 3 × CH_3), 4.29 (t, 2H, CH_2, $^3J_{H\text{-}H}$= 5.5 Hz), 6.24 (d, 1H, aromatic-H $^4J_{H\text{-}H}$=2.3 Hz), 6.66 (d, 1H, aromatic-H $^4J_{H\text{-}H}$=2.3 Hz), 6.99 (d, 1H, aromatic-H, $^3J_{H\text{-}H}$=8.8 Hz), 7.65-7.85 (m, 17H, aromatic-H) ppm.

^{13}C-NMR (62.9 MHz, $CDCl_3$) δ (ppm): 174.0, 162.9, 160.8, 158.6, 152.6, 150.7, 148.6, 141.0, 135.1, 135.7, 133.7 (d, $^3J_{(13C/31P)}$= 10.1 Hz), 130.5 (d, $^2J_{(13C/31P)}$= 12.5 Hz), 123.2,

121.8, 118.0 (d, $^{1}J_{(13C/31P)}$= 86.1 Hz), 111.0, 110.7, 95.7, 93.7, 67.3, 59.8, 56.6, 56.3, 55.9, 29.1 (d, $^{2}J_{(13C/31P)}$= 17.7 Hz), 22.4 (d, $^{1}J_{(13C/31P)}$= 50.9 Hz), 19.2 ppm.

ESI-MS: m/z 676, $[M]^{+}$.

Bibliography

[1] Sheu, S. S.; Nauduri, D.; Anders, M. W. Targeting antioxidants to mitochondria: a new therapeutic direction. Biochim. Biophys. Acta **1762:** 256-265; 2006.
[2] Murphy, M. P.; Smith, R. A. Targeting antioxidants to mitochondria by conjugation to lipophilic cations. Annu. Rev. Pharmacol. Toxicol. **47**: 629-656; 2007.
[3] Hoye, A. T.; Davoren, J. E.; Wipf, P.; Fink, M. P.; Kagan, V. E. Targeting mitochondria. Acc. Chem. Res. **41:** 87-97; 2008.
[4] Smith, R. A.; Adlam, V. J.; Blaikie, F. H.; Manas, A. R.; Porteous, C. M.; James, A. M.; Ross, M. F.; Logan, A.; Cochemé, H. M.; Trnka, J.; Prime, T. A.; Abakumova, I.; Jones, B. A.; Filipovska, A.; Murphy, M. P. Mitochondria-targeted antioxidants in the treatment of disease. Ann. N. Y. Acad. Sci. **1147:** 105-111; 2008.
[5] Victor, V.M.; Apostolova, N.; Herance, R.; Hernandez-Mijares, A.; Rocha, M. Oxidative stress and mitochondrial dysfunction in atherosclerosis: mitochondria-targeted antioxidants as potential therapy. Curr. Med. Chem. **16**: 4654-4667; 2009.
[6] Skulachev, V. P.; Anisimov, V. N.; Antonenko, Y. N.; Bakeeva, L. E.; Chernyak, B. V.; Erichev, V. P.; Filenko, O. F.; Kalinina, N. I.; Kapelko, V. I.; Kolosova, N. G.; Kopnin, B. P.; Korshunova, G. A.; Lichinitser, M. R.; Obukhova, L. A.; Pasyukova, E. G.; Pisarenko, O. I.; Roginsky, V. A.; Ruuge, E. K.; Senin, I. I.; Severina, I. I.; Skulachev, M. V.; Spivak, I. M.; Tashlitsky, V. N.; Tkachuk, V. A.; Vyssokikh, M. Y.; Yaguzhinsky, L. S.; Zorov, D. B. An attempt to prevent senescence: a mitochondrial approach. Biochim. Biophys. Acta **1787:** 437-461; 2009.
[7] Rocha, M.; Apostolova, N.; Hernandez-Mijares, A.; Herance, R.; Victor, V.M. Oxidative stress and endothelial dysfunction in cardiovascular disease: mitochondria-targeted therapeutics. Curr. Med. Chem. **17**: 3827-3841; 2010.
[8] Smith, R. A.; Murphy, M. P. Animal and human studies with the mitochondria-targeted antioxidant MitoQ. Ann. N. Y. Acad. Sci. **1201**: 96-103; 2010.
[9] Dong, L. F.; Low, P.; Dyason, J. C.; Wang, X. F.; Prochazka, L.; Witting, P. K.; Freeman, R.; Swettenham, E.; Valis, K.; Liu, J.; Zobalova, R.; Turanek, J.; Spitz, D. R.; Domann, F. E.; Scheffler, I. E.; Ralph, S. J.; Neuzil, J. Alpha-tocopheryl succinate induces apoptosis by targeting ubiquinone-binding sites in mitochondrial respiratory complex II. Oncogene **27**: 4324-4335; 2008.
[10] Dong, L. F.; Freeman, R.; Liu, J.; Zobalova, R.; Marin-Hernandez, A.; Stantic, M.; Rohlena, J.; Valis, K.; Rodriguez-Enriquez, S.; Butcher, B.; Goodwin, J.; Brunk, U. T.; Witting, P. K.; Moreno-Sanchez, R.; Scheffler, I. E.; Ralph, S. J.; Neuzil, J. Suppression of tumor growth in vivo by the mitocan alpha-tocopheryl succinate requires respiratory complex II. Clin. Cancer Res. **15**: 1593-1600, 2009.
[11] Dong, L. F.; Jameson, V. J.; Tilly, D.; Cerny, J.; Mahdavian, E.; Marín-Hernández, A.; Hernández-Esquivel, L.; Rodríguez-Enríquez, S.; Stursa, J.; Witting, P. K.; Stantic, B.; Rohlena, J.; Truksa, J.; Kluckova, K.; Dyason, J. C.; Ledvina, M.; Salvatore, B. A.; Moreno-Sánchez, R.; Coster, M. J.; Ralph, S. J.; Smith, R. A.; Neuzil, J. Mitochondrial targeting of vitamin E succinate enhances its pro-apoptotic and anti-cancer activity. J. Biol. Chem. 2010, in press (doi: 10.1074/jbc.M110.186643).
[12] Rodriguez-Cuenca, S.; Cochemé, H. M.; Logan, A.; Abakumova, I.; Prime, T. A.; Rose, C.; Vidal-Puig, A.; Smith, A. C.; Rubinsztein, D. C.; Fearnley, I. M.; Jones, B. A.;

Pope, S.; Heales, S. J.; Lam, B. Y.; Neogi, S. G.; McFarlane, I.; James, A. M.; Smith, R. A.; Murphy, M. P. Consequences of long-term oral administration of the mitochondria-targeted antioxidant MitoQ to wild-type mice. Free Radic. Biol. Med. **48**: 161-172; 2010.
[13] Doughn, A. K.; Dikalov, S. I. Mitochondrial redox cycling of mitoquinone leads to superoxide production and cellular apoptosis. Antiox. Redox Signal. **9**: 1825-1836; 2007.
[14] Cao, G.; Sofic, E.; Prior, R. L. Antioxidant and prooxidant behavior of flavonoids: structure–activity relationships. Free Rad. Biol. Med. **22**: 749–760; 1997.
[15] Galati, G.; Chan, T.; Wu, B.; O'Brien, P. J. Glutathione-dependent generation of reactive oxygen species by the peroxidase-catalyzed redox cycling of flavonoids. Chem. Res. Toxicol. **12**: 521–525; 1999.
[16] Choi, E. J.; Chee, K. M.; Lee, B. H. Anti- and prooxidant effects of chronic quercetin administration in rats. Eur. J. Pharmacol. **482**: 281–285; 2003.
[17] Halliwell, B. Are polyphenols antioxidants or pro-oxidants? What do we learn from cell culture and in vivo studies? Arch. Biochem. Biophys. **476**: 107–112; 2008.
[18] Robaszkiewicz, A.; Balcerczyk, A.; Bartosz, G. Antioxidative and prooxidative effects of quercetin on A549 cells. Cell Biol. Int. **31**: 1245-1250; 2007.
[19] Schmalhausen, E. V.; Zhlobek, E. B.; Shalova, I. N.; Firuzi, O.; Saso, L.; Muronetz, V. I. Antioxidant and prooxidant effects of quercetin on glyceraldehyde-3-phosphate dehydrogenase. Food Chem. Toxicol. **45**: 1988-1993; 2007.
[20] De Marchi, U.; Biasutto, L.; Garbisa, S.; Toninello, A.; Zoratti, M. Quercetin can act either as an inhibitor or an inducer of the mitochondrial permeability transitino pore: A demonstration of the ambivalent redox character of polyphenols. Biochim. Biophys. Acta **1787**: 1425-1432; 2009.
[21] Ferraresi, R.; Troiano, L.; Roat, E.; Lugli, E.; Nemes, E.; Nasi, M.; Pinti, M.; Fernandez, M. I.; Cooper, E. L.; Cossarizza, A. Essential requirement of reduced glutathione (GSH) for the anti-oxidant effect of the flavonoid quercetin. Free Radic. Res. **39**: 1249-1258; 2005.
[22] Ramos, A. M.; Aller, P. Quercetin decreases intracellular GSH content and potentiates the apoptotic action of the antileukemic drug arsenic trioxide in human leukemia cell lines. Biochem. Pharmacol. **75**: 1912-1923; 2008.
[23] Mattarei, A.; Sassi, N.; Biasutto, L.; Durante, C.; Sandonà, G.; Marotta, E.; Garbisa, S.; Gennaro, A.; Zoratti, M.; Paradisi, C. Isomeric mitochondriotropic quercetin derivatives have different redox properties and cytotoxicity. Free Radic. Biol. Med., submitted.
[24] Biasutto, L.; Sassi, N.; Mattarei, A.; Marotta, E.; Cattelan, P.; Toninello, A.; Garbisa, S.; Zoratti, M.; Paradisi, C. Impact of mitochondriotropic quercetin derivatives on mitochondria. Biochim. Biophys. Acta **1797:** 189-196; 2010.
[25] Lowry, O. H.; Rosebrough, N. J.; Farr, A. L.; Randall, R. J. Protein measurement with the Folin phenol reagent. J. Biol. Chem. **193**: 265–275; 1951.
[26] Ellman, G. L. Tissue sulfhydryl groups. Arch. Biochem. Biophys. **82**: 70–77; 1959.
[27] Kanadzu, M.; Lu, Y.; Morimoto, K. Dual function of (-)-epigallocatechin gallate (EGCG) in healthy human lymphocytes. Cancer Lett. **241:** 250-255; 2006.
[28] Kim, E. J.; Choi, C. H.; Park, J. Y.; Kang, S. K.; Kim, Y. K. Underlying mechanism of quercetin-induced cell death in human glioma cells. Neurochem. Res. **33**: 971-979; 2008.
[29] Zielonka, J.; Kalyanaraman, B. Hydroethidine- and MitoSOX-derived red fluorescence is not a reliable indicator of intracellular superoxide formation: another inconvenient truth. Free Radic. Biol. Med. **48**: 983-1001; 2010.
[30] Dickinson, B. C.; Srikun, D.; Chang, C. J. Mitochondrial-targeted fluorescent probes for reactive oxygen species. Curr. Opin. Chem. Biol. **14:** 50-56; 2010.

[31] Awad, H. M.; Boersma, M. G.; Vervoort, J.; Rietjens, I. M. Peroxidase-catalyzed formation of quercetin quinone methide-glutathione adducts. Arch. Biochem. Biophys. **378**: 224-233; 2000.
[32] Awad, H. M.; Boersma, M. G.; Boeren, S.; van der Woude, H.; van Zanden, J.; van Bladeren, P. J.; Vervoort, J.; Rietjens, I. M. Identification of o-quinone/quinone methide metabolites of quercetin in a cellular in vitro system. FEBS Lett. **520**: 30-34; 2002.
[33] Awad, H. M.; Boersma, M. G.; Boeren, S.; van Bladeren, P. J.; Vervoort, J.; Rietjens, I. M. Quenching of quercetin quinone/quinone methides by different thiolate scavengers: stability and reversibility of conjugate formation. Chem. Res. Toxicol. **16**: 822-831; 2003.
[34] Gliszczyńska-Swigło, A.; van der Woude, H.; de Haan, L.; Tyrakowska, B.; Aarts, J. M.; Rietjens, I. M. The role of quinone reductase (NQO1) and quinone chemistry in quercetin cytotoxicity. Toxicol. In Vitro **17**: 423-431; 2003.
[35] van der Woude, H.; Alink, G. M.; van Rossum, B. E.; Walle, K.; van Steeg, H.; Walle, T.; Rietjens, I. M. Formation of transient covalent protein and DNA adducts by quercetin in cells with and without oxidative enzyme activity. Chem. Res. Toxicol. **18**: 1907-1916; 2005.
[36] van der Woude, H.; Boersma, M. G.; Alink, G. M.; Vervoort, J.; Rietjens, I. M. Consequences of quercetin methylation for its covalent glutathione and DNA adduct formation. Chem. Biol. Interact. **160**: 193-203; 2006.
[37] Murphy, M. P. How mitochondria produce reactive oxygen species. Biochem. J. **417:** 1-13; 2009.
[38] Kim, E.J.; Choi, C. H.; Park, J. Y.; Kang, S. K.; Kim, Y. K. Underlying mechanisms of quercetin-induced cell death in human glioma cells. Neurochem. Res. **33**: 971-979; 2008.
[39] Nicholls, D. G. Oxidative stress and energy crises in neuronal dysfunction. Ann. N. Y. Acad. Sci. **1147**: 53-60; 2008.
[40] Nicholls, D. G. Spare respiratory capacity, oxidative stress and excitotoxicity. Biochem. Soc. Trans. **37**: 1385-1388; 2009.
[41] Chan, T.; Galati, G.; O'Brien, P. J. Oxygen activation during peroxidase catalyzed metabolism of flavones or flavanones. Chem. Biol. Interact. **122**: 15-25; 1999.
[42] Galati, G.; Chan, T.; Wu, B.; O'Brien, P. J. Glutathione-dependent generation of reactive oxygen species by the peroxidase-catalyzed redox cycling of flavonoids. Chem. Res. Toxicol. **12**: 521-525; 1999.
[43] Metodiewa, D.; Jaiswal, A. K.; Cenas, N.; Dickancaité, E.; Segura-Aguilar, J. Quercetin may act as a cytotoxic prooxidant after its metabolic activation to semiquinone and quinoidal product. Free Radic. Biol. Med. **26**: 107-116; 1999.
[44] Marí, M.; Morales, A.; Colell, A.; García-Ruiz, C.; Fernández-Checa, J.C. Mitochondrial glutathione, a key survival antioxidant. Antiox. Redox Signal. **11**: 2685-2700; 2009.
[45] Franco, R.; Cidlowski, J. A. Apoptosis and glutathione: beyond an antioxidant. Cell Death Differ. **16**: 1303-1314; 2009.
[46] Circu, M. L.; Aw, T. Y. Glutathione and apoptosis. Free Radic. Res. **42**: 689-706; 2008.
[47] Circu, M. L.; Aw, T. Y. Reactive oxygen species, cellular redox systems, and apoptosis. Free Radic. Biol. Med. **48**: 749-762; 2010.
[48] Wefers, H.; Sies, H. Oxidation of glutathione by the superoxide radical to the disulfide and the sulfonate yielding singlet oxygen. Eur. J. Biochem. **137**: 29-36; 1983.
[49] Winterbourn, H.; Metodiewa, D. The reaction of superoxide with reduced glutathione. Arch. Biochem. Biophys. **314**: 284-290; 1994.

[50] Jones, C. M.; Lawrence, A.; Wardman, P.; Burkitt, M. J. Kinetics of superoxide scavenging by glutathione: an evaluation of its role in the removal of mitochondrial superoxide. Biochem. Soc. Trans. **31**: 1337-1339; 2003.
[51] Kurata, M.; Suzuki, M.; Takeda, K. Effects of phenol compounds, glutathione analogues and a diuretic drug on glutathione S-transferase, glutathione reductase and glutathione peroxidase from canine erythrocytes. Comp. Biochem. Physiol. B **103**: 863-867; 1992.
[52] Elliott, A. J.; Scheiber, S. A.; Thomas, C.; Pardini, R. S. Inhibition of glutathione reductase by flavonoids: A structure-activity study. Biochem. Pharmacol. **44**: 1603–1608; 1992.
[53] Zhang, K.; Yang, E.B.; Tang, W.Y.; Wong, K.P.; Mack, P. Inhibition of glutathione reductase by plant polyphenols. Biochem. Pharmacol. **54**: 1047–1053; 1997.
[54] Choi, E. J.; Lee, B. H.; Lee, K.; Chee, K. M. Long-term combined administration of quercetin and daidzein inhibits quercetin-induced suppression of glutathione antioxidant defenses. Food Chem. Toxicol. **43**: 793-798; 2005.
[55] van Zanden, J. J.; Ben Hamman, O.; van Iersel, M. L.; Boeren, S.; Cnubben, N. H.; Lo Bello, M.; Vervoort, J.; van Bladeren, P. J.; Rietjens, I. M. Inhibition of human glutathione S-transferase P1-1 by the flavonoid quercetin. Chem. Biol. Interact. **145**: 139-148; 2003.
[56] Hayeshi, R.; Mutingwende, I.; Mavengere, W.; Masiyanise, V.; Mukanganyama, S. The inhibition of human glutathione S-transferases activity by plant polyphenolic compounds ellagic acid and curcumin. Food Chem. Toxicol. **45**: 286-295; 2007.
[57] Lu, J.; Papp, L. V.; Fang, J.; Rodriguez-Nieto, S.; Zhivotovsky, B.; Holmgren, A. Inhibition of mammalian thioredoxin reductase by some flavonoids: implications for myricetin and quercetin anticancer activity. Cancer Res. **66**: 4410-4418; 2006.
[58] Lavoie, S.; Chen, Y.; Dalton, T. P.; Gysin, R.; Cuénod, M.; Steullet, P.; Do, K. Q. Curcumin, quercetin, and tBHQ modulate glutathione levels in astrocytes and neurons: importance of the glutamate cysteine ligase modifier subunit. J. Neurochem. **108**: 1410-1422; 2009.
[59] Arredondo, F.; Echeverry, C.; Abin-Carriquiry, J. A.; Blasina, F.; Antúnez, K.; Jones, D. P.; Go, Y. M.; Liang, Y. L.; Dajas, F. After cellular internalization, quercetin causes Nrf2 nuclear translocation, increases glutathione levels, and prevents neuronal death against an oxidative insult. Free Radic. Biol. Med. **49**: 738-747; 2010.
[60] Blum, J.; Fridovich, I. Inactivation of glutathione peroxidase by superoxide radical. Arch. Biochem. Biophys. **240**: 500-508; 1985.
[61] Han, Y. H.; Kim, S. Z.; Kim, S. H.; Park, W. H. Pyrogallol as a glutathione depletor induces apoptosis in HeLa cells. Int. J. Mol. Med. **21**: 721-730; 2008.
[62] Loor, G.; Kondapalli, J.; Schriewer, J. M.; Chandel, N. S.; Vanden Hoek, T. L.; Schimaker, P. T. Menadione triggers cell death through ROS-dependent mechanisms involving PARP activation without requiring apoptosis. Free Radic. Biol. Med. 2010, in press (doi: 10.1016/j.freeradbiomed.2010.09.021).
[63] Strathmann, J.; Klimo, K.; Sauer, S. W.; Okun, J. G.; Prehn, J. H.; Gerhäuser C. Xanthohumol-induced transient superoxide anion radical formation triggers cancer cells into apoptosis via a mitochondria-mediated mechanism. FASEB J. **24**: 2938-2950; 2010.
[64] Kessler, M.; Ubeaud, G.; Jung, L. Anti- and pro-oxidant activity of rutin and quercetin derivatives. J. Pharm. Pharmacol. **55**: 131-142; 2003.
[65] Kim, G. N.; Jang, H. D. Protective mechanism of quercetin and rutin using glutathione metabolism on HO-induced oxidative stress in HepG2 cells. Ann. N. Y. Acad. Sci. **1171**: 530-537; 2009.
[66] Vargas, A. J.; Burd, R. Hormesis and synergy: pathways and mechanisms of quercetin in cancer prevention and management. Nutr. Rev. **68**: 418-428; 2010.

[67] Brisdelli, F.; Coccia, C.; Cinque, B.; Cifone, M. G.; Bozzi, A. Induction of apoptosis by quercetin: different response of human chronic myeloid (K562) and acute lymphoblastic (HSB-2) leukemia cells. Mol. Cell. Biochem. **296**: 137-149; 2007.
[68] Chien, S. Y.; Wu, Y. C.; Chung, J. G.; Yang, J. S.; Lu, H. F.; Tsou, M. F.; Wood, W. G.; Kuo, S. J.; Chen, D. R. Quercetin-induced apoptosis acts through mitochondrial- and caspase-3-dependent pathways in human breast cancer MDA-MB-231 cells. Hum. Exp. Toxicol. **28**: 493-503; 2009.
[69] Soria, E. A.; Eynard, A. R.; Bongiovanni, G. A. Cytoprotective effects of silymarin on epithelial cells against arsenic-induced apoptosis in contrast with quercetin cytotoxicity. Life Sci. **87**: 309-315; 2010.
[70] Priyadarsini, R. V.; Murugan, R. S.; Maitreyi, S.; Ramalingam, K.; Karunagaran, D.; Nagini, S. The flavonoid quercetin induces cell cycle arrest and mitochondria-mediated apoptosis in human cervical cancer (HeLa) cells through p53 induction and NF-kB inhibition. Eur. J. Pharmacol. **649**: 84-91; 2010.
[71] Chou, C. C.; Yang, J. S. ; Lu, H. F. ; Ip, S. W. ; Wu, C. C.; Lin, J. P. ; Tang, N. Y. ; Chung, J. G.; Chou, M. J.; Teng, Y. H.; Cehn, D. R. Quercetin-mediated cell cycle arrest and apoptosis involving activation of a caspase cascade through the mitochondrial pathway in human breast cancer MCF-7 cells. Arch. Pharm. Res. **33**: 1181-1191; 2010.
[72] Cheng, S.; Gao, N.; Zhang, Z.; Chen, G.; Budhraja, A.; Ke, Z.; Son, Y.; Wang, X.; Luo, J.; Shi, X. Quercetin Induces Tumor-Selective Apoptosis through Downregulation of Mcl-1 and Activation of Bax. Clin. Cancer Res. **16**: 5679-5691; 2010.
[73] Jamison, J. M.; Gilloteaux, J.; Taper, H. S.; Calderon, P. B.; Summers, J. L. Autoschizis: a novel cell death. Biochem. Pharmacol. **63:** 1773-1783; 2002.
[74] Nicotera, P.; Leist, M.; Ferrando-May, E. Intracellular ATP, a switch in the decision between apoptosis and necrosis. Toxicol. Lett. **102-103:** 139-142; 1998.
[75] Mattarei, A.; Biasutto, L.; Marotta, E.; De Marchi, U.; Sassi, N.; Garbisa, S.; Zoratti, M.; Paradisi, C. A mitochondriotropic derivative of quercetin: a strategy to increase the effectiveness of polyphenols. ChemBioChem **9:** 2633-2642; 2008.
[76] Son, T. G.; Camandola, S.; Mattson, M.P. Hormetic dietary phytochemicals. Neuromolecular Med. **10**: 236-246; 2008.
[77] Calabrese, E. J. Hormesis is central to toxicology, pharmacology and risk assessment. Hum. Exp. Toxicol. **29**: 249-261; 2010.
[78] Calabrese, V.; Cornelius, C.; Trovato, A.; Cavallaro, M.; Mancuso, C.; Di Rienzo, L.; Condorelli, D.; De Lorenzo, A.; Calabrese, E. J. The hormetic role of dietary antioxidants in free radical-related diseases. Curr. Pharm. Des. **16**: 877-883; 2010.
[79] Tanigawa, S.; Fujii, M.; Hou, D. X. Action of Nrf2 and Keap1 in ARE-mediated NQO1 expression by quercetin. Free Radic. Biol. Med. **42**: 1690-1703; 2007.
[80] Eggler, A. L.; Gay, K. A.; Mesecar, A. D. Molecular mechanisms of natural products in chemoprevention: induction of cytoprotective enzymes by Nrf2. Mol. Nutr. Food Res. **52** (Suppl. 1): S84-S94; 2008.
[81] Kimura, S.; Warabi, E.; Yanagawa, T.; Ma, D.; Itoh, K.; Ishii, Y.; Kawachi, Y.; Ishii, T. Essential role of Nrf2 in keratinocyte protection from UVA by quercetin. Biochem. Biophys. Res. Comm. **387**: 109-114; 2009.
[82] Miyamoto, N.; Izumi, H.; Miyamoto, R.; Kondo, H.; Tawara, A.; Sasaguri, Y.; Kohno, K. Quercetin induces the expression of peroxiredoxins 3 and 5 via the Nrf2/NRF1 transcription pathway. Invest. Ophtalmol. Vis. Sci. 2010, in press.
[83] Ding, M.; Zhao, J.; Bowman, L.; Lu, Y.; Shi, X. Inhibition of AP-1 and MAPK signaling and activation of Nrf2/ARE pathway by quercitrin. Int. J. Oncol. **36**: 59-67; 2010.
[84] Chen, L. B. Mitochondrial membrane potential in living cells. Annu. Rev. Cell Biol. **4:** 155-181; 1988.

[85] Modica-Napolitano, J. S.; Aprille, J. R. Delocalized lipophilic cations selectively target the mitochondria of carcinoma cells. Adv. Drug Deliv. Rev. **49:** 63-70; 2001.
[86] Fantin, V. R.; Berardi, M. J.; Scorrano, L.; Korsmeyer, S. J.; Leder, P. A novel mitochondriotoxic small molecule that selectively inhibits tumor cell growth. Cancer Cell **2:** 29-42;

Chapter 7

Absorption and metabolism of resveratrol carboxyesters and methanesulfonate by explanted rat intestinal segments[7]

Summary

Model prodrugs of resveratrol carrying protecting substituents at the hydroxyls have been synthesised and tested. Resveratrol triacetate and resveratrol-tri-mPEG$_{1900}$ were formed by linking methyl groups or poly(ethylene glycol) chains, respectively, via carboxyester bonds. Resveratrol trimesylate, a molecule less susceptible to hydrolytic attack, was synthesised as well. This latter compound proved to be stable *in vitro*, while the carboxyester derivatives were slowly hydrolysed in solutions mimicking the gastric or intestinal environment, and rapidly converted to resveratrol in blood. In *ex vivo* permeation experiments with explanted intestinal segments, resveratrol and its triacetate derivative appeared in the basolateral compartment essentially as a mixture of Phase II metabolites. When the PEGylated derivative was provided on the apical side, unconjugated resveratrol accounted for about 50% of the compounds in the basolateral-side chamber. The same result was obtained by providing an equivalent physical mixture of resveratrol and PEG polymer, indicating that this behaviour is likely due to an adjuvating effect of PEG rather than to the covalent polymer conjugation. These observations suggest that the ester derivatives are rapidly hydrolysed at the intestinal surface or inside enterocytes, and are then processed as resveratrol. On the other hand, the mesylate was transported from the apical to the basolateral side without modification. It may thus be possible to enhance absorption and hinder metabolism of natural polyphenols by constructing pro-drugs incorporating bonds with appropriate resistance to enzymatic hydrolysis.

Introduction

Polyphenols are a huge family of natural compounds exhibiting a variety of biological activities.

[7] Published as: Biasutto, L.; Marotta, E.; Mattarei, A.; Beltramello, S.; Caliceti, P.; Salmaso, S.; Bernkop-Schnürch, A.; Garbisa, S.; Zoratti, M.; Paradisi, C. *Cell. Physiol. Biochem.* **2009**, 24, 557-566.

A vast literature documents effects of potential relevance for such major health-care endeavours as protection of the cardiovascular system [1], improving performance impaired by old age or neurodegeneration [2,3], and prevention and therapy of cancer [4,5]. Several biochemical pathways underlying these effects have been identified (e.g.: cardio- and neurovascular protection [5,6]; neuroprotection and anti-aging [7,8]). Studies dealing with the mechanisms underlying the bioactivity of resveratrol, the model polyphenol used in the present work, have been summarized in recent reviews [8-11]. The biological processes involved are by no means limited to the general chemical reactivity of polyphenols as anti- or pro-oxidants. Various members of the family are known to modulate signal-transducing proteins ranging from channels [12] to cyclooxygenases [13]. Effects on gene expression are important [8,14].

A few polyphenols display high affinity for proteins. For example, epigallocatechin gallate (EGCG) binds the laminin receptor with nM affinity [15]. In many other cases, however, potentially useful interactions are considerably weaker. For example the IC_{50} for the inhibition of cyclooxygenases 1 and 2 by quercetin is around 5 μM [16]. Resveratrol and other polyphenols inhibit IkB kinase (IKK), thus reducing phosphorylation and degradation of IkB and downregulating NF-kB. IKK is half-inhibited at a concentration of resveratrol around 1 μM [17]. Relatively poor affinities constitute an obstacle to the utilization of these compounds, since their bioavailability is notoriously low [18-20]. Polyphenols such as quercetin and resveratrol can diffuse into enterocytes as aglycones, as shown by experiments with cultured cells. *In vivo*, they do the same after being generated from naturally occurring glycosides by the activity of glycosidases such as Lactase Phloridzin Hydrolase and Broad Specificity Glucosidase. Some evidence has also been presented that they can be also taken as glycosides, mainly via hexose carriers, to be then hydrolysed in the cytoplasm of enterocytes ([21,22] and references therein). There, polyphenols are rapidly converted by conjugating enzymes to metabolites that are re-exported, largely to the intestinal lumen, by ABC transporters such as P-glycoprotein. Liver sulfotransferases (SULTs) and glucuronosyltransferases (UGTs) then intervene on the molecules which have entered the circulation. Thus, only low concentrations (nM-μM) of polyphenols, mostly in the form of conjugates, are found in plasma and lymph even after a polyphenol-rich meal. At least two dozen different quercetin derivatives have been detected in human plasma [19] and resveratrol undergoes similar processing [23-25].

"Detoxification" by conversion into sulfates and glucuronides entails faster elimination by the renal and biliary routes. The study of the properties and activities of metabolites is still

in the initial phases (e.g.: [26-34]), but it is clear that conjugation also determines at least a partial loss of bioefficacy. Since metabolites are present at much higher concentrations than the parent molecule, in some cases they may actually be more relevant than the latter in terms of biomedical activity. While these aspects remain to be investigated, a reduction or delay of phase II metabolism would allow progress in the exploitation of natural polyphenols. Furthermore, new, synthetic polyphenols are beginning to be explored as drugs (for resveratrol-inspired ones see, e.g., [35-45]). They are certain to be affected by the same (or worse) bioavailability problems as the natural compounds.

One of the main strategies used to prevent drug metabolism and enhance bioavailability and effectiveness is based on the development of "prodrugs" by protecting the reactive sites with removable groups. "Capping" the hydroxyls with chemical structures less prone hydrogen bond formation is also expected to decrease the well-known tendency of these compounds to bind aspecifically to proteins, which decreases their effective concentration and slows their distribution in the organism.

We report here the synthesis of three prodrugs of resveratrol, *in vitro* stability studies and investigations of their absorption by explanted rat intestinal segments. Resveratrol was adopted as polyphenol model because of its remarkable biomedical properties, relative structural simplicity and stability. Among the various conceivable derivatives the peracetylated molecule was chosen as a representative simple carboxyester derivative. Resveratrol triacetate has recently been reported to inhibit the proliferation of human colon adenocarcinoma cells [46]. With the intent of improving passage through the intestinal barrier we also produced a PEGylated derivative. "PEGylation" often leads to the improvement of drug absorption and pharmacokinetics [47-49]. PEG is non-toxic, non-antigenic and biocompatible, is rapidly eliminated from the body, is soluble both in water and many organic solvents and has pronounced solubilizing properties. It may also increase resistance to hydrolases and stability in the gastrointestinal tract. Also in this compound the polymeric chains were linked to the polyphenol kernel via carboxy ester bonding. To test an expectedly more stable type of chemical bond we also synthesized and tested per-methylsulfonated resveratrol. Little is known about the behaviour of sulfonates in biological systems; this group may be a potentially useful prodrug building block.

The various compounds were compared to resveratrol itself in experiments with explanted intestine segments to provide information on their relative efficiency and metabolic transformations in the specific step of permeation of the intestinal wall. To our knowledge, none of the previous studies with polyphenol prodrugs has dealt with the effects of the

modifications on permeation of the intestinal epithelium (as distinct from overall bioavailability or permeation of cultured cell monolayers). Experiments involving *ex vivo* intestinal tissue have however proven useful in assessing mechanistic aspects of polyphenol absorption [19,50-52].

Results

Syntheses. The new resveratrol derivatives RTA, RmPEG and RTM were synthesised from resveratrol as shown in Scheme 1. Details about synthetic procedures, product purification and characterization are provided in the Experimental Section.

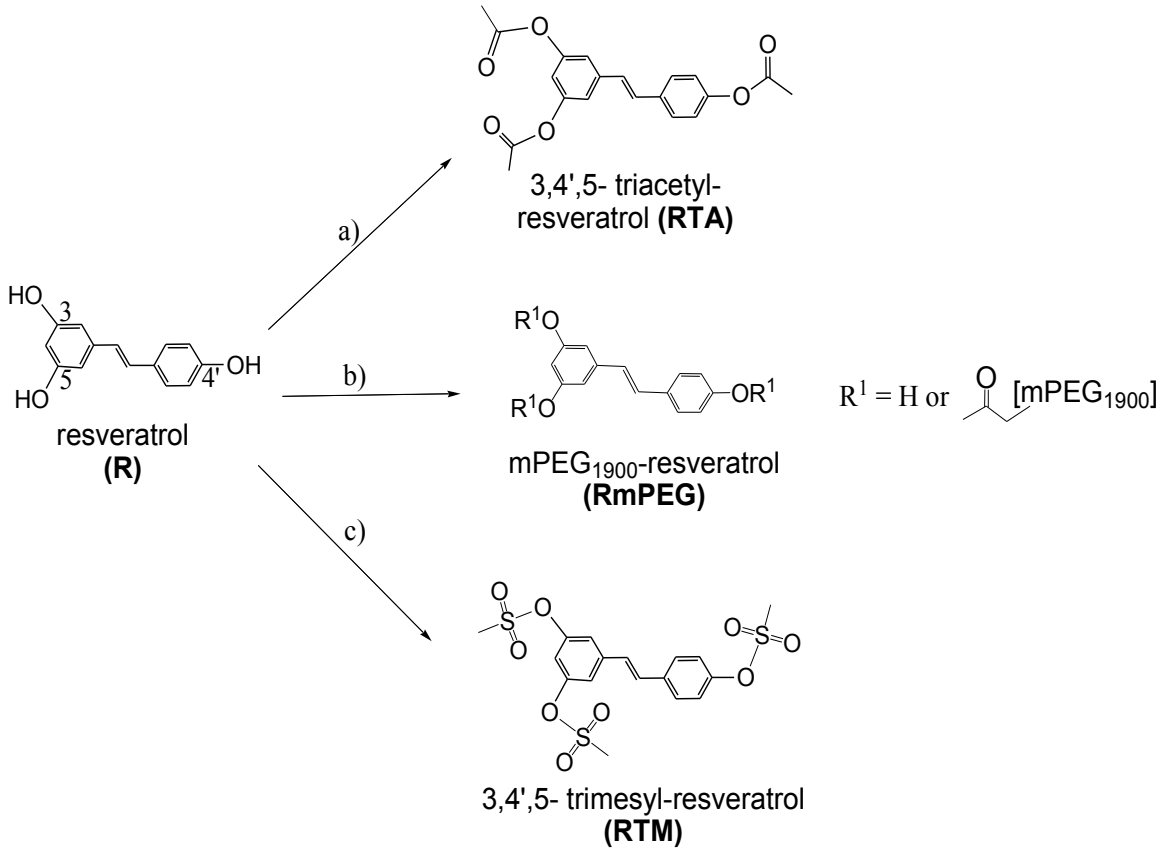

Scheme 1. Synthesis of the resveratrol derivatives. Reaction conditions: a) $(CH_3CO)_2O$ (16.7 eq.), pyridine, room temperature, 40 min; b) $mPEG_{1900}$ (5.8 eq.), CH_2Cl_2, DCC, DMAP, room temperature, 72 h; c) CH_3SO_2Cl (5.9 eq.), pyridine, 100°C, 3h.

Solubility in water. The solubility in water of the new derivatives differs markedly depending on the protecting group. While both RTA and RTM turned out to be poorly soluble (≤ 2 μM), the PEGylated compound is highly soluble, and saturation was not reached even dissolving 400 mg in 1 mL water (> 70 mM).

Stability in gastric and intestinal-like environment. All three compounds proved to be sufficiently stable over a 6 h period, both in gastric and intestinal environment-mimicking solutions (0.1 N HCl and 0.1 M PBS at pH 6.8, respectively). RTM was stable throughout the experimental period, while RTA and RmPEG underwent slow hydrolysis of the ester bonds, with up to 20% loss of the starting compound in 6 h (Fig.1). Over this period, RmPEG hydrolysis regenerated resveratrol, while RTA hydrolysis produced intermediate products (di- and mono- acetylated derivatives).

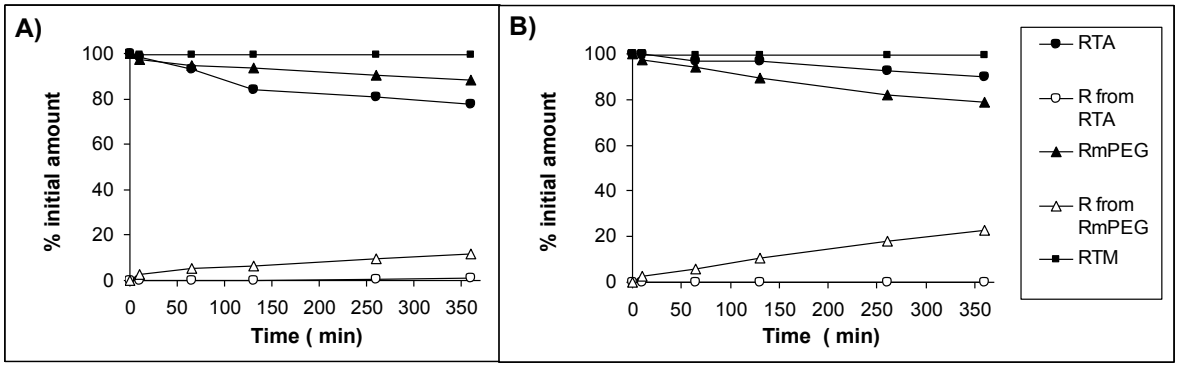

Figure 1. Stability of resveratrol-derivatives in media mimicking A) gastric and B) intestinal environment (at 37°C). Data are expressed as molar % of the initial amount.

Stability in blood. Stability studies showed that complete hydrolysis of both resveratrol carboxyesters (RTA and RmPEG) occurred over 1 hour incubation in whole blood at 37°C, with resveratrol being the unique final released product. The sulfonyl derivative RTM, on the contrary, was stable.

Intestinal wall permeability

The susceptibility to hydrolysis of the carboxyesters might constitute an advantage, allowing regeneration of the parent compound. However, rapid *in vivo* hydrolysis may reflect in metabolism during absorption. To investigate this point, the epithelial absorption of the compounds was examined in *ex vivo* intestinal wall permeation assays using segments of excised rat jejunum mounted in Ussing chambers. This experimental system allows the study of transepithelial transport separately from processes taking place *in vivo* in the intestinal lumen, blood, or liver.

The results show that the powerful hydrolytic and conjugation enzyme activities, namely esterases and glucoronyl and sulphate transferases, associated with the intestinal membrane have strong effects on the derivative stability and metabolism. RTA and RmPEG were completely hydrolysed within 2.5 hours. The process is certainly due to enzymatic activities, since only a small amount of hydrolysis products were formed upon parallel incubation of the derivatives under the same conditions but without the intestine. Analyses

of the contents of the basolateral compartments (Fig. 2) confirmed that resveratrol (i.e. the reference compound) is mainly metabolized into glucuronyl- and sulphate- derivatives during passage across the intestinal wall. RTA produced a similar mix of basolateral resveratrol derivatives, whereas the PEGylated derivative yielded a significant amount of non-metabolized resveratrol on the basolateral side.

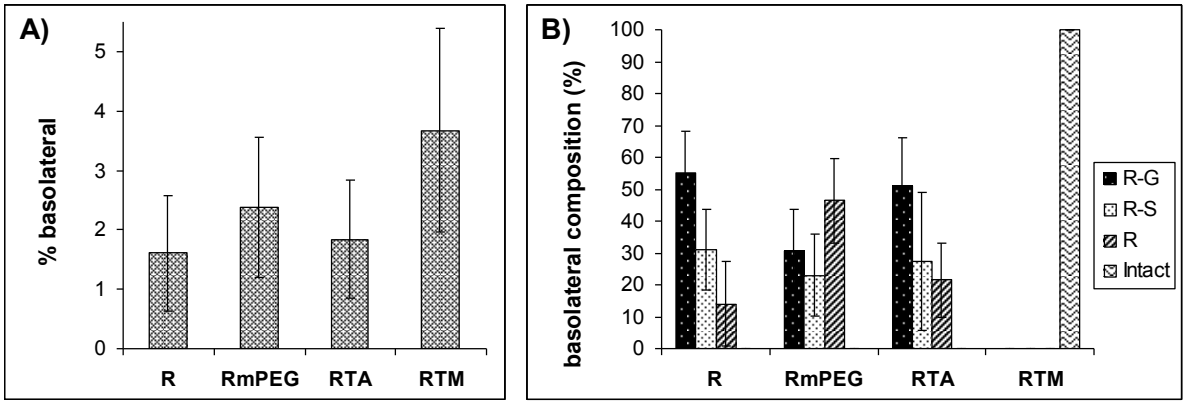

Figure 2. Composition of the basolateral compartment after 2.5 h incubation with 20 μM apical compounds (see text for details). A) Total basolateral species. Data are expressed as percentage of the total amount recovered in the apical and basolateral compartments (mean ± standard deviation, N=4 for all compounds). B) Relative amounts of basolateral resveratrol metabolites (R-3-glucuronide and R-3-sulfate), resveratrol and intact loaded compound. Data are expressed as percentages considering the total amount recovered in the basolateral compartment as 100% (mean ± standard deviation, N=4 for all compounds).

An analogous transfer of unmetabolised resveratrol was observed when the apical-side chamber was loaded with a physical resveratrol/mPEG$_{1900}$ mixture at the same concentration of the two components as used in the conjugate experiment (Fig. 3). In contrast RTM crossed the intestine as such (Fig. 2).

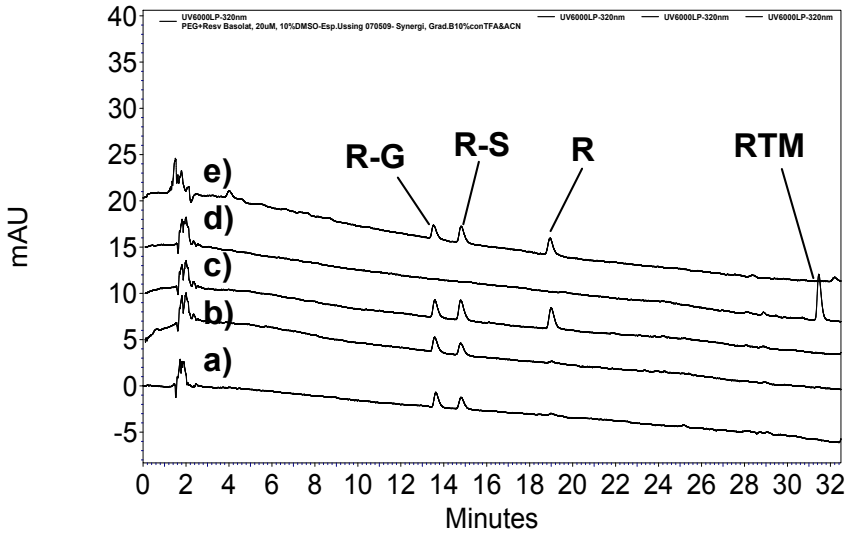

Figure 3. HPLC chromatograms (320 nm) of the basolateral compartment after 2.5 h incubation with 20 μM of: a) resveratrol; b) RTA; c) RmPEG; d) RTM; e) R and mPEG$_{1900}$.

Discussion

The resveratrol conjugates investigated in this study (acetylated, PEGylated and mesylated resveratrol) constitute a new set of derivatives intended to explore the feasibility of the pro-drug approach to improve polyphenol absorption and efficacy [56].

Bond stability represents a key parameter for the preparation of effective prodrugs. A desirable property of ester-based protecting groups is that they can be removed by esterases at the action site. For example, in acetylsalycilic acid (aspirin), in which the leaving group is formally a phenoxy anion, the ester bond is stable enough for the molecule to reach cycloxygenase and inhibit the enzyme by transferring the acetyl group to a specific serine. The resistance of the ester to hydrolysis is, in general, expected to be an inverse function of the stability of the products, i.e. mainly of the phenoxide anion leaving group. Polyphenols in which the negative charge of the deprotonated form is more widely delocalised by resonance are expected to be better leaving groups, and their ester derivatives are expected to be more fragile.

Ester precursors intended to improve bioavailability and/or stability have been obtained with several drugs bearing alcoholic or phenolic hydroxyls and with a few polyphenols [57-61]. These derivatives have been tested so far mainly on cultured cells, but peracetylated EGCG administered by intraperitoneal injection has been reported to be more effective than EGCG itself against human prostate [60] and breast [62] cancers implanted in SCID mice. In our own work, quercetin aminoacyl derivatives showed an increased protection against metabolization by epithelial cell monolayers [56].

Among the several other chemical groups that may be considered for a protective role we tested a different class of esters, namely those of sulfonic acids, using the mesylate as the representative specie. It may be worthwhile to clarify that the type of derivatives we considered are unlikely to be toxic. Alkylsulfonates ($RSO_2O\text{-}CH_2R'$) are known genotoxic agents: the methylsulfonate group can be easily displaced by a nucleophile (such as a DNA base) to produce RSO_3^- and the alkylated nucleophile. However, in the case of aromatic sulphonates, such as our resveratrol derivative, an analogous reaction cannot take place. Neither displacement of the mesylate group by nucleophilic attack at an aromatic carbon nor substitution at the S-linked carbon are expected to occur under the conditions prevailing in living organisms. The only type of reaction that one might expect is the desired one: (enzyme-catalyzed) hydrolysis to regenerate the phenolic component and RSO_3H.

The PEGylated derivatives were designed to improve both solubility and stability of resveratrol and to enhance its oral bioavailability. PEGylation of low molecular weight molecules has indeed been developed to tune biopharmaceutical and pharmacokinetic properties of drugs whose performance, clinical efficacy, and market potential are substantially limited by their poor oral bioavailability, solubility, half-life, or immediate clearance by first-pass metabolism [63]. Actually, small PEGs can easily penetrate the epithelial barrier and few studies have demonstrated that conjugation of small PEGs yields derivatives with enhanced trans-membrane penetration properties [63-65]. Accordingly, 1.9 kDa PEG was activated to produce a reversible PEG-resveratrol ester prodrug suitable for oral delivery. The product had an average substitution ratio of two PEG polymers per resveratrol molecule, which represented a compromise between the requisite for hydroxyl protection and solubilisation on one side and bulkiness on the other. The presence of a fraction of monosubstituted resveratrol explains why free resveratrol was produced by the PEGylated product, but not by RTA, in stability tests (Fig. 1).

The experiments reported here show that rat intestine possesses powerful carboxyesterase and conjugation enzyme activity involved in resveratrol and resveratrol derivative metabolism. In 2.5 hours, 64 mm^2 of apical intestinal surface were able to convert 100% of the carboxyesters supplied (20 nmoles) to the unsubstituted parental resveratrol. This activity readily accounts for the similarity of the transepithelial transport data obtained with RTA and RmPEG, which may well have acted only as a source of resveratrol. A first conclusion is therefore that acetylated resveratrol derivatives (and presumably other polyphenols with extensive charge delocalisation) have little chance of constituting a significant improvement over the parent polyphenol if administered orally. Due to the limited stability in blood, these derivatives seem to be not suitable for intravenous administration either.

A further observation is that PEGylation enhances resveratrol bioavailability, but this effect can be obtained by co-administration of PEG and unmodified polyphenol at the luminal side, indicating that the polymer can by itself play a role in the biotransport of this compound. The PEG effect may be interpreted in terms of the influx/efflux mechanisms involved in the transport of the drug. Resveratrol is known to cross biomembranes either passively or by exploiting active transporters [66] and to undergo efflux transport mediated exocytosis involving MRP transporters located in intestinal enterocytes [67,68]. Although PEG-resveratrol is expected to undergo passive transmembrane diffusion, the data obtained in the present study show that PEGyated resveratrol is at least partially hydrolysed to the

parent molecule by esterases. Since PEG is known to interfere with a variety of efflux mechanisms involved in drug clearance, including MRP-mediated transport, it seems reasonable to conclude that the enhanced resveratrol permeation may be due to MRP-mediated efflux inhibition by the polymer [69,70].

Methanesulfonates join ethers as a potentially useful class of polyphenol derivatives capable of escaping early metabolism. Permethylethers of polyphenols have already been considered as possible prodrugs and pharmacological agents [71,72]. Methanesulfonates may thus be useful in pathological contexts, leading to the creation of new molecules with their own, possibly advantageous, properties.

Our results indicate however that to develop prodrugs in the traditional sense it will be necessary to identify a type of protecting group based on a bond with considerable, but not indefinite, resistance to enzymatic hydrolysis *in vivo*. They thus identify the goals and directions of future studies in this sector. The bioavailability of new compounds being developed with the intention of building on the biomedical effectiveness of natural compounds ought to be tested at an early stage, and the stability of any prodrugs should be verified in a physiologically relevant environment. PEG chains may well be one of most promising substituents to be tested once the opportune bond type is identified.

Experimental section

Materials and methods:

Starting materials and reagents were purchased from Aldrich, Fluka, Merck-Novabiochem, Riedel de Haen, J.T. Baker, Cambridge Isotope Laboratories Inc., Acros Organics, Carlo Erba and Prolabo, and were used as received. Carboxyl terminating monomethoxypoly(ethylene glycol) (mPEG-COOH) was synthesised in our laboratory according to the procedure reported elsewhere [53]. Briefly, 1.9 kDa PEG-OH was activated as p-nitrophenol ester and then reacted with glycin. PEG-COOH was purified by extraction in dichloromethane. Resveratrol metabolites (R-G and R-S) were synthesised as described in the literature [54], and used as standards. ^{1}H NMR and ^{13}C spectra were recorded with a Bruker AC 250F spectrometer. Chemical shifts (δ) are given in ppm relative to the signal of the solvent. TLCs were run on silica gel supported on plastic (Macherey-Nagel Polygram®SIL G/UV$_{254}$, silica thickness 0.2 mm), or on silica gel supported on glass (Fluka) (silica thickness 0.25 mm, granulometry 60Å, medium porosity) and visualized by UV detection. Flash chromatography was performed on silica gel (Macherey-Nagel 60, 230-400 mesh granulometry, 0.063-0.040 mm) under air pressure. The solvents were

analytical or synthetic grade and were used without further purification. HPLC-UV analyses were performed by a Thermo Separation Products Inc. system with a P2000 Spectra System pump and a UV6000LP diode array detector (190-500 nm). LC-MS analyses and mass spectra were performed with a 1100 Series Agilent Technologies system, equipped with binary pump (G1312A) and MSD SL Trap mass spectrometer (G2445D SL) with ESI source.

Synthetic procedures.

3,4',5-triacetyl-resveratrol (RTA). Acetic anhydride (1.5 mL, 14.7 mmol, 16.7 eq) was added to a solution of resveratrol (200 mg, 0.88 mmol) in dry pyridine (0.5 mL), and the mixture was stirred at room temperature. After 40 min, a white solid was precipitated with ice-cold water. The precipitate was then filtered to afford 233.6 mg of the desired product (75% yield). ^{1}H-NMR (250 MHz, DMSO-d_6) δ (ppm): 2.28 (m, 9H, OAc), 6.90 (t, 1H, H-4), 7.12-7.38 (m, 6H, H-3', H-5', H-2, H-6, H-7, H-8); 7.62 (d, 2H, H-2', H-6', J=8.8 Hz). ^{13}C-NMR (62.9 MHz, DMSO-d_6) δ (ppm): 20.75, 20.79, 114.93, 117.09, 122.14, 126.70, 127.63, 129.44, 134.16, 139.29, 150.16, 151.12, 168.93, 169.10. ESI-MS (ion trap): m/z 355, $[M+H]^+$.

mPEG$_{1900}$-resveratrol (RmPEG). DMAP (21.4 mg, 0.17 mmol, 2 eq), DCC (180.7 mg, 0.88 mmol, 10 eq) and resveratrol (20 mg, 0.09 mmol, previously dissolved in 100 mL DMF) were added to a solution of mPEG$_{1900}$-COOH (1 g, 0.51 mmol, 5.8 eq) in CH_2Cl_2 (1 mL). The mixture was stirred at room temperature in the dark for 2 days. The suspension was then filtered and a white solid was precipitated from the liquid phase with diethyl ether (15 mL). The solvent was decanted and the precipitation procedure repeated 3 more times. The precipitate was then dried and purified by gel filtration (Sephadex G-25 superfine, GE Healthcare) using water as eluent to afford 407 mg of product (40% yield). HPLC-UV analysis (see below) showed no free resveratrol in the final product, which consisted of mono-, di- and tri-PEGylated resveratrol in an approximately 1:8:1 ratio. The overall PEG:resveratrol molar ratio was about 2 as determined through UV-Vis spectrometric analysis of 3 different solutions of known concentration (w/v) of the product. In these assays the resveratrol content in the solutions was determined by a calibration curve obtained by plotting the absorbance at 300 nm against resveratrol concentration. The PEG concentration was assessed by the iodine assay [55] using a calibration curve obtained by plotting the absorbance at 535 nm against PEG concentration in the range 2-5 mg/mL ($y=0.0664x+0.001$, $R^2=0.99$).

3,4',5-trimesyl-resveratrol (RTM). Methanesulfonyl chloride (2 mL, 25.8 mmol, 5.9 eq) was added to a solution of resveratrol (1 g, 4.38 mmol, 1 eq) in dry pyridine (5 mL). After stirring 3 h at 100 °C, the mixture was diluted in EtOAc (150 mL) and washed with 1 M HCl (3×100 mL). The organic layer was dried over $MgSO_4$ and filtered. The solvent was finally evaporated under reduced pressure, and the residue purified by flash chromatography using 8:1:1 CH_2Cl_2:petroleum ether:EtOAc v/v ratio as eluent, to afford 1.05 g of the desired product (88%, white solid). ^{1}H-NMR (250 MHz, DMSO-d_6) δ (ppm): 3.41 (s, 3H, OCH_3), 3.49 (s, 6H, OCH_3), 7.32-7.53 (m, 5H, H-4, H-3', H-5', H-7, H-8); 7.65 (d, 2H, H-2, H-6, J=2.5 Hz), 7.75 (d, 2H, H-2', H-6', J=7.5 Hz). ^{13}C-NMR (62.9 MHz, DMSO-d_6) δ (ppm): 37.39, 37.56, 115.53, 119.05, 122.56, 126.96, 128.32, 130.27, 135.45, 140.42, 148.74, 149.68. ESI-MS (ion trap): m/z 463, $[M+H]^+$.

Solubility in water. Calibration curves were built by plotting absorbance at 320 nm *vs* concentration for seven standard resveratrol solutions in the 10^{-6} - 10^{-4} M range, prepared from a 10^{-3} M mother solution in CH_3CN by dilution with 9:1 water:CH_3CN v/v ratio. Aqueous saturated solutions were prepared by vigorous stirring and sonication of 4, 2, 1, 0.5 or 0.25 mg of the compound in 1 mL of water. The resulting suspensions were then centrifuged (14000*g*, 30 min) and the clear supernatant was transferred into a cuvette and absorbance was measured at 320 nm. The concentration of aqueous saturated solutions of the derivatives was determined by interpolation (N = 5). The presence of significant amounts of colloidal particles could be excluded because similar absorbance readings were obtained starting with different amounts of undissolved material. The concentration of colloids would be expected to be a function of the latter parameter. Absorbance values remained similar (after correcting for dilution) also after the addition of 10% CH_3CN to the final solution to insure solubilisation of all organic material.

Stability in gastric and intestinal environment. The chemical stability of the compounds was tested in aqueous media mimicking gastric (0.1 N HCl) and intestinal environment (0.1 M PBS buffer, pH 6.8). A 20 mM solution of compounds, made diluting stock solutions in DMSO, was incubated at 37°C for 6 hours. Samples were withdrawn at different reaction times and analyzed by HPLC-UV (see below).

Stability in blood. Heparinized, EDTA-supplemented blood samples (1 mL) were spiked with 5 mM compound and incubated at 37°C for 1 hour. An internal standard was then added and the samples were extracted with organic solvents. The extracts were analyzed by HPLC-UV (see below).

Permeation studies. Intestine was excised from 18 h fasted rats and transferred into a saline solution (154 mM NaCl in water) at 37°C. The jejunum was cut into 1 cm long strips, opened longitudinally, rinsed free of luminal content and mounted in Ussing-type chambers. Apical and basolateral compartments were filled with 1 mL of oxygenated Hepes buffer each (248 mM NaCl, 55.3 mM Glucose, 50 mM $NaHCO_3$, 9.9 mM KCl, 1.9 mM $MgSO_4$, 40 mM Hepes, pH 6.8), and incubated in a water bath at 37°C until all chambers were assembled. The buffer was then removed and substituted with 1 mL of a 20 mM solution of the compound to be tested in the same buffer on the apical side (dilution from a 0.2 mM stock solution in DMSO, 10% final DMSO), and with 1 mL of fresh Hepes buffer plus 10% DMSO on the basolateral one. In the controls, only Hepes buffer plus 10% DMSO was present on both sides. This relatively high content of DMSO was necessary to insure solubility of the sulfonate derivative, and was thus used in all three cases to allow a proper comparison. During the experiment, oxygen was continuously bubbled in each basolateral compartment. An aliquot of the initial apical solutions was incubated separately at 37°C for the period of the experiment, to verify the stability of each compound in the absence of jejunum. At the end of the experiment (2.5 h) 800 mL of chamber contents on both apical and basolateral sides were collected and mixed with 8 mL of 100 mM ascorbic acid in water and 8 mL of 6 M acetic acid. All samples were frozen and maintained at -20°C until HPLC-UV analysis as described below.

The experiments were performed with the permission and supervision of the University of Padova Central Veterinary Service, which acts as Institutional Animal Care and Use Committee and certifies compliance with Italian Law DL 116/92, embodying UE Directive 86/609.

HPLC-UV analysis. Samples (20 mL) were analyzed using a reversed-phase column (Synergi-MAX, 4 μm, 150 x 4.6 mm i.d.; Phenomenex). Solvents A and B were 0.1% TFA supplemented H_2O and CH_3CN, respectively. The gradient for B was as follows: 10% for 2 min, from 10% to 35% in 20 min, then from 35% to 100% in 20 min; the flow rate was 1 mL/min. The eluate was monitored at 320 nm. Since absorption coefficients e_{320} of resveratrol and resveratrol derivatives are very similar, for quantification purposes we assumed the same absorption coefficient e_{320} of resveratrol also for hydrolysis products and resveratrol metabolites. Results were expressed as percentages, where the total amounts of recovered compounds represent 100%.

LC-ESI/MS analysis. Before LC-MS analysis, samples were further concentrated under vacuum (about 10 ×) and analyzed using the same column, solvents and gradient profile

used for HPLC-UV analyses. LC-ESI/MS analyses and mass spectra were performed with a 1100 Series Agilent Technologies system, equipped with binary pump (G1312A) and MSD SL Trap mass spectrometer (G2445D SL) with ESI source operating in full-scan mode in both positive and negative ion mode.

Statistics. Data are presented as means ± standard deviation. Experiments were performed at least in triplicate. Statistical data analyses were performed using Student's t-test with $p < 0.1$ as a minimal level of significance, using the software Origin 7.5 (OriginLab, Northampton, MA, USA).

Bibliography

[1] Leifert WR, Abeywardena MY: Cardioprotective action of grape polyphenols. Nutr Res 2008;28:729-737.
[2] Spencer JP: Food for thought: the role of dietary flavonoids in enhancing human memory, learning and neuro-cognitive performance. Proc Nutr Soc 2008;67:238-252.
[3] Singh M, Arseneault M, Sanderson T, Murthy V, Ramassamy C: Challenges for research on polyphenols from foods in Alzheimer's disease: bioavailability, metabolism, and cellular and molecular mechanisms. J Agric Food Chem 2008;56:4855-4873.
[4] Ramos S: Cancer chemoprevention and chemotherapy: dietary polyphenols and signalling pathways. Mol Nutr Food Res 2008;52:507-526.
[5] Yang CS, Lambert JD, Sang S: Antioxidative and anti-carcinogenic activities of tea polyphenols. Arch Toxicol 2009;83:11-21.
[6] Darra E, Shoji K, Mariotto S, Suzuki H: Protective effect of epigallocatechin-3-gallate on ischemia/reperfusion-induced injuries in the heart: STAT1 silencing flavonoid. Genes Nutr 2007;2:307-310.
[7] Ramassamy C: Emerging role of polyphenolic compounds in the treatment of neurodegenerative diseases: a review of their intracellular targets. Eur J Pharmacol 2006;545:51-64.
[8] Harikumar KB, Aggarwal BB: Resveratrol: a multitargeted agent for age-associated chronic diseases. Cell Cycle 2008;7:1020-1035.
[9] Baur JA, Sinclair DA: Therapeutic potential of resveratrol: the in vivo evidence. Nat Rev Drug Discov 2006;5:493-506.
[10] Pervaiz S, Holme AL: Resveratrol: Its Biological Targets and Functional Activity. Antioxid Redox Signal DOI: 10.1089/ARS.2008.2412.
[11] Shakibaei M, Harikumar KB, Aggarwal BB: Resveratrol addiction: to die or not to die. Mol Nutr Food Res 2009;53:115-128.
[12] Illek B, Fischer H: Flavonoids stimulate Cl conductance of human airway epithelium in vitro and in vivo. Am J Physiol 1998;275:L902-L910.
[13] Szewczuk LM, Forti L, Stivala LA, Penning TM: Resveratrol is a peroxidase-mediated inactivator of COX-1 but not COX-2: a mechanistic approach to the design of COX-1 selective agents. J Biol Chem 2004;279:22727-22737.
[14] Narayanan BA: Chemopreventive agents alters global gene expression pattern: predicting their mode of action and targets. Curr Cancer Drug Targets 2006;6:711-727.
[15] Umeda D, Yano S, Yamada K, Tachibana H: Green tea polyphenol epigallocatechin-3-gallate signaling pathway through 67-kDa laminin receptor. J Biol Chem 2008;283:3050-3058.

[16] Al-Fayez M, Cai H, Tunstall R, Steward WP, Gescher AJ: Differential modulation of cyclooxygenase-mediated prostaglandin production by the putative cancer chemopreventive flavonoids tricin, apigenin and quercetin. Cancer Chemother Pharmacol 2006;58:816-825.
[17] Kundu JK, Shin YK, Kim SH, Surh YJ: Resveratrol inhibits phorbol ester-induced expression of COX-2 and activation of NF-kappaB in mouse skin by blocking IkappaB kinase activity. Carcinogenesis 2006;27:1465-1474.
[18] Kroon PA, Clifford MN, Crozier A, Day AJ, Donovan JL, Manach C, Williamson G: How should we assess the effects of exposure to dietary polyphenols in vitro? Am J Clin Nutr 2004;80:15-21.
[19] Manach C, Williamson G, Morand C, Scalbert A, Rémésy C: Bioavailability and bioefficacy of polyphenols in humans. I. Review of 97 bioavailability studies. Am J Clin Nutr 2005;81(1 Suppl):230S-242S.
[20] Yang CS, Sang S, Lambert JD, Lee MJ: Bioavailability issues in studying the health effects of plant polyphenolic compounds. Mol Nutr Food Res 2008;52 Suppl 1:S139-S151.
[21] Walle T: Absorption and metabolism of flavonoids. Free Rad Biol Med 2004;36:829-837.
[22] Passamonti S, Terdoslavich M, Franca R, Vanzo A, Tramer F, Braidot E, Petrussa E, Vianello A: Bioavailability of flavonoids: a review of their membrane transport and the function of bilitranslocase in animal and plant organs. Curr Drug Metab 2009;10:369-394.
[23] Wenzel E, Somoza V: Metabolism and bioavailability of trans-resveratrol. Mol Nutr Food Res 2005;49:472-481.
[24] Maier-Salamon A, Hagenauer B, Reznicek G, Szekeres T, Thalhammer T, Jäger W: Metabolism and disposition of resveratrol in the isolated perfused rat liver: role of Mrp2 in the biliary excretion of glucuronides. J Pharm Sci 2008;97:1615-1628.
[25] Burkon A, Somoza V: Quantification of free and protein-bound trans-resveratrol metabolites and identification of trans-resveratrol-C/O-conjugated diglucuronides - two novel resveratrol metabolites in human plasma. Mol Nutr Food Res 2008;52:549-557.
[26] Day AJ, Bao Y, Morgan MR, Williamson G: Conjugation position of quercetin glucuronides and effect on biological activity. Free Radic Biol Med 2000;29:1234-1243.
[27] de Pascual-Teresa S, Johnston KL, DuPont MS, O'Leary KA, Needs PW, Morgan LM, Clifford MN, Bao Y, Williamson G: Quercetin metabolites downregulate cyclooxygenase-2 transcription in human lymphocytes ex vivo but not in vivo. J Nutr 2004;134:552-557.
[28] Mochizuki M, Kajiya K, Terao J, Kaji K, Kumazawa S, Nakayama T, Shimoi K: Effect of quercetin conjugates on vascular permeability and expression of adhesion molecules. Biofactors 2004;22:201-204.
[29] Donnini S, Finetti F, Lusini L, Morbidelli L, Cheynier V, Barron D, Williamson G, Waltenberger J, Ziche M: Divergent effects of quercetin conjugates on angiogenesis. Br J Nutr 2006;95:1016-1023.
[30] Lambert JD, Sang S, Yang CS: Biotransformation of green tea polyphenols and the biological activities of those metabolites. Mol Pharm 2007;4:819-825.
[31] Lodi F, Jiménez R, Menendez C, Needs PW, Duarte J, Perez-Vizcaino F: Glucuronidated metabolites of the flavonoid quercetin do not auto-oxidise, do not generate free radicals and do not decrease nitric oxide bioavailability. Planta Med 2008;74:741-746.
[32] Loke WM, Proudfoot JM, Stewart S, McKinley AJ, Needs PW, Kroon PA, Hodgson JM, Croft KD: Metabolic transformation has a profound effect on anti-inflammatory activity of flavonoids such as quercetin: lack of association between antioxidant and lipoxygenase inhibitory activity. Biochem Pharmacol 2008;75:1045-1053.

[33] Murias M, Miksits M, Aust S, Spatzenegger M, Thalhammer T, Szekeres T, Jaeger W: Metabolism of resveratrol in breast cancer cell lines: impact of sulfotransferase 1A1 expression on cell growth inhibition. Cancer Lett 2008;261:172-182.
[34] Winterbone MS, Tribolo S, Needs PW, Kroon PA, Hughes DA: Physiologically relevant metabolites of quercetin have no effect on adhesion molecule or chemokine expression in human vascular smooth muscle cells. Atherosclerosis 2009;202:431-438.
[35] Murias M, Handler N, Erker T, Pleban K, Ecker G, Saiko P, Szekeres T, Jäger W: Resveratrol analogues as selective cyclooxygenase-2 inhibitors: synthesis and structure-activity relationship. Bioorg Med Chem 2004;12:5571-5578.
[36] Murias M, Jäger W, Handler N, Erker T, Horvath Z, Szekeres T, Nohl H, Gille L: Antioxidant, prooxidant and cytotoxic activity of hydroxylated resveratrol analogues: structure-activity relationship. Biochem Pharmacol 2005;69:903-912.
[37] Minutolo F, Sala G, Bagnacani A, Bertini S, Carboni I, Placanica G, Prota G, Rapposelli S, Sacchi N, Macchia M, Ghidoni R: Synthesis of a resveratrol analogue with high ceramide-mediated proapoptotic activity on human breast cancer cells. J Med Chem 2005;48:6783-6786.
[38] Murias M, Luczak MW, Niepsuj A, Krajka-Kuzniak V, Zielinska-Przyjemska M, Jagodzinski PP, Jäger W, Szekeres T, Jodynis-Liebert J: Cytotoxic activity of 3,3',4,4',5,5'-hexahydroxystilbene against breast cancer cells is mediated by induction of p53 and downregulation of mitochondrial superoxide dismutase. Toxicol In Vitro 2008;22:1361-1370.
[39] Lee KW, Kang NJ, Rogozin EA, Oh SM, Heo YS, Pugliese A, Bode AM, Lee HJ, Dong Z: The resveratrol analogue 3,5,3',4',5'-pentahydroxy-trans-stilbene inhibits cell transformation via MEK. Int J Cancer 2008;123:2487-2496.
[40] Meng XL, Yang JY, Chen GL, Zhang LJ, Wang LH, Li J, Wang JM, Wu CF: RV09, a novel resveratrol analogue, inhibits NO and TNF-alpha production by LPS-activated microglia. Int Immunopharmacol 2008;8:1074-1082.
[41] Gosslau A, Pabbaraja S, Knapp S, Chen KY: Trans- and cis-stilbene polyphenols induced rapid perinuclear mitochondrial clustering and p53-independent apoptosis in cancer cells but not normal cells. Eur J Pharmacol 2008;587:25-34.
[42] Bernhaus A, Ozsvar-Kozma M, Saiko P, Jaschke M, Lackner A, Grusch M, Horvath Z, Madlener S, Krupitza G, Handler N, Erker T, Jaeger W, Fritzer-Szekeres M, Szekeres T: Antitumor effects of KITC, a new resveratrol derivative, in AsPC-1 and BxPC-3 human pancreatic carcinoma cells. Invest New Drugs 2009; in press (DOI: 10.1007/s10637-008-9183-7).
[43] Jung JC, Lim E, Lee Y, Kang JM, Kim H, Jang S, Oh S, Jung M: Synthesis of novel trans-stilbene derivatives and evaluation of their potent antioxidant and neuroprotective effects. Eur J Med Chem 2009;44:3166-3174.
[44] Fan GJ, Liu XD, Qian YP, Shang YJ, Li XZ, Dai F, Fang JG, Jin XL, Zhou B: 4,4'-Dihydroxy-trans-stilbene, a resveratrol analogue, exhibited enhanced antioxidant activity and cytotoxicity. Bioorg Med Chem 2009;17:2360-2365.
[45] Guha P, Dey A, Sarkar B, Dhyani MV, Chattopadhyay S, Bandyopadhyay SK: Improved antiulcer and anticancer properties of a trans-resveratrol analog in mice. J Pharmacol Exp Ther 2009;328:829-838.
[46] Marel AK, Lizard G, Izard JC, Latruffe N, Delmas D: Inhibitory effects of trans-resveratrol analogs molecules on the proliferation and the cell cycle progression of human colon tumoral cells. Mol Nutr Food Res 2008;52:538-548.
[47] Veronese FM, Mero A: The impact of PEGylation on biological therapies. BioDrugs 2008;22:315-329.
[48] Jain A, Jain SK: PEGylation: an approach for drug delivery. A review. Crit Rev Ther Drug Carrier Syst 2008;25:403-447.

[49] Bailon P, Won CY: PEG-modified biopharmaceuticals. Expert Opin Drug Deliv 2009;6:1-16.
[50] Matsumoto M, Matsukawa N, Mineo H, Chiji H, Hara H: A soluble flavonoid-glycoside, alphaG-rutin, is absorbed as glycosides in the isolated gastric and intestinal mucosa. Biosci Biotechnol Biochem 2004;68:1929-1934.
[51] Day AJ, Gee JM, DuPont MS, Johnson IT, Williamson G: Absorption of quercetin-3-glucoside and quercetin-4'-glucoside in the rat small intestine: the role of lactase phlorizin hydrolase and the sodium-dependent glucose transporter. Biochem Pharmacol 2003;65:1199-1206.
[52] Gee JM, DuPont MS, Day AJ, Plumb GW, Williamson G, Johnson IT: Intestinal transport of quercetin glycosides in rats involves both deglycosylation and interaction with the hexose transport pathway. J Nutr 2000;130:2765-2771.
[53] Sartore L, Caliceti P, Schiavon O, Veronese FM: Enzyme modification by MPEG with an amino acid or peptide as spacer arms. Appl Biochem Biotechnol 1991;27:45-54.
[54] Wenzel E, Soldo T, Erbersdobler H, Somoza V: Bioactivity and metabolism of trans-resveratrol orally administered to Wistar rats. Mol Nutr Food Res 2005;49:482-494.
[55] Sims GE, Snape TJ: A method for estimation of poly(ethylene glycol) in plasma protein fractions. Anal Biochem 1980;107:60–63.
[56] Biasutto L, Marotta E, De Marchi U, Zoratti M, Paradisi C: Ester-based precursors to increase the bioavailability of quercetin. J Med Chem 2007;50:241-253.
[57] Mulholland PJ, Ferry DR, Anderson D, Hussain SA, Young AM, Cook JE, Hodgkin E, Seymour LW, Kerr DJ: Pre-clinical and clinical study of QC12, a water-soluble, pro-drug of quercetin. Ann Oncol 2001;12:245-248.
[58] Montenegro L, Carbone C, Maniscalco C, Lambusta D, Nicolosi G, Ventura CA, Puglisi G: In vitro evaluation of quercetin-3-O-acyl esters as topical prodrugs. Int J Pharm 2007;336:257-262.
[59] Kuhn D, Lam WH, Kazi A, Daniel KG, Song S, Chow LM, Chan TH, Dou QP: Synthetic peracetate tea polyphenols as potent proteasome inhibitors and apoptosis inducers in human cancer cells. Front Biosci 2005;10:1010-1023.
[60] Lee SC, Chan WK, Lee TW, Lam WH, Wang X, Chan TH, Wong YC: Effect of a prodrug of the green tea polyphenol (-)-epigallocatechin-3-gallate on the growth of androgen-independent prostate cancer in vivo. Nutr Cancer 2008;60:483-491.
[61] Hirpara KV, Aggarwal P, Mukherjee AJ, Joshi N, Burman AC: Quercetin and its derivatives: synthesis, pharmacological uses with special emphasis on anti-tumor properties and prodrug with enhanced bio-availability. Anticancer Agents Med Chem 2009;9:138-161.
[62] Landis-Piwowar KR, Huo C, Chen D, Milacic V, Shi G, Chan TH, Dou QP: A novel prodrug of the green tea polyphenol (-)-epigallocatechin-3-gallate as a potential anticancer agent. Cancer Res 2007;67:4303-4310.
[63] Riley T, Riggs-Sauthier J: The Benefits and Challenges of PEGylating Small Molecules. Pharm Tech 2008;32:88-94.
[64] Gursahani H, Riggs-Sauthier J, Pfeiffer J, Lechuga-Ballesteros D, Fishburn CS: Absorption of polyethylene glycol (PEG) polymers. The effect of PEG size on permeability. J Pharm Sci 2009;98:2957-2856.
[65] Ashada H, Douen T, Mizokoshi Y, Fujita T, Murakami M, Yamamoto A, Muranishi S: Absorption characteristics of chemically modified insulin derivatives with various fatty acids in the small and large intestine. J Pharm Sci 1995;84:682–687.
[66] Lançon A, Delma D, Osman H, Thénot JP, Jannin B, Latruffe N: Human hepatic cell uptake of resveratrol: involvement of both passive diffusion and carrier-mediated process. Biochem Biophys Res Comm 2004;316:1132-1137.

[67] Kaldas MI, Walle UK, Walle T: Resveratrol transport and metabolism by human intestinal Caco-2 cells. J Pharm Pharmacol 2003;55:307-312.
[68] Henry C, Vitrac X, Decendit A, Ennamany R, Krisa S, Mérillon JM: Cellular uptake and efflux of trans-piceid and its aglycone trans-resveratrol on the apical membrane of human intestinal Caco-2 cells. J Agric Food Chem 2005;53:798-803.
[69] Torres-Lugo M, Santos-Román N, Méndez J, Licha M: Poly(Ethylene Glycol) Hydrogels as Possible Multidrug Resistance Associated Protein (MRP) Inhibitors. Proceedings of the 29th Annual International Conference of the IEEE EMBS Cité Internationale, Lyon, France, August 23-26, 2007.
[70] Werle M: Polymeric and Low Molecular Mass Efflux Pump Inhibitors for Oral Drug Delivery. J Pharm Sci 2008;97:60-70.
[71] Walle T, Wen X, Walle UK: Improving metabolic stability of cancer chemoprotective polyphenols. Expert Opin Drug Metab Toxicol 2007;3:379-388.
[72] Pan MH, Gao JH, Lai CS, Wang YJ, Chen WM, Lo CY, Wang M, Dushenkov S, Ho CT: Antitumor activity of 3,5,4'-trimethoxystilbene in COLO 205 cells and xenografts in SCID mice. Mol Carcinog 2008;47:184-196.

Chapter 8

Soluble polyphenols: synthesis and bioavailability of 3,4',5-tri(α-D-glucose-3-O-succinyl) resveratrol[8]

Summary

We report the development of a chemical modification method of general applicability to polyphenols, which increases solubility to influence absorption. Glucosyl groups were added to the resveratrol kernel via a succinate linker, yielding 3,4',5-tri-(α-D-glucose-3-O-succinyl) resveratrol. The construct was only slowly hydrolysed in acid and at pH 6.8, but it was destroyed by blood esterases in less than one hour. In rats its administration resulted in a blood concentration vs. time curve shifted to longer times in comparison to resveratrol, a useful modulation of pharmacokinetics. The area-under-curve parameter and the metabolite mix were similar to those of resveratrol. The method may be advantageously employed to solubilise other polyphenols and to make them more palatable.

Introduction

Optimization of bioavailability is fundamental for the full realization of the biomedical potential of nutraceuticals such as plant polyphenols. The research efforts of dozens of groups worldwide have proven that many polyphenols possess potentially very useful biochemical properties [1], offering promise for the fight against aging, cancer, cardiovascular diseases and chronic inflammation. The promise however is only partially fulfilled: polyphenols are poorly absorbed and are present in the circulatory streams at very low levels, mostly as conjugates produced by phase II metabolism in the intestinal enterocytes and in the liver. Solubility is recognized as a key factor for bioaccessibility and thus bioavailability [2]. The problems and approaches to the improvement of the bioavailability of antioxidants and polyphenols via formulations and modifications have been reviewed [3].

The generally low solubility of polyphenol aglycones can be attributed largely to a tendency to form aggregates via hydrophobic interaction of the aromatic systems and

[8] Published as: Biasutto L., Marotta E., Bradaschia A., Fallica M., Mattarei A., Garbisa S., Zoratti M., Paradisi C. *Bioorganic & Medicinal Chemistry Letters*, **2009**, 19, 6721-6724.

hydrogen-bond formation by the hydroxyls. In nature polyphenols occur mainly as glycosylated derivatives. The current paradigm describing the absorption of these compounds in the intestine is that they are first deglycosylated at the intestinal wall, and then enter the cell by diffusion or via transport by carriers [4]. The presence of glycosyl groups may nonetheless improve bioavailability by influencing phenomena taking place upstream of entry into enterocytes. A well-studied case is that of quercetin and its 3-O-glycosides [5]. Kinetics and extent of absorption by rats depend strongly not only on the presence, but also on the identity of the sugar group, with uptake being most efficient for the most soluble derivatives. Following nature's lead, as a proof of principle we linked a prototypical glycosyl group, glucose, to a model polyphenol, resveratrol (**1**), via succinic acid.

Results

Synthetic procedures were optimized using 4,4'-dihydroxybiphenyl as a model compound. The final optimized protocol was then successfully applied to resveratrol (Scheme 1).

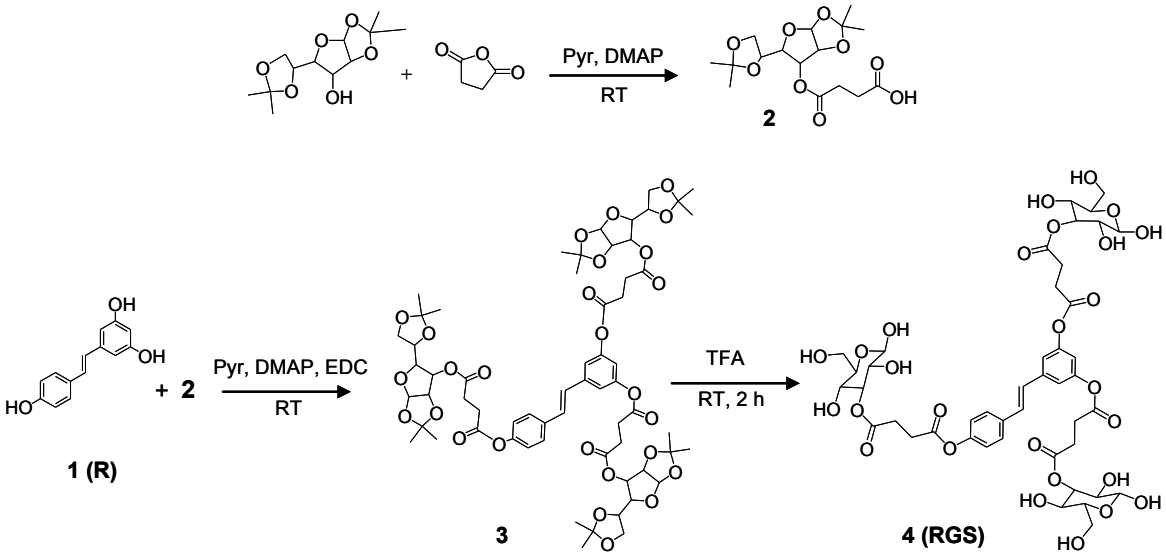

Scheme 1. Synthesis of 3, 4', 5-tri(α-D-glucose-3-O-succinyl)-resveratrol (RGS, **4**).

In the first step of the synthesis of a succinyl linker is attached to the 3-hydroxyl group of a glucose molecule used in a protected form (diacetone-D-glucose, DAG) to avoid reactions of the other hydroxyls, yielding diacetone-α-D-glucose-3-O-succinyl ester (**2**). Per-esterification of 4,4'-dihydroxybiphenyl or **1** to give 4, 4'-di(diacetone-α-D-glucose-3-O-succinyl)-biphenyl or 3,4',5-tri(diacetone-α-D-glucose-3-O-succinyl)-resveratrol (**3**), respectively, was then performed by activating the free carboxylic group of **2** with 1-ethyl-3-(3-dimethylaminopropyl) carbodiimide hydrochloride (EDC), using 4-N,N-

dimethylamino pyridine (DMAP) as catalyst. The final step consisted in the deprotection of the glucose hydroxyl groups with trifluoroacetic acid (TFA), affording 4,4'-di(α-D-glucose-3-O-succinyl)-biphenyl or 3,4',5-tri(α-D-glucose-3-O-succinyl)-resveratrol (**4**; RGS) respectively. The solubility of **4** in water at room temperature is at least 90 mg/mL (89 mM). The major resveratrol phase II metabolites were also synthesised according to published procedures [7] as described in the Materials and Methods. They were used as standards to identify metabolites.

RGS (**4**) underwent slow hydrolysis in 1N HCl (Fig. 1). After 6 h at 37°C, 80% of the starting material was still present as such, with the main product of hydrolysis being the di-substituted derivatives.

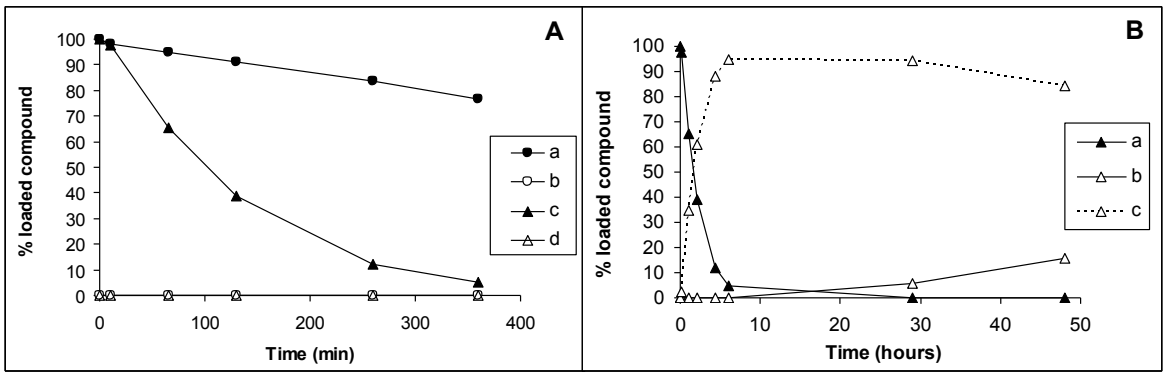

Figure 1. Stability of **4** in media mimicking gastric and intestinal environment (37°C). **A)** Over 6 hours: a) **4** and b) **1** in 1N HCl; c) **4** and d) **1** in PBS, pH 6.8. **B**) Over 48 hours: a) **4**, b) **1**, c) Mono- and di-(α-D-glucose-3-O-succinyl)-resveratrol in PBS, pH 6.8. Data are expressed as % of the initial molar amount used.

At pH 6.8 in phosphate-buffered saline (PBS) disappearance was faster. The process consisted in the loss of one entire glucose-O-succinyl moiety at a time. Loss of the first one was nearly complete after 6 hours, as showed by LC-MS analysis [8]. Formation of resveratrol was observed after 28 h. At no time were detectable amounts of products arising from the loss of glucose molecules formed.

In pharmacokinetics experiments (see Supporting data for the experimental procedures) individual variability is generally high. We therefore performed our experiments utilizing the same set of rats for the administration of both resveratrol and the new derivative **4**. The identity of the circulating species was confirmed by LC-MS analysis using standards and by enzymatic treatment (Fig 2).

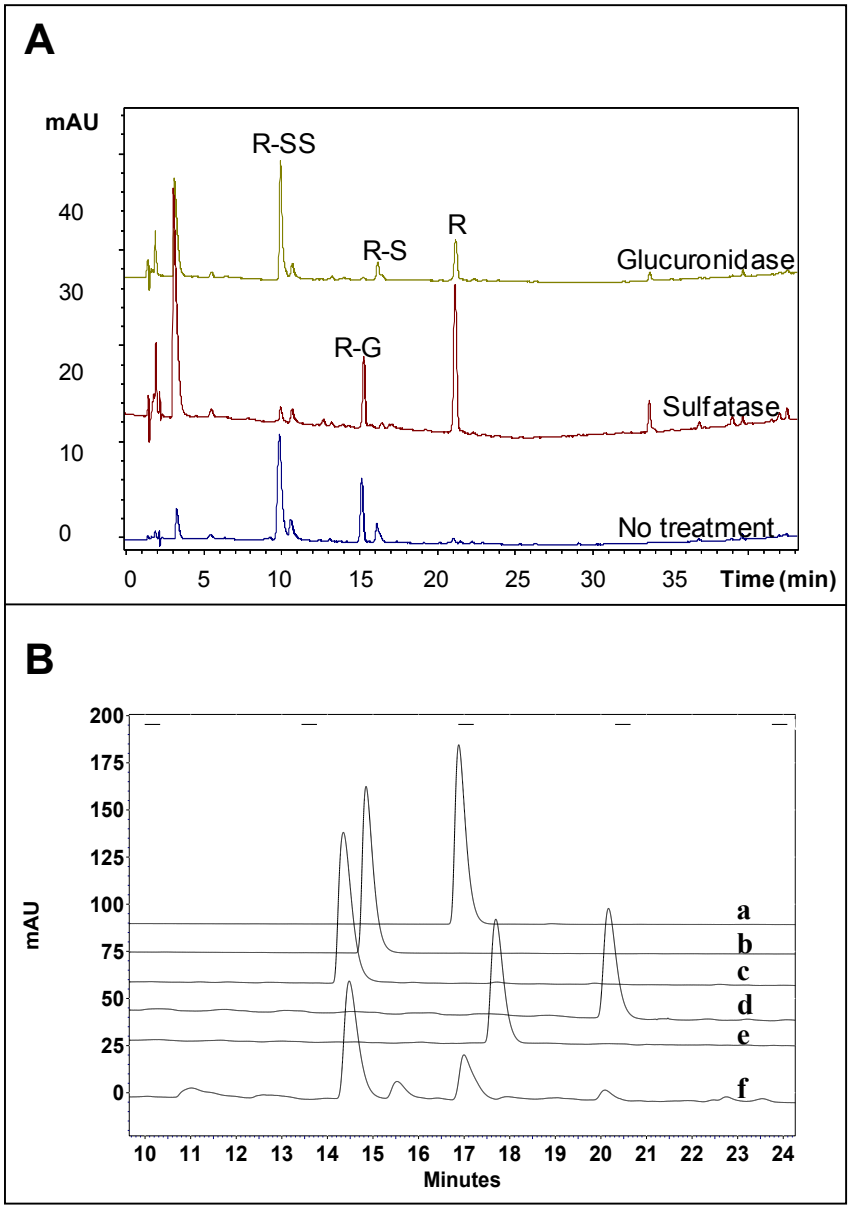

Fig. 2. Identification of resveratrol metabolites. **A)** HPLC-UV chromatograms (320 nm) of a blood sample withdrawn 4h after intragastric administration of **4**. The chromatograms were obtained from aliquots of the same sample: without any enzymatic treatment, and after treatment with sulfatase or with glucuronidase, as indicated. R-S: resveratrol-sulfate; R-G: resveratrol-glucuronide; R: resveratrol. **B)** Comparison between synthetic resveratrol conjugates and *in vivo* metabolites. HPLC chromatograms recorded at 320 nm of: a) R-3-glucuronide; b) R-4'-glucuronide; c) R-3,4'-disulfate; d) R-3-sulfate; e) R-4'-sulfate; f) rat blood sample collected 30 min after administration of 0.22 mmol/kg resveratrol.

In the case of resveratrol, blood analyses revealed relatively high amounts of resveratrol sulfate- and glucuronide-conjugates. In agreement with literature reports [9], C_{max} for the sum of all resveratrol-derived species (9.4 ± 8.5 μM) was reached at about 60 minutes after administration (Fig. 3A). The concentration vs. time curves of all metabolites followed the same pattern. Intact resveratrol appeared only at low levels (C_{max}: 1.2 ± 1.2 μM), and the corresponding peak earlier, at about 10 min. Administration of **4** resulted in a delayed

absorption, with the maximum concentration of total species in blood reached after approximately 4 hours (Fig. 3B).

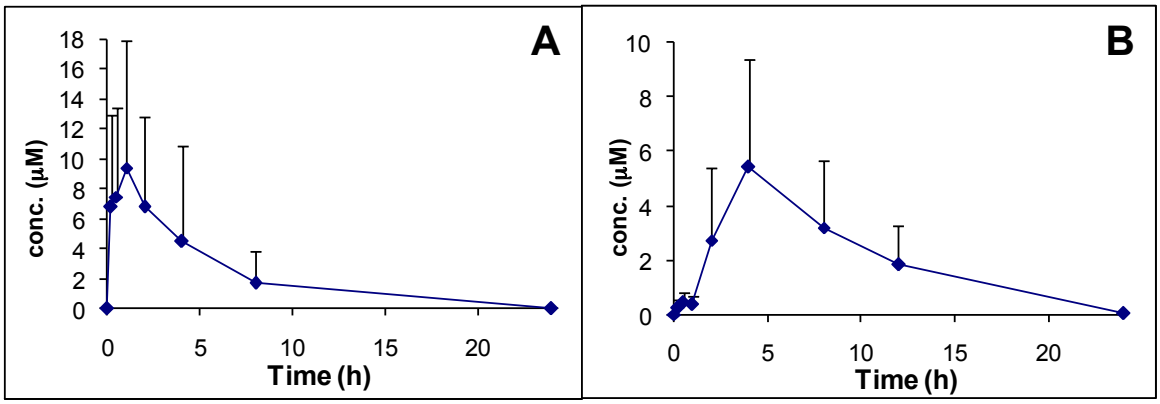

Figure 3. Pharmacokinetics of **A) 1** and **B) 4**. Mean values of total circulating species derived from the respective parent compounds (N = 3).

The overall C_{max} was 5.4 ± 4.0 μM. The species present in the bloodstream were also in this case resveratrol (at low levels) and mostly its metabolites, in proportions similar to those observed after administration of resveratrol itself (Fig. 4). When values of the area under concentration-time curves (AUC) are compared, no significant differences can be noted depending on whether resveratrol or **4** was administered. Similar results were obtained administering **4** as a water, rather than a DMSO, solution (not shown; N = 3).

Compound **4** is water-soluble and its stability vs. chemical hydrolysis is satisfactory. In particular, it is nearly stable in an acidic environment mimicking that of the stomach, so that it can be supposed to survive the gastric stage with only very limited destruction. Interestingly, hydrolysis of the succinate-resveratrol bond is much faster than that of the succinate-glucose bond, so that **4** is destroyed via successive losses of whole glucosylsuccinyl groups.

Administration of this solubilised form of resveratrol results in delayed absorption in comparison to the aglycone, without a significant difference in total absorption. Thus, administration of a proper mix of aglycone and derivative is expected to produce a prompt as well as long-lasting increase in circulating and body levels of the polyphenol and of its metabolites. The delay may be tentatively attributed to the time needed for complete hydrolysis of **4** to resveratrol in the intestinal tract, with the subsequent absorption of the resveratrol thus formed.

A

Circulating specie	AUC (μM * h)	
	Resveratrol	RGS
R	1,1 ± 1,1	0,2 ± 0,2
R-S	2,4 ± 1,7	3,5 ± 2,6
R-G	35,5 ± 36,9	21,2 ± 15,8
R-SS	14,4 ± 20,0	27,0 ± 18,7
Total	53,4 ± 57,7	51,8 ± 37,2

B

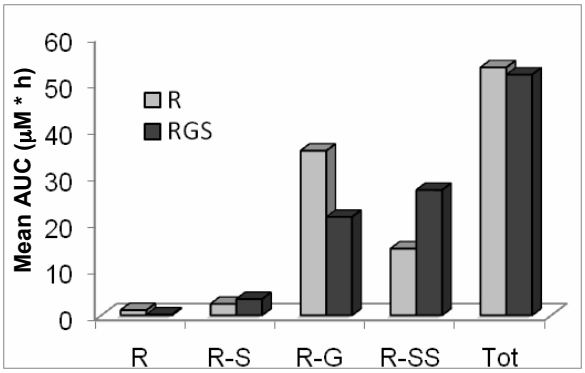

Figure 4. Mean AUC values for resveratrol and its main metabolites. The determinations were performed using three rats, each of which received both resveratrol and **4** with a 2-week interval. R: Resveratrol; R-S: Resveratrol sulfate; R-G: Resveratrol glucuronide; R-SS: Resveratrol disulfate. **A)** Error notations are standard deviations. **B)** Column plots of the data tabulated in A) (error notations omitted).

While polyphenols generally occur in nature as glycosylated derivatives, in many cases these products are not commercially available. Furthermore, monoglycosylation in some cases does not make the molecule soluble. For example rutin (quercetin-3-*O*-rutinoside, an abundant glycoside of quercetin) only dissolves at about 1 gram in 8 liters of water [10], i.e. about $2x10^{-4}$ M (2.3 grams/liter at pH 9 and decreasing with pH [11]). Quercitrin and genistin, common glucosides of quercetin and genistein respectively, have very low solubility in cold water [10]. The procedures described above provide a straightforward approach to soluble polyphenol prodrugs. Linkage to more than one sugar residue is expected to lead to products with higher water solubility. Bioavailability may be improved by optimizing the choice of the glycosyl component or by linkage to a polymeric soluble molecule. New synthetic polyphenols are beginning to be explored as drugs and they are certain to be affected by the same (or worse) bioavailability problems as the natural compounds. Modulating solubility may have an impact and it would facilitate administration.

Modification of OHs may have to do not only with bioavailability, but also with complex formation with salivary proteins in the mouth. Sensations of bitterness and astringency are often associated with these compounds and in particular with their polymers [12], but they would not be expected to be induced by derivatives with "capped" hydroxyls. The other components forming RGS, succinic acid and glucose, are molecules already abundant and ubiquitous in the body, and thus certainly safe or beneficial as nutrients. Therefore, this type of molecules may find relevant technological applications in the food industry, such as, in the formulation of fortifying ingredients and supplements.

Experimental section

Materials and Methods

Materials and instrumentation. Resveratrol was purchased from Waseta Int. Trading Co. (Shangai, P.R.China). Other starting materials and reagents were purchased from Aldrich, Fluka, Merck-Novabiochem, Riedel de Haen, J.T. Baker, Cambridge Isotope Laboratories Inc., Acros Organics, Carlo Erba and Prolabo, and were used as received. ^{1}H NMR spectra were recorded with a Bruker AC 250F spectrometer operating at 250 MHz. Chemical shifts (δ) are given in ppm relative to the signal of the solvent. HPLC-UV analyses were performed by a Thermo Separation Products Inc. system with a P2000 Spectra System pump and a UV6000LP diode array detector (190-500 nm). LC-ESI/MS analyses and mass spectra were performed with a 1100 Series Agilent Technologies system, equipped with binary pump (G1312A) and MSD SL Trap mass spectrometer (G2445D SL) with ESI source. TLCs were run on silica gel supported on plastic (Macherey-Nagel Polygram®SIL G/UV$_{254}$, silica thickness 0.2 mm), or on silica gel supported on glass (Fluka) (silica thickness 0.25 mm, granulometry 60Å, medium porosity) and visualized by UV detection. Flash chromatography was performed on silica gel (Macherey-Nagel 60, 230-400 mesh granulometry (0.063-0.040 mm)) under air pressure. The solvents were analytical or synthetic grade and were used without further purification.

Stability under gastric and intestinal-like conditions. The chemical stability of **4** was tested in aqueous media mimicking gastric (0.1 N HCl) and intestinal (PBS buffer 0.1 M, pH 6.8) environment. A 50 μM solution of the compound was made diluting a 1000× stock solution in DMSO, and incubated at 37°C for 48 hours; samples withdrawn at different times were analyzed by HPLC-UV. Hydrolysis products were identified by LC-MS analysis of selected samples.

Stability in blood. Rats were anesthetized and blood was withdrawn from the jugular vein, heparinized and transferred to tubes containing EDTA. Blood samples (1 mL) were spiked with 5 μM of compound (dilution from a 1000× stock solution in DMSO), incubated at 37°C for 1 hour and then treated as described below. Cleared blood samples were finally subjected to HPLC-UV analysis.

HPLC-UV analysis. Samples (20 μl) were analyzed using a reversed phase column (Synergi-MAX, 4 μm, 150 x 4.6 mm i.d.; Phenomenex). Solvents A and B were H_2O containing 0.1% TFA and CH_3CN, respectively. The gradient for B was as follows: 10% for 2 min, from 10% to 35% in 20 min, then from 35% to 100% in 20 min; the flow rate was 1 mL/min. The eluate was preferentially monitored at 286, 300 and 320 nm.

Alternatively, a Gemini C18, 3 μm, 150 x 4.6 mm i.d.; Phenomenex column was used. In this case the gradient for B was as follows: 10% for 2 min, from 10% to 30% in 15 min, from 30% to 60% in 15 min, from 60% to 100% in 3 min; the flow rate was 0.7 mL/min.

LC-ESI/MS analysis. Samples (20 μl) were analyzed using the same column, solvents and gradient profile used for HPLC-UV analyses. MS analysis was performed with an ESI source operating in full-scan mode in both positive and negative ion mode. Before LC-MS analysis, samples were further concentrated under vacuum (about 10×).

Pharmacokinetics. Resveratrol or **4** were administered to overnight-fasted rats as a single intragastric dose (0.09 mmol/Kg, dissolved in 250 μl DMSO). Blood samples were obtained by the tail bleeding technique: before drug administration, rats were anesthetized with isoflurane and the tip of the tail was cut off; blood samples (80-100 μl each) were then taken from the tail tip at different time points after drug administration. Blood was collected in heparinized tubes, kept in ice and treated as described below within 20 min. A two-week recovery interval was obligatorily allowed between experiments utilising the same rat. The experiments were performed with the permission and supervision of the University of Padova Central Veterinary Service, which acts as Institutional Animal Care and Use Committee and certifies compliance with Italian Law DL 116/92, embodying UE Directive 86/609. The area under the concentration-time curves (AUC) were determined by the linear trapezoidal method.

Blood sample treatment and analysis. Before starting the treatment, 4,4'-dihydroxybiphenyl was added as internal standard (25 μM final concentration). Blood was then stabilized with a freshly-prepared 10 mM solution of ascorbic acid (0.1 vol) and acidified with 0.6 M acetic acid (0.1 vol); after mixing, an excess of acetone (4 vol) was added, followed by sonication (2 min) and centrifugation (10,000 *g*, 8 min, 4°C). The supernatant was finally collected (measuring its volume) and stored at -20°C. Before analysis, acetone was allowed to evaporate at room temperature under N_2 flow, and 30 μL of CH_3CN were added to precipitate residual proteins; after centrifugation, cleared samples were directly subjected to HPLC-UV analysis. Metabolites were identified by LC-MS analysis, enzymatic treatment on selected samples, and/or direct comparison with chromatograms of synthetic purified metabolites (main text, Fig. 2).

The recovery yield for resveratrol and the major metabolites was determined in a preliminary set of experiments using spiked blood samples. Internal standard recovery was 68.7 ± 6.3% (N = 7). The method was found to ensure a constant recovery ratio of the analytes to the internal standard: 1.18 ± 0.14 (N = 7), 0.90 ± 0.01 (N = 3), 0.64 ± 0.04 (N =

6) and 0.90 ± 0.02 (N = 3), for resveratrol and its 3,4'-disulfate, 3-glucuronide and 3-sulfate, respectively. Knowledge of these ratios allowed us to determine the unknown amount of analyte in a blood sample by measuring the recovery of the internal standard.

Enzymatic treatment (Fig. 2A). Selected samples (100 μl) were diluted with the same volume of PBS 0.1M, pH 7, and then incubated with sulfatase (*Aerobacter aerogenes*, 10-20 U/mL, Sigma-Aldrich, 25 μl) or glucuronidase (*E. Coli K12*, 140 U/mL, Roche, 25 μl) at 37°C for 30 min. Acetone (200 μl) was then added to stop the reaction; the mixture was centrifuged (12000*g*, 4°C, 5 min), and supernatants were collected and stored at -20°C until analysis. Acetone was evaporated under a flow of nitrogen, and the concentrated samples were injected into the HPLC-UV system. Comparison of the chromatographic profiles of treated and untreated samples allowed the attribution of peaks representing sulfated or glucuronated species.

Chromatographic comparison of synthetic conjugates with metabolites observed in vivo (Fig. 2B). Synthesized resveratrol conjugates were dissolved in a water:CH_3CN 7:3 (5 μM final concentration) and then analyzed as described above. A straightforward comparison of the chromatograms recorded at 320 nm allowed isomer-specific identification.

Synthesis of resveratrol sulfates. Synthesis was performed by a slight modification of the procedure reported in literature (Kawai, N.; Fujibayashi, Y.; Kuwabara, K.-I.; Ijuin, Y.; Kobayashi, S. *Tetrahedron* **2000**, *56*, 6467. Wenzel, E.; Soldo, T.; Erbersdobler, H.; Somoza, V. *Mol. Nutr. Food Res.* **2005**, *49*, 482). Briefly, **1** (1 g, 4.39 mmol) and sulfur trioxide pyridine complex (2.6 g, 16.35 mmol) were dissolved in dry pyridine (10 mL). After stirring under nitrogen for 2 h at 60°C, the mixture was purified by flash chromatography using first $CHCl_3$:MeOH 9:1 as eluent to eliminate pyridine. The trisulfate was not formed in detectable amounts. Mono- and di- sulfate isomers were separated by semi-preparative HPLC. Synthesis mixtures (about 20 mg/mL, dissolved in the starting mobile phase) were separated by injecting 100 μl samples in a semi-preparative HPLC column (Gemini C18, 5 μm, 250 x 10 i.d. mm). Solvents A and B were 50 mM Ammonium Acetate (pH 6.5) and CH_3CN, respectively. The gradient for B was as follows: 18% for 6 min, from 18% to 22% in 1 min, 22% for 10 min and then from 22% to 90% in 5 min. The two isomers were identified by ^{1}H-NMR.

Synthesis of resveratrol glucuronides. The published procedure (Brandolini, V.; Maietti, A.; Tedeschi, P.; Durini, E.; Vertuani, S.; Manfredini, S. *J. Agric. Food Chem*. **2002**, *50*, 7407. Wenzel, E.; Soldo, T.; Erbersdobler, H.; Somoza, V. *Mol. Nutr. Food Res.* **2005**, *49*, 482) was followed with some modification. **1** (2.28 g, 10 mmol), acetobromo-α-D-

glucuronic acid methyl ester (2 g, 6.3 mmol) and metallic Na (0.23 g, 1 mmol) were dissolved in methanol (MeOH; 30 mL). Sodium reacts immediately to produce resveratrol anion. After stirring for 2 h at room temperature, the solvent was evaporated and the mixture was diluted in ethylacetate (EtOAc) (20 mL) and then washed with 0.01 N HCl (5 x 50 mL). The organic layer was dried over $MgSO_4$ and filtered. The solvent was finally evaporated under reduced pressure and the residue was purified by flash chromatography on silica gel using $CHCl_3$:MeOH 95:5 as eluent to afford a mixture of two mono-aceto-α-D-glucuronide-methyl-esters (44%). No di- or tri-substitution products were obtained. The corresponding glucuronides were obtained incubating the product (1.8 g, 4.44 mmol) with NaOH 0.1 M (20 mL) and MeOH (20 mL). The mixture was stirred at reflux for 2 hours, and then diluted in EtOAc (20 mL) and washed with 0.01 N HCl (5 x 50 mL). The organic layer was dried over $MgSO_4$ and filtered. The solvent was finally evaporated under reduced pressure and the residue dissolved in MeOH (50 mL). 50 mL water were added, and the mixture was stirred with ion-exchange (H^+) Amberlist resin until pH 3 was reached. The resin was finally filtered off, and the solution dried under vacuum and purified by flash chromatography using EtOAc:MeOH 9:1 as eluent (78%). The two isomers were separated by semi-preparative HPLC as above; the gradient for B was as follows: 18% for 10 min, from 18% to 90% in 5 min, then 90% for 2 min. The two isomers were identified by ^{1}H-NMR.

Synthetic procedures.

Diacetone-α-D-glucose-3-O-succinyl ester (**2**). Synthesis was performed modifying a published procedure.[13] Briefly, DMAP (120 mg, 0.98 mmol, 0.26 eq) and succinic anhydride (1.6 g, 16 mmol, 4.2 eq) were added to a solution of DAG (1 g, 3.8 mmol) in dry pyridine (15 mL). After stirring for 20 h at room temperature, the mixture was diluted in $CHCl_3$ (30 mL) and washed with 0.5 N HCl (6 x 50 mL). The organic layer was dried over $MgSO_4$ and filtered. The solvent was finally evaporated under reduced pressure to afford 1.08 g of the desired product (78%). ^{1}H NMR (250 MHz, $CDCl_3$) δ (ppm) : 1.47,1.36,1.27 (s, 12H, CH_3); 2.64 (m, 4H, CH_2); 3.99 (m, 2H, CH-4, CH-5); 4.17 (m, 2H, CH-6); 4.45 (m, 1H, CH-2); 5.22 (d, 1H, CH-3); 5.82 (d, 1H, CH-1);10.7 (br, 1H, OH).

4, 4'-di(diacetone-α-D-glucose-3-O-succinyl)-biphenyl. DMAP (120 mg, 0.98 mmol, 1.3 eq), EDC (0.58 g, 3 mmol, 4 eq) and 4,4'-diidroxybiphenyl (**2**; 140 mg, 0.75 mmol) were added to a solution of **3** (1.08 g, 3 mmol, 4 eq) in dry pyridine (15 mL). After stirring for 24 h at room temperature, the mixture was diluted in $CHCl_3$ (30 mL) and washed with 0.5 N HCl (6 x 50 mL) and then with 5% $NaHCO_3$ (3 x 50 mL). The organic layer was dried

over $MgSO_4$ and filtered. The solvent was finally evaporated under reduced pressure, to afford 560 mg of the desired product (86%). ^{1}H-NMR (250 MHz, $CDCl_3$) δ (ppm) : 1.44,1.33,1.23 (s, 24H, CH_3); 2.72-2.84 (m, 8H, CH_2); 3.98 (m, 4H, CH-4, CH-5); 4.16 (m, 4H, CH-6); 4.45 (m, 2H, CH-2); 5.22 (m, 2H, CH-3); 5.79 (d, 2H, CH-1); 7.09 (m, 4H, H-3, H-5, H-3', H-5', $J_{3\text{-}2}$=8.1 Hz); 7.47 (m, 4H, H-2, H-6, H-2', H-6', $J_{2\text{-}3}$=8.1 Hz). MS-ESI (CH_3CN): m/z 893, $[M+Na]^+$.

4,4'-di(α-D-glucose-3-O-succinyl)-biphenyl. 4,4'-di(diacetone-α-D-glucose-3-O-succinyl)-biphenyl (150 mg, 0.17 mmol) was dissolved in 12 M TFA (3 mL). After stirring for 1.5 h at room temperature, the product was precipitated with diethyl ether (10 mL) 3 times, and the solvent decanted after each precipitation. The white solid was dried under vacuum and then dissolved in 3 mL water to hydrolyse trifluoroacetic esters at glucose hydroxyls. The solution was finally lyophilized to afford 98 mg of the desired product (81%). ^{1}H-NMR (250 MHz, DMSO-d_6) δ (ppm) : 2.73-2.8 (m, 8H, CH_2); 3.07-5.05 (m, CH_2 D-glucose); 7.21 (d, 4H, H-3, H-5, H-3', H-5', $J_{3\text{-}2}$=8.1 Hz); 7.69 (d, 4H, H-2, H-6, H-2', H-6', $J_{2\text{-}3}$=8.1 Hz). MS-ESI (CH_3CN): m/z 733, $[M+Na]^+$.

3,4',5-tri(diacetone-α-D-glucose-3-O-succinyl)-resveratrol (**3**). DMAP (120 mg, 0.98 mmol, 1.8 eq), EDC (0.58 g, 3 mmol, 5.7 eq) and **1** (120 mg, 0.53 mmol) were added to a solution of **3** (990 mg, 2.75 mmol, 5.2 eq) in dry pyridine (15 mL). After stirring for 24 h at room temperature, the mixture was diluted in $CHCl_3$ (30 mL) and washed with 0.5 N HCl (6 x 50 mL). The organic layer was dried over $MgSO_4$ and filtered. The solvent was finally evaporated under reduced pressure and the residue was purified by flash chromatography using ethylacetate/hexane 5:3 as eluent to afford 475 mg of the desired product (74%). ^{1}H-NMR (250 MHz, $CDCl_3$) δ (ppm) : 1.49,1.39,1.28 (s, 36H, CH_3); 2.77-2.9 (m, 12H, CH_2); 4.04-4.08 (m, 6H, CH-4,CH-5); 4.21 (m, 6H, CH-6); 4.5 (m, 3H, CH-2); 5.29 (m, 3H, CH-3); 5.85 (d, 3H, CH-1); 6.85 (t, 1H, H-4, J=2 Hz); 6.92-6.99 (d, 1H, H-7, J=16 Hz); 7.07-7.11 (d, 2H, H-5', H-3', J=8.6 Hz); 7.10 (d, 2H, H-2, H-6, J=2 Hz);7.49 (s, 2H, H-2', H-6', J=8.6 Hz). ^{1}H-NMR (250 MHz, DMSO-d_6) δ (ppm) : 1.39,1.27,1.19,1.18 (s, 36H, CH_3); 2.7-2.85 (m, 12H, CH_2); 3.8-3.9 (m, 6H, CH-4, CH-5); 4.15 (m, 6H, CH-6); 4.49 (m, 3H, CH-2); 5.04 (m, 3H, CH-3); 5.86 (d, 3H, CH-1); 6.83 (t, 1H, H-4, J=2 Hz); 7.12 (d, 2H, H-3', H-5', J=8.6 Hz); 7.25 (d, 2H, H-2, H-6, J=2 Hz); 7.28 (d, 1H, H-7, J=16 Hz);7.59 (d, 2H, H-2', H-6', J=8.7 Hz). MS-ESI (CH_3CN): m/z 1277, $[M+Na]^+$.

3,4',5-tri(α-D-glucose-3-O-succinyl)-resveratrol (**4**). **3** (150mg, 0.12 mmol) was dissolved in 12 M TFA (3 mL). After stirring for 1.5 h at room temperature, the product was

precipitated with diethyl ether (10 mL) 3 times, and the solvent decanted after each precipitation. The white solid was dried under nitrogen and then dissolved in 3 mL water to hydrolyse trifluoroacetic esters at glucose hydroxyls. The solution was finally lyophilised to afford 121 mg of the desired product (98%). ^{1}H-NMR (250 MHz, DMSO-d_6) δ (ppm): 2.74-2.83 (d, 12H, CH_2); 3.07-5.06 (m, CH_2 D-glucose); 6.88 (s, 1H, H-4); 7.16 (d, 2H, H-3', H-5', J=7.9 Hz); 7.28 (s, 2H, H-2, H-6); 7.31-7.36 (d, 1H, H-7, J=16 Hz);7.64-7.67 (d, 2H, H-2', H-6', J=8.1 Hz). MS-ESI (CH_3CN): m/z 1037, $[M+Na]^+$.

Bibliography and notes

[1] For recent reviews on resveratrol see, e.g.: (a) Baur, J.A.; Sinclair, D.A. Nat. Rev. Drug Discov. **2006**, 5, 493. (b) Shakibaei, M.; Harikumar, K.B.; Aggarwal, B.B. Mol. Nutr. Food Res. **2009**, 53, 115. (c) Athar, M.; Back, H.H.; Kopelovich, D.R.; Bickers, D.R.; Kim, A.L. Arch. Biochem. Biophys. **2009**, 486, 95.
[2] (a) Fahr, A.; Liu, X. Expert Opin. Drug Deliv. **2007**, 4, 403. (b) Hurst, S.; Loi, C.M.; Brodfuehrer, J.; El-Kattan, A. Expert. Opin. Drug Metab. Toxicol. **2007**, 3, 469. (c) Stegemann, S.; Levellier, F.; Franchi, D.; de Jong, H.; Lindèn, H. Eur. J. Pharm. Sci. **2007**, 31, 249.
[3] (a) Ratnam, D.V.; Ankola, D.D.; Bhardwaj, V.; Sahana, D.K.; Kumar, M.N. J. Control. Release **2006**, 113, 189. (b) Scholz, S.; Williamson, G. Int. J. Vitam. Nutr. Res. **2007**, 77, 224.
[4] Passamonti, S.; Terdoslavich, M.; Franca, R.; Vanzo, A.; Tramer, F.; Braidot, E.; E. Petrussa, E.; Vianello, A. Curr. Drug Metab. **2009**, 10, 369.
[5] (a) Manach, C. ; Morand, C. ; Demigné, C. ; Texier, O. ; Régérat, F. ; Rémésy, C. FEBS Lett. **1997**, 409, 12. (b) Graefe, E.U.; Wittig, J.; Mueller, S.; Riethling, A.K.; Uehleke, B.; Drewelow, B.; Pforte, H.; Jacobasch, G.; Derendorf, H.; Veit, M. J. Clin. Pharmacol. **2001**, 41, 492. (c) Shimoi, K.; Yoshizumi, K.; Kido, T.; Usui, Y.; Yumoto, T. J. Agric. Food Chem. **2003**, 51, 2785. (d) Arts, I.C.; Sesink, A.L.; Faassen-Peters, M.; Hollman, P.C. Br. J. Nutr. **2004**, 91, 841.
[7] (a) Kawai, N.; Fujibayashi, Y.; Kuwabara, K.-I.; Ijuin, Y.; Kobayashi, S. Tetrahedron **2000**, 56, 6467. (b) Wenzel, E.; Soldo, T.; Erbersdobler, H.; Somoza, V. Mol. Nutr. Food Res. **2005**, 49, 482. (c) Brandolini, V.; Maietti, A.; Tedeschi, P.; Durini, E.; Vertuani, S.; Manfredini, S. J. Agric. Food Chem. **2002**, 50, 7407.
[8] LC-ESI/MS analyses and mass spectra were performed with a 1100 Series Agilent Technologies system using a reversed phase column (Synergi-MAX, 4 μm, 150 x 4.6 mm i.d.; Phenomenex). Solvents A and B were H_2O containing 0.1% TFA and CH_3CN. See the Supplementary data for further information.
[9] (a) Walle, T. Free Radic. Biol. Med. **2004**, 36, 829. (b) Manach, C.; Donovan, J.L. Free Radic. Res. **2004**, 38, 771. (c) Yang, C.S.; Sang, S; Lambert, J.D.; Lee, M.J. Mol. Nutr. Food Res. **2008**, 52 Suppl 1, S139.
[10] The Merck Index, 13th edition (2001). Merck and Co., Inc., Whitehouse Station, NJ, USA.
[11] Barreto, M.; Buescher, R.W.: http://ift.confex.com/ift/2004/ techprogram/paper_ 23374.htm
[12] (a) Lesschaeve, I.; Noble, A.C. Am. J. Clin. Nutr. **2005**, 81 suppl. 1, 330S. (b) Bajec, M.R.; Pickering, G.J. Crit. Rev. Food Sci. Nutr. **2008**, 48, 858.

[13] Bonina, F.; Puglia, C.; Rimoli, M.G.; Avallone, E.; Abignente, E.; Boatto, G.; Nieddu, M.; Meli, R.; Amorena, M.: de Caprariis, P. Eur. J. Pharm. Sci. **2002**, 16, 167.

Chapter 9

Synthesis and characterization of novel daidzein derivatives. A Dual Drug approach to improve the activity toward Arginase 1 expression.

Summary

Recently it was discovered that daidzein, a soy isoflavone, induces arginase 1 (Arg 1) expression in a hippocampal cell line. Arg 1 has been shown to protect motor neurons from trophic factor deprivation and to allow sensory neurons to overcome neurite outgrowth inhibition by myelin proteins. Daidzein is a known agonist of the β estrogen receptor, and preliminary data suggested that it might also weakly inhibit histone deacetylase (HDAC) enzymes. Furthermore the HDAC inhibitor TSA robustly induces arginase expression whereas estrogen itself does not. Based on this and on the observation that estrogen receptor activation is required for daidzein to induce the Arg 1 promoter, we synthesized a novel series of compounds by incorporating a histone deacetylase (HDAC) inhibitory functionality into the phytoestrogen daidzein to verify the possibility of a synergy between estrogenic activity and HDAC inhibition, potentiating the effect of these derivatives.

Introduction

Phytoestrogens are plant-derived chemicals that possess estrogenic activity, being effective in combining with estrogen receptors and initiating estrogen-dependent transcription [1]. Their affinity for estrogen receptors, however, is at least 1000–10,000 times lower than of estradiol and this is an important factor when considering dietary intake of these chemicals and their subsequent circulating concentrations. Phytoestrogens are classified according to their chemical structure; the most widely studied are isoflavones, present in high concentrations in soy products and red clover, followed by flavones and coumestans. Genistein and daidzein (Figure 1), the major isoflavones in soybeans [2] are currently receiving much attention because of their potential role in preventing and treating cancer as well as other chronic diseases [3,4].

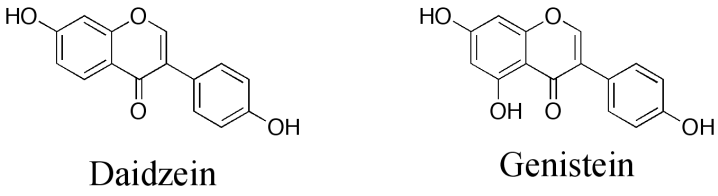

Figure 1. Molecular structures of the major soy isoflavones daidzein and genistein.

These compounds are antioxidants [5] and are proposed to be anticarcinogenic è [6-8]. Furthermore daidzein affords bone-protective action by stimulation of osteoblast [9-11] and inhibition of osteoclast functions [12] through the estrogen receptors. Recently it was discovered [13] that daidzein exhibits a concentration-dependent induction of activity at the Arg1 promoter. Arginase 1 can increase polyamine synthesis by catalyzing the hydrolysis of arginine to ornithine and urea [14]. Ornithine is then converted to putrescine by ornithine decarboxylase. Cai et al. demonstrated that transduction of DRG (Dorsal root ganglion) neurons with a viral vector encoding arginase 1 rendered these neurons resistant to the neurite outgrowth-suppressing effects of myelin, presumably by enhancing polyamine synthesis and putrescine production [15]. An ideal therapeutic agent for stroke or spinal cord injury should promote survival and regeneration in the CNS. Despite significant focus on neuroprotection, stroke and spinal cord injury (SCI) remain prevalent causes of disability worldwide as therapeutics designed to limit cell death have failed to enhance recovery in humans [16-18]. Functional recovery after injury requires many barriers to be surmounted, including inhibitory myelin proteins [19-20]. Indeed, direct neutralization of these proteins has resulted in improved recovery after injury [21]. Regenerative effects are transcription-dependent and are mediated by arginase 1 (Arg1), a notable gene target for cAMP-mediated transcription. Collectively, these studies suggest that increasing arginase activity by elevating cAMP may be a promising therapeutic approach to promote CNS protection and regeneration. Daidzein has been reported to be neuroprotective to CNS neurons in glutamate excitotoxicity and oxygen/glucose deprivation models and to promote axonal outgrowth of hippocampal neurons cultured on permissive substrates; these effects were attributed to the activity of daidzein on estrogen receptors [22-24]. However, it is unlikely that the estrogenic properties of daidzein alone can account for its ability to induce Arg1, as compounds with superior estrogenic activity (e.g. genistein) failed to induce high Arg1 protein levels. Daidzein has shown a weak activity as inhibitor of histone deacetylases (HDACs), an important class of enzymes that modulate gene expression. Additionally, the HDAC inhibitor TSA (trichostatin A) has been shown to robustly induce arginase expression whereas estrogen itself does not. Prof Raj Ratan et al. at Burke/Cornell Medical

Research Institute have demonstrated that estrogen receptor activation is required for daidzein to induce Arg 1 expression [13]. Based on these results, we undertook the synthesis of a series of daidzein derivatives (Figure 2) that incorporate an HDAC-inhibitory functionality into the molecular structure of the soy isoflavone.

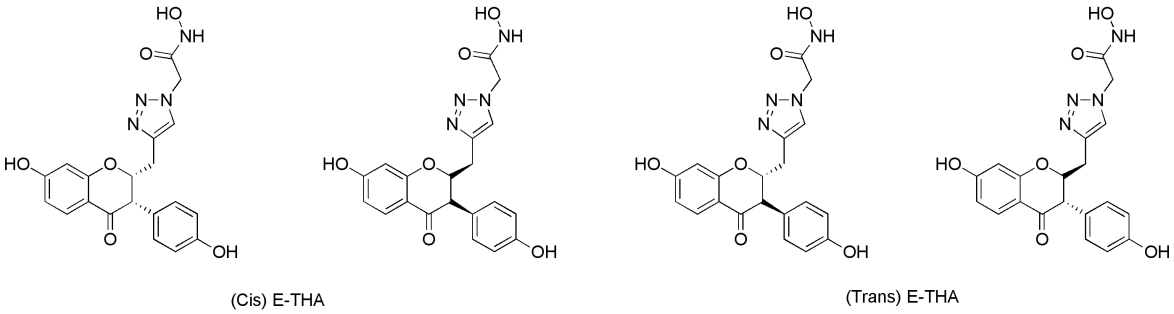

Figure 2. Derivatives of daidzein synthesized in this study

For this study we decided to combine daidzein with the pharmacophore of a class of HDAC inhibitors, namely hydroxamic acid. These inhibitors have a high affinity for HDACs; their hydroxamic acid moiety binds to the catalytic domain of HDACs, blocking access of the substrate to a crucial Zn^{2+} ion that sits at the bottom of a "pocket" formed by the polypeptide chain. The general structure of these inhibitors comprises a linker, which allows hydroxamic acid to coordinate with the cation, while the rest of the molecule blocks the entry of the "pocket" (Figure 3).

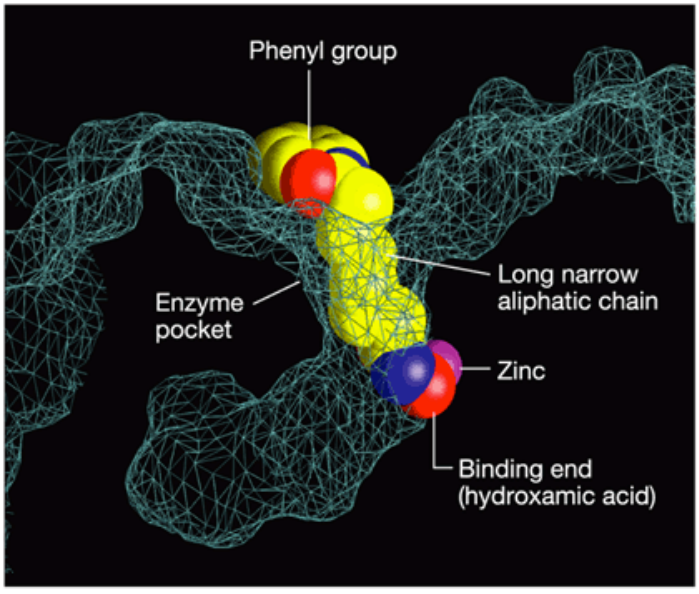

Figure 3. Structure of SAHA bound to an HDAC-like protein[25]

The new compounds hopefully will in turn allow us to assess whether the combination of estrogenic activity and enhanced HDAC inhibitory activity might lead to an enhancement of the neuroprotective action.

Results

The design of the synthesis of daidzein derivatives bearing a hydroxamic acid group linked to a spacer is derived by the need to keep intact the features of daidzein that are alleged to have estrogenic properties. Based on analysis of structure-activity relationships the following features have been identified as important for determining estrogen receptor binding [26]:

- Presence of a hydroxyl group that can mimic the function of the 3-hydroxy of estradiol through the formation of a hydrogen bond with Glu 353 and Arg 394;
- Formation of a hydrogen bond between His 524 and a second hydroxyl group placed at an optimal distance of 11 Å from the first, as in estradiol;
- Structures characterized by a degree of hydrophobicity allow a better interaction with the apolar site;
- Presence of a ring, usually aromatic, which contributes to the rigidity of the molecule.

Based on these features we chose to modify the molecule by binding a linker with the hydroxamic acid in position 2 by replacing the double bond (Figure 4).

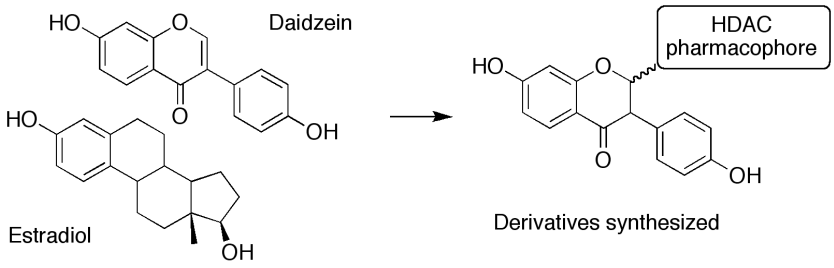

Figure 4. Comparison between daidzein and estradiol and derivatives synthesized

The addition to the 2-3 double bond affects the rigidity of the molecule, but published studies [27] shown that equol (isoflavandiol produced from daidzein by metabolism, with very similar structure to the isoflavone but hydrogenated in position 2-3, Figure 5) is an estrogen 100 times more potent than daidzein. Thus, the 2-3 double bond should not be closely related to the estrogenic activity of the isoflavone and its reduction may even lead to increased estrogenic activity.

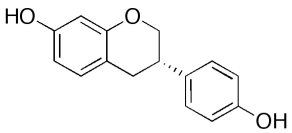

4', 7-Isoflavandiol (Equol)

Figure 5. Molecular structure of equol.

Synthesis

The desired compounds were synthesized as described in the Experimental Section following the strategy outlined in Scheme 1.

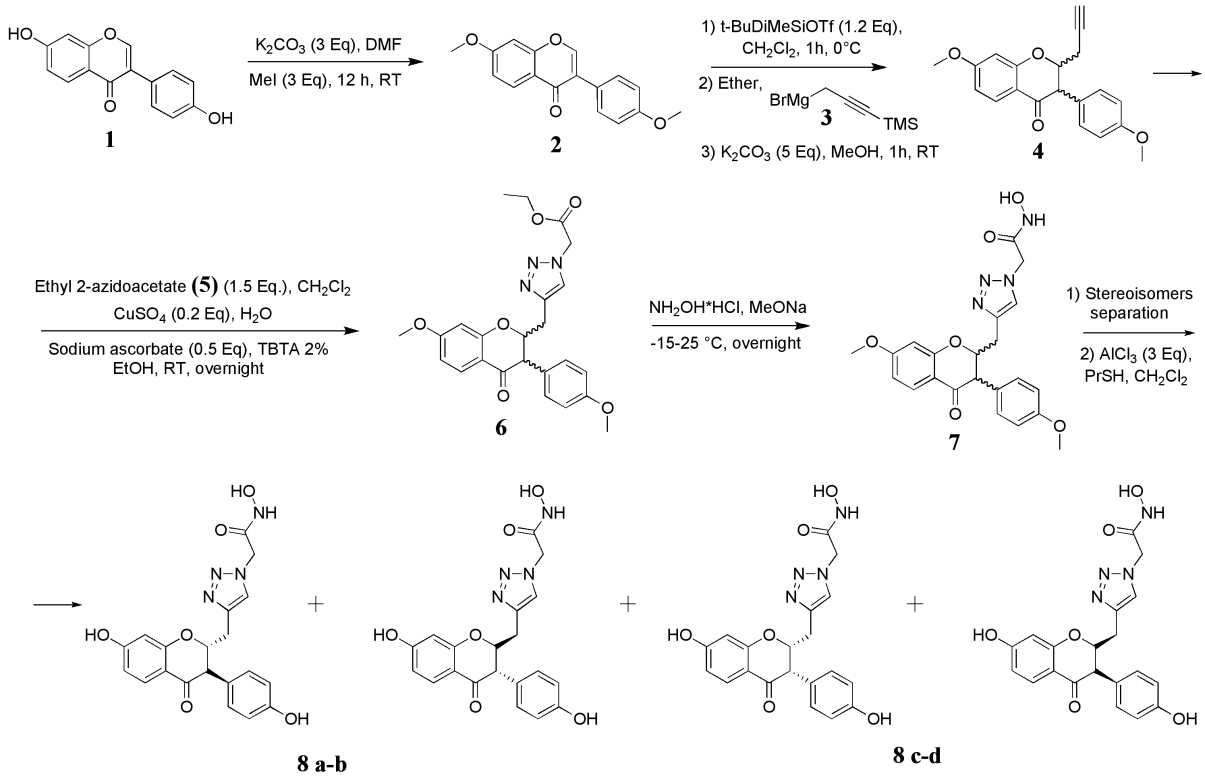

Scheme 1. Synthesis of daidzein derivatives **8 a-d**

The crucial step for obtaining the desired products is the Michael addition on the protected daidzein in order to obtain **4**. The Grignard reagent **3** was obtained by reaction between 3-(trimethylsilyl)propargyl bromide and magnesium chips catalyzed by zinc bromide as reported by Acharya et al. [28]. The direct reaction of dimethyl daidzein (**2**) with **3** results in the formation of complex mixtures, due to competing attack of the Grignard reagent onto the carbonyl group and onto the double bond (conjugate addition). The previous protection of the carbonyl moiety using *tert*-Butyldimethylsilyl trifluoromethanesulfonate resulted in the formation of the corresponding 4-silyloxybenzopyrylium triflates [29-30]. The addition of Grignard reagent onto the latter and the subsequent addition of an aqueous solution of ammonium chloride (1 M) followed by deprotection of the propargyl moiety in potassium carbonate resulted in regioselective formation of **4** in satisfying yield (Scheme 2).

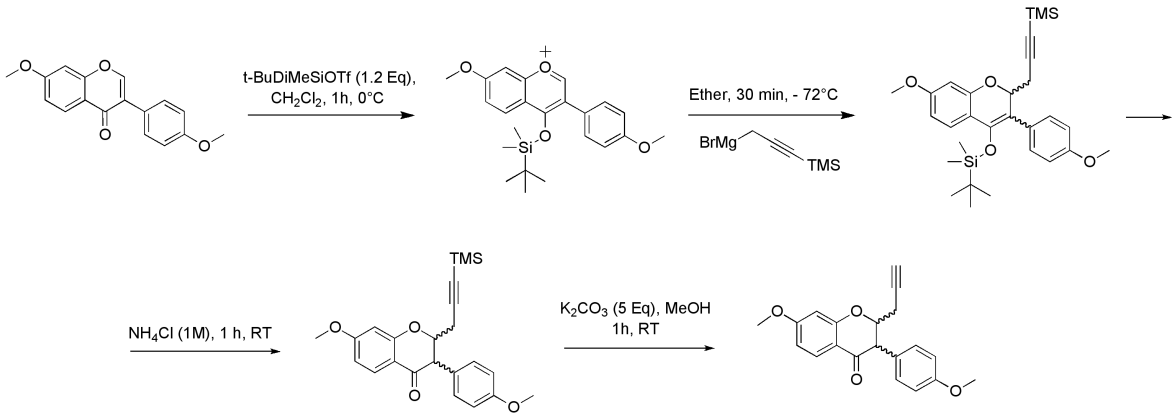

Scheme 2. Mechanism of the Michael addition on **2**

Using "click chemistry" we then formed a triazole ring bearing the ethyl ester of acetic acid (**6**), which was then converted to hydroxamic acid using hydroxylamine hydrochloride (**7**). The separation of the synthesized stereoisomers was performed using a chiral preparative coloumn AD-H Chiralpack (Figure 5, see Materials and Methods) and the relative stereoisomery (cis/trans 1:2) was confirmed by the analysis of the coupling constant J for the proton in position 3 coupled with the proton in position 2, higher in the trans isomer.

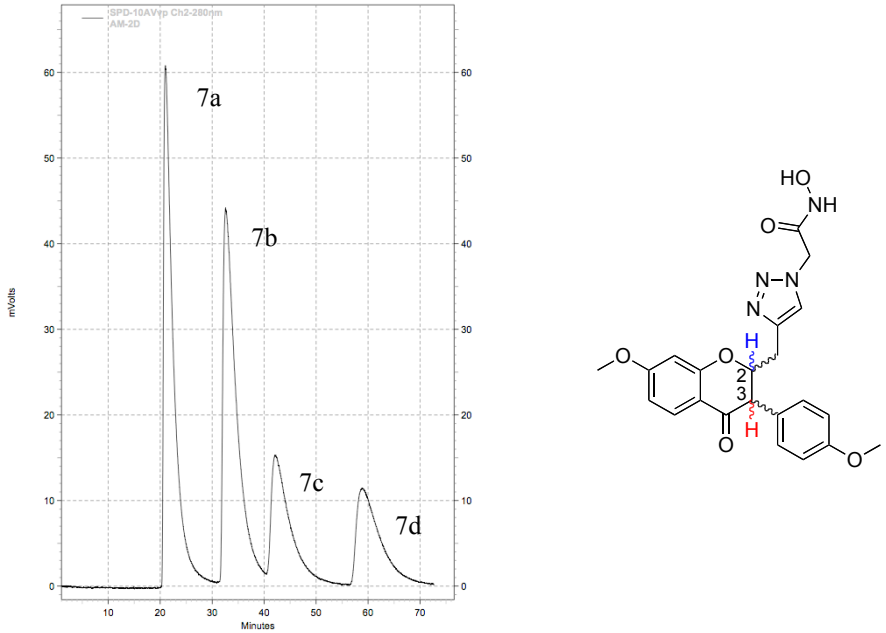

Figure 5. Semipreparative chiral stereoisomers separation of **7** (**7 a-d**)

Finally demethylation was performed using $AlCl_3$ in presence of 1-propanethiol to obtain the desired daidzein derivatives (**8 a-d**). These new compounds are presently being tested at Burke/Cornell Medical Research Institute to assess possible effects on the expression of Arginase 1.

Experimental section

Materials and Methods

Daidzein (98%) was purchased from AmplaChem, Inc. and reagents were purchased from Aldrich and were used as received. Proton and carbon NMR spectra were recorded on a 400 MHz Bruker spectrometer. Chemical shifts (δ) are given in ppm relative to the residual signal of the solvent (for ^{1}H: $CDCl_3$: δ = 7.26 ppm, DMSO-d_6: δ = 2.50 ppm, DMF-d_6: δ = 8.03 ppm, CD_3CN: δ = 1.94 ppm; for ^{13}C: $CDCl_3$: δ = 77.00 ppm, DMSO-d_6: δ = 39.52 ppm, DMF-d_6: δ = 29.76 ppm, CD_3CN: δ = 1.32 ppm). Optical rotation was detected on an Autopol IV automatic polarimeter. Mass spectra were measured in the ESI mode at an ionization potential of 70 eV using the LCMS MSD spectrometer (Hewlett-Packard). Column chromatography was performed using Merck silica gel (40-60 mesh). Purity of compounds (> 95%) was established by HPLC, which was carried out on an Agilent 1100 HPLC system with a Synergy 4 μm Hydro-RP 80A column, with detection at 254 (or 280) nm on a G1314A variable wavelength detector; flow rate = 1.4 mL/min; gradient elution over 20-29 min, from 30% methanol water to 100% methanol (both containing 0.05 vol % of CF_3COOH).

Preparative HPLC Conditions (Water/Acetonitrile System- Gradient A).

An ACE AQ 150 mm × 21.2 mm 5 μm particle size column was used with UV detection at both 254 and 280 nm. Conditions: flow 10.0 mL/min; gradient of 0-50% acetonitrile in water (both containing 0.05 vol % of CF_3COOH) for 25 min, to 100% for another 5 min, return to 0% for the next 5 min, finally balanced at 0% for the final 5 min at 25 °C.

Preparative HPLC Conditions (Water/Methanol System- Gradient B).

Column and detection as above. Conditions: flow 10.0 mL/min; gradient of 0-50% methanol in water (both containing 0.05 vol % of CF_3COOH) for 20 min, to 100% for another 5 min, maintain 100 % for another 5 min, return to 0% for the next 5 min, finally balanced at 0% for the final 5 min.

Preparative Chiral HPLC Conditions (Hexanes/Ethanol System- Gradient C).

An AD-H chiralpak 20 mm × 250 mm, 10 μm particle size column was used with UV detection at both 254 and 280 nm. Conditions: flow 9 mL/min; isocratic 55 % ethanol / 45 % hexanes.

Synthetic procedures.

7,4'-Dimethoxy Daidzein (2): Methyl Iodide (3.35 g, 23.6 mmol, 3 equiv.) was added to a solution of Daidzein (2.00 g, 7.9 mmol) plus suspended K_2CO_3 (3.26 g, 3 equiv.) in dry DMF (20 mL). The mixture was stirred overnight at room temperature, and was then

diluted in CH_2Cl_2 (200 mL) and washed with 0.5 M HCl (5 × 100 mL). The organic layer was dried over $MgSO_4$ and filtered. The solvent was evaporated under reduced pressure and the crude compounds were purified by MPCC (middle pressure chromatography column) using dichloromethane/ethyl acetate (0% EtOAc for 10 minutes and from 0% to 10% of EtOAc in 20 minutes) as eluent to afford 1.45 g of product as a bright white solid (65 % yield).^{1}H-NMR (d_6-DMSO, 400 MHz): δ = 3.78 (s, 3H, -OCH_3), 3.91 (s, 3H, -OCH_3), 6.99 (d, $^3J_{H\text{-}H}$ = 8.8 Hz, 2H, 3',5'-H), 7.08 (dd, $^4J_{H\text{-}H}$ = 2.4 Hz, $^3J_{H\text{-}H}$ = 8.8 Hz, 1H, 6-H), 7.15 (d, $^4J_{H\text{-}H}$ = 2.4 Hz, 8-H), 7.52 (d, $^3J_{H\text{-}H}$ = 8.8 Hz, 2H, 2',6'-H), 8.03 (d, $^3J_{H\text{-}H}$ = 8.8 Hz, 5-H), 8.42 (s, 1H, 2-H). ESI-MS (ion trap): m/z 283, $[M+H]^+$; HRESI: m/z 283.0973; calcd for $C_{17}H_{14}O_4 \cdot H^+$ 283.0973.

3-(Trimethylsilyl)propargyl magnesium bromide (3): A flask containing $ZnBr_2$ (50 mg, 0.22 mmol, 2.5% w/w) and Mg (505 mg, 2 equiv.) was heated under vacuum and flushed with Ar. Et_2O (6 mL) was added. Upon slow (30 min) addition of TMS-propargylic bromide (2.0 g, 10.4 mmol, 1 equiv.) in Et_2O (8 mL) an exothermic reaction took place and the mixture was cooled to 0 °C (ice cold water). After the addition had been completed, the mixture was stirred while kept in an ice-water bath for 2 h to afford a light yellow solution and pulverized excess solid Mg. The mixture was used without further purification. 86% yield [28].

7-methoxy-3-(4-methoxyphenyl)-2-propargyl-chroman-4-one (4): A solution of t-BuDiMeSiOTf (2.25 g, 8.5 mmol, 1.2 equiv) in CH_2Cl_2 (5 mL) was added to a CH_2Cl_2 (30 mL) solution of 7,4'-Dimethoxy Daidzein (2.00 g, 7.1 mmol, 1 equiv) at 0 °C. After stirring for 1 h at 0 °C, the mixture was cooled to -78 °C and the TMS-Propargylic Grignard Reagent (preceeding compound, 1.5 equiv. in ether) was added. After stirring for 30 min at -78 °C an aqueous solution of NH_4Cl (20 mL, 1 M) was added. The mixture was allowed to warm to ambient temperature and the organic and aqueous layers were separated. The latter was extracted with CH_2Cl_2 (3 × 30 mL). The combined organic layers were dried over $MgSO_4$, filtered and the filtrate was concentrated *in vacuo*. K_2CO_3 (4.90 g, 35.5 mmol, 5 equiv.) was then added to a solution of the above residue in 30 mL of methanol and 5 mL of CH_2Cl_2. The mixture was then stirred at R.T. for 1 h and diluted with saturated aqueous NH_4Cl (40 mL) and CH_2Cl_2 (40 mL) with vigorous stirring. The phases were separated, and the aqueous phase was extracted with CH_2Cl_2 (3 × 40 mL). The solvent was evaporated under reduced pressure and the crude products were purified by MPCC using dichloromethane/ethyl acetate (0% EtOAc for 10 minutes and from 0% to 10% of EtOAc in 20 minutes) as eluent to afford 0.79 g of product as a pale yellow solid

(34 % yield), as a mixture of cis/trans-isomers 2:1. ^{1}H-NMR ($CDCl_3$, 400 MHz): δ = 2.12-2.21 (2 × t, $^{4}J_{H\text{-}H}$ = 2.8 Hz, 1H Propargylic-C*H*), 2.33-2.72 (m, 2H, Propargylic-C*H*$_2$), 3.77-4.82 (m, 8H, 2 × -OC*H*$_3$, H-2, H-3), 6.53 (m, 1H), 6.61-6.69 (m, 1H), 6.81-6.93 (m, 2H), 7.13-7.17 (m, 2H), 7.78-7.92 (m, 1H). ESI-MS (ion trap): m/z 323, $[M+H]^+$; HRESI: m/z 323.1277; calculated for $C_{20}H_{18}O_4 \cdot H^+$ 323.1278.

Ethyl 2-azidoacetate (5): NaN_3 (2.0 equiv) was added to a solution of ethyl bromoacetate in water/acetone (1:3, 0.25 M) and the mixture was stirred at room temperature for 30 min. The reaction mixture was diluted with CH_2Cl_2 and washed with water. The organic layer was dried over $MgSO_4$ and evaporated. The crude material is generally clean enough to be used without further purification. ^{1}H-NMR ($CDCl_3$, 400 MHz): δ = 4.23 (q, $^{3}J_{H\text{-}H}$ = 7.1 Hz, 2 H, CH_3-C*H*$_2$-), 3.83 (s, 2 H, -C*H*$_2$-N_3), 1.28 (t, $^{3}J_{H\text{-}H}$ = 7.1 Hz, 3 H, -CH_2-C*H*$_3$).

7-methoxy-3-(4-methoxyphenyl)-2-methyl-[1,2,3]triazol-3-acetic acid ethyl ester-chroman-4-one (6): To a solution of azide (**5**) (0.61 g, 3.7 mmol, 1.5 eq. in 3 mL of ethanol) and **4** (0.79 g, 2.5 mmol, 1.0 equiv. in 8 mL ethanol, 6 mL chloroform and 2 mL H_2O) at R.T., sodium ascorbate (0.24 g, 1.25 mmol, 0.5 eq. in 0.75 mL H_2O), $CuSO_4$*$5H_2O$ (0.13 g, 0.5 mmol, 0.2 equiv.) and TBTA (Tris[(1-benzyl-1H-1,2,3-triazol-4-yl)methyl] amine) catalyst (2% w/w in 2 mL chloroform) were added and the resulting yellow mixture was stirred vigorously overnight. The reaction mixture was diluted and extracted with EtOAc. The organic layer was dried over $MgSO_4$ and the solvents were evaporated under reduced pressure. The crude products were purified by MPCC using chloroform/ethyl acetate (0% to 20% of EtOAc in 30 minutes) as eluent to afford 0.74 g of product as a pale yellow solid (66 % yield). ^{1}H-NMR ($CDCl_3$, 400 MHz): δ = 1.29-1.36 (m, 3H, -CH_2-C*H*$_3$), 3.05-3.13 (m, 2H), 3.67-3.87 (m, 7H), 4.25-4.33 (m, 2H), 4.89-5.22 (m, 3H), 6.45-6.50 (m, 1H), 6.59-6.66 (m, 1H), 6.81-6.91 (m, 2H), 7.07-7.14 (m, 2H), 7.57-7.62 (2 × s, broad 1H –N*H*-) 7.84-7.88 (m, 1H). ESI-MS (ion trap): m/z 452, $[M+H]^+$; HRESI: m/z 452.1822; calcd for $C_{24}H_{25}N_3O_6 \cdot H^+$ 452.18161.

7-methoxy-3-(4-methoxyphenyl)-2-methyl-[1,2,3]triazol-3-hydroxamic acid-chroman-4-one (7a-d): Hydroxylamine hydrochloride (0.65 g, 9.3 mmol, 6 eq.) was added to a solution of **6** (0.70 g, 1.6 mmol, 1 eq.) in MeOH (20 mL) at -15°C. MeONa (12.4 mmol, 8 eq.) was then added and the reaction mixture was warmed to room temperature and stirred at 25 °C overnight. The reaction mixture was neutralized with 10 mL of a saturated aqueous solution of $NaHCO_3$ and diluted with 40 mL of water. The resulted solution was extracted with chloroform (4 × 50 mL). The organic layer was dried over $MgSO_4$ and the solvents were evaporated under reduced pressure to yield a crude mixture which was

purified by reverse-phase preparative HPLC to give the title compounds as a bright white solid (0.44 g, 63 % yield). The resulting stereoisomers were then separated by chiral preparative HPLC (AD-H chiralpak 20 × 250 mm, 10 μm particle size) using 55% Ethanol/45% Hexanes (isocratic). **7a-7b** (trans stereoisomers) ^{1}H-NMR (d_6-DMSO, 400 MHz): δ = 2.82-3.06 (m, 2H, -C*H*$_2$-), 3.76 (s, 3H, -OC*H*$_3$), 3.84 (s, 3H, -OC*H*$_3$), 3.98 (d, 1H, H-3, $^{3}J_{H-H}$ = 10.8 Hz), 4.95-5.29 (m, 2H), 6.59 (d, 1H, $^{4}J_{H-H}$ = 2.4 Hz), 6.68 (dd, 1H, $^{3}J_{H-H}$ = 8.8 Hz, $^{4}J_{H-H}$ = 2.4 Hz), 6.92 (d, 2H, $^{3}J_{H-H}$ = 8.4 Hz), 7.16 (d, 2H, $^{3}J_{H-H}$ = 8.4 Hz), 7.71 (d, 1H, $^{3}J_{H-H}$ = 8.8 Hz) 7.98 (s, 1H). ESI-MS (ion trap): m/z 439, $[M+H]^{+}$; HRESI: m/z 439.1609; calcd for $C_{24}H_{25}N_3O_6 \cdot H^{+}$ 439.1612, **7a** $[\alpha]^{25}_{D}$ = - 55.0°, **7b** $[\alpha]^{25}_{D}$ = + 55.0° (c = 0.0005 g/mL $CHCl_3$). **7c-7d** (cis stereoisomers) ^{1}H-NMR (d_6-DMSO, 400 MHz): δ = 2.79-2.93 (m, 2H, -C*H*$_2$-), 3.72 (s, 3H, -OC*H*$_3$), 3.77 (d, 1H, H-3, $^{3}J_{H-H}$ = 3.6 Hz), 3.86 (s, 3H, -OC*H*$_3$), 4.96-5.31 (m, 2H), 6.65 (d, 1H, $^{4}J_{H-H}$ = 2.4 Hz), 6.73 (dd, 1H, $^{3}J_{H-H}$ = 8.8 Hz, $^{4}J_{H-H}$ = 2.4 Hz), 6.89 (d, 2H, $^{3}J_{H-H}$ = 8.4 Hz), 7.07 (d, 2H, $^{3}J_{H-H}$ = 8.4 Hz), 7.75 (d, 1H, $^{3}J_{H-H}$ = 8.8 Hz) 7.97 (s, 1H). ESI-MS (ion trap): m/z 439, $[M+H]^{+}$; HRESI: m/z 439.1611; calcd for $C_{24}H_{25}N_3O_6 \cdot H^{+}$ 439.1612, **7c** $[\alpha]^{25}_{D}$ = - 102.0°, **7d** $[\alpha]^{25}_{D}$ = + 103.0° (c = 0.0005 g/mL $CHCl_3$).

3-phenyl-2-methyl-[1,2,3]triazol-3-hydroxamic acid-chroman-4-one (8a-d): $AlCl_3$ (1 g, 7.5 mmol) was added under the protection of dry argon to a stirred solution of 1-propanethiol (PrSH) (10 mL) at 0 °C. After stirring for 5 min, **7a-d** (0.05 g, 0.11 mmol) in 2 mL CH_2Cl_2 was added. The reaction mixture was stirred at 0 °C for 30 min, and then was warmed slowly to room temperature. After 3 hours a new fresh solution of $AlCl_3$ (1 g, 7.5 mmol) in 1-propanetiol (10 mL) was added at room temperature. The reaction mixture was stirred at 25 °C for 3 hours, then quenched with water (50 mL). The PrSH and the CH_2Cl_2 were evaporated under reduced pressure then, the resulting mixture was extracted with EtOAc (10 mL × 6). The organic layers were combined, and dried with $MgSO_4$. After filtration, the filtrate was concentrated *in vacuo* and purified by reverse-phase preparative HPLC to give the title compounds as a bright white solid (0.038 g, 84% yield). **8a-8b** (trans stereoisomers) ^{1}H-NMR (d_6-DMSO, 400 MHz): δ = 2.93-3.05 (m, 2H, -C*H*$_2$), 3.76 (d, 1H, H-3, $^{3}J_{H-H}$ = 10.8 Hz), 5.01 (s, 2H), 6.36 (d, 1H, $^{4}J_{H-H}$ = 2.4 Hz), 6.48 (dd, 1H, $^{3}J_{H-H}$ = 8.8 Hz, $^{4}J_{H-H}$ = 2.4 Hz), 6,76 (d, 2H, $^{3}J_{H-H}$ = 8.4 Hz), 6.99 (d, 2H, $^{3}J_{H-H}$ = 8.4 Hz), 7.69 (d, 1H, $^{3}J_{H-H}$ = 8.8 Hz) 7.87 (s, 1H). ESI-MS (ion trap): m/z 411, $[M+H]^{+}$; HRESI: m/z 411.1296; calcd for $C_{20}H_{18}N_4O_6 \cdot H^{+}$ 411.1299, **8a** $[\alpha]^{25}_{D}$ = - 58.0°, **8b** $[\alpha]^{25}_{D}$ = + 56.0° (c = 0.001 g/mL EtOH). **8c-8d** (cis stereoisomers) ^{1}H-NMR (d_6-DMSO, 400 MHz): δ = 2.94-2.96 (m, 2H, -C*H*$_2$), 3.63 (d, 1H, H-3, $^{3}J_{H-H}$ = 3.6 Hz), 5.06 (s, 2H), 6.43 (d, 1H, $^{4}J_{H-H}$ = 2.4

Hz), 6.56 (dd, 1H, $^{3}J_{H\text{-}H}$ = 8.8 Hz, $^{4}J_{H\text{-}H}$ = 2.4 Hz), 6,73 (d, 2H, $^{3}J_{H\text{-}H}$ = 8.4 Hz), 7.01 (d, 2H, $^{3}J_{H\text{-}H}$ = 8.4 Hz), 7.76 (d, 1H, $^{3}J_{H\text{-}H}$ = 8.8 Hz) 7.87 (s, 1H). ESI-MS (ion trap): m/z 411, $[M+H]^{+}$; HRESI: m/z 411.1298; calcd for $C_{20}H_{18}N_4O_6 \cdot H^{+}$ 411.1299, **8c** $[\alpha]^{25}_{D}$ = - 92.0°, **8d** $[\alpha]^{25}_{D}$ = + 93.0° (c = 0.001 g/mL EtOH).

Bibliography

[1] Kuiper GG, Lemmen JG, Carlsson BO, Corton JC, Safe SH, van der Saag PT, van der Burg V, Gustafsson JA. (1998) Interaction of estrogenic chemicals and phytestrogens with estrogen receptor. Endocrinol 139:4252– 4263.

[2] Xu X, Wang H, Murphy PA, Cook L, Hendrich S. (1994) Daidzein is more bioavailable soymilk isoflavone than is genistein in adult women. J Nutr. 124:825–832.

[3] Bielecki A, Roberts J, Mehta R, Raju J. (2011) Estrogen Receptor-β Mediates the Inhibition of DLD-1 Human Colon Adenocarcinoma Cells by Soy Isoflavones. Nutrition and cancer 63:139-150

[4] Martinez-Montemayor MM, Otero-Franqui E, Martinez J, De La Mota-Peynado A, Cubano LA, Dharmawardhane S. (2010) Individual and combined soy isoflavones exert differential effects on metastatic cancer progression. Clinical and Experimental Metastasis 27:465-480.

[5] Liang J, Tian Y, Fu L, Wang T, Li H, Wang P, Han R, Zhang J, Skibsted LH. (2008) Daidzein as an Antioxidant of Lipid: Effects of the Microenvironment in Relation to Chemical Structure. J. Agric. Food Chem. 56:10376-10383.

[6] Yamamoto S, Sobue T, Kobayashi M, Sasaki S, Tsugane S. (2003) Based Prospective Study on Cancer Cardiovascular Diseases Group. Soy, soflavones, and breast cancer risk in Japan. J. Natl. Cancer Inst. 95:906-913.

[7] Adlercreutz H. (2002) Phytoestrogens and cancer. Lancet Oncol. 3:364-373

[8] Morrissey C, Watson RW. (2003) Phytoestrogens and prostate cancer. Curr Drug Targets 4:231-241.

[9] Jia TL, Wang HZ, Xie LP, Wang XY, Zhang RQ. (2003) Daidzein enhances osteoblast growth that may be mediated by increased bone morphogenetic protein (BMP) production. Biochem. Pharmacol. 65:709-715.

[10] Setchell KD, Lydeking-Olsen E. (2003) Dietary phytoestrogens and their effect on bone: evidence from in vitro and in vivo, human observational, and dietary intervention studies. Am. J. Clin. Nutr. 78:593S-609S.

[11] Yamaguchi M, Ono R, Ma ZJ. (2001) Prolonged Intake of Isoflavone- and Saponin- containing soybean extract (Nijiru) supplement enhances Circulating γ-Carboxylated osteocalcin concentrations in healthy individuals. Journal of Health Science, 47:579,582.

[12] Rassi CM, Lieberherr M, Chaumaz G, Pointillart A, Cournot GJ. (2002) Down-regulation of osteoclast differentiation by daidzein via caspase 3. Bone Miner. Res. 17:630-638.

[13] Ma TC, Campana A, Lange PS, Lee HH, Banerjee K, Bryson JB, Mahishi L, Alam S, Giger RJ, Barnes S, Morris SM Jr, Willis DE, Twiss JL, Filbin MT, Ratan RR. (2010) A large scale chemical screen for regulators of the arginase 1 promoter identifies the soy isoflavone, daidzein as a clinically approved, small molecule that can promote neuronal protection or regeneration via a cAMP-independent pathway. J. Neurosci. 30:739-748.

[14] Guoyao WU, Morris MM. (1998) Arginine metabolism: nitric oxide and beyond. Biochem, J. 336:1-17.

[15] Cai D, Deng K, Mellado W, Lee J, Ratan RR, Filbin MT (2002) Arginase I and polyamines act downstream from cyclic AMP in overcoming inhibition of axonal growth MAG and myelin in vitro. Neuron 35:711–719.
[16] Baptiste DC, Fehlings MG. (2007) Update on the treatment of spinal cord injury. Prog Brain Res 161:217-233.
[17] Savitz SI, Fisher M. (2007) Future of neuroprotection for acute stroke: in the aftermath of the SAINT trials. Ann Neurol 61:396-402.
[18] Ratan RR, Noble M. (2009) Novel multi-modal strategies to promote brain and spinal cord injury recovery. Stroke 40:S130-132.
[19] Cafferty WB, Strittmatter SM. (2006) The Nogo-Nogo receptor pathway limits a spectrum of adult CNS axonal growth. J Neurosci 26:12242-12250.
[20] Hannila SS, Filbin MT. (2008) The role of cyclic AMP signaling in promoting axonal regeneration after spinal cord injury. Exp Neurol 209:321-332.
[21] Rossignol S, Schwab M, Schwartz M, Fehlings MG. (2007) Spinal cord injury: time to move? J. Neurosci. 27:11782-11792.
[22] Zhao L, Chen Q, Diaz Brinton R. (2002) Neuroprotective and neurotrophic efficacy of phytoestrogens in cultured hippocampal neurons. Exp Biol Med (Maywood) 227:509-519.
[23] Wang P, Jeng CJ, Chien CL, Wang SM (2008) Signaling mechanisms of daidzein-induced axonal outgrowth in hippocampal neurons. Biochem Biophys Res Commun 366:393-400.
[24] Schreihofer DA, Redmond L (2009) Soy phytoestrogens are neuroprotective against stroke-like injury in vitro. Neuroscience 158:602-609.
[25] Marks PA, Rifkind RA, Richon VM, Breslow R, Miller T, Kelly WK. (2001) Histone deacetylases and cancer: causes and therapies. Nature Reviews Cancer 1:194-202.
[26] Fang H, Tong W, Shi LM, Blair R, Perkins R, Branham W, Hass BS, Xie Q, Dial SL, Moland CL, Sheehan DM. (2001). Structure-activity relationships for a large diverse set of natural, synthetic, and environmental estrogens. Chem. Res. Toxicol. 14:280–294.
[27] Sathamoorthy N, Wang TT. (1997) Differential effects of dietary phyto-oestrogens daidzein and equol on human breast cancer MCF-7 cells. Eur. J. Cancer 33:2384-2389.
[28] Acharya HP, Miyoshi K, Kobayashi Y. (2007) Mercury-Free Preparation and Selective Reactions of Propargyl (and Propargylic) Grignard Reagents. Org. Lett 18:3535-3538.
[29] Lee YG, Ishimaru K, Iwasaki H, Ohkata K, Akiba K. (1991) Tandem Reactions in 4-Siloxy-1-benzopyryliumSalts: Introduction of Substituents and Cyclohexene and Cyclopentane Annulation in Chromones. J. Org. Chem. 56:2058-2066.
[30] Hoettecke N, Rotzoll S, Albrecht U, Lalk M, Fisher C, Langer P. (2008) Synthesis and antimicrobial activity of 2-alkenylchroman-4-ones, alkenylthiochroman-4-ones and 2-alkenylquinol-4-ones. Bioorg. & Med. Chem. 16:10319-10325.

Abbreviations

ARG 1: Arginase 1

AUC: Area Under Curve (in pharmacokinetics)

BTPI: (n-butyl-4-triphenylphosphonium) iodide

COX: Cyclooxygenase

CSP: Cyclosporin A

DMEM: Dulbecco's Modified Eagle Medium

DMF: Dimethylformamide

DMSO: Dimethylsulfoxide

EDC: N-ethyl-N'-(3-dimethylaminopropyl)-carbodiimide

EDTA: N,N,N',N'etilendiamminotetraacetic acid

EGCG: EpiGalloCatechinGallate

ER: Endoplasmic reticulum

ESI: ElectroSpray Ionization

EtOAc: Ethyl Acetate

FBS: Fetal Bovine Serum

GSH: Glutatione

GST: Glutathione-S-Transferase

HBSS: Hank's balanced saline solution

HDAC: Histone Deacetylase

HEPES: N-(2-idroxyethyl)-piperazin-N'-2-ethansolfonic acid

HPLC: High Performance Liquid Chromatography

IMM: Inner mitochondrial membrane

I/R: Ischemia/Riperfusion

MAPK: Mitogen-Activated Protein Kinase

MDR: Multi-Drug Resistance

MEF: Mouse Embryo Fibroblast

MeOD: Deuterated methanol

MeOH: Methanol

MPCC: Middle pressure chromatography coloumn

MPT: Mitochondrial Permeability Transition

MPTP: Mitochondrial Permeability Transition Pore

MS: Mass Spectrometry

MTT: (3-(4,5-Dimethylthiazol-2-yl)-2,5-diphenyltetrazolium bromide, a tetrazolium salt)

OAc: Acetyl-

OMM: Outer mitochondrial membrane

Q: Quercetin

QBCl: Chlorobutyl-quercetin

QBI: Iodobutyl-quercetin

QBTPI: (n-butyl-4-triphenylphosphonium)-quercetin-iodide

QTA: Tetraacetyl-quercetin

QTABCl: Chlorobutyl-tetraacetyl-quercetin

QTABI: Iodobutyl-tetraacetyl-quercetin

QTABTPI: (n-butyl-4-triphenylphosphonium)-tetraacety-quercetin-iodide

PrSH: 1-Propanethiol

Pyr: Pyridine

RSV: Resveratrol

RDA: Diacetyl-resveratrol

RT: Room temperature

TBTA: Tris[(1-benzyl-1H-1,2,3-triazol-4-yl)methyl] amine

TPMP: Methyl-triphenylphosphonium

TPP: Tetraphenylphosphonium

RBCl: Chlorobutyl-resveratrol

RDABCl: Chlorobutyl-diacetyl-resveratrol

PEG: PolyEthyleneGlycol

P_i: Phosphate

PTFE: Politetrafluoroetilene (Teflon®)

RLM: Rat Liver Mitochondria

ROS: Reactive Oxygen Species

TLC: Thin layer chromatography

TSA: Trichostatin A

SOD: Superoxide Dismutase

SULT: Sulfotransferase

UGT: UDP-Glucuronosyltransferase

Partecipation to congresses

- Andrea Mattarei, Lucia Biasutto, Ester Marotta, Umberto De Marchi, Spiridione Garbisa, Mario Zoratti, Cristina Paradisi. Synthesis and characterization of mitochondriotropic derivatives of quercetin, oral presentation, *WISPOC Winter School in Physical Organic Chemistry, Bressanone* (Italy), January 27-31, 2008.
- Andrea Mattarei, Lucia Biasutto, Ester Marotta, Armando Gennaro, Christian Durante, Mario Zoratti, Cristina Paradisi. Oxidation potentials and radical-scavenging properties of novel mitochondrion-targeted quercetin derivatives, poster, *International Symposium on Natural Compounds in Cancer Therapy, Naples* (Italy), September 22-26, 2008.
- A. Mattarei, L. Biasutto, E. Marotta, A. Bradaschia, U. De Marchi, N. Sassi, S. Garbisa, C. Paradisi, M. Zoratti. Mitochondria-targeted polyphenol derivates, oral communication, *International PSE Symposium on Natural Products in Cancer Therapy*, Napoli (Italy), September 23-26, 2008.
- L. Biasutto, A. Bradaschia, A. Mattarei, E. Marotta, S. Garbisa, M. Zoratti, C. Paradisi, The fate of polyphenols and their mitochondriotropic derivatives in blood - accumulation by mitochondria slow metabolic conjugation, poster, *International PSE Symposium on Natural Products in Cancer Therapy*, Napoli (Italy), September 23-26, 2008.
- L. Biasutto, A. Mattarei, E. Marotta, U. De Marchi, A. Bradaschia, S. Garbisa, C. Paradisi, M. Zoratti, Mitochondriotropic polyphenol derivates", poster, *International Symposium on Mitochondrial Physiology and Pathology IUBMB Symposium S1/2008*, Bari (Italy), June 22-26, 2008.
- L. Biasutto, A. Mattarei, E. Marotta, U. De Marchi, A. Bradaschia, S. Garbisa, C. Paradisi, M. Zoratti, Mitochondriotropic polyphenol derivates, poster, *COST Action 926 Conference – Benefits and risks of bioactive plant compounds*, Krakow (Poland), March 27-28, 2008. Acta Biochim. Pol. 55 (1, Suppl), 12 (P1.18).
- M. Zoratti, L. Biasutto, E. Marotta, A. Mattarei, M. Fallica, U. De Marchi, A. Bradaschia, S. Garbisa, C. Paradisi. Bioavailability-enhancing prodrugs of polyphenols, oral presentation, *COST Action 926 Conference – Benefits and risks of bioactive plant compounds*, Krakow (Poland), March 27-28, 2008. Acta Biochim. Pol. 55 (1, Suppl), 26 (O2.3).

- Mario Zoratti, Lucia Biasutto, Andrea Mattarei, Silvia Beltramello, Alice Bradaschia, Nicola Sassi, Ester Marotta, Spiridione Garbisa, Cristina Paradisi: Mitochondrially targeted polyphenols: antioxidants or chemotherapeutic drugs? *EMBO Workshop "Mitochondria, Apoptosis and Cancer: Targeting Mitochondria to defeat Cancer" Prague,* (Czech Republic), Oct. 1-3, 2009. Short Talk (MZ) ST9 (Abstract book, p.46).
- Andrea Mattarei, Lucia Biasutto, Ester Marotta, Spiridione Garbisa, Mario Zoratti, Giancarlo Sandona', Cristina Paradisi, Armando Gennaro, Christian Durante: Novel mitochondrially targeted quercetin derivatives: synthesis, oxidation potential, radical-scavenging properties and cytotoxicity EMBO Workshop *"Mitochondria, Apoptosis and Cancer: Targeting Mitochondria to defeat Cancer"* Prague, (Czech Republic), Oct. 1-3, 2009. Poster (AM) P35 (Abstract book, p. 88).
- Lucia Biasutto, Mario Zoratti, Andrea Mattarei, Alice Bradaschia, Silvia Beltramello, Nicola Sassi, Spiridione Garbisa: *"Developing prodrugs of polyphenols"*. 4th International Conference on Polyphenols and Health Harrogate, UK, 7-11 Dec. 2009 (Abstracts, P161, page 253).
- Lucia Biasutto, Andrea Mattarei, Ester Marotta, Nicola Sassi, Spiridione Garbisa, Cristina Paradisi and Mario Zoratti: *"Mitochondriotropic polyphenols: effects on mitochondria"*. 4th International Conference on Polyphenols and Health Harrogate, UK, 7-11 Dec. 2009 (Abstracts, P392, page 382).
- L. Biasutto, A. Mattarei, A. Bradaschia, S. Beltramello, E. Marotta, S. Garbisa, C. Paradisi, M. Zoratti: "Prodrugs of polyphenols" WineHealth 2010 Rosazzo (UD), Italy, 3-6 october 2010 Abstracts, page 48 (oral communication).
- N. Sassi, L. Biasutto, A. Mattarei, E. Marotta, S. Garbisa, C. Paradisi, M. Zoratti: "Mitochondriotropic quercetin and resveratrol derivatives" WineHealth 2010 Rosazzo (UD), Italy, 3-6 october 2010 Abstracts, page 58 (oral communication).
- A. Mattarei, Raj Ratan, A. P. Kozikowski: "Synthesis and characterization of novel daidzein derivatives. A Dual Drug Approach to improve the activity toward Arginase 1 expression" CSB 2010, Italy, S. Vito di Cadore, (BL) 9-11 Sept. 2010 (poster).
- A. Mattarei, L. Biasutto, N. Sassi, E. Marotta, C. Durante, A. Gennaro, M. Zoratti, C. Paradisi: "Redox behavior and biological action of novel mitochondrion-targeted quercetin and resveratrol derivatives" CSB 2010, Italy, S. Vito di Cadore, (BL) 9-11 Sept. 2010 (poster).